MTI 78TR71

POWER GENERATION WITH BINARY CYCLES

by
D. D. Colosimo, R. K. Rose and O. Decker

for Presentation at

1977-78 Lecture Series
Combined Cycles for Power Generation
Von Karman Institute for Fluid Dynamics
Rhode-Saint-Genese, Belgium

April 27, 1978

Revised October 1978

Mechanical Technology Incorporated

Research and Development Division

MTI 78TR71

POWER GENERATION WITH BINARY CYCLES

by
D. D. Colosimo, R. K. Rose and O. Decker

for Presentation at

1977-78 Lecture Series
Combined Cycles for Power Generation
Von Karman Institute for Fluid Dynamics
Rhode-Saint-Genese, Belgium

April 27, 1978

Revised October 1978

MECHANICAL TECHNOLOGY INCORPORATED
968 Albany-Shaker Road
Latham, N.Y. U.S.A. 12110

MTI 78TR71

POWER GENERATION WITH BINARY CYCLES

Prepared by:

D. D. Colosimo
R. K. Rose
O. Decker

For Presentation at

1977-78 Lecture Series
Combined Cycles for Power Generation
Von Karman Institute for Fluid Dynamics
Rhode-Saint-Genese, Belgium

April 27, 1978

Revised October, 1978

MECHANICAL TECHNOLOGY INCORPORATED
968 Albany-Shaker Road
Latham, New York 12110

TABLE OF CONTENTS

NUMBER		PAGE
1.0	INTRODUCTION	1-1
	1.1 Background	1-1
	1.2 Assumptions and Caveats	1-4
2.0	FLUID SELECTION CRITERIA	2-1
	2.1 User Acceptance	2-1
	2.2 Working Fluid Thermodynamics	2-3
	2.3 Machinery Considerations	2-5
	2.4 Heat Transfer Considerations	2-12
	2.5 Fluid Stability	2-17
	2.6 Fluid Safety	2-17
	2.7 Fluid Cost and Availability	2-18
3.0	SYSTEM COMPARISON FOR HIGH TEMPERATURES	3-1
	3.1 High Temperature Gas Source	3-2
	3.2 Cycle Comparisons	3-3
	3.2.1 Simple Steam Cycle	3-3
	3.2.2 Fluorinol Cycle	3-4
	3.2.3 Toluene Cycle	3-4
	3.2.4 Butane Cycle	3-5
	3.2.5 R-114 Cycle	3-6
	3.2.6 Binary Steam/R-11 Cycle	3-7
	3.2.7 Two Level Steam Cycle	3-7
	3.3 System Comparisons	3-8
4.0	SYSTEM COMPARISON FOR MEDIUM TEMPERATURES	4-1
	4.1 Cycle Comparisons	4-2
	4.1.1 Simple Steam Cycle	4-2
	4.1.2 Fluorinol Cycle	4-2
	4.1.3 Toluene Cycle	4-2
	4.1.4 Butane Cycle	4-3
	4.1.5 R-114 Cycle	4-3
	4.1.6 Binary Steam/R-11 Cycle	4-4
	4.2 System Comparisons	4-4

APPENDIX A

LIST OF FIGURES

Figure	Caption
1	An Illustration of the Conventional Definition of a Combined Cycle
2	Illustration of Energy Cascading Concept
3	Example of Partial Energy Cascaded Techniques
4	Binary Cycle Simplified
5	A Thermodynamically Perfect Rankine Fluid Duplicates a Carnot Cycle
6	Illustration of a Rankine Cycle with an Isentropic Fluid
7	Illustration of a Rankine Cycle with a Wetting Fluid
8	Illustration of a Rankine Cycle with a Drying Fluid
9	Illustration of a Supercritical Rankine Cycle
10	Temperature-Entropy Diagram of a Two Level Steam System Presented in Reference 18
11	Temperature Entropy Diagram of a Two Level Steam System Presented in Reference 6
12	Temperature Entropy Diagram of a Two Level Steam System
13	Temperature Entropy Diagram of a Binary Steam and Organic Cycle
14	Performance Map For a Single Stage Radial Inflow Turbine
15	Comparison of Allowable Enthalpy Drops For Different Fluids
16	Effect of Pressure Ratio on Turbine Efficiency
17	Illustration of Three Working Fluid Enthalpy-Temperature Characteristics
18	Temperature-Heat Flow for Water
19	Temperature-Heat Flow for Fluorinol-85
20	Temperature-Heat Flow for Butane
21	Temperature-Heat Flow for Toluene
22	Illustration of Heat Transfer In a Heat Exchanger
23	Variation in Unit Surface Cost of Shell and Tube Heat Exchangers (Reference 31)
24	Sealed Tube Test Data for Thermal Decomposition of R-11 and R-114
25	General Classification of Applications for Rankine Bottoming Cycles
26	Sample Output from MTI Rankine Design Program (a) Temperature Heat Flow From Waste Heat Source to Working Fluid (b) Cycle and Machinery Calculations for Top Cycle (c) Cycle and Machinery Calculations for Bottom Cycle (d) Cycle Cost Estimate

LIST OF FIGURES (Cont'd)

Figure	Caption
27	Effect of Fuel Sulfur Content on Dew Point Temperature of Sulfuric Acid in Exhaust Gas
28	Cost Comparison of Various Cycle Conditions With Simple Steam With 700°F Hot Gas Source
29	Illustration of Rankine Cycle With Simple Steam For Most Cost Effective Case Considered
30	Power Output and Machinery Cost for Various Steam Cycles With a 700°F Hot Gas Source
31	Cost Comparison of Various Cycle Conditions With Fluorinol-85 With 700°F Hot Gas Source
32	Illustration of Rankine Cycle With Flourinol-85 For Most Cost Effective Case Considered
33	Cost Comparison of Various Cycle Conditions With Toluene With 700°F Hot Gas Source
34	Illustration of Rankine Cycle With Toluene For Most Cost Effective Case Considered
35	Cost Comparison of Various Cycle Conditions With Butane With 700°F Hot Gas Source
36	Illustration of Rankine Cycle With Butane For Most Cost Effective Case Considered for a 600°F Turbine Inlet
37	Illustration of Rankine Cycle with Butane For Most Cost Effective Case Considered for a 500°F Turbine Inlet Case
38	Cost Comparison of Various Cycle Conditions With R-114 With 700°F Hot Gas Source
39	Illustration of Rankine Cycle With R-114 For Most Cost Effective Case Considered
40	The Effect of Regeneration on System Cost and Power Output For an R-114 Cycle With 600 psia and 400°F Turbine Inlet Conditions
41	Cost Comparison For a Binary Steam/R-11 System With 700°F Hot Gas Source
42	Schematic of Binary Steam/R-11 Cycle
43	Schematic of Simple Two Level Steam Cycle
44	Cost Comparison of Various Cycle Conditions With Two Level Steam With 700°F Hot Gas Source
45	Alternate Working Fluids For Cost Optimized Heat Recovery With a 700°F Waste Gas Source and 100°F Condensing Temperature
46	Conventional System Design Approach
47	MTI/Turbonetic System Design Approach

LIST OF FIGURES (Cont'd)

Figure	Caption
48	Illustration of Rankine Cycle With Simple Steam Cycle For Most Cost Effective Case Considered With 500°F Gaseous Source
49	Cost Comparison of Simple Steam Cycle With 500°F Hot Gas Source
50	Cost Comparison of Fluorinol-85 Cycles With 500°F Hot Gas Source
51	Illustration of Rankine Cycle With Fluorinol-85 For Most Cost Effective Case Considered With 500°F Gaseous Source
52	Cost Comparison of Toluene Cycle With 500°F Gas Source
53	Illustration of Rankine Cycle With Toluene For Most Cost Effective Case Considered With 500°F Gaseous Source
54	Cost Comparison of Butane Cycle With 500°F Hot Gas Source
55	Illustration of Rankine Cycle With Butane For Most Cost Effective Case Considered With 500°F Gaseous Source
56	Cost Comparison of R-114 Cycles With 500°F Hot Gas Source
57	Illustration of Rankine Cycle With R-114 For Most Cost Effective Case Considered With 500°F Gaseous Source
58	Schematic of Binary Steam/R-11 Cycle With a 500°F Hot Gas Source
59	Cost Comparison of Binary Steam/R-11 Cycle With 500°F Hot Gas Source
60	Alternate Working Fluids For Cost Optimized Heat Recovery With a 500°F Waste Gas Source and 81°F Condensing Temperature
61	Cycle Schematic For Binary Demonstration System
62	General Arrangement of MTI Binary Rankine Cycle System For Waste Heat Recovery/Electric Power Generation
63a	Schematic of Exhaust Gas Ducting For Heat Recovery
63b	Mockup of Exhaust Gas Management System and Steam Generator
64	Machinery Building Mockup
65	Mockup of Heat Exchanger Skid
66	Dimensions and Spacing Pattern For Steam Evaporator
67	Layout of Waste Heat Recovery Vaporizer System
68	Construction Details of Steam Evaporator
69	Gearbox and Assembled Machinery Package for the Binary Steam/R-11 System
70	Steam Turbine Components
71	Steam and Freon Turbine Wheels
72	Critical Speed Map For the Three Shafts of the Binary Steam/R-11 System
73	Parametric Plot of Radial-Inflow Turbine Geometry Variables
74	Flowpath Cross-Section for Radial-Inflow Steam Turbine

LIST OF FIGURES (Cont'd)

Figure	Caption
75	Flowpath Cross-Section for Radial-Inflow R-11 Turbine
76	Gear Life Factor Versus Number of Fatigue Cycles, Illustrating Conservative MTI Practice Compared to AGMA Standard
77	Partial Assembly of Gearbox
78	Linearized Controller Block Diagram
79	System Schematic
80	Accumulative Distribution of Industries and Utilities That Should Be Willing To Invest at a Given Rate of Return (Source: Reference 41)
81	Sample Printout from the Waste Heat Recovery Investment Analysis Program
82	Effect of Energy Cost on the Discounted Cash Flow
83	Effect of Energy Inflation Rate on the Discounted Cash Flow
84	Effect of Annual Operating Hours on Discounted Cash Flow
85	Effect of Marginal Tax Rate on the Discounted Cash Flow
86	Effect of Investment Tax Credit Rate on the Discounted Cash Flow
87	Effect of Depreciation Period on the Discounted Cash Flow
88	Variation of DCF With Available Heat Flow For Organic Cycles With a Condensing Heat Source
89	Variation of DCF With Available Heat Flow For Organic and Binary Cycles With a Sensible Hot Gas Source
90	Variation in DCF With Hot Gas Source Temperature For Organic and Binary Cycles With a 10-million Btu/Hr Heat Flow
91	Variation in Delivered Net Power With Hot Gas Source Temperature For Organic and Binary Cycles With a 10-million Btu/Hr Heat Flow
92	Economic Applications For Bottoming Cycles
93	Comparison of Rejected Heat and Suitable Power Fluids

APPENDIX B

LIST OF TABLES

Number	
1	Fluids and System Concepts Being Developed as Bottoming Cycles for Power Generation
2	Selected Characteristics of Working Fluids Considered
3	Fluid and Machinery Configurations Considered
4	Cycle Points for Determination of Working Fluid Thermodynamic Efficiency With Ideal Hardware
5	Comparison of Working Fluid Performance
6	Comparison Fluid Selection on Turbine Size
7	The Combined Effect of Heat Transfer and Thermodynamics on Delivered Power
8	Overall Heat Transfer Coefficient
9	Comparison of Transport Properties of Working Fluids and Their Effect on Condensing Heat Transfer Coefficient
10	Effect of Condensing Heat Transfer Coefficient on System Cost per Unit Output
11	Overall Heat Transfer Coefficient Used in the Comparison Analyses
12	Comparison of the Effect of Turbine Inlet Temperatures With a Supercritical Butane Cycle
13	Working Fluid Comparison For Heat Recovery From A 700°F Waste Gas Source
14	Comparison of Butane Supercritical and Regular Rankine Cycles
15	Comparison of R-114 Supercritical and Regular Rankine Cycles
16	Working Fluid Comparison For Heat Recovery From A 500°F Waste Gas Source
17	Heat Energy Available for Recovery
18	Diesel Engine Maintenance Requirements
19	Design Point Exhaust Flow Conditions
20	Gas Side Data for Steam Evaporator
21	Steam Side Data for Steam Evaporator
22	Gear Data For Binary System Integral Double Gear Set
23	Economic Factors Used in Economic Acceptance Analysis
24	Cycles for Investment Screening

1.0 INTRODUCTION

1.1 Background

> "The continued upward trend of fuel and other operating costs is providing the impetus now apparent in the electric power industry for the use of high-efficiency power cycles. Every effort is being made to produce a kilowatt-hour with the minimum expenditure of fuel and at the lowest possible cost".

This quotation is taken from a 1951 paper describing the advances of mercury-steam central power stations [1]. This illustrates the fact that the electric utility industry has had a long and continued interest in combined cycles ranging from their historic operation of mercury-steam Rankine stations, to their more recent use of gas turbine-steam turbine stations. Thus, the use of combined cycles for utility applications has received considerable attention (e.g., the extensive discussions here on gas turbine-steam turbine systems).

The continued upward trend of energy costs has prompted the consideration of Rankine systems to generate power in non-utility situations. In fact, it is the inability of the electric power industry to maintain its historic trend of selling power at a cost that was continually decreasing in real terms that is now motivating its customers to look at internal power generation. As opposed to the development of combined cycles in the utilities, the Rankine cycle in non-utility applications must be matched to a heat source that is a by-product of an operation that is not related to nor optimized for power generation. The use of combined and binary cycles in these applications poses an entirely different set of constraints and economics than those faced in utility power generation. The objective of this paper is to explore the use of binary cycles as the bottom cycle of combined cycles to produce small levels of power in non-utility environments.

The first step in exploring this subject is to clarify the terms "combined cycle", "binary cycle", "small power levels", and "non-utility environment". As typically used, "combined cycle" means the cascading of two heat engines, the top heat engine deriving its energy from a fuel and the bottom heat engine deriving its energy from the reject heat of the top cycle. This is shown in Figure 1 for the case of a gas turbine steam turbine cycle. We believe that this conventional definition of combined cycles is unnecessarily restrictive

and tends to mask useful and desirable applications. We prefer to consider that the definition of a cycle includes not only heat engines, but any process that changes the thermodynamic potential of heat in the extraction of useful work, the processing of chemicals, or the heating or cooling of process materials [2]. Figure 2 shows a number of "cycles" operating over the available energy potential spectrum. The combining of any or all of these cycles can produce the same amount of useful output with only the amount of fuel that the highest cycle alone consumes. Perhaps the term "energy cascading" should be used instead of combined cycles. Nevertheless, under our definition of combined cycles, cogeneration (the production of electricity and process steam) and total energy (the production of electricity and building space conditioning) are examples of combined cycles (see Figure 3). This paper is concerned with those combined cycles which combine a Rankine cycle with the rejected heat from any other cycle.

The term "binary cycle" has been used to mean many different types of systems. As used in this paper, a binary cycle is a Rankine bottoming cycle consisting of separate cycles using water and organic working fluids to better match the available source and sink temperatures and the source temperature - heat flow, and to produce simplified machinery designs. An example of a binary cycle is shown in Figure 4. A specific demonstration of this design in the recovery of power with a single stage of steam expansion and a single stage of organic expansion with no pressure in the system going below atmospheric pressure will be discussed in detail in this paper. The use of water and organics for power generation is not new. Organic working fluids have properties which considerably reduce the size of the turbomachinery, the number of stages required, and even the condenser size relative to steam. These attributes were discussed as a reason to replace the low pressure steam turbine section in a large (1000 megawatt) power station with an organic turbine [3]. The combination of a steam-organic cycle is referred to as a "binary plant" in Reference 3 .

In the context of this paper, the term "small power levels" means power levels below four megawatts. This level of power is about the maximum that could be expected to be recovered from industrial installations. The most typical level of power will be in the range of 0.5 to 1.0 megawatts.

The application of these systems will occur more and more in industrial situations - that is, in situations where the investment decision criteria used will be based on industrial economics and not utility economics. This is what is meant by "non-utility environment".

It will be noted that virtually all of the current organic and binary Rankine systems are scheduled for installation in municipal utilities. These are electric utilities owned and operated by a city government. As you are aware, government operated utilities have some economic peculiarities. These peculiarities increase when it is a city government and not the central government that is operating the utility. The municipal utilities are typically small with total generation capacity in the range of 20 to 30 megawatts. Many have base loaded diesel engines which have rejected heat characteristics that are very nice to consider for Rankine bottoming cycles. Also, since their primary cost is fuel, municipal utilities were severely affected by the increased oil prices following the oil embargo and are very eager to try anything to reduce their operating costs. Therefore, municipal utilities are a ready customer for Rankine bottoming cycles.

While the municipal utilities provide a receptive and technically attractive area for Rankine bottoming cycles, meaningful energy savings can be realized only when industry fully adopts bottoming cycles. Industry's delay in using bottoming cycles has been a result of the uncertain economics and technology of bottoming cycles. However, industry is now beginning to move. We fully expect that a very sizeable business will exist in Rankine cycles for industry in four to five years.

This lecture will present a survey of the state-of-the-art in Rankine bottoming cycles in order to illustrate the applicability and nonapplicability of binary cycles. The first topic covered will be the typical criteria used in the selection of working fluids for Rankine cycles. Next, we will show how these criteria are reflected in the application of steam, organic, and binary cycles to two favorite waste heat sources - a gas turbine and a diesel. Next, we will discuss how various governmental policies and alternative energy prices affect the industrial economics of energy recovery. Finally, we will cover screening techniques to match organic and binary cycles to industrial processes.

1.2 Assumptions and Caveats

In this discussion of the applicability of binary cycles, some assumptions have been made to make the problem tractable. Specifically, it has been assumed that the binary cycle will be compared only to those Rankine bottoming cycles that are being developed and offered for the same range of applications as those shown in Table 1. The general machinery configuration for each system has been retained in general, but not necessarily the exact configuration in terms of specific speeds, actual rotation rates, or stages. The major exception is our assumption of a multistage axial machine configuration for use with toluene rather than the supersonic single stage being developed by Sundstrand [11]. The total stage efficiency is taken to be the highest that can reasonably be expected for the class of machinery. The six fluids (Table 2) currently being considered are assumed to be the best fluids available - at least in the judgement of their respective developers. Thus, it must be assumed that any fluid or cycle concept must compete with these six fluids and the systems in which they are configured. Examining the system concepts listed in Table 1, we have selected the eight combinations presented in Table 3 for analysis here.

The two level steam cycle considered here has a single stage for the expansion of each level. The use of multistage expansions at each level as suggested in References 6 and 18 can result in better overall performance and economics than might be implied by the system considered here. The problem is that selection of a specific two level steam configuration is highly application-dependent. The specification of a temperature and heat flow does not result in a general two level cycle configuration. The two level cycle selected for evaluation here should be considered as an illustration only.

The comparison of the systems in Table 3 is done on a consistent basis for specific applications to provide system performance and cost estimates. The results presented here are valid for the applications considered, and may be construed as being generally valid. There are, however, some special applications for which the system selection criteria are different than those assumed

here. For example, air condensing presents a different cycle and equipment cost constraints. Arctic pipeline applications [9] present fluid selection constraints that are not present in most applications and not considered here. Thus, the definitive suitability of any fluid or cycle configuration must be judged by the operating and economic criteria of the end user.

POWER GENERATION

WITH BINARY CYCLES

78P79

The continued upward trend of fuel and other operating costs is providing the impetus now apparent in the electric power industry for the use of high efficiency power cycles. Every effort is being made to produce a kilowatt-hour with the minimum expenditure of fuel and at the lowest possible cost.

Hackett
Mechanical Engineering
July 1951

78P79

Binary Cycles as the Bottom Cycle of **Combined Cycles** to Produce **Small Levels of Power** in **Non-Utility Environments**

78P79

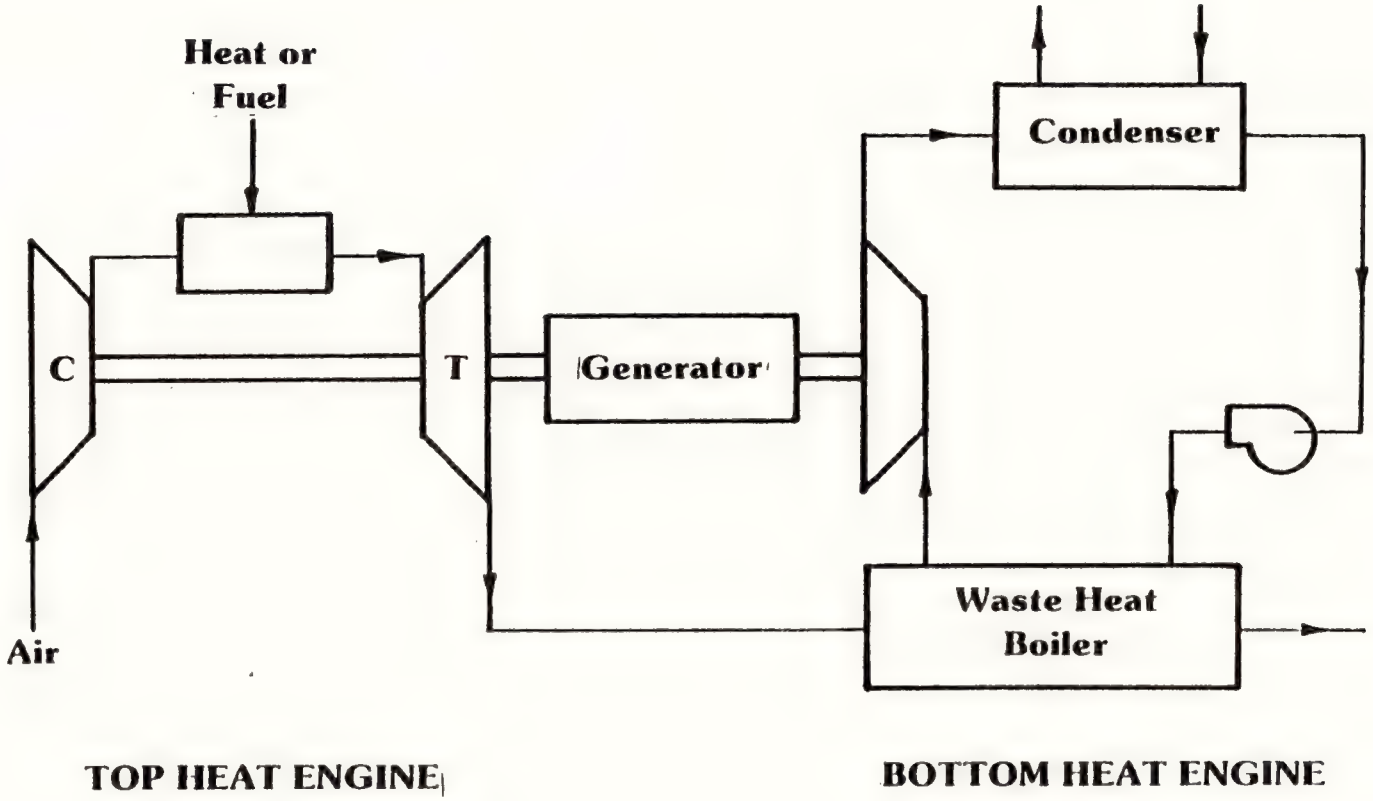

Figure 1 An Illustration of the Conventional Definition of a Combined Cycle

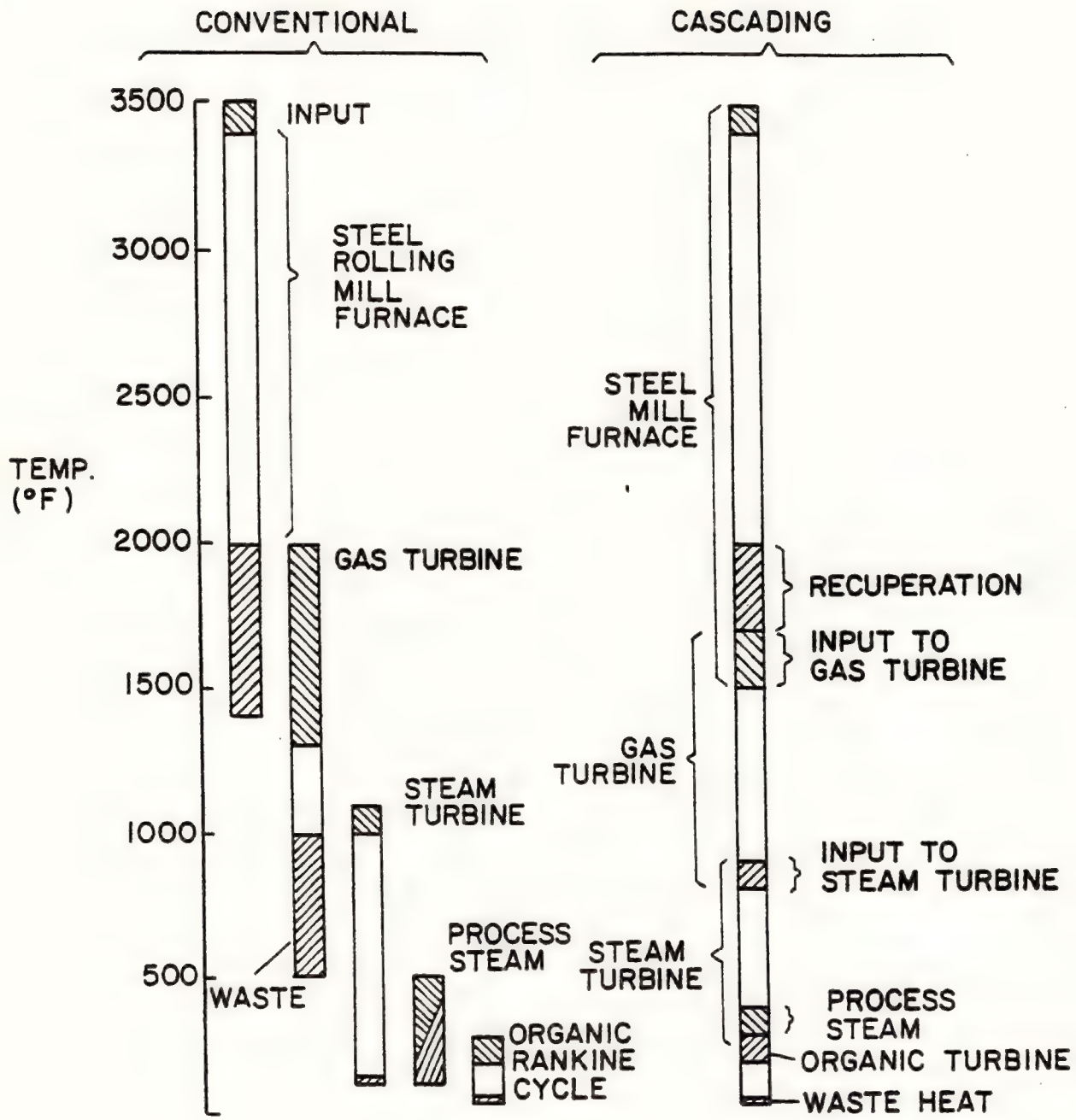

Figure 2 Illustration of Energy Cascading Concept

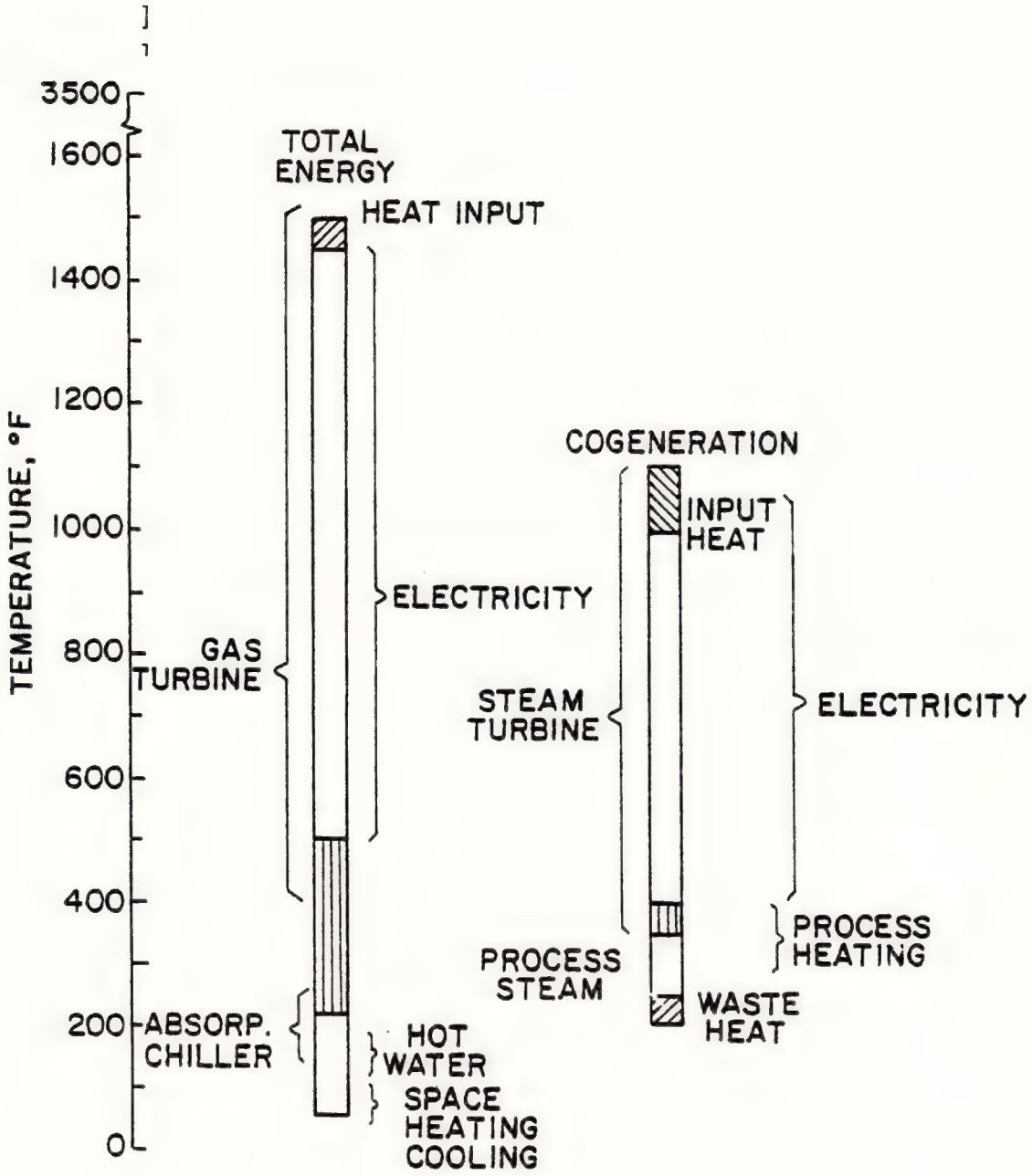

Figure 3 Example of Partial Energy Cascaded Techniques

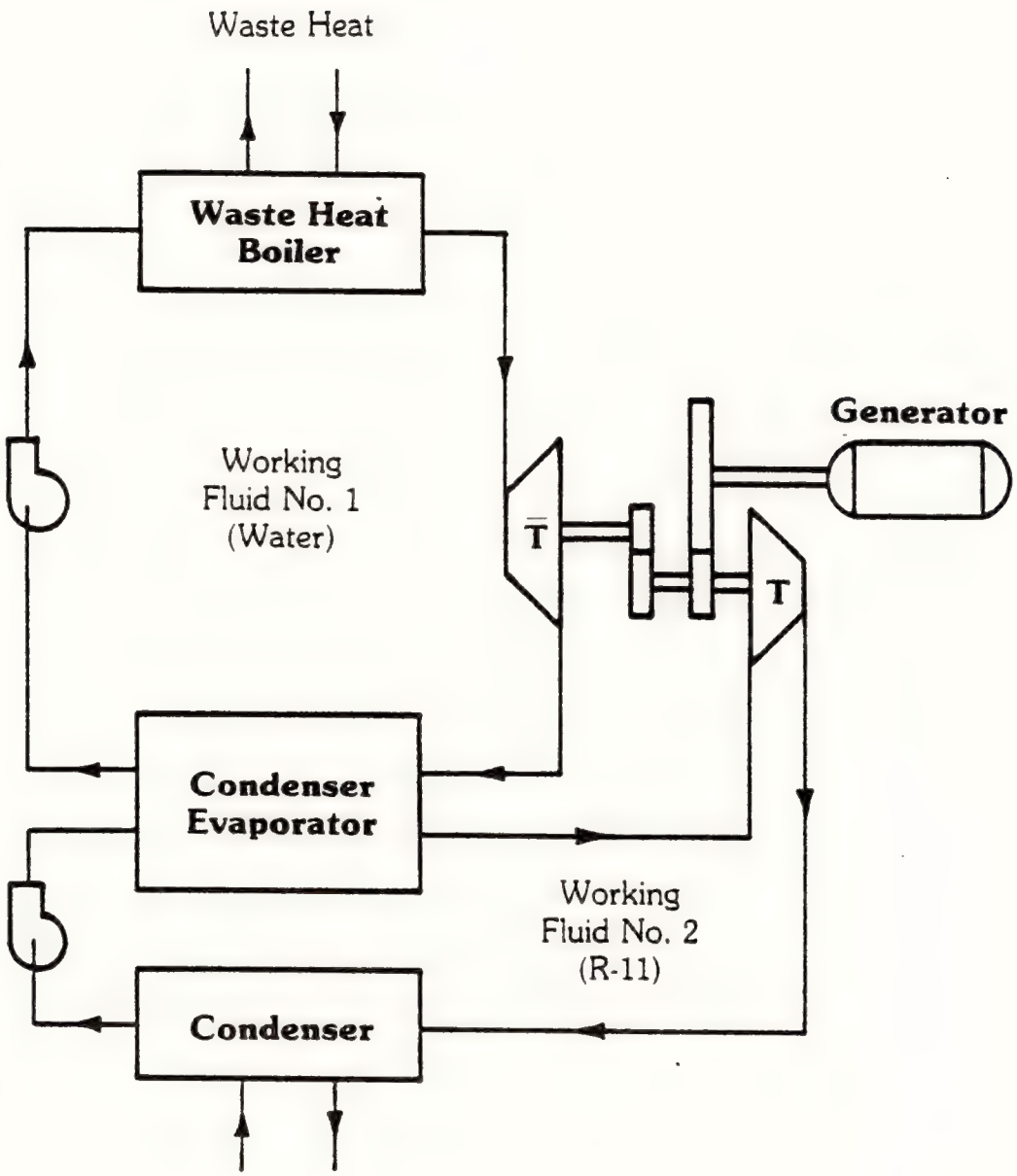

Figure 4 Binary Cycle Simplified

SMALL POWER LEVELS

78P79

NON-UTILITY ENVIRONMENT

78P79

ASSUMPTIONS

78P79

TABLE 1

FLUIDS AND SYSTEM CONCEPTS BEING DEVELOPED
AS BOTTOMING CYCLES FOR POWER GENERATION

FLUID	PROBABLE RANGE OF APPLICATION	MACHINERY DESCRIPTION	DEVELOPER OR ADVOCATE	REF.
Binary (Water/R-11)	400° - 800°F	Single stage radial steam; single stage radial R-11	MTI	4
Water	>500°F	Two level, multi-stage axial	Solar	6
		Multi-stage axial	Hawthorne Leslie	7
		Multi-stage axial	Thermo Electron	8
		Multi-stage axial	MTI	5,9
		Two level, single stage at each level	MTI	5,9
Normal Butane	>400°F	Single stage radial	Therma Technology	10
Toluene	>500°F	Single stage axial	Sundstrand	11
Fluorinol-85	500° - 800°F	Multi-stage axial	Thermo Electron	12,13,14
R-114 (Dichlorotetrafluoroethane)	400° - 700°F	Single stage radial	MTI	9
R-11 (Trichlorofluoromethane)	<500°F	Single stage radial	IHI Allied	15,16
		Single stage radial	MTI	4,5,17

TABLE 2

SELECTED CHARACTERISTICS OF WORKING FLUIDS CONSIDERED

NAME	CHEMICAL FORMULA	MOLECULAR WEIGHT	CRITICAL TEMP	CRITICAL PRESSURE	VAPOR PRESSURE AT 100°F	SATURATED VAPOR SPECIFIC VOLUME AT 100°F	MAXIMUM RECOMMENDED OPERATING TEMP	TYPE OF FLUID
Water	H_2O	18	705	3206	0.949	350.4		Wetting
R-11 (Trichlorofluoromethane)	$C\ Cl_3F$	137.4	388	640	23.4	1.765	300°F	Wetting Isentropic
R-114 (Dichlorotetrafluoroethane)	$C_2Cl_2F_4$	170.9	294.3	473	45.8	0.696	400°F	Drying
Fluorinol-85	85% Mole $C_2F_3H_3O$ 15% Mole H_2O	87.7	448	778	3.2	21.41	625°F	Drying Isentropic
Toluene	C_7H_8	92.1	609	592	1.04	62.5	900°F	Drying
Butane	C_4H_7	58.1	305	550	51.4	1.80	500°F	Drying

TABLE 3

FLUID AND MACHINERY CONFIGURATIONS CONSIDERED

FLUID	MACHINERY DESCRIPTION
Binary (water/R-11)	Single stage radial turbine for each fluid
Water	Single level steam with multi-stage axial turbine
Water	Two level steam with a single stage radial turbine for each level of steam
R-114	Single stage radial turbine
R-11	Single stage radial turbine
Butane	Single stage radial turbine
Fluorinol-85	Multi-stage axial turbine
Toluene	Multi-stage axial turbine

CAVEATS

78P79

2.0 FLUID SELECTION CRITERIA

Each branch of engineering seems to have its ideal material requirement. Thus, there is always a search for the perfect lubricating fluid, the perfect bearing metal, the perfect tool metal, the perfect structural metal, etc., Rankine cycles are no exception. There is a continual debate on the perfect Rankine fluid. We believe that there is no perfect Rankine fluid, but that there are a number of fluids that are acceptable for a given application when compared against some reasonable selection criteria [3,5,19,20,21,22,23,24]. The selection criteria presented in the order an engineer would consider are:

1. Thermodynamics - how closely the fluid approaches a Carnot cycle
2. Fluid machinery considerations
3. Heat transfer characteristics - the match between the temperature - heat flow required by the fluid compared to the available temperature-heat flow available from the source and the transport properties of the fluid
4. Fluid stability and material compatibility
5. Safety - toxicity and flammability
6. Fluid cost and availability
7. User perception and acceptance of the fluid

The first six items are typical engineering considerations. The last item is really a marketing consideration but should dominate engineering considerations. Regardless of an engineer's selection of the best Rankine fluid, it would be to no avail if his company could not sell the product because of the user's perception of the fluid. In our selection of fluids, we view the last item as the most important, and will discuss it first in combination with Items 5 and 6.

2.1 User Acceptance

There are two factors which have significant impact on the potential purchaser of a Rankine system when considering the working fluid: availability and perceived risk.

Availability of the fluid or any critical component in the system is important to the potential purchaser because it affects the ability of the machine to continue to run at the rate necessary to justify an investment. Many plant managers have been hurt by having a piece of equipment inoperative because of some part having to be flown in from Los Angeles or Tokoyo, for example. A system which would depend upon a fluid that is exotic in that it is not a generally available commercial item, or a fluid that is exclusive to one manufacturer would have a competitive disadvantage against a Rankine system with a conventional fluid with comparable performance and cost.

The only safety risk that is important is the one perceived by the potential buyer. Whether this perception is based upon health, safety, government regulations, or community relations and is not justified by engineering fact is totally immaterial. Perceived risk is entirely different from the risk considered by an engineer under Item 5. As an engineer, I can accept that a Rankine system using a hydrocarbon can be safely designed. After all, refineries run high distillate hydrocarbons through heaters, distillation towers, and condensers with no problems resulting. But as a plant manager of a cement plant, for example, this would be of little importance to me, as I have a cement plant and not a refinery. For example, my personnel are accustomed to using butane to light cigarettes, not to run through a heat exchanger in a clinker cooler. Thus, a Rankine system using a hydrocarbon or any working fluid with a perceived risk will have a competitive disadvantage when compared to a system with a working fluid that does not have a perceived risk with comparable performance and cost.

Given the above, we at MTI decided that we would consider only fluids that are generally available, nonflammable, nontoxic, and have no other psychological barriers. Specifically, we restricted our working fluid selection to water and commonly used fluorocarbon refrigerants. As we will show later, in the range of temperatures in which the more exotic fluids and hydrocarbons are considered, comparable performance and machinery costs can be obtained by using binary Rankine systems or simple steam systems.

2.2 Working Fluid Thermodynamics

The ideal thermodynamic cycle is the Carnot cycle. A thermodynamically perfect Rankine cycle fluid would permit the Carnot cycle to be duplicated, as shown in Figure 5. This perfect fluid would have a vapor dome that has isentropic saturated liquid and saturated vapor lines. The degree of fluid imperfection is the degree to which it deviates from a Carnot cycle. This is a rather simplistic view, but one that has dominated much thought on fluid selection. While no fluid has an isentropic saturated liquid line, there are fluids with very nearly isentropic saturated vapor lines (Figure 6), as well as fluids with negatively sloped and positively sloped saturated lines. The fluids with negatively sloped lines, such as water, are called wetting fluids since any expansion tends to enter the vapor dome or wet area (Figure 7). The fluids with positively sloped lines, such as some hydrocarbons and fluorocarbons, are called drying fluids since any expansion results in a superheated vapor (Figure 8). There is a deviation of the Rankine cycle that is often considered. This is called a supercritical Rankine cycle, as shown in Figure 9. Actually, this cycle is a hybrid Brayton-Rankine cycle. It consists of isentropic compressions and expansions as does both the Brayton and Rankine. The heat addition occurs isobarically as in the Brayton cycle, while the heat rejection occurs isothermally as in the Rankine.

Examination of the sketches in Figures 6 through 9 suggests that a fluid with an isentropic saturated vapor line will achieve the highest percentage of Carnot efficiency of any of the other fluid types. This is why there is much interest in isentropic fluids. However, suggestions from sketches do not necessarily reflect facts, as will be shown later in this section. An isentropic fluid may not achieve the best thermodynamic performance nor the best system performance. In fact, a drying fluid used in either a regular or supercritical cycle may achieve very high efficiencies relative to Carnot when regeneration is used.

Rankine cycles may be combined either with one working fluid as in multi-level steam, or with two fluids as in a binary. The use of either approach to the stacking of cycles is not readily justified by the ideal thermodynamic efficiency that is obtained. In fact, the idealist in thermodynamics may argue against the use of this approach. However, it is the effect of this approach on overall system performance and cost that is the ultimate decision factor.

The use of two level steam for gas turbine steam turbine applications has been considered for rather typical utility sized applications [18] and for smaller applications [6]. The cycle represented in Figure 10 is the cycle selected in Reference 18 as the optimum. The cycle in Figure 11 is discussed in Reference 6. Figure 12 presents the cycle for a two level steam system that will be used here for comparison with the other systems. These cycles will be further discussed at a later point.

The binary cycle is illustrated in a temperature entropy diagram in Figure 13. The vapor domes used are typical of water and R-11. Depending on fluid selection and matching, and the temperature differential between the two fluids, the binary cycle can achieve a closer approximation to Carnot than single fluid systems. This is demonstrated below.

In order to illustrate the thermodynamic performance of the fluids and cycles under consideration, cycles were set for each fluid between a peak turbine temperature of 650°F and 100°F. It was assumed that there are no losses in heat transfer, pumping, or expansion. The only restriction which affects both steam and R-11 is that the isentropic expansion cannot enter the vapor dome. Since real machinery increases entropy, entering the vapor dome on an isentropic expansion is normally practiced with steam even when a dry turbine exhaust is desired. In the case of R-11, the shape of its vapor dome is such that, except near the critical point, all isentropic expansions enter the vapor dome. Thus, R-11 could not be used in this simplified analysis. Instead, R-113 (trichloro-trifluoroethane) is used as the bottom half of the binary cycle. The state points for the cycles are presented in Table 4.

In computing the thermodynamic performance, any pumping losses were ignored since they tend to be small in the ideal case, e.g., less than 2 Btu/lb in the most severe case of Fluorinol-85. For the drying fluids, the efficiency was computed without regeneration and with 100 percent effective regeneration. In practice, the amount of regeneration is a tradeoff between cycle losses, increased heat exchanger costs, and overall system costs. The results shown in Table 5 indicate that, without regeneration, the ideal binary cycle achieves the highest thermodynamic efficiency. With full regeneration, however, toluene very closely approximates Carnot. Steam appears to be the worst fluid.

partly because a dry expansion was assumed. If this condition were relaxed to the point of a 10 percent wet expansion isentropically, the steam efficiency would increase, as shown in Tables 4 and 5. Obviously, this comment is equally applicable to the top half of the binary cycle. As shown again in Tables 4 and 5, if the steam in the binary cycle is allowed to go into the wet region on the isentropic expansion to 10 percent liquid, the overall binary efficiency would exceed butane and Fluorinol with 100 percent efficient regeneration.

A general conclusion might be that steam is not a good working fluid when comparing its potential thermodynamic performance to the other fluids presented. Indeed, if thermodynamic performance were the sole criteria, any of the three organic fluids would appear to be a more attractive selection. However, ideal thermodynamic cycles must be fitted into the real world (e.g., machinery).

2.3 Machinery Considerations

The theoretical cycle efficiencies previously discussed were arrived at independent of any machinery considerations. When the various power fluids are applied to specific applications, it becomes apparent that certain design constraints are imposed by the equipment. Some of the more significant constraints are:

- Maximum enthalpy and pressure drop across a single turbine stage for maximum turbine efficiency
- Maximum turbine tip speed
- Size of piping and machinery to accommodate the required volumetric flow rate of the fluid

In an attempt to satisfy the above design requirements, it is necessary to make compromises as a result of the conflicting influences of the fluid properties. The approach typically used is to start with the turbomachinery design relations developed by Balje [25] and Wood [26]. The use of this approach was first developed by Bjerklie [19] and has been used most recently by Woodson [5]. Horn [3] used a different method but obtained similar results. The approach here will follow the Bjerklie methodology.

Balje defined a number of similarity parameters which would characterize a turbine's performance. From the point of view of design, the key parameters are:

Specific speed $N_s = \frac{NQ^{1/2}}{H^{3/4}}$

Specific diameter $D_s = \frac{DH^{1/4}}{Q^{1/2}}$

Velocity ratio U/C_o

Spouting velocity $C_o = \sqrt{2\ H}$

The definition of the various terms and their usual U.S. engineering dimensions are as follows:

D Turbine diameter, feet

g Gravitational constant, 32.2 ft^2/sec^2

H Isentropic enthalpy drop across the stage $ft\text{-}lbs_f/lb_m$ $(ft^2/sec^2/lb_m)$

N Turbine rotational rate, revolutions per minute

Q Turbine exit volumetric flow rate, ft^3/sec

u Turbine tip speed, ft/sec

You will note that the specific speed and diameter are not dimensionless quantities as typically defined. These quantities have been used to present possible turbine stage efficiencies for axial, multi-stage axial and radial inflow turbines. Figure 14 duplicates Balje's performance data for a radial inflow turbine. From Figure 14 it can be seen that a maximum efficiency radial inflow turbine should have:

$N_s = 70$

$D_s = 1.5$

$u/C_o = 0.7$

There are, however, some restrictions. The Reynolds number should be over 10^6 and the maximum total pressure ratio should be equal to or less than 6.

In order to start this analysis, let us deal with the radial turbine and specify that the pressure ratio is 6. This implies an isentropic enthalpy drop across the turbine, given by:

$$H = \frac{\gamma}{\gamma-1} RT \left[1 - \pi^{-(\gamma-1)/\gamma}\right] \qquad (1)$$

where:

R is the gas constant for the gas

T is the turbine inlet total temperature °R

γ is the ratio of specific heats

π is the total pressure ratio, turbine inlet to turbine exit

We note that the gas constant for any gas is simply given by:

$$R = \frac{R_o}{m} \qquad (2)$$

where:

R_o is the universal gas constant, 1.9589 Btu/°R lb-mole

or cal/°k g-mole

or 1545.43 ft-lb/°R lb-mole

m is the gas molecular weight

Combining Equations 1 and 2, we obtain:

$$H = (1545.43)\left(\frac{\gamma}{\gamma-1}\right)\frac{T}{m}\left[1 - \pi^{-(\gamma-1)/\gamma}\right] \qquad (3)$$

which can be written as:

$$H = f \frac{T}{m} \tag{3a}$$

where:

$$f = 1545.43 \left(\frac{\gamma}{\gamma-1}\right)\left[1 - \pi^{-(\gamma-1)/\gamma}\right] \tag{4}$$

Using various values for γ and π=6, we find that:

γ	1.4	1.3	1.2	1.1
f	2166.0	2268.0	2394.0	2555.0

Since the fluids of interest here have a γ in the range of 1.1 to 1.3, a single value of f will be taken for screening purposes. This results in an expression for the isentropic enthalpy drop as:

$$H = 2400 \frac{T}{m} \tag{3b}$$

This relation implies that a gas of low molecular weight would be desirable since it can result in the greatest enthalpy drop and power per stage. The relation in Equation 3b is presented in Figure 15.

There is another consideration which defines the maximum enthalpy drop across the stage. This consideration is the stress levels in the turbine. Turbine stress is proportional to the square of the turbine tip velocity. If we wish to have high efficiency, we know from Figure 14 that the turbine tip velocity is related to the enthalpy drop as follows:

$$u = .7\sqrt{2gH} \tag{5}$$

or

$$H = \frac{1}{2g}\left(\frac{u}{.7}\right)^2 \tag{5a}$$

We can set the maximum value of tip speed to a level that is currently state-of-the-art, 1600 ft/sec for instance, which will then provide the maximum enthalpy drop from a mechanical stress consideration:

$$H = 81{,}125 \text{ ft-lb/lb} \qquad (5b)$$

This mechanical limiting enthalpy drop is also presented in Figure 15.

The implication is that, for a given turbine inlet temperature and power level, a high molecular weight fluid will have a lower turbine tip speed. The actual head drops depend on the properties of the working fluid. To provide an indication, the actual enthalpy drops for the ideal cycles discussed in Table 4 are presented in Figure 15. Steam far exceeds the mechanical and aerodynamic limitations. Toluene also exceeds the mechanical and aerodynamic limitations. Only R-113 can reasonably satisfy both the mechanical and aerodynamic enthapy requirements. This does not mean, however, that the other requirements, specifically pressure ratio, are satisfied.

The restriction on the pressure ratio is basically a limitation on the velocities relative to sonic conditions. Balje gives a correction factor to determine the change in the stage efficiency as follows:

$$\eta = \eta_o - N_s^3 D_s^5 (5 \times 10^{-9}) [\pi^{1/\gamma} - \pi_o^{1/\gamma}] \qquad (6)$$

where the subscript o denotes the efficiency of Figure 14. Since we are dealing with a design point of $\eta_o = 85\%$, $N_s = 70$, $D_s = 1.5$, and $\pi_o = 6$, Equation 6 may be written as:

$$\eta = .85 - (1.302 \times 10^{-2}) [\pi^{1/\gamma} - (6)^{1/\gamma}] \qquad (6a)$$

This function is plotted in Figure 16 for $\gamma = 1.4$ and 1.1. Also shown on this plot are the pressure ratios for the ideal cycles in Table 4. All the fluids have pressure ratios above 6. Based on pressure ratio, the fluorocarbons, butane, and steam can be used with a single stage turbine with reasonable efficiency. In the case of steam, the enthalpy limitations are

more constraining and limit pressure ratios to be of the order of 3 or 4. Based both on enthalpy and pressure limitations, toluene and Fluorinal should have multistage turbines.

As with any generalization, there are exceptions. Supersonic axial turbines have been built to take pressure ratios of 100 [11]. Also, by changing cycle state points such as the condensing temperature by only a few degrees, a large difference can be realized on the pressure ratio. For example, if toluene were to condense at 150°F instead of 100°F, the pressure ratio would be 89.9 instead of 288.

If simple machinery designs such as single stage radial inflow turbines are desired, a combination of Equations 3b and 5a present a screening criteria for fluids or cycle state points:

$$u_{max}^2 \leq 75734 \frac{T}{m} \tag{7}$$

This implies that high molecular weight fluids are desirable. However, as a result of their lower enthalpy drops, the flow rates of the high molecular weight fluids must be higher than the low molecular weight fluids. If the density of the high molecular weight fluid does not increase faster than its enthalpy drop relative to the low molecular weight fluids, the tradeoff could be the question of small multistage machinery relative to large single stage machinery. This brings up the question of fluid selection impact on machinery size.

To evaluate the effects of fluid on machinery size, we start with the assumptions that an optimum specific speed and specific diameter are used, and that the enthalpy drop and stress levels are within the limitations stated above. Thus, the machinery size is given by the specific diameter relation:

$$D_s = \frac{DH^{\frac{1}{4}}}{Q^2} \tag{8}$$

By using the definition of power and the continuity relation, we note that:

$$P = \dot{\omega} H \tag{9}$$

$$\dot{\omega} = \rho_3 Q \tag{10}$$

where:

P is power

$\dot{\omega}$ is mass flow

ρ_3 is the turbine exit density

Combining Equations 8, 9, and 10, we can express the relationship for the turbine diameter as follows:

$$D^2 = (PD_s^2) \frac{1}{\rho_3 H^{3/2}} \tag{11}$$

If we want to maintain the same power output and the same specific diameter, then the term PD_s^2 would be a constant. The enthalpy drop is given by either 3b or 5b, depending upon whether aerodynamics or mechanical stress is the limiting constraint. Thus, we can write:

$$D^2 = (PD_s^2) \frac{1}{\rho_3 (2400\ T/m)^{3/2}} \tag{12a}$$

or

$$D^2 = (PD_s^2) \frac{1}{\rho_3 (81{,}125)^{3/2}} \tag{12b}$$

The value of the density at the turbine exit is not readily identifiable in a general case, and does not lend itself to screening of fluids. We assume that the density at the turbine exit is approximated by the density of the saturated vapor at the condensing conditions:

$$\rho_3 \cong \rho_c$$

where:

ρ_c is the density of the saturated vapor at condensing conditions

This assumption introduces an error, since some of the fluids exit with considerable superheat. But this error is normally relatively small. In the worst case considered here, the difference in densities in butane is 93 percent, which results in only a 39 percent difference in turbine diameter. We can then determine the ratio of turbine diameter between two fluids by ignoring stress limitations and rewriting Equation 12a as follows:

$$\frac{D_1}{D_2} = \left(\frac{\rho c_2}{\rho c_1}\right)^{1/2} \left(\frac{T_2}{T_1}\right)^{3/4} \left(\frac{m_1}{m_2}\right)^{3/4} \qquad (13)$$

If we assume further that the turbine inlet temperature is the same for the two fluids, Equation 13 is reduced to:

$$\frac{D_1}{D_2} = \left(\frac{\rho c_2}{\rho c_1}\right)^{1/2} \left(\frac{m_1}{m_2}\right)^{3/4} \qquad (13a)$$

This relationship is shown in Table 6.

Examination of Figure 15 and Table 6 indicates that fluids such as butane and the fluorocarbons can be used with simple and small one stage machinery. Also implicit in these data is the fact that these fluids would be very desirable where relatively cold condensing temperatures are available, such as in air condensing in arctic or subarctic regions, and in areas where cold river water or low wet bulb temperatures are available.

2.4 Heat Transfer Considerations

There are two aspects of heat transfer as it relates to the selection of working fluids. The first aspect is the match between the working fluid enthalpy - temperature change relative to the heat source. For example, if a totally sensible heat source, such as hot gas, is available, it might be

desired that the working fluid have an enthalpy - temperature characteristic with very little latent heat. Or, if a totally sensible heat source, such as a condensing hydrocarbon, is available, it might be desired that the working fluid have an enthalpy - temperature characteristic with very little sensible heat and no superheat. The second aspect is the transport characteristics that will result in high heat transfer coefficients to reduce the heat exchanger area.

In this discussion, we shall consider only the selection of a working fluid with a sensible heat source, since it introduces a tradeoff between heat transfer and thermodynamics. The selection of a working fluid with a latent heat source is rather straightforward. Figure 17 illustrates three alternatives of working fluid enthalpy - temperature characteristics relative to a sensible heat source. Examination of Figure 17 produces some obvious, although not necessarily correct, conclusions. First, a working fluid that behaves as a sensible heat transfer results in the highest peak turbine inlet temperature for a given exit temperature of the heat source. The obvious conclusion is that such a fluid results in the maximum cycle efficiency. If a given turbine inlet temperature is specified, the working fluid with a sensible heat transfer characteristic can extract more heat from the heat source. In the extreme case where a minimum approach temperature is specified as the difference between the peak heat source temperature and the turbine inlet, any fluid with only latent heat transfer would be unable to extract any heat.

The problem with simplistic comparisons on heat transfer is that heat transfer and the cycle thermodynamics are very closely interrelated. A supercritical Rankine cycle that maximizes the heat flow from the sensible heat source can can also deviate most for a true Rankine cycle. An additional consideration is the tradeoff between the value of additional heat recovered from the heat source and the cost of the additional heat exchanger surface. This later point will be covered in Section 3.0. Here we shall illustrate the tradeoff between the heat transfer mode and cycle thermodynamics for the cycles considered in Section 2.3 (see Table 4).

Let us specify a heat source that has a total heat capacity of 10×10^6 Btu/hr between 700°F and 260°F. Now let us determine the heat that can be recovered by the cycles listed in Table 7 and the power that can be delivered by each

cycle. Figures 18 through 21 present the heat flow data in the form of temperature-heat flow plots. As can be seen in Table 7, the advantages, in terms of delivered power, between supercritical and non-supercritical cycle are not very significant or are non-existent. Also, trading thermodynamic efficiency for less recovered heat through regeneration produces little effect in the case of toluene and a negative effect for butane in terms of delivered power. Economically though, the tradeoff is in terms of heat exchanger surface, so that regeneration is economically attractive.

Another heat transfer consideration is the transport properties of the working fluid to increase the effective heat transfer coefficient. In practice, this has little effect on the design of an evaporator with a hot gas source. The heat transfer in a heat exchanger involves heat transfer at the wall on both the hot and cold sides, and through the wall as shown in Figure 22. The overall heat transfer coefficient is given by the relation [27]:

$$\frac{1}{h_o} = \frac{1}{h_h} + \frac{\tau}{k} + \frac{1}{h_c} \qquad (14)$$

where:

h_o is the overall heat transfer coefficient

h_h is the hot side heat transfer coefficient

h_c is the cold side heat transfer coefficient

τ is the wall thickness

k is the thermal conductivity of the wall

For typical steel piping, the value of $k/\tau \cong 3500$ Btu/hr/ft^2 °F. Typical values for h_h in gas side equipment range from 5 to 15 hr/ft^2 °F and the average is 10. If we insert these values into Equation 14, we get:

$$\frac{1}{h_o} = .10028 + \frac{1}{h_c} \qquad (14a)$$

Table 8 presents the effect of the heat transfer coefficient of the working fluid on the overall heat transfer coefficient. As can be seen, a two order magnitude change in the heat transfer coefficient of the working fluid changes the overall heat transfer coefficient of the evaporator by less than 10 percent.

The effect on the condenser is more sizable. Here, the heat transfer coefficient of water in the condenser tubes is of the order of 1000 Btu/hr ft^2 °F. This results in Equation 14, expressed as:

$$\frac{1}{h_o} = .00128 + \frac{1}{h_h} \tag{14b}$$

where the working fluid is the hot side heat transfer coefficient. Table 8 presents values for the overall heat transfer coefficient as a function of various working fluid heat transfer coefficients. As can be seen, the impact on heat transfer in the condenser can be changed by a factor of 5 with a factor of 10 change in the heat transfer coefficient of the working fluid from 100 to 1000. After the heat transfer coefficient of the working fluid exceeds that of the condensing medium, the changes are less spectacular.

Because of its importance, the heat transfer coefficient in the condenser should be a consideration in fluid selection. The heat transfer coefficient of a condensing medium [28, 29, 30] is given by:

$$h = a\left[\frac{1}{G}\right]^{1/3}\left[\frac{k^3\rho_1}{\mu}\right]^{1/3} \tag{15}$$

where:

a is a constant

G is a loading factor for the heat exchanger, mass flow of condensate per unit length of tubing

ρ_1 is the density of the liquid condensate

For most fluids under consideration, the loading and density will be approximately the same. Thus, any variations in the condensing heat transfer coefficent will be given by:

$$h \propto k/\mu^{1/3} \qquad (16)$$

Values of thermal conductivity and viscosity and the ratio given in Equation 16 are presented in Table 9. Table 9 shows that relative values of the heat transfer coefficient might vary by a factor of 7 from a fluorocarbon to water.

The implication of the comparison in Table 9 is that a considerable savings can be made in the condenser cost by using a fluid with higher heat transfer coefficients.

Let us assume that we have two fluids, one with a condensing coefficient of 150 Bth/hr ft^2 °F (which is typical of the fluorocarbons and butane), and another with a condensing coefficient of 1200 Btu/hr ft^2 °F (which is typical of steam). Applying Equation 14b, we note in Table 10 that the overall heat transfer coefficients differ by a factor of three. This implies that the condensing surface area would differ by a factor of four. However, the fluids have different thermodynamic efficiencies. For example, in Table 5, the cycle efficiency of the steam cycle is 27.4 percent and the binary cycle with a condensing flourocarbon is 37.5 percent. This means that the steam cycle rejects 37 percent more heat per unit output than the binary cycle, and that the steam cycle will need 37 percent more condenser surface per unit output. Combining these two factors, we see in Table 10 that only a factor of three reduction in surface area results per unit output. This would seem to be a significant factor. However, we must examine the impact of this change on cost per unit output. The condenser costs in systems where there is water condensing in shell and tube heat exchangers typically account for about 12 percent of the total machinery cost. Thus, at best, the selection of steam over a fluorocarbon, for example, will result in 6.6 percent reduction in the cost per unit output, assuming everything else is constant. There is, however, a problem in that heat exchanger surface cost is not a linear function. Figure 23 shows the variation in heat exchanger cost per unit area (see Reference 31). A nominal 3 megawatt system has a surface area

of about 24,000 ft^2. Referring to Figure 23, a factor of three reduction in surface area means that each square foot of surface in an 8000 ft^2 condenser costs 6 to 10 percent more than that in a 24,000 ft^2 condenser. Applying this factor to adjust overall savings, we see in Table 10 that a factor of ten change in a fluid's heat property results in only 5 to 6 percent change in the overall system cost. Such a change can be totally obscured by other cost considerations.

A final observation is that the above considerations have totally ignored the application of fouling factors which will reduce even further the differences between fluids.

No generalized conclusions can be made for the heat transfer characteristics of the working fluid. The selection must involve an engineering tradeoff among thermodynamic efficiency, the match to the heat source, heat transfer coefficients, and heat exchanger cost. Some of this system tradeoff is presented in later sections.

2.5 Fluid Stability

All the organic fluids are unstable at high temperatures and will decompose over time. The rates of decomposition for the fluid vary. The fluorocarbons are the most sensitive, and the hydrocarbons the least sensitive. The decomposition rates for R-11 and R-114 are shown in Figure 24. In fluid selection, care must be taken to consider not only the thermal decomposition of the pure fluid, but also the effects of various materials and contaminants upon fluid stability. For example, the presence of oil in R-11 greatly accelerates its decomposition.

2.6 Fluid Safety

The effects of perceived risk in fluid selection have been discussed previously. From an engineering consideration, it is necessary to know the actual risk associated with the fluid, and to provide the appropriate safe design practices as are specified by the various codes. There are two types of safety problems: fluid toxity and fluid flammability. Some of the design considerations are applicable to both safety problems.

The major problem with both types of hazards is system leakage. Seals, flanges, and valves are perennial sources of leaks. Thus, a system design should try to minimize or, if possible, eliminate all seals, flanges and valve stem penetrations. The hermetric design typical of small sized refrigeration and air conditioning equipment is the ultimate design goal. Also, the system design must take into account the need for rupture disks, relief valves and system purges. With a flammable fluid it would make very little sense to comply with a boiler code by providing a relief valve if the relief valve exhausts into an area where there is an ignition source. Thus, the system design must also include either the capture or safe disposition of the working fluid in emergency, or planned release of the fluid.

Having designed the system to minimize leakage potential, sensors connected to automatic purge or fire supression equipment are also necessary.

While none of the fluids considered here are classified as toxic, both butane and toluene are flammable and would require safety provisions.

2.7 Fluid Cost and Availability

From the user's perspective, the cost of a Rankine cycle includes normal maintanance costs as well as considerations for major repairs. The cost of the working fluid and its availability affect the cost of ownership of a Rankine system in two ways. The first is simply the cost associated with system make-up or refill. The second is lost time due to the unavailability of the working fluid. This latter factor can have significant economic impact if an industrial plant's production output is tied to a Rankine cycle. While a low cost, readily available fluid (like water) is desired, a higher cost, readily available fluid would be acceptable if overall system economics justified the selection. High cost, low availability fluids will need a strong justification.

FLUID SELECTION CRITERIA

- Thermodynamics
- Fluid Machinery
- Heat Transfer
- Fluid Stability

FLUID SAFETY

- Fluid Cost
- User Acceptability

USER ACCEPTANCE

PERCEIVED RISK
VERSUS
ACTUAL RISK

78P79

WORKING FLUID

THERMODYNAMICS

78P79

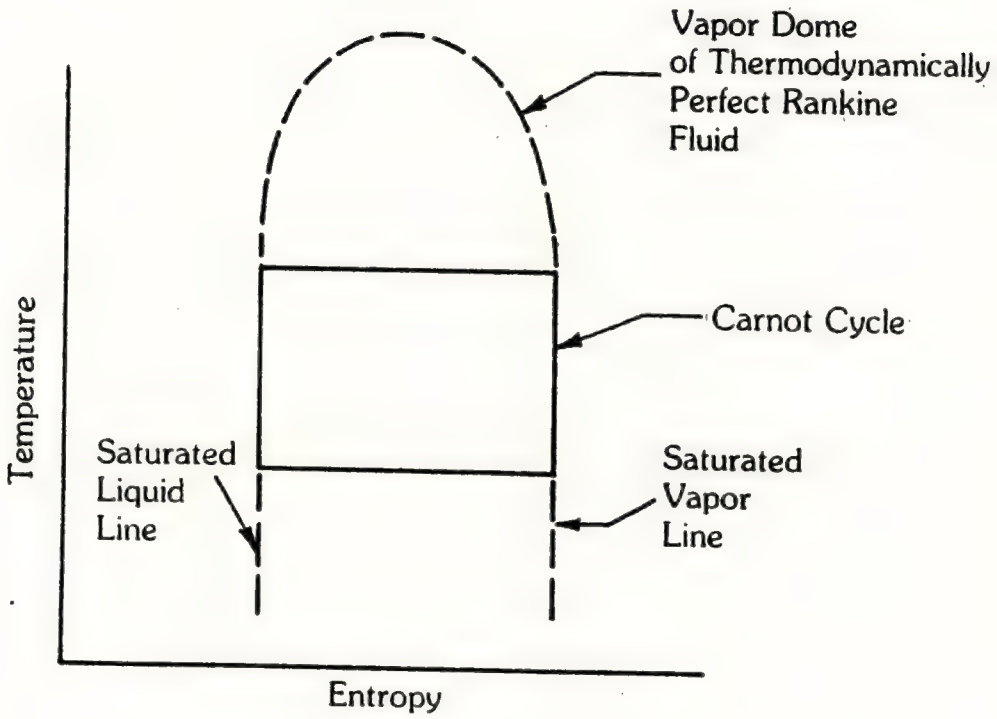

Figure 5 A Thermodynamically Perfect Rankine Fluid Duplicates a Carnot Cycle

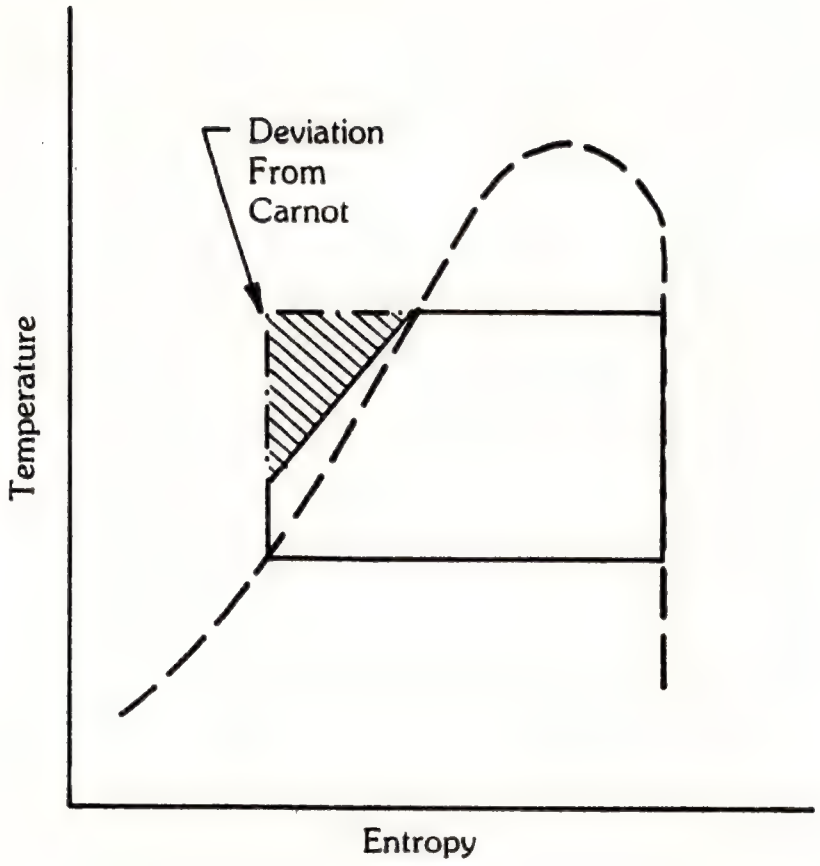

Figure 6 Illustration of a Rankine Cycle with an Isentropic Fluid

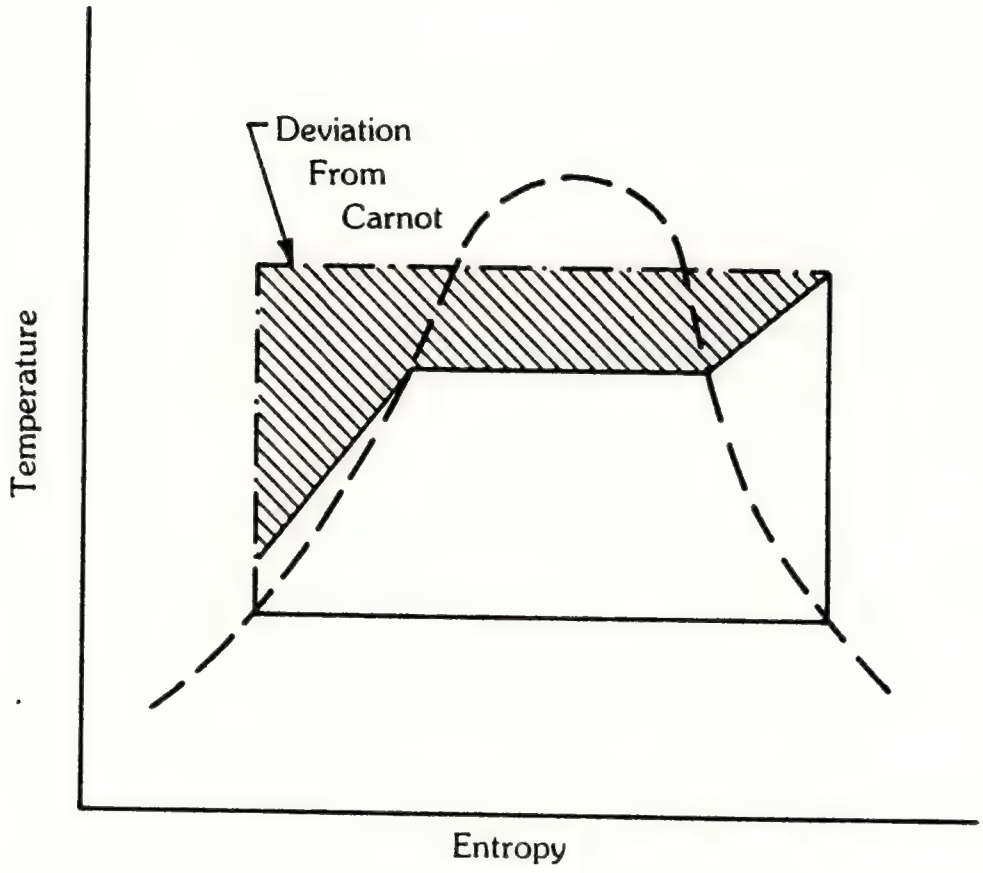

Figure 7 Illustration of a Rankine Cycle with a Wetting Fluid

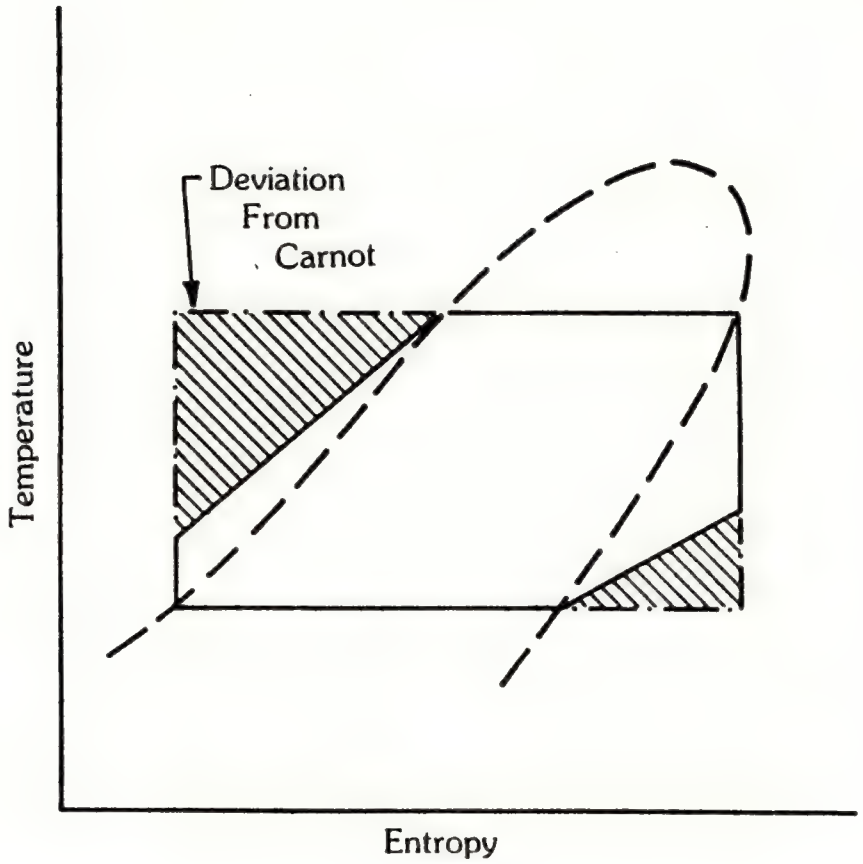

Figure 8 Illustration of a Rankine Cycle with a Drying Fluid

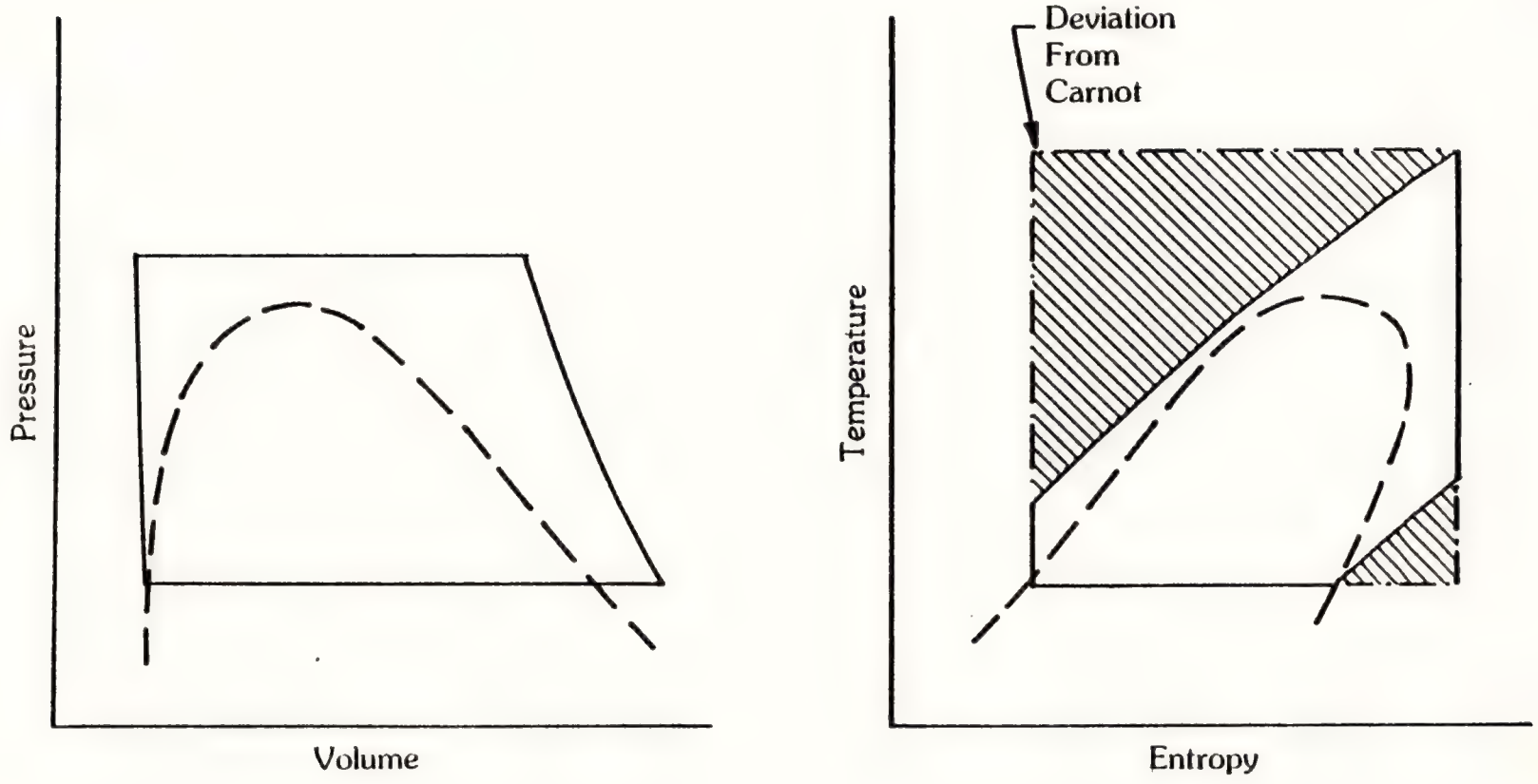

Figure 9 Illustration of a Supercritical Rankine Cycle

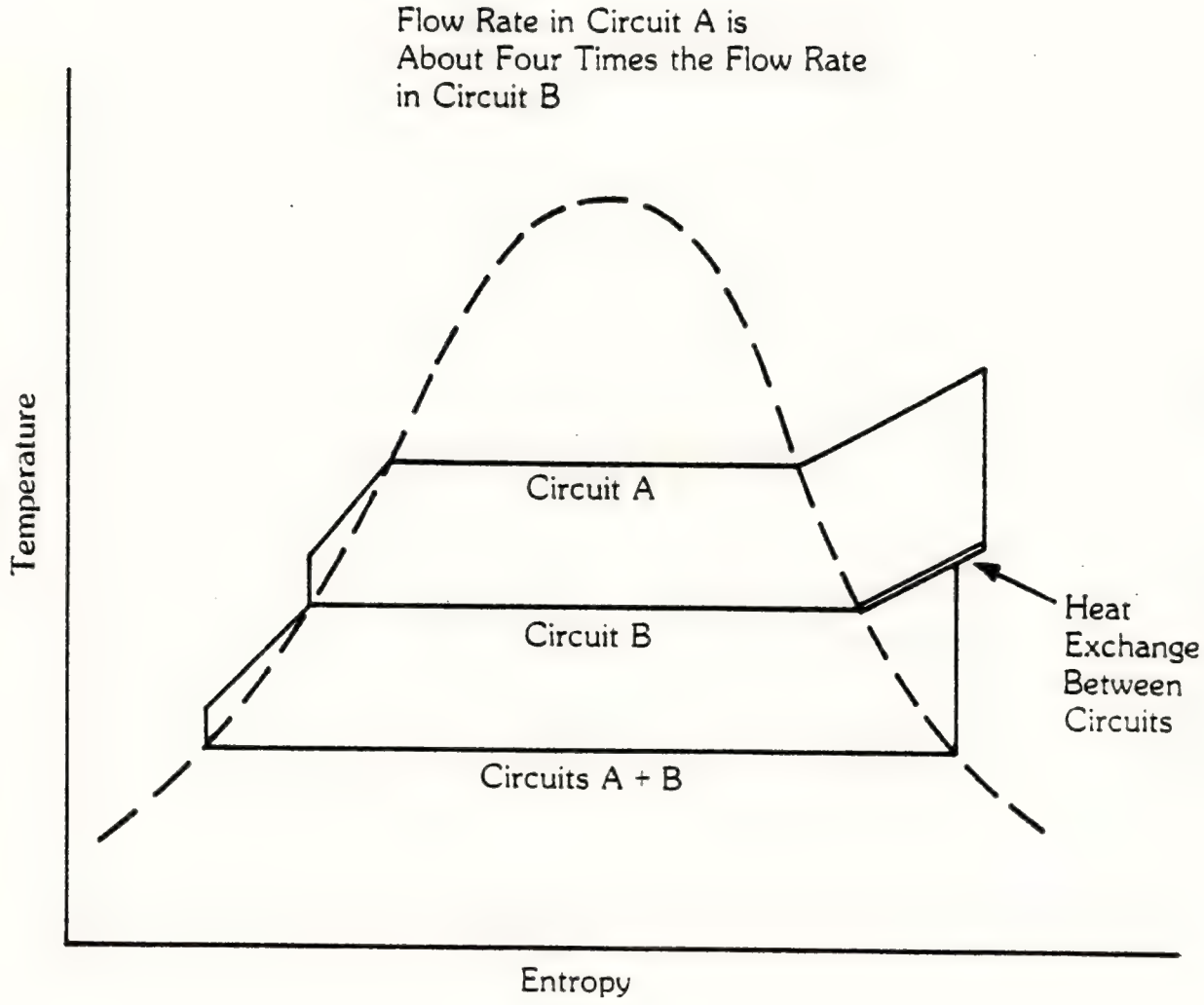

Figure 10 Temperature-Entropy Diagram of a Two Level Steam System Presented in Reference 18

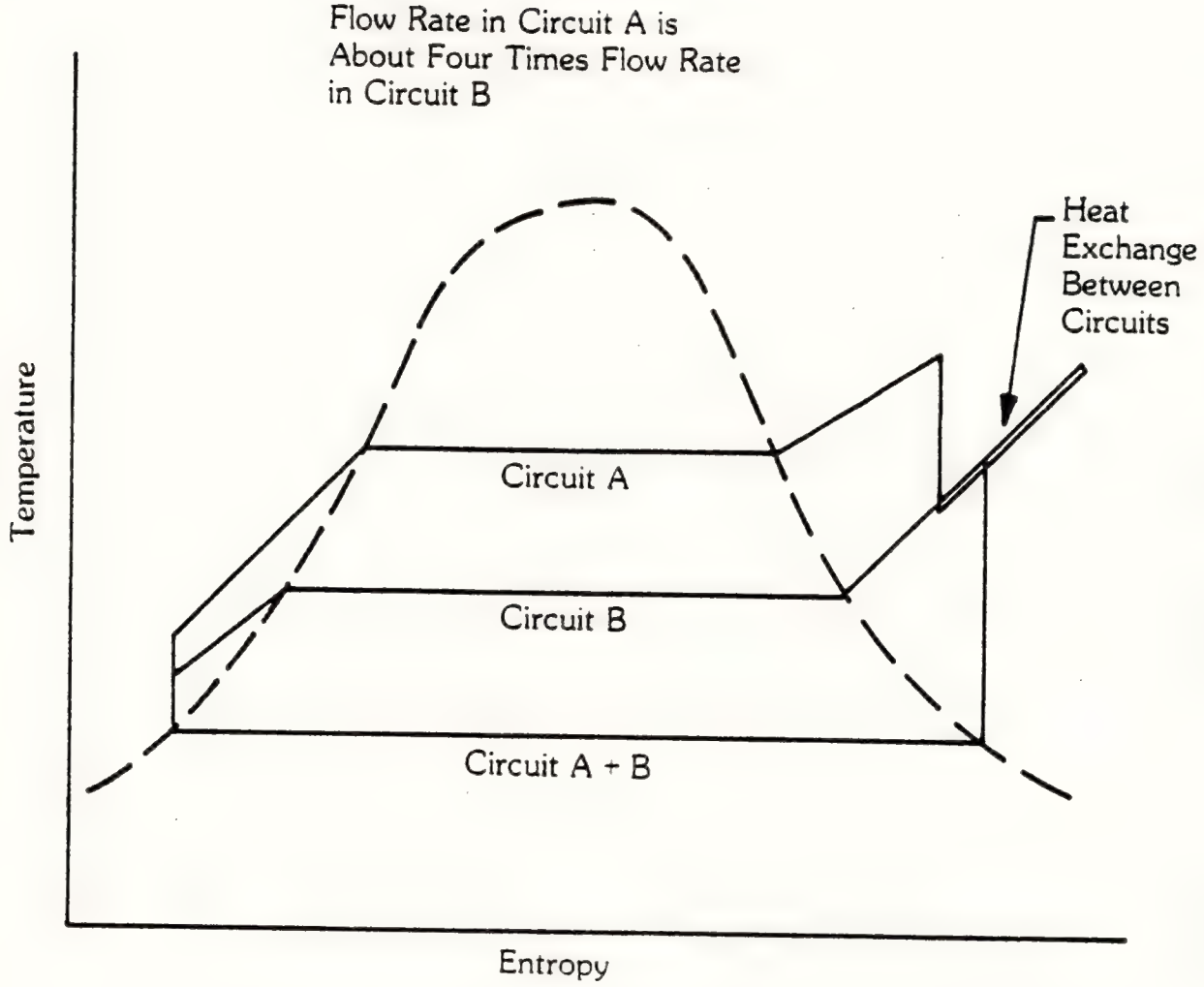

Figure 11 Temperature Entropy Diagram of a Two Level Steam System Presented in Reference 6

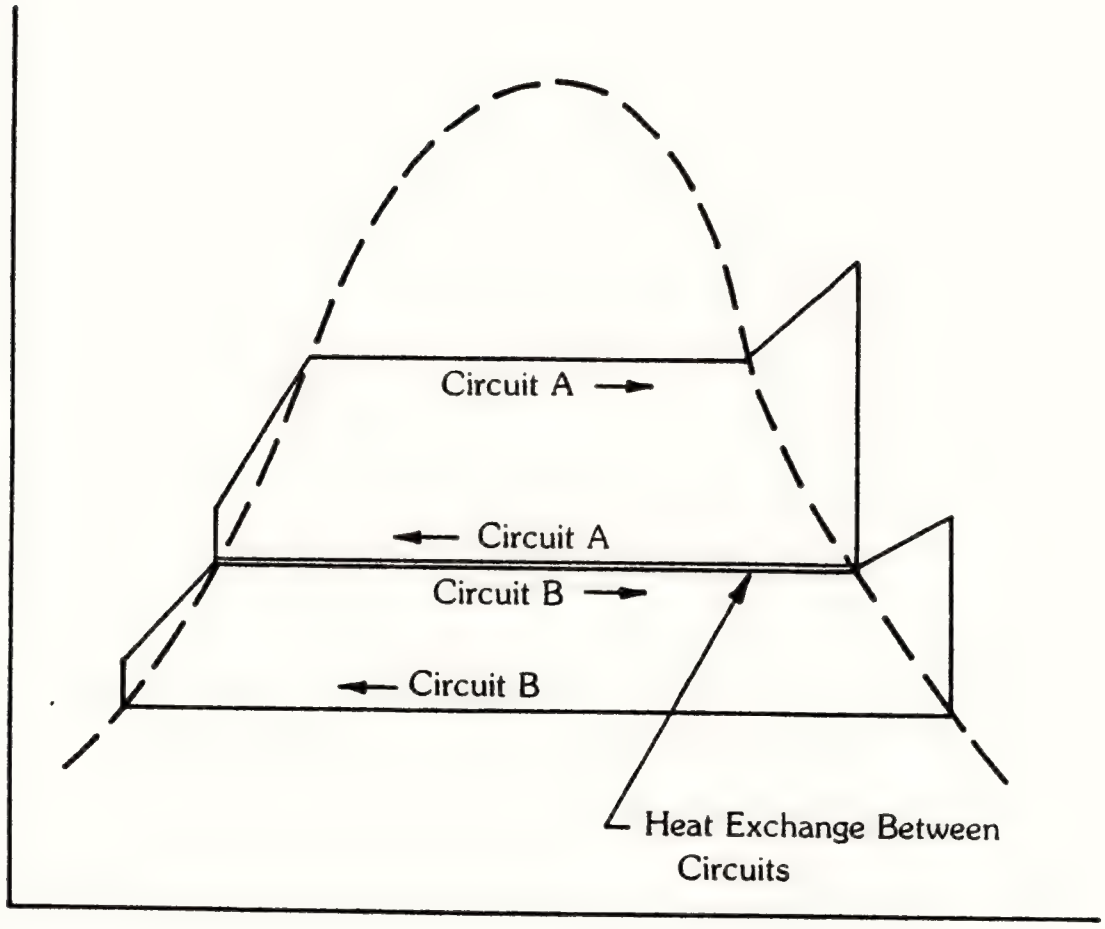

Figure 12 Temperature Entropy Diagram of a Two Level Steam System

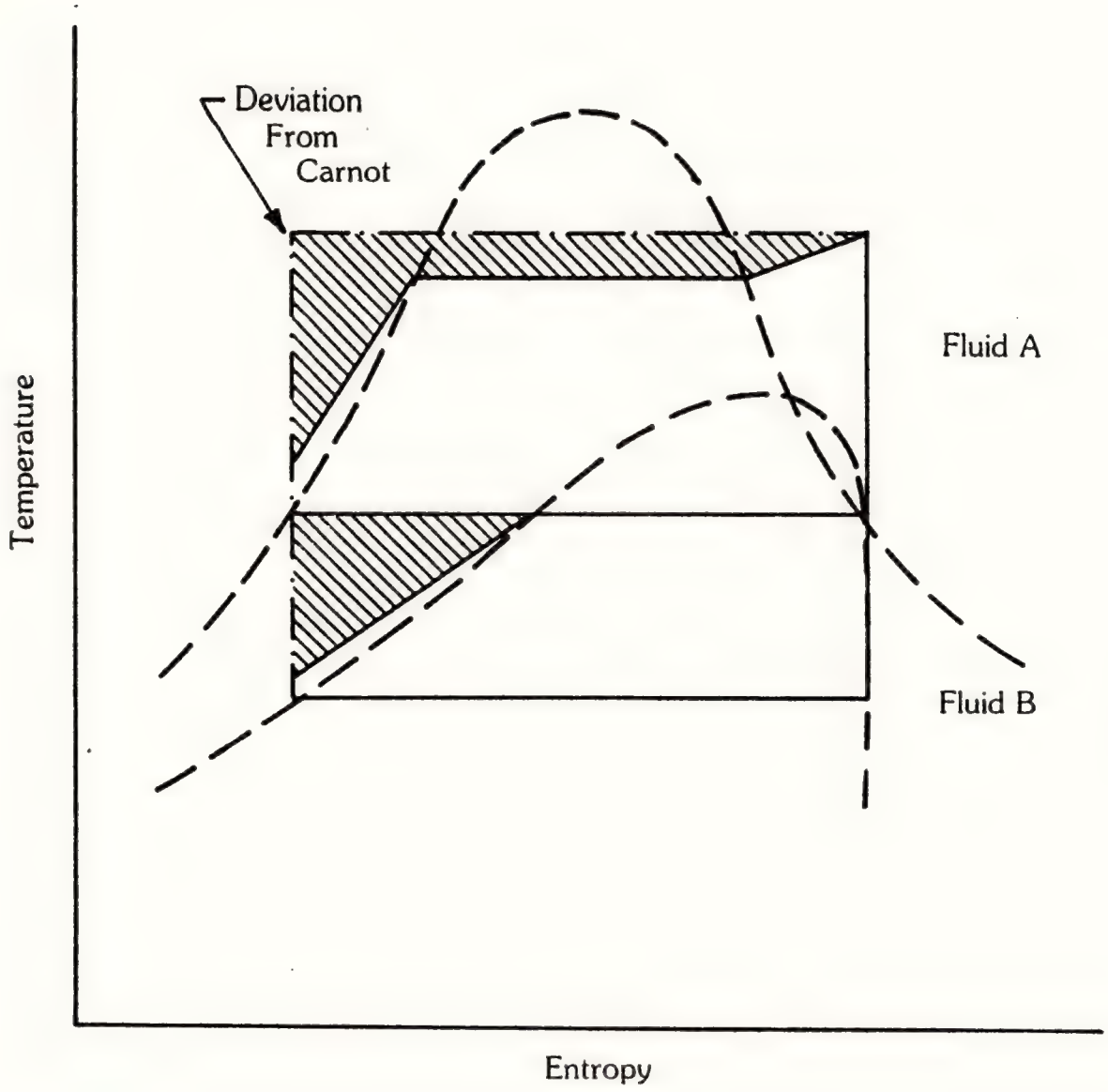

Figure 13 Temperature Entropy Diagram of a Binary Steam and Organic Cycle

TABLE 4

CYCLE POINTS FOR DETERMINATION OF WORKING FLUID THERMODYNAMIC EFFICIENCY WITH IDEAL HARDWARE

FLUID/CYCLE	TURBINE INLET 650°F		TURBINE EXIT			CONDENSER 100°F		
	PRESS.	ENTHALPY	TEMP.	PRESS.	ENTHALPY	PRESS.	ENTHALPY VAPOR	ENTHALPY LIQUID
Steam (Dry) Steam (Wet)	16 87	1358.9 1354.7	100 100	0.949 0.949	1105.2 1001.1	0.949 0.949	1105.2 1105.2	67.9 67.9
Fluorinol-85	700	378.0	275	3.2	277.0	3.2	218.9	30.3
Butane	600	-283.3	500	51.4	-370.0	51.4	-587.5	-737.7
Toluene	300	215.7	296	1.04	95.9	1.04	17.8	-155.1
Binary — Steam (Dry)	340	1339.2	300	67.0	1179.7	67 / 300°F	1179.7	269.6
Binary — Steam (Wet)	825	1304.0	300	67.0	1088.6	67 / 300°F	1179.7	269.6
Binary — R-113	176.5 / 300°F	120.1	146	10.5	100.8	10.5	93.4	29.0

TABLE 5

COMPARISON OF WORKING FLUID PERFORMANCE

WORKING FLUID	EFFICIENCY %	% OF CARNOT
Carnot	49.5	-
Steam (Dry)	19.6	39.6
Steam (10% wet isentropically)	27.4	55.4
Fluorinol-85	28.5* (36.6)	57.6
Butane	29.04* (34.9)	58.7
Toluene	32.3* (46.6)	65.3
Binary Steam/R-113** (Dry)	32.9	66.5
Binary Steam/R-113 (Wet)	37.5	75.8

* Without any regeneration, efficiency in parentheses assumes 100% effective regeneration.

** The relative flow between R-113 and the steam is 9.98 R-113 to steam in the dry expansion and 8.93 R-113 to steam in the wet expansion.

MACHINERY

CONSIDERATIONS

78P79

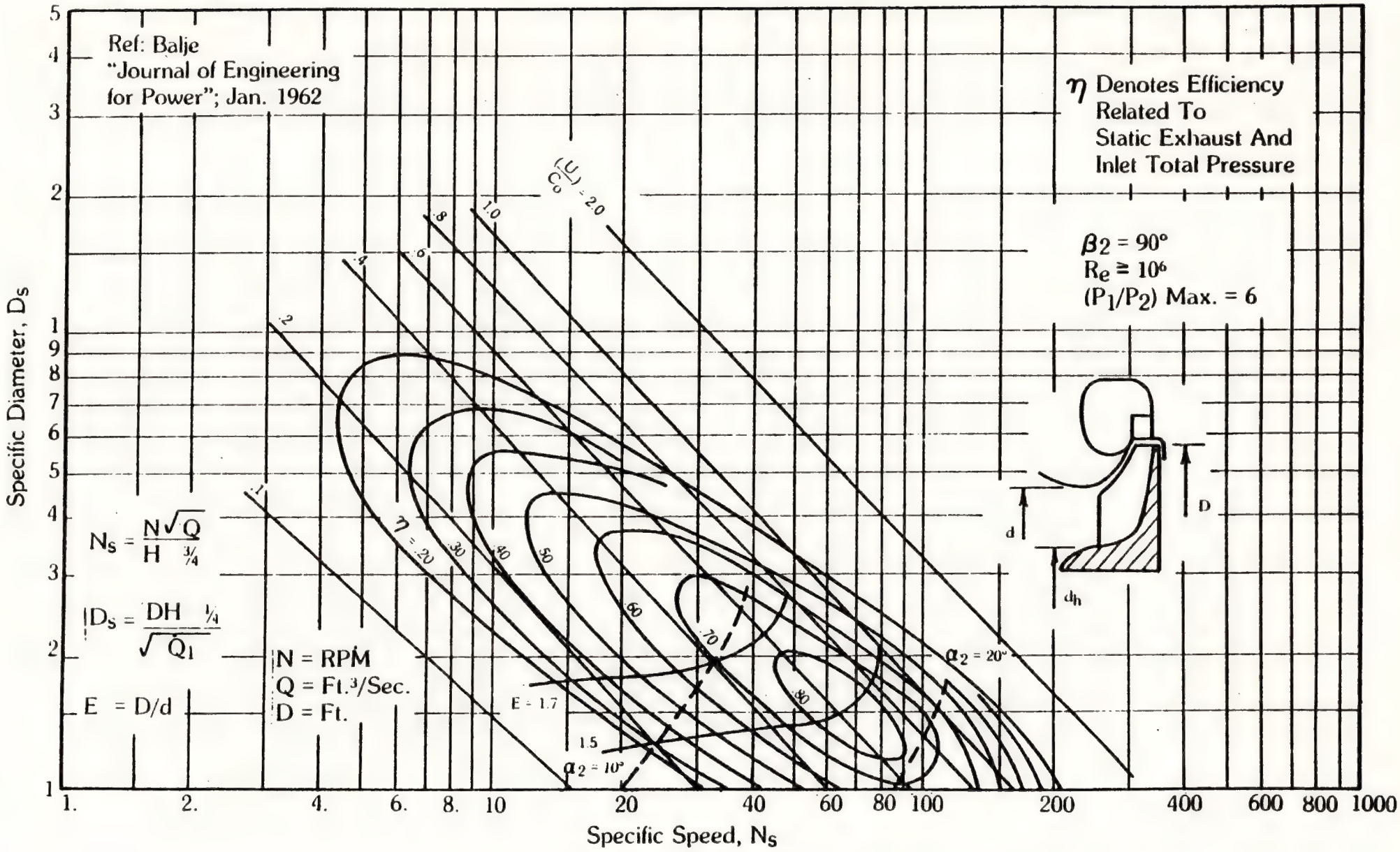

Figure 14 Performance Map For a Single Stage Radial Inflow Turbine

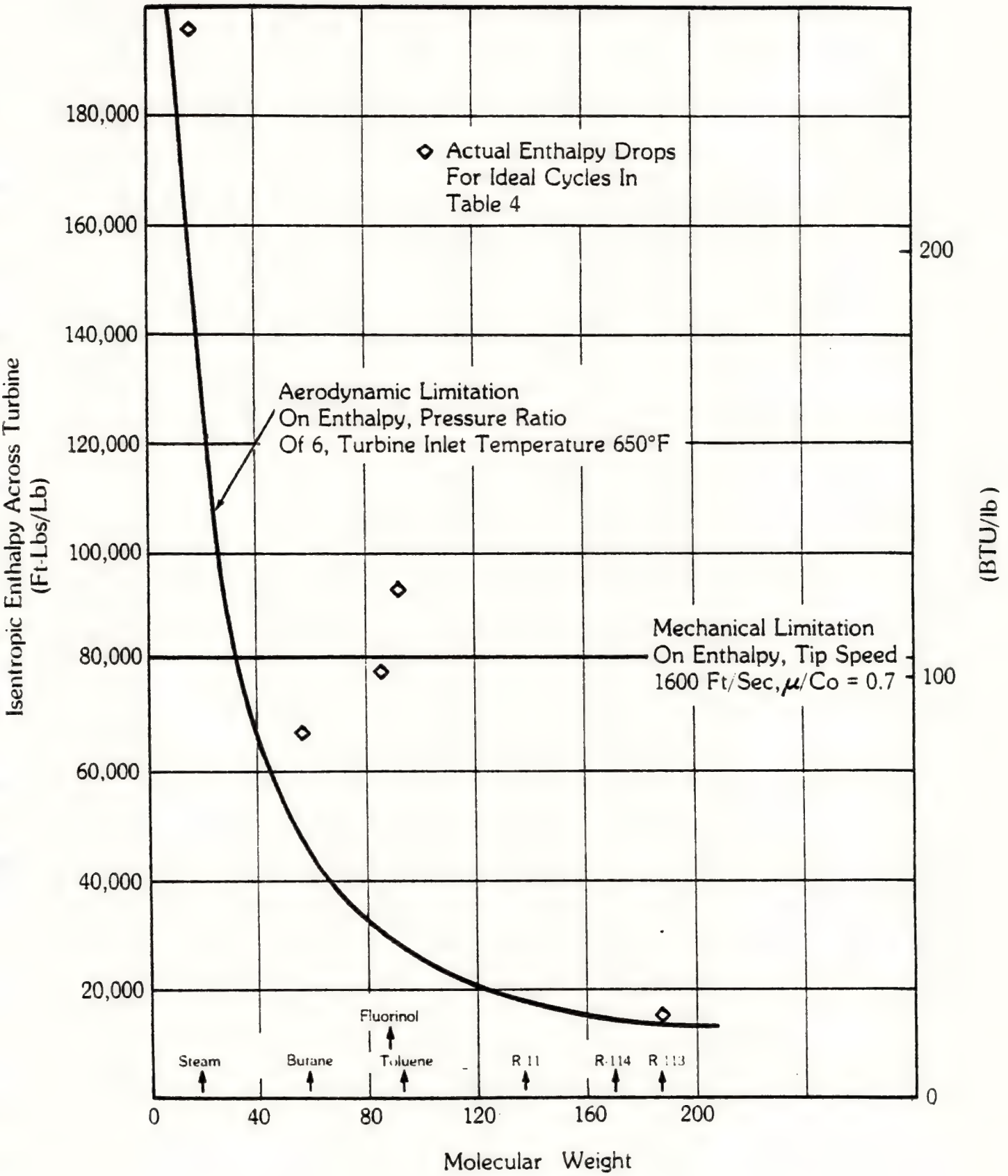

Figure 15 Comparison of Allowable Enthalpy Drops
For Different Fluids

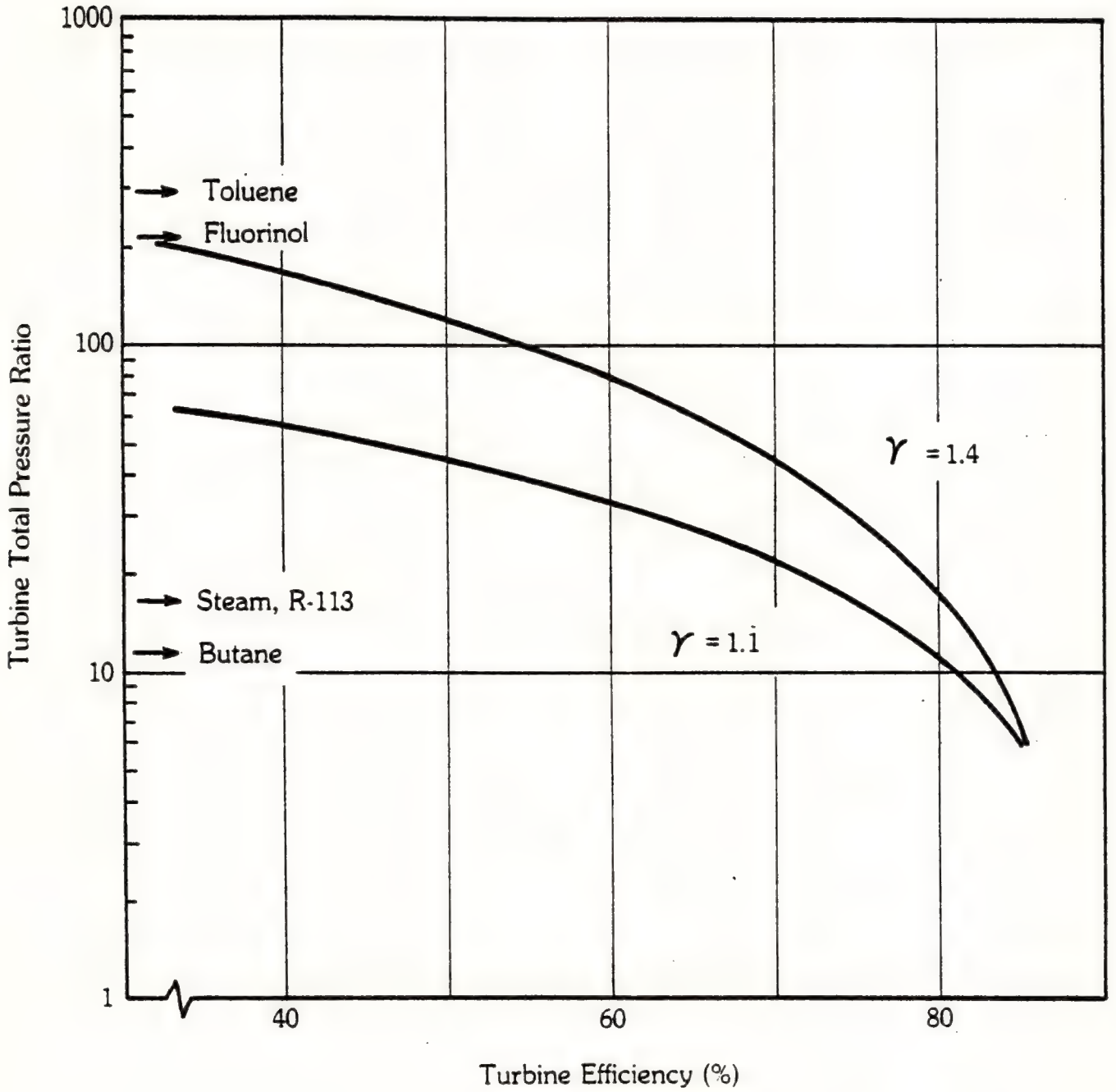

Figure 16 Effect of Pressure Ratio on Turbine Efficiency

TABLE 6

COMPARISON FLUID SELECTION ON TURBINE SIZE

FLUID	MOLECULAR WEIGHT	DENSITY AT CONDENSING CONDITIONS OF 100°F (lb/ft^3)	RATIO OF DIAMETERS
Water	18.0	2.85×10^{-3}	1.00
Butane	58.1	0.555	0.172
Fluorinol-85	87.7	4.67×10^{-2}	0.810
Toluene	92.1	1.60×10^{-2}	1.435
R-11	137.4	.566	0.325
R-114	170.9	1.437	0.241

HEAT TRANSFER CONSIDERATIONS

- **Enthalpy Temperature Consideration**
- **Transport Properties**

78P79

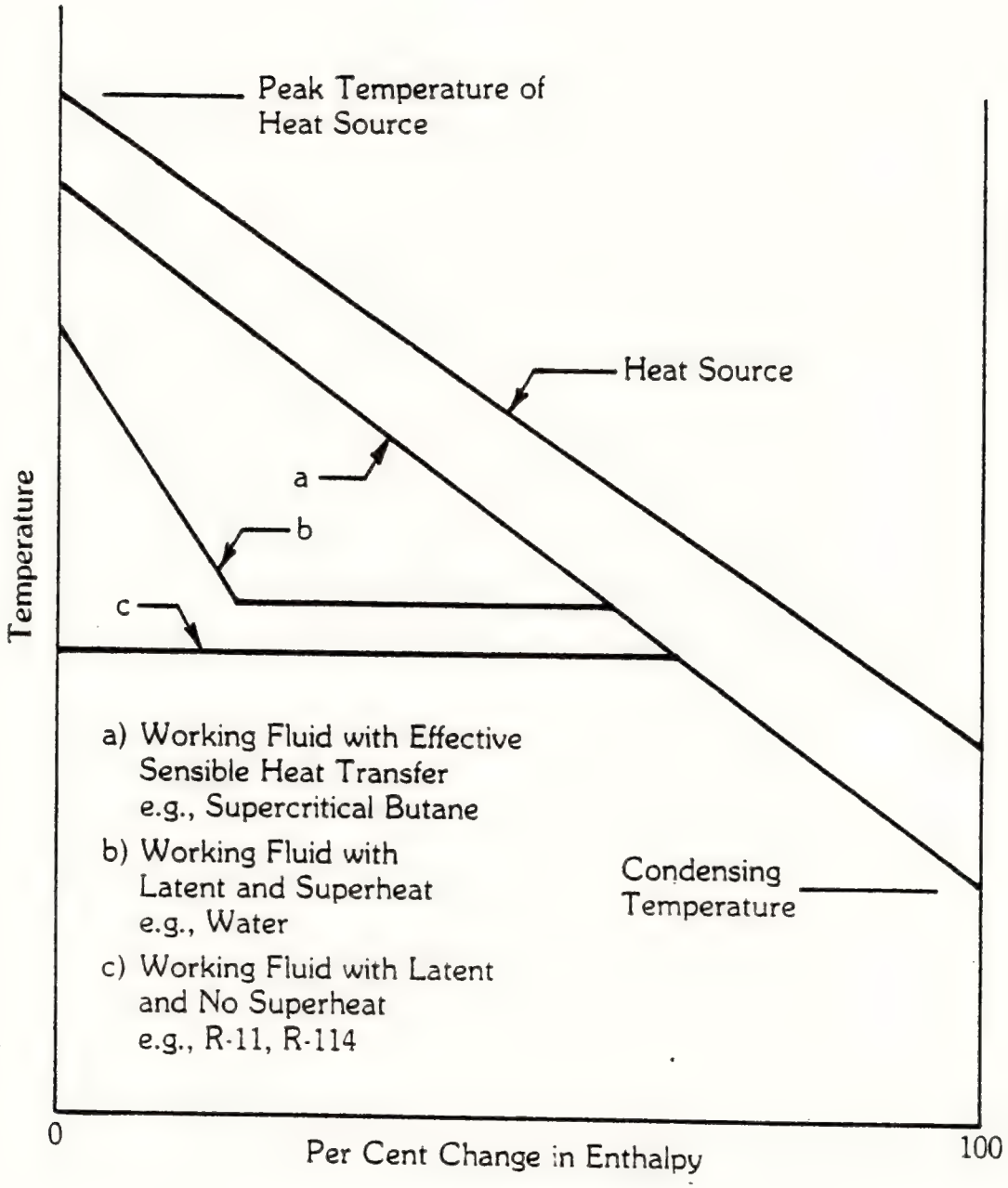

Figure 17 Illustration of Three Working Fluid Enthalpy-Temperature Characteristics

TABLE 7

THE COMBINED EFFECT OF HEAT TRANSFER AND THERMODYNAMICS ON DELIVERED POWER

FLUID CYCLE	TURBINE INLET		TURBINE EXIT		CONDENSER EXIT		HEAT RECOVERED Btu/hr)	FLUID FLOW (lb/hr)	CYCLE EFFICIENCY	DELIVERED POWER (kw)
	TEMP.	ENTHALPY	TEMP.	ENTHALPY	TEMP.	ENTHALPY				
Steam	650	1358.9	100	1105.2	100	67.9	10×10^6	7,746	19.6 27.4	574 802
Fluorinol-85	650	378.0	275	277.0	100	30.3				
Unregenerated							10×10^6	28,802	28.5	835
Regenerated							10×10^6	34,590	36.6	1072
Butane (Supercritical)	650	-283.3	500	-370.0	100	-737.7				
Unregenerated							10×10^6	22,007	29.04	850
Regenerated							7.3×10^6	30,725	34.9	746
Toluene	650	215.7	297	95.8	100	-155.1				
Unregenerated							10×10^6	25,743	32.3	946
Regenerated							7.3×10^6	24,838	46.6	997
Binary Steam/R-113	650	1339.2	300	1179.7	300	269.6	6.8×10^6	6,374	32.9	655

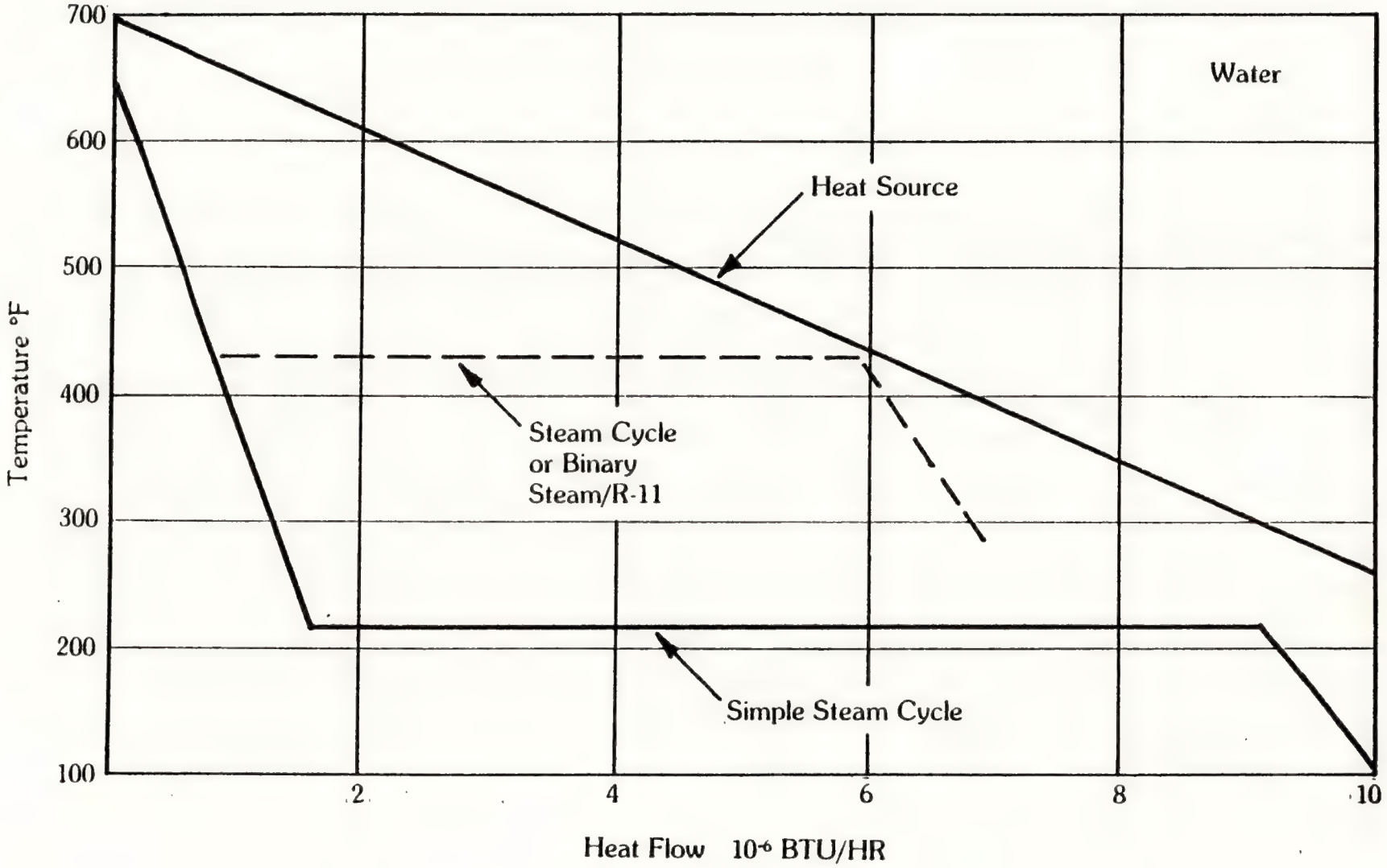

Figure 18 Temperature-Heat Flow for Water

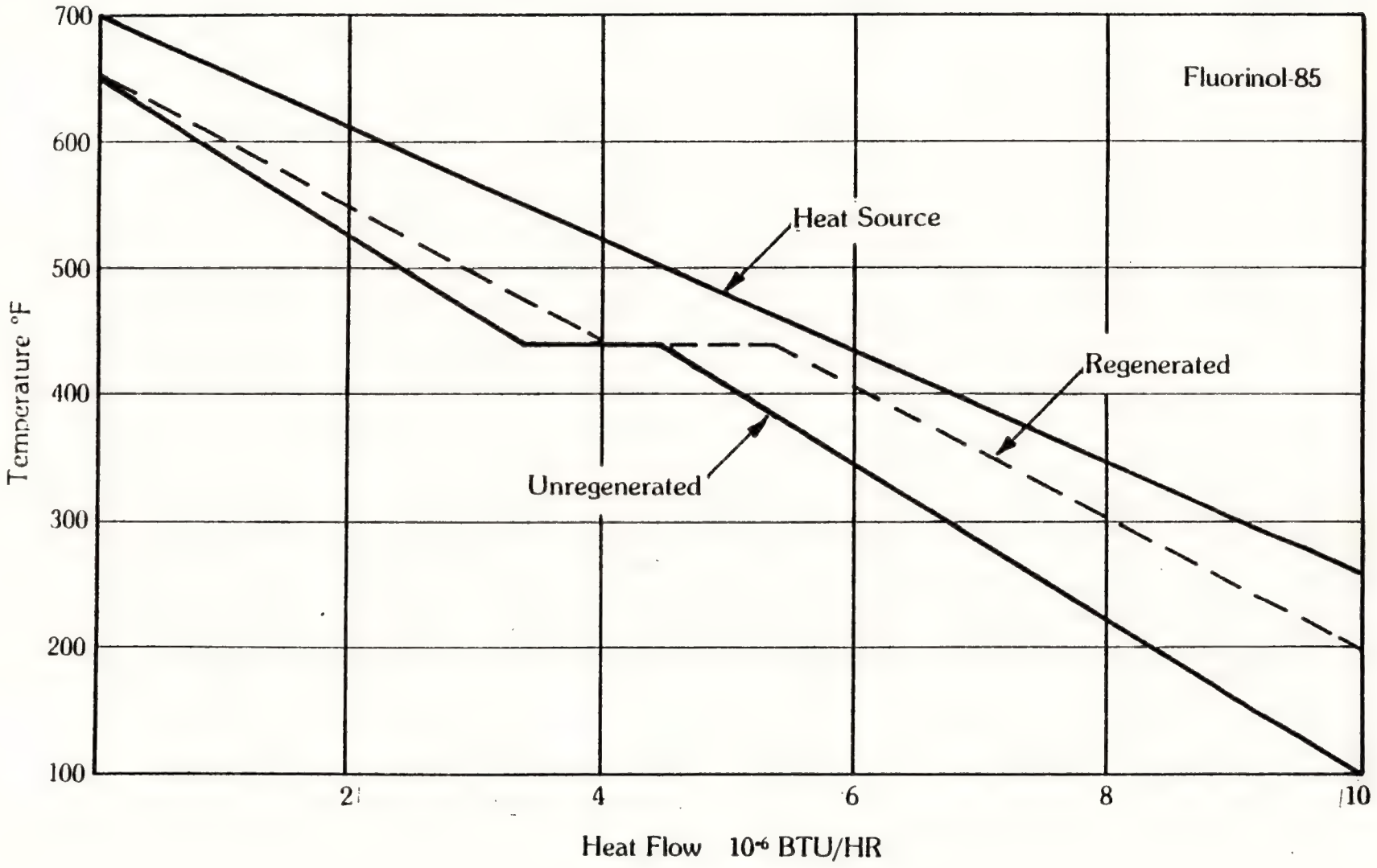

Figure 19 Temperature-Heat Flow for Fluorinol-85

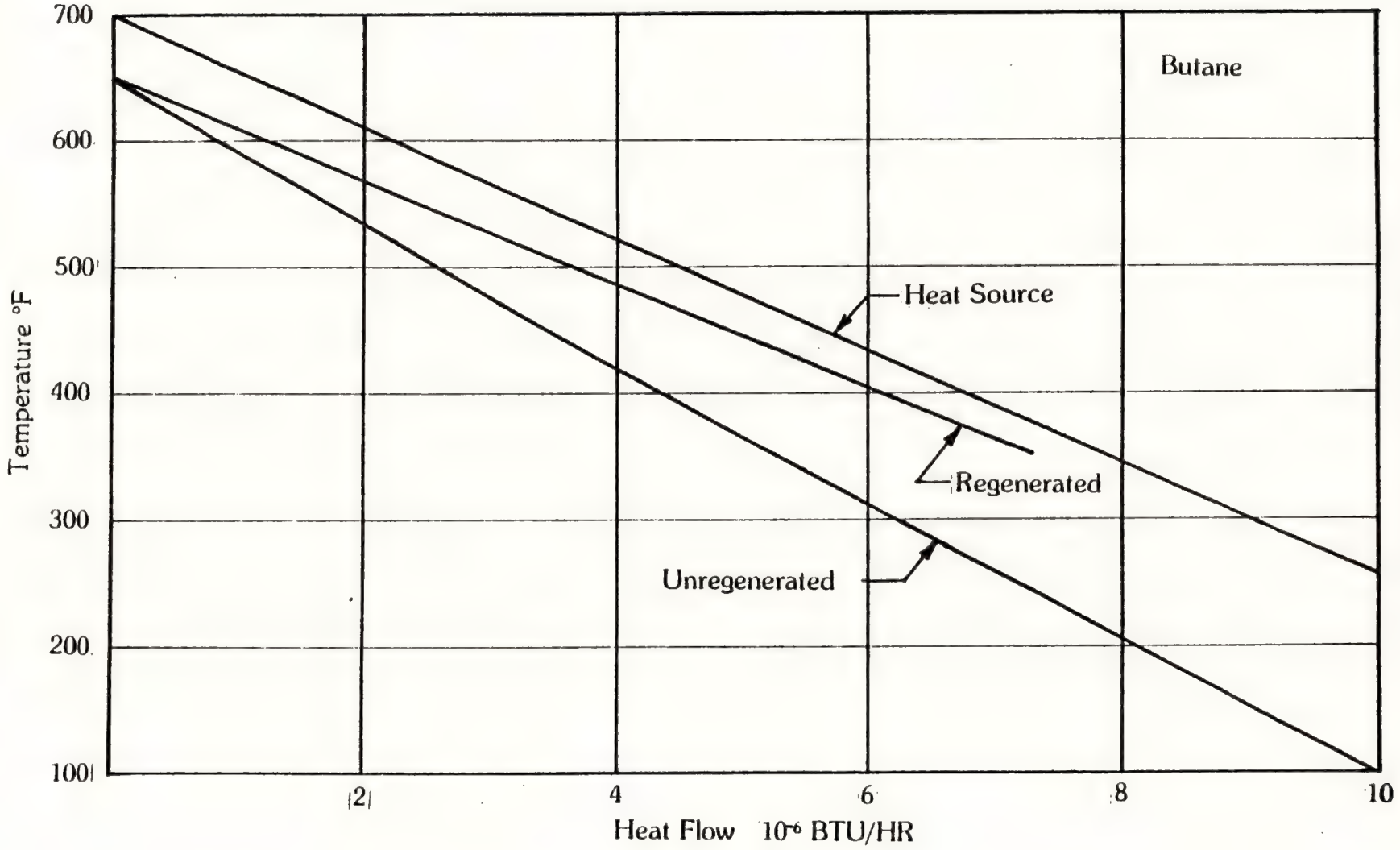

Figure 20 Temperature-Heat Flow for Butane

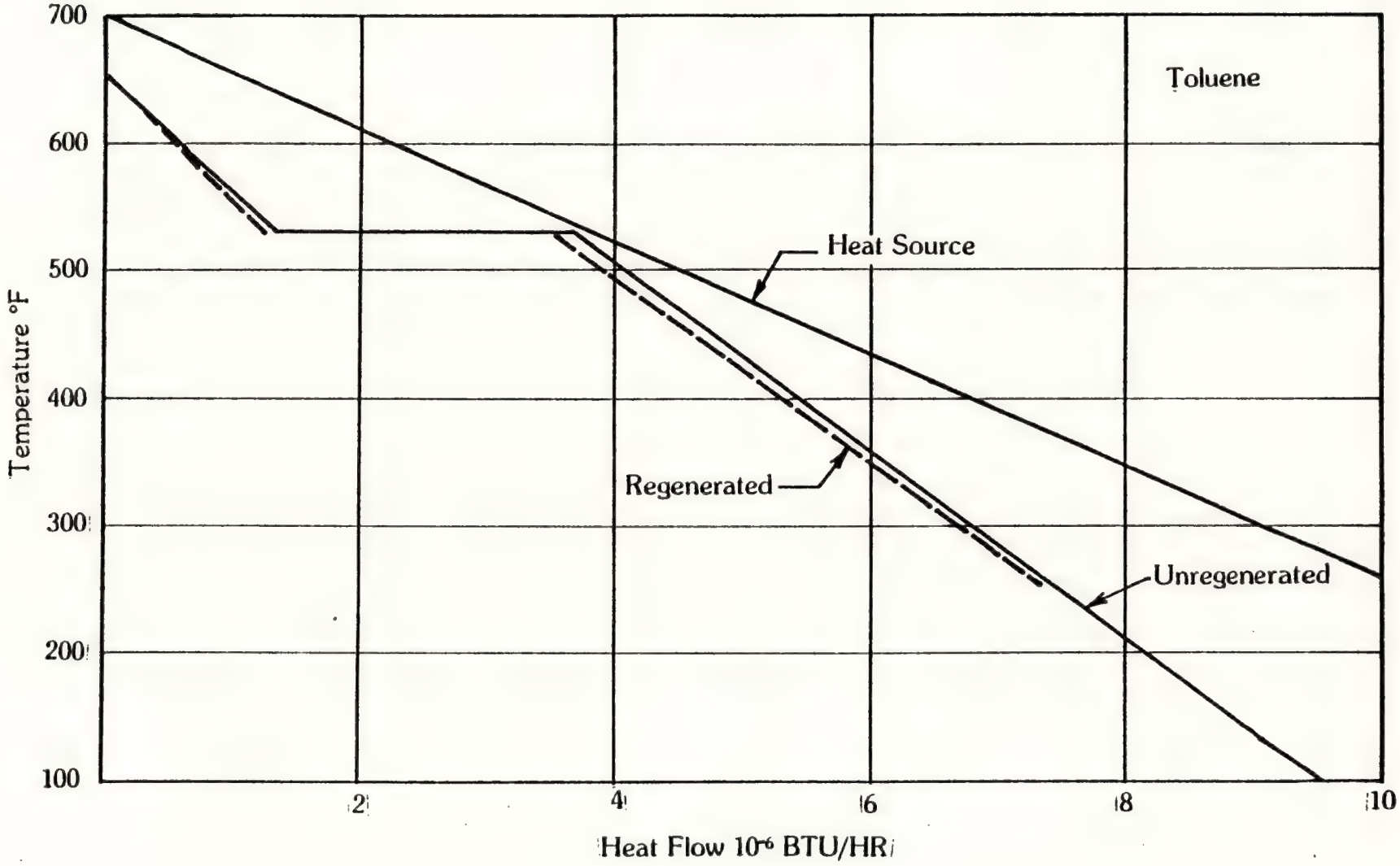

Figure 21 Temperature-Heat Flow for Toluene

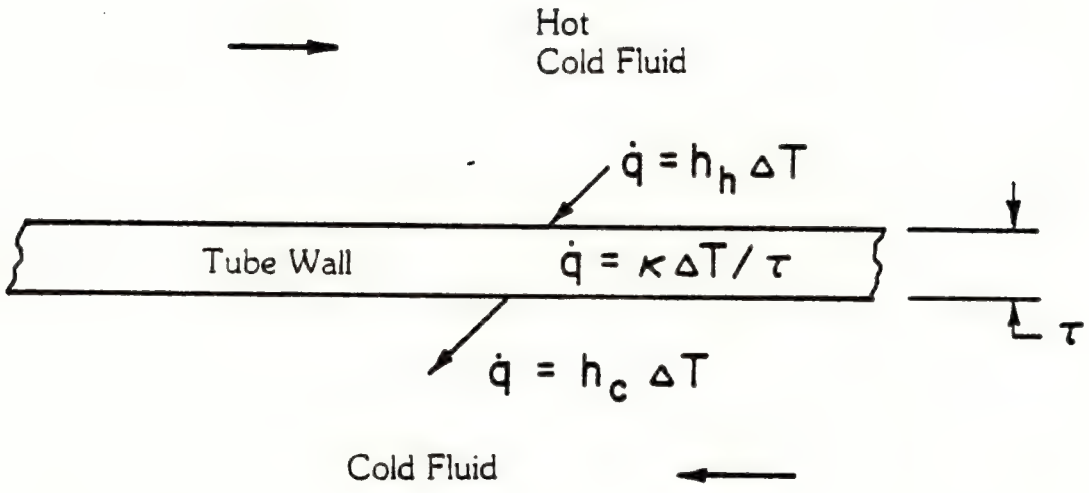

Overall Heat Transfer

$$\dot{q} = h_o \Delta T$$

Where $$\frac{1}{h_o} = \frac{1}{h_h} + \frac{\tau}{\kappa} + \frac{1}{h_c}$$

Figure 22 Illustration of Heat Transfer
In a Heat Exchanger

TABLE 8

OVERALL HEAT TRANSFER COEFFICIENT

HEAT TRANSFER COEFFICIENT OF WORKING FLUID	HEAT TRANSFER COEFFICIENT OF SOURCE OR SINK FLUID	
	AIR (h = 10)	WATER (h = 1000)
100	9.06	88
200	9.49	159
1,000	9.87	438
2,000	9.92	562
10,000	9.96	724

TABLE 9

COMPARISON OF TRANSPORT PROPERTIES OF WORKING FLUIDS AND THEIR EFFECT ON CONDENSING HEAT TRANSFER COEFFICIENT

Fluid	Thermal Conductivity (Btu/ft/hr)	Viscosity (Lb_m/ft^2 hr)	Ratio of Condensing Heat Transfer Coefficient
R-11	0.049	0.97	1.00
R-114	0.033	0.86	0.70
Butane	0.09	0.36	1.29
Toluene	0.080	1.18	1.53
Fluorinol-85	0.071	2.27	1.09
Water	0.364	1.53	6.38

TABLE 10

EFFECT OF CONDENSING HEAT TRANSFER COEFFICIENT
ON SYSTEM COST PER UNIT OUTPUT

Fluid Condensing Coefficient (Btu/hr ft^2 °F)	Overall Heat Transfer (Btu/hr ft^2 °F)	Thermodynamic Efficiency	Relative Surface Area Per Unit Output	Unadjusted Change in Cost Per Unit Output	Heat Transfer Surface Area Unit Cost Factor	Actual Change in Cost Per Unit Output
150	125	37.5% [1]	1.00	-	1.00	-
1200	473	27.4% [2]	0.45	-6.6%	1.10	-6%

[1] Binary see Table 5

[2] Steam see Table 5

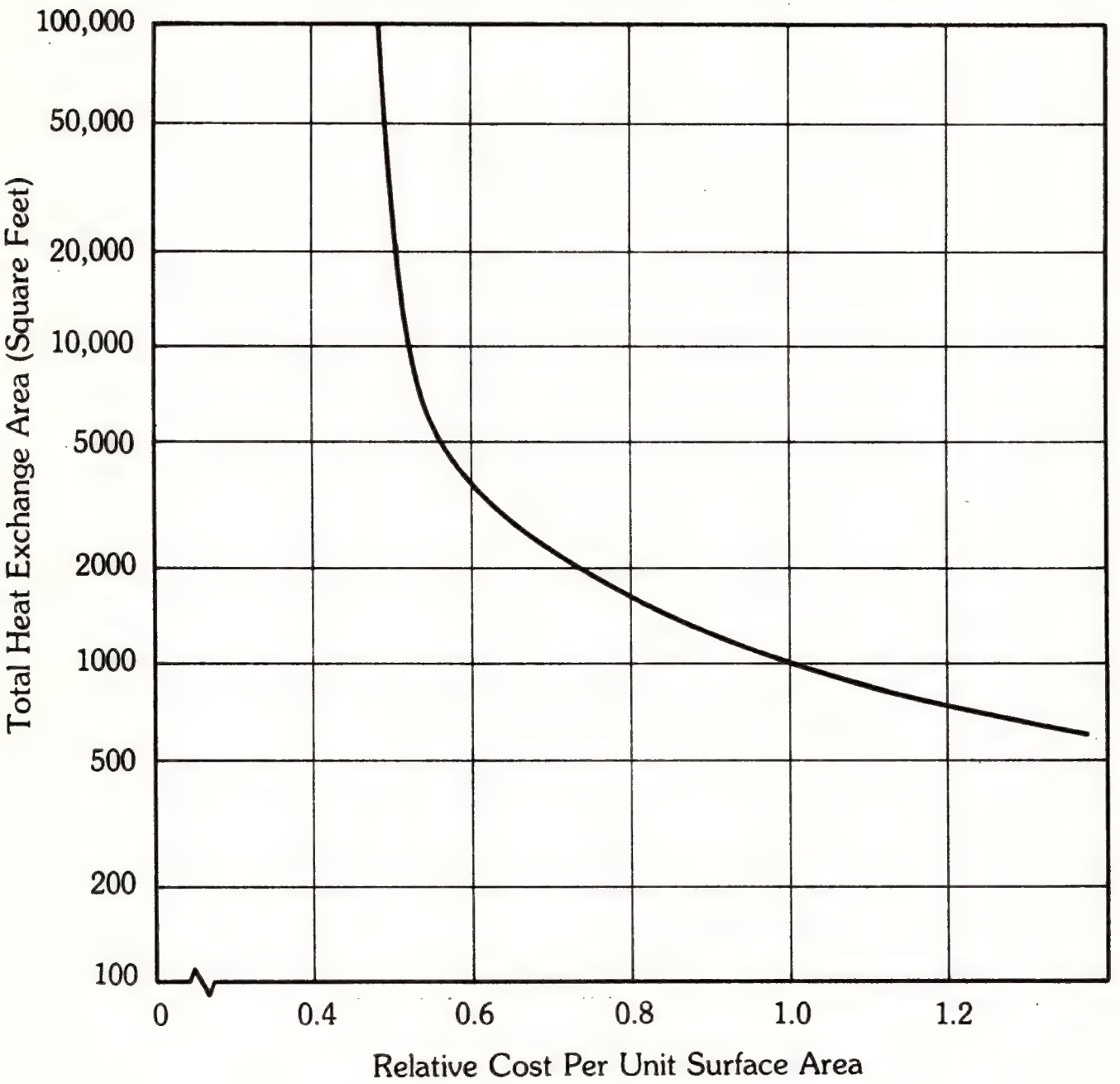

Figure 23 Variation in Unit Surface Cost of Shell and Tube Heat Exchangers (Reference 31)

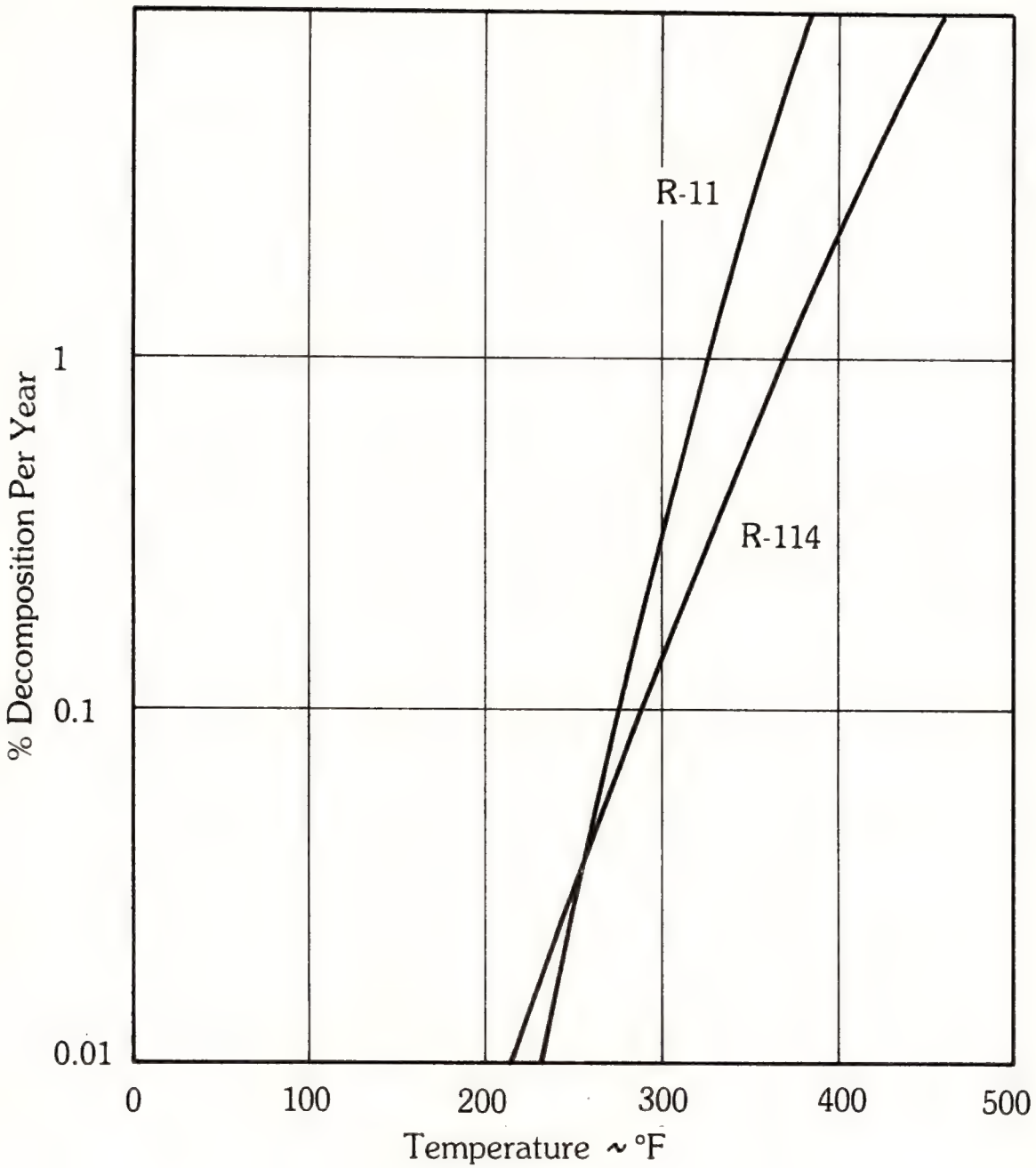

Figure 24 Sealed Tube Test Data for Thermal Decomposition of R-11 and R-114

3.0 SYSTEM COMPARISON FOR HIGH TEMPERATURES

A review of the previous section would lead to the conclusion that fluid and cycle selection criteria are good only for general conclusions. The selection of a fluid and cycle must be made for a specific application or class of applications. Such a selection must also be done on a consistent basis. The objective of this and the following section is to examine the fluids and cycles presented in Table 3 for two specific applications. Figure 25 presents the general classification of applications for which steam, organic, and binary cycles would be considered competitive. In this section, the high temperature gas source is examined. In Section 4.0, the medium temperature gas source is examined. Section 7.0 presents cost correlations for the latent heat and the sensible gas cases.

The approach for the analyses in Sections 3.0, 4.0, and 7.0 is to use a Rankine cycle design and costing program developed at MTI for the purpose of screening Rankine cycle designs. This program matches a given cycle to a heat source, sizes the heat exchangers, piping, turbomachinery, and generator. Cost correlations based upon recent purchase orders and production experience are used to cost the components. While the turbomachinery portion of the program is specifically suited to the design of radial single stage inflow, the costing algorithms are valid for all turbomachinery types. In making the evaluation, the heat transfer coefficients were assumed to be independent of the working fluid, as shown in Table 11. As explained in Section 3.2, the largest impact that might be expected is less than a 5 percent variation on the cost estimate. Since the overall costing estimate is not accurate to more than ± 10 percent, the added complexity of defining precise heat transfer coefficients was not felt to be justified. A sample output from this program is presented in Figure 26.

An additional assumption made for these analyses was that the pressure drop through the evaporator was 10 percent of the turbine inlet pressure. A zero pressure drop from the turbine exit to the condenser was assumed. In practice, this pressure drop can be a significant percentage of the turbine exit pressure, especially if there is any regeneration. The liquid side pressure drop from the condenser hot well to the entry of the evaporator is based upon relative elevations and piping lengths.

A uniform condensing temperature was assumed, along with an adequate supply of 75°F water for the condenser. A 15°F temperature rise was assumed for the water across the condenser.

Various types of turbine configurations and efficiencies were assumed, depending upon the fluid and configuration. Uniform mechanical losses of 5 percent and generator losses of 4 percent were assumed. The feed pump is assumed to be 60 percent efficient.

3.1 High Temperature Gas Source

MTI has analyzed a number of gas turbine applications. The one selected for use here is a gas pipeline installation in which a Cooper-Bessemer turbine-compressor set is installed. The gas generator for the Cooper-Bessemer power turbine is a 11,500 hp Rolls Royce AVON MK.1533 gas generator. The gas generator has an exhaust flow of about 562,000 lb/hr at 900°F at a pressure of 3.15 atmospheres. The Cooper-Bessemer power turbine drops the exhaust temperature to 700°F and essentially ambient pressure. If an exhaust temperature limit of 260° is selected, 63,140,000 Btu/hr (18,500 kw) is available for recovery. The selection of the exhaust temperature limitation is based upon the condensation temperature of the sulfur oxides in the exhaust steam. Figure 27 shows that, at 260°F, condensation will start to occur with about 2 percent sulfur in the fuel. The important temperature is not the gas temperature, but the coldest wall temperature on the heat exchanger. If the wall temperature is less than 175°F, sulfuric acid condensation is a possibility with more than 0.1 percent sulfur in the fuel. The hot side tube wall temperation depends upon the heat transfer coefficients on both the hot and cold sides, as well as the tube characteristics (conductivity and thickness). In general, if the fluid temperature is less than 140°F and the gas temperature is 260°F, condensation of sulfuric acid is likely for all fuels with more than 0.1 percent sulfur. All the cycles considered, except the simple steam cycle, avoid this condition, as will be discussed latter in this section.

The 700°F hot gas source with an available energy flow of 143,500 Btu/hr per degree of temperature drop was matched to a steam cycle, a Fluorinol-85 cycle, a toluene cycle, a butane cycle, an R-114 cycle, a binary steam/R-11 cycle,

and a two level steam cycle. Generally, a number of cycle state points were considered and optimized for minimum machinery cost as a function of stack exit temperature (or pinch point temperature). The following sections describe the cycles analyzed.

3.2 Cycle Comparisons

3.2.1 Simple Steam Cycle

Water is a marvelous fluid for Rankine cycles. It is almost universally available, usually low cost in a treated state, nontoxic, nonflammable and used in Rankine machinery for over 150 years. But water has some drawbacks. Unless the expansion goes well into the wet regime, the thermodynamic cycle potential is low relative to the organics. Also, the specific volume of water at normal condensing temperatures is extremely high compared to most organics. These and other disadvantages of water as a working fluid in bottoming cycles (and even power cycles) has prompted people to look toward the organics as alternatives. The question is really how bad is water as a working fluid.

A number of Rankine cycles using water were examined using the MTI Rankine design program. Each cycle was constrained to have a turbine exit condition that was approximately dry (no more than 3 percent wet). A multistage axial turbine was assumed with a total turbine efficiency of 78 percent. Figure 28 presents the results of cost comparison of four steam cycle alternatives. The minimum cost system is a cycle with a 650°F and 60 psia turbine inlet and a stack gas exit temperature of 310°F. Figure 29 presents a cycle schematic for the cost optimum case.

The tradeoffs among cycle efficiency, heat exchanger surface, and total recovered power often determine that the cost optimum system is usually not the maximum power system. Figure 30 presents the cycles considered here as a function of net power and unit cost. Industrial and ultility economics dictate that the lowest cost system be installed in order to maximize return for industry or to stimulate additional demand for the utility. Using these economic criteria, a steam cycle would be selected that yields 380 kw less than the highest recovery system at a 260°F stack exit.

It should be observed that, as illustrated in Figure 29, sulfuric acid will condense on the boiler tubes where the 100°F water returns from the condenser. To avoid this, an additional heat exchanger is needed to preheat the water so that the water entering the stack evaporator section is at least 150°F for use with 0.1 percent sulfur fuel.

3.2.2 Fluorinol Cycle

Fluorinol is the trade name of a proprietary fluid developed by Halocarbon Products Corporation. The fluid trifluoroethanol ($C_2F_3H_3O$) is totally miscible in water in all proportions, and produces a mixture that has a nearly isentropic saturated vapor line to a drying condition depending on the percentage mixture of trifluoroethanol and water. The usual concentration used is 85 percent mole weight water and 15 percent mole weight trifluoroethanol [14, 32, 33].

A number of Fluorinol-85 cycle points were evaluated for the heat recovery conditions analyzed here. A multistage axial turbine with an 80 percent total turbine efficiency was assumed. The results of this comparison are shown in Figure 31. The optimum (least cost) cycle is for 500°F, 700 psia turbine inlet conditions and a stack exhaust temperature of 320°F. An 80 percent effective regenerator was assumed. For a similar heat source condition, the developers of Fluorinol systems selected virtually the same turbine inlet conditions [12, 13, 14].

The schematic of the cost optimized Fluorinol-85 cycle is shown in Figure 32.

3.2.3 Toluene Cycle

Toluene is an extremely good Rankine cycle fluid. It has high temperature stability and high thermodynamic efficiency relative to Carnot. It is a highly energetic fluid so that a multistage turbine would be used in usual practice. However, the developers of the toluene system have chosen to use a single stage supersonic axial turbine [11]. Toluene also results in machinery that is larger than comparable steam cycle machinery. Toluene has a safety problem in that it is a flammable fluid.

A number of toluene cycles were considered for the heat source being analyzed. A multistage axial turbine with total turbine efficiency of 80 percent was

assumed. The results are shown in Figure 33. The cost optimized cycle condition was a turbine inlet pressure of 300 psia and a turbine inlet temperature of 550°F. An 80 percent effective regenerator was assumed. For a similar heat source condition, the developer selected virtually the same turbine inlet conditions [11].

A schematic of the cost optimized cycle is shown in Figure 34.

3.2.4 Butane Cycle

The use of butane and other hydrocarbons has been considered for Rankine cycles in power generation applications [23]. The selection of butane was made by its developer for use on gas and oil pipelines in arctic and subarctic regions [10]. The use of a fluid such as butane results in rather simple singe stage radial machinery, avoids the freezing problem associated with water, and can readily take advantage of the very low condensing temperature available in such locations. When MTI studied the artic pipeline application [9], we selected R-114 because of its nonflammable nature. Since both the butane cycles and R-114 cycles were selected for an application that is somewhat different from the hot gas application considered here, it should not be too surprising that their costs are higher than the other cycles.

A number of butane cycles were considered for the heat source being analyzed. A single stage radial inflow turbine was assumed with an efficiency of 85 percent. The overall pressure ratio across the turbine is 12 as compared to the desired level of 6. This should result in a turbine efficiency that is degraded to 79 percent (see Figure 16). This difference was ignored for the purpose of this analysis. A regenerator effectiveness of 45 percent was used. The selected cycle condition is for turbine inlet conditions of 600 psia and 500°F. The temperature is based upon the stability of butane. Although higher pressures do not appear to be justified since the turbine efficiency losses may become significant, the developer [10] uses turbine inlet conditions of 1000 psia and 500°F, but maintains a pressure ratio of 12 by having turbine exit conditions of 95 psia and 360°F. The cost comparisons of the cycle conditions are shown in Figure 35.

To illustrate the effect of turbine inlet temperature conditions on a super critical cycle, Figures 36 and 37 present schematics for a 600°F and 500°F turbine inlet temperature.

Some comparisons between two supercritical butane cycles are shown in Table 12. It is interesting to note some anomalies. A reduction by 100°F in peak turbine inlet temperature results in an expected decrease in overall cycle efficiency, but an unexpected increase in total power delivered and lower net costs. The increased power comes about by means of a lowering of the cost optimum stack exhaust temperature, and by making about 12 percent more heat available to the cycle. The decreased cost comes about by means of a sizeable reduction (30 percent) in total evaporator surface area, and a more sizeable reduction (35 percent) in evaporator surface area per unit output. This illustrates the problem with using generalized selection criteria to optimize a cycle selection for a specific application.

3.2.5 R-114 Cycle

R-114 has the highest temperature stability of the fluorocarbons that exhibit good Rankine power fluid characteristics. It is limited to a peak cycle temperature of 400°F. Its characteristics make it nicely suited to arctic pipeline applications [9]. Unlike butane, R-114 is not flammable, but like butane, the R-114 has higher cost than the other cycles considered.

Two levels of turbine inlet pressure were considered (Figure 38). The 600 psia case resulted in a supercritical cycle. The 400 psia case has a small amount of latent heat addition. The supercritical cycle was more cost effective. A single stage radial inflow turbine was assumed with 85 percent efficiency. The cycle pressure ratio is 13 as compared to the desired level of 6. As with the butane case, no degredation of turbine efficiency was assigned for the high stage pressure ratio. An 80 percent effective regenerator was assumed. The cost optimum case is for the supercritical cycle with turbine inlet conditions of 600 psia and 400°F, and a stack exit temperature of 300°F.

A schematic of the cost optimized system is shown in Figure 39.

The effect of regeneration on cycle cost and power output is shown in Figure 40. For R-114, 60 percent effective regeneration appears optimal, but with little cost difference between 40 percent and 80 percent effectiveness. Since 80 percent effectiveness provides significantly more power output, it was used in the cost comparsions.

3.2.6 Binary Steam/R-11 Cycle

The binary steam/R-11 cycle has the advantages that it can achieve high peak cycle temperatures without a flammable fluid, and that it can achieve low condensing temperatures without large machinery.

Binary cycles were selected for the heat source being analyzed in this section. Some constraints were imposed upon the cycle selection. Specifically, each fluid will have a single stage radial turbine which will satisfy all the conditions set for it in Section 2.0. The steam turbine has a 1636 ft/sec tip speed and the R-11 turbine has a pressure ratio of 6. A cost optimized cycle was not determined since the number of variables involved are rather extensive. We feel that a non-optimized cycle is adequate for this analysis.

Figure 41 presents the optimization of the stack exit temperature for the single binary cycle considered. Figure 42 presents a schematic of the cycle.

3.2.7 Two Level Steam Cycle

There has been some effort directed toward two level steam cycles with multi-stage axial turbines at each level [6, 18]. As an extreme example, a two level steam cycle was selected for the heat source considered here. This cycle is constrained to have a single stage radial turbine for each level of steam. The cycle schematic is shown in Figure 43. It should be noted that, with the turbine configuration constraint, the condensing temperature increased to 141°F from 100°F. This cycle is cost optimized in Figure 44.

Due to the constraining machinery requirements and the resulting higher condensing temperature, the system costs are much higher than the other cycles considered in this section. For the same reasons, this two level steam cycle is not directly comparative to the other systems. It is included here as an extreme example of what might be obtained by a rather simple two level steam system. Cycle optimization with multistage axial turbines will improve the performance and economics of two level steam systems. This will take considerable engineering and development time, and would be justified only in a case where a number of identical systems could be sold. Such an application is a packaged gas turbine-steam turbine system as discussed in Reference 6.

3.3 System Comparisons

Seven alternative approaches to recovering power from a waste gas source at 700°F have been presented. Let us now look at these seven alternatives in a plot of their estimated machinery cost and net delivered power in Figure 45. Each alternative has shown a ±10 percent band in estimated cost. Depending upon design approach, production volume, and manufacturing techniques, four of the alternatives (Fluorinol, toluene, steam, and binary) can be cost competive for the machinery packager. Butane and R-114 would have higher costs for the machinery. The two level steam is unrealistically high. However, machinery cost is only part of the story. As is well known, the installed cost of a system can be many times the cost of the base machinery.

The conventional approach to building power recovery systems is for the end user or his consulting engineer to design a power recovery system, procure individual components, and erect them in the field. This approach is illustrated in Figure 46. This results in extremely costly field labor, extensive startup costs, and possible reliability problems. The cost of field erection is well known and needs no further discussion. As the first time the system is going to operate is in the field, the normal problems of any hardware development effort are compounded by the fact that field instrumentation and engineering support is limited, and that the startup depends on a production operating unit. Reliability problems could result since there is a tendency to use catalog components and match their operating ranges. The combination of a number of components operating in different portions of their design range can result in problems with unexpected couplings.

All of the developers of Rankine power recovery systems recognize this problem and have provided some degree of packaging. The MTI packaging approach is shown in Figure 47 and will be discussed further in Section 5.

Table 13 shows a number of considerations regarding the fluids and turbomachinery. The turbomachinery design approach is shown in Table 12. MTI uses an integral gearing arrangment to eliminate any high speed couplings. A similar approach is taken for the toluene system in Reference 11. A direct drive approach is taken in Reference 7. This approach imposes limitations on the application and the turbines such that there could be severe performance penalties for some applications or even complete incompatibility. The usual approach is to use a separate gear box with a high speed coupling to the turbine. Three of the fluids offer potential thermal stability problems. Butane and R-114 operate at their thermal stability limiting temperature. Since the supply temperature is significantly hotter than their thermal stability, evaporator hot spots or plugged tubes could result in rapid deterioration of these fluids. Fluorinol is operating well below its thermal stability limit. However, the supply temperature is above its recommended operating temperature and evaporator hot spots might cause thermal deterioriation problems.

In terms of fluid safety, toluene and butane are flammable. Toluene and Fluorinol may have toxicity problems. Except for Fluorinol, all the fluids are generally available in large commercial volumes from many suppliers.

A consideration of fluid working pressures is also important. It would be desirable from an operating standpoint to avoid extremely high or low pressures. Only the binary system avoids high vacuums and/or high pressures. Fluorinol requires both a high vacuum and a high pressure. The operating pressures impose design constraints upon the heat exchangers, both in terms of wall thicknesses and volumes, and upon feed pumps, valving, and other plumbing components. These factors impose cost penalties.

A question typically asked about binary systems is that of the added cost of the binary condenser/evaporator heat exchanger. All the systems considered here need three heat exchangers. The organics need regenerators for cycle efficiency. Steam needs a boiler preheater to avoid stack gas condensation. Thus, there is little (if any) cost penalty for the added heat exchanger.

There is, of course, a second law thermodynamic potential penalty. In the binary system, the tradeoff between second law losses and heat exchanger cost is part of the cost optimization of the system.

All of the above criteria result in the bottom line cost-total installed cost per unit output. This must be a qualitative estimate since no real comparative figures are available. However, the binary and Fluorinol systems should be cost competive. Toluene would be in the competitive range, depending upon the packaging approach taken. Butane would probably be slightly higher but has a better chance for a highly integrated package design which could make it very cost competitive. Steam and R-114 would be the highest cost on an installed basis. In the case of steam, this would be a result of equipment installation. For that of R-114, this would be a result of its overall high machinery cost.

Based on cost and fluid characteristics, the selection of a binary system would obviously be our choice and our expectation of the market's choice.

Referring to Figure 45, it is obvious that four of the five fluids produce more delivered output than the binary system. However, although it would be desirable from the point of view of society, a utility or non-utility end user has no economic incentive to select a system with higher output and the same cost per unit output as a system which entails less risk. From a national policy consideration, it would be more desirable to develop and initiate the use of cost effective, low risk systems that will be used by industry, rather than promote high performance systems that present cost or perceived risk difficulties.

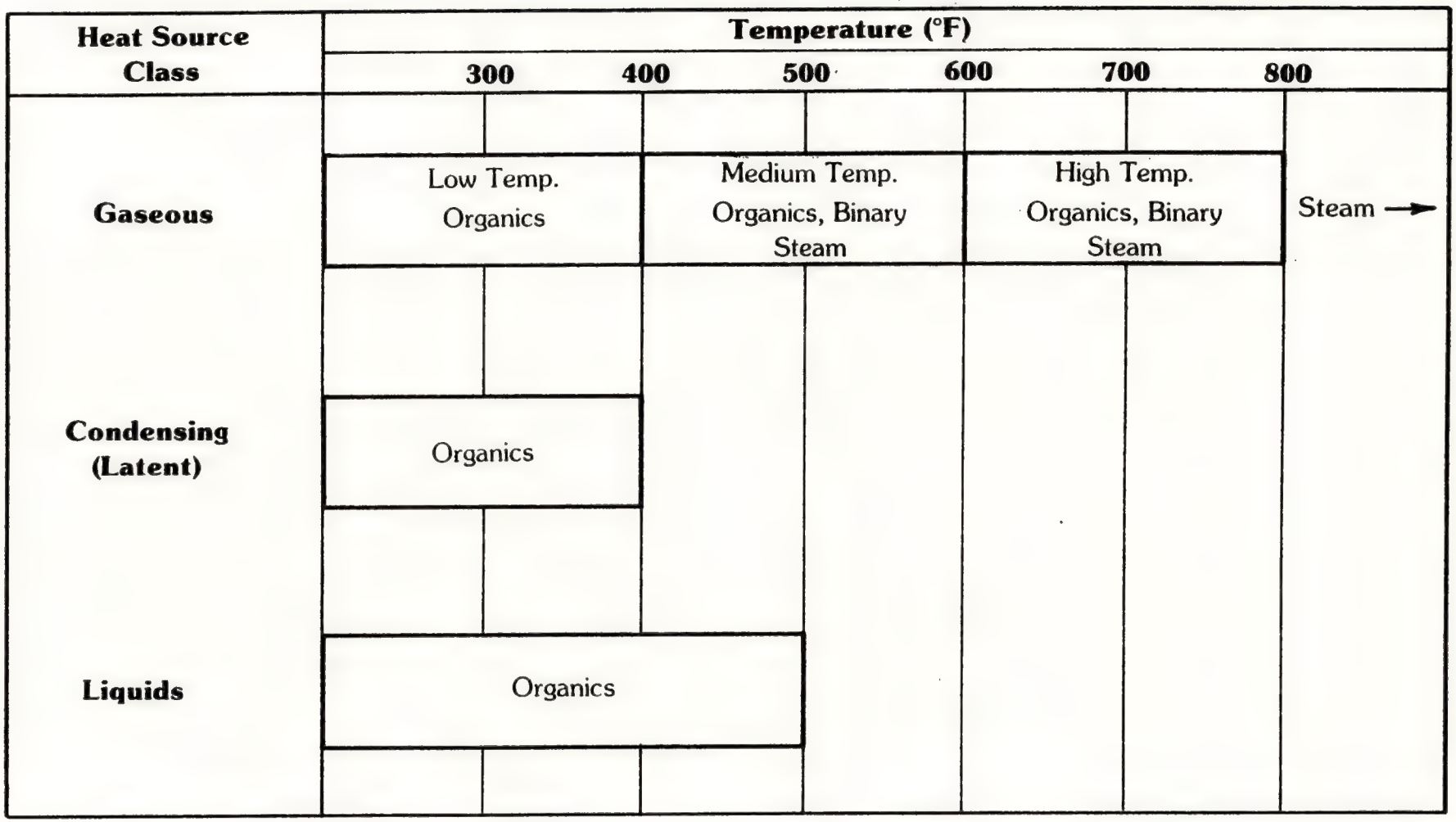

Figure 25 General Classification of Applications For Rankine Bottoming Cycles

SYSTEM COMPARISON

ASSUMPTIONS

78P79

TABLE 11

OVERALL HEAT TRANSFER COEFFICIENT
USED IN THE COMPARISON ANALYSES

Evaporator		
Gas Source	Liquid	9
	Boiling	9
	Superheat	5
Condensing Source		75 [1]
Liquid Source		125 [1]
Regenerator		30
Condenser		100

[1] Organics only, without superheat

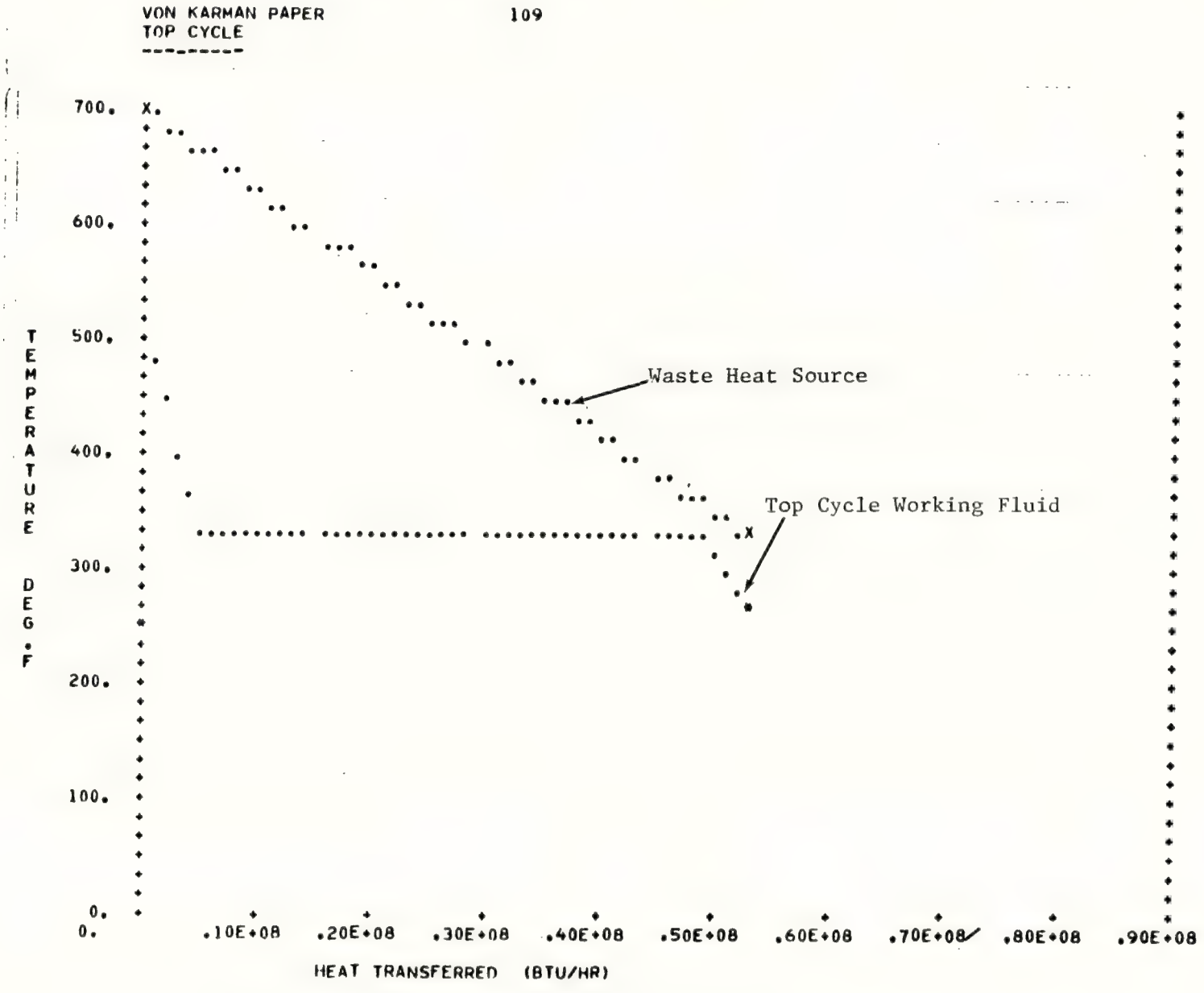

Figure 26 Sample Output from MTI Rankine Design Program
(a) Temperature Heat Flow From Waste Heat Source to Working Fluid

TOP CYCLE

STATE POINTS

	TURBINE INLET	TURBINE EXHAUST	BOILER 2 OUTLET (RECEIVER)	PUMP OUTLET
P (PSIA).....	100.000	30.000	30.000	158.170
T (DEG.F).....	500.000	295.200	250.000	250.651
H (BTU/LB).....	1279.100	1186.400	218.800	219.471
V (CU FT/LB).....	5.589	14.650	.017	.017

SYSTEM PIPING AND RECEIVER

	LENGTH (FT)	ID (IN)	WALL THICKNESS (IN)	NUMBER FLANGES	FLUID VELOCITY (FPS)	FLUID WEIGHT (LBS)
BOILER OUTLET TO TURBINE INLET,	100.000	8.709	.212	10	190.000	7.401
TURBINE EXHAUST TO BOILER 2....	10.000	14.486	.168	2	180.000	.781
BOILER 2 TO RECEIVER TO PUMP...	50.000	2.703	.133	12	6.000	117.185
RECEIVER (L/D=4).....	11.697	35.091	.230	3	---	716.152
PUMP DISCHARGE TO BOILER.....	100.000	2.702	.168	10	6.000	234.371
BOILER.....	---	---	---	---	---	2504.870

TOTAL FLUID INVENTORY (LBS)... 3580.761
RECEIVER VOLUME (FT**3)..... 76.091
NET ELEVATION CHANGE (FT)..... 20.000

MACHINERY

	NPSH (FT)	SPECIFIC SPEED	PRESSURE RATIO	HEAD (FT)	EXIT VOLUME FLOW (CFS,GPM)	SHAFT POWER	RPM	OD (IN)	U/C	EFF	TIP SPEED (FPS)
TURBINE...	---	70.000	3.333	84847.765	206.012	1843.950	24245.556	15.465	.700	.850	1635.893
PUMP.....	2.209	486.404	---	313.559	107.235	13.362	3500.000	9.301	---	.600	142.038

HEAT EXCHANGERS

	AVERAGE HT COEF	FLUID TEMPERATURES (DEG.F) HOT IN	HOT OUT	COLD IN	COLD OUT	HEAT FLOW (BTU/HR)	SURFACE AREA (FT**2)	EFFECTIVENESS
BOILER.....	---	700.000	326.183	250.651	500.000	.536E+08	.574E+05	---

POWER FLUID FLOW RATE.... .506E+05

Figure 26 Sample Output from MTI Rankine Design Program
(b) Cycle and Machinery Calculations for Top Cycle

BOTTOM CYCLE

STATE POINTS

	TURBINE INLET	TURBINE EXHAUST	CONDENSER OUTLET (RECEIVER)	PUMP OUTLET
P (PSIA).....	138.000	23.400	23.400	170.313
T (DEG.F).....	225.000	110.000	100.000	102.382
H (BTU/LB).....	117.440	105.400	28.700	29.198
V (CU FT/LB).....	.320	1.759	.011	.011

SYSTEM PIPING AND RECEIVER

	LENGTH (FT)	ID (IN)	WALL THICKNESS (IN)	NUMBER FLANGES	FLUID VELOCITY (FPS)	FLUID WEIGHT (LBS)
BOILER 2 OUTLET TO TURBINE INLET	10.000	13.876	.316	2	47.000	32.808
TURBINE EXHAUST TO CONDENSER....	10.000	33.246	.203	2	45.000	34.266
CONDENSER TO RECEIVER TO PUMP...	10.000	7.199	.142	4	6.000	256.994
RECEIVER (L/D=4).....	13.538	40.614	.220	3	---	1715.991
PUMP DISCHARGE TO BOILER 2.....	10.000	7.197	.248	2	6.000	256.994
BOILER 2.....	---	---	---	---	---	6282.903

TOTAL FLUID INVENTORY (LBS)...	8579.957
RECEIVER VOLUME (FT**3).....	117.974
NET ELEVATION CHANGE (FT).....	10.000

MACHINERY

	NPSH (FT)	SPECIFIC SPEED	PRESSURE RATIO	HEAD (FT)	EXIT VOLUME FLOW (CFS,GPM)	SHAFT POWER	RPM	OD (IN)	U/C	EFF	TIP SPEED (FPS)
TURBINE...	---	70.000	5.897	11020.141	271.278	2626.129	4571.208	29.561	.700	.850	589.560
PUMP.....	8.157	1621.157	---	232.539	760.780	108.657	3500.000	8.010	---	.600	122.318
GENERATOR.	---	---	---	---	---	4291.276	---	---	---	.950	---

THERMAL EFFICIENCY.....	.212
MECHANICAL EFFICIENCY...	.960
DELIVERED GENERATOR KW..	3041.227

HEAT EXCHANGERS

	AVERAGE HT COEF	FLUID TEMPERATURES (DEG.F) HOT IN	HOT OUT	COLD IN	COLD OUT	HEAT FLOW (BTU/HR)	SURFACE AREA (FT**2)	EFFECTIVENESS
CONDENSER.....	100.000	110.000	100.000	75.000	90.000	.426E+08	.260E+05	.600
BOILER 2.....	---	295.200	250.000	102.382	225.000	.490E+08	.131E+05	---

POWER FLUID FLOW RATE....	.555E+06
CONDENSER FLOW RATE.....	.284E+07

Figure 26 Sample Output from MTI Rankine Design Program
(c) Cycle and Machinery Calculations for Bottom Cycle

COST SUMMARY

1 UNITS PURCHASED

TOP CYCLE

PIPE AND FLANGES

	(PIPE / FLANGE)			PERCENT OF HARDWARE COST	PERCENT OF PRICE
TURBINE EXHAUST....	$ 197.89	/ $ 653.80			
RECEIVER.....	291.74	/ 297.05			
BOILER INLET.....	367.52	/ 688.22			
TURBINE INLET.....	1497.77	/ 4283.77			
	$ 2354.91	$ 5922.84	$ 8277.75	1.04	.64
BOILER			216180.89	27.03	16.60
CONTROL			43396.78	5.43	3.33
FLUID			1790.38	0.00	0.00
RECEIVER			2107.65	.26	.16
TOP CYCLE HARDWARE SUB TOTAL..			$ 271753.45		

BOTTOM CYCLE

PIPE AND FLANGES

	(PIPE / FLANGE)			PERCENT OF HARDWARE COST	PERCENT OF PRICE
TURBINE EXHAUST....	$ 546.73	/ $ 2386.30			
RECEIVER.....	165.62	/ 443.11			
BOILER INLET.....	144.48	/ 635.50			
TURBINE INLET.....	356.13	/ 1779.17			
	$ 1212.96	$ 5244.07	$ 6457.03	.81	.50
CONDENSER			155007.16	19.38	11.90
BOILER			105288.75	13.17	8.09
CONTROL			53278.73	6.66	4.09
FLUID			12869.93	1.61	.99
RECEIVER			2983.70	.37	.23
PRIME MOVER			143430.70	17.93	11.01
GENERATOR			48692.71	6.09	3.74
BOTTOM CYCLE HARDWARE SUB TOTAL..			$ 528008.72		
ALL HARDWARE SUB TOTAL..			$ 799762.17		
MATERIAL HANDLING			39988.11		3.07
INTEREST AND INSURANCE			35989.30		2.76
WARRANTY COST			15995.24		1.23
FIXED CHARGES(ASSY,TEST,SHIP,INSTALL)			150000.00		11.52
LEARNING CURVE DISCOUNT			0.00		0.00
ALLOCATION OF O.T.C.(TOOLING + DESIGN)			0.00		0.00
MANUFACTURING COST			1041734.82		
ROYALTY			0.00		0.00
MARKUP			260433.70		20.00
					100.00
PRICE..			$ 1302168.52		
DOLLARS/KW =			428.17		

Figure 26 Sample Output from MTI Rankine Design Program
(d) Cycle Cost Estimate

HIGH TEMPERATURE GAS SOURCE

COOPER-BESSEMER

GAS PIPELINE TURBINE-COMPRESSOR

ROLLS ROYCE AVON MK, 1533
11,500 hp
562,000 lb/hr
700°F

78P79

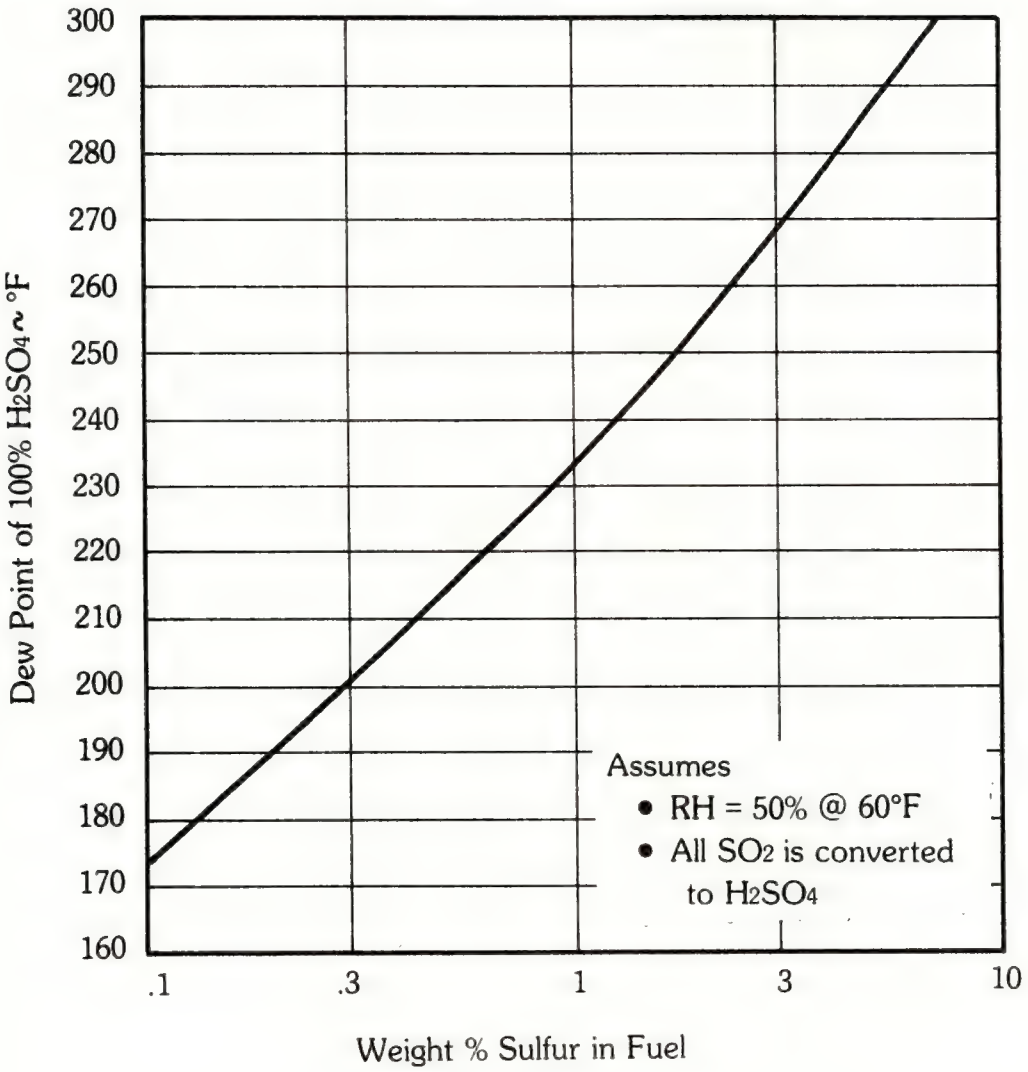

Figure 27 Effect of Fuel Sulfur Content on Dew Point Temperature of Sulfuric Acid in Exhaust Gas

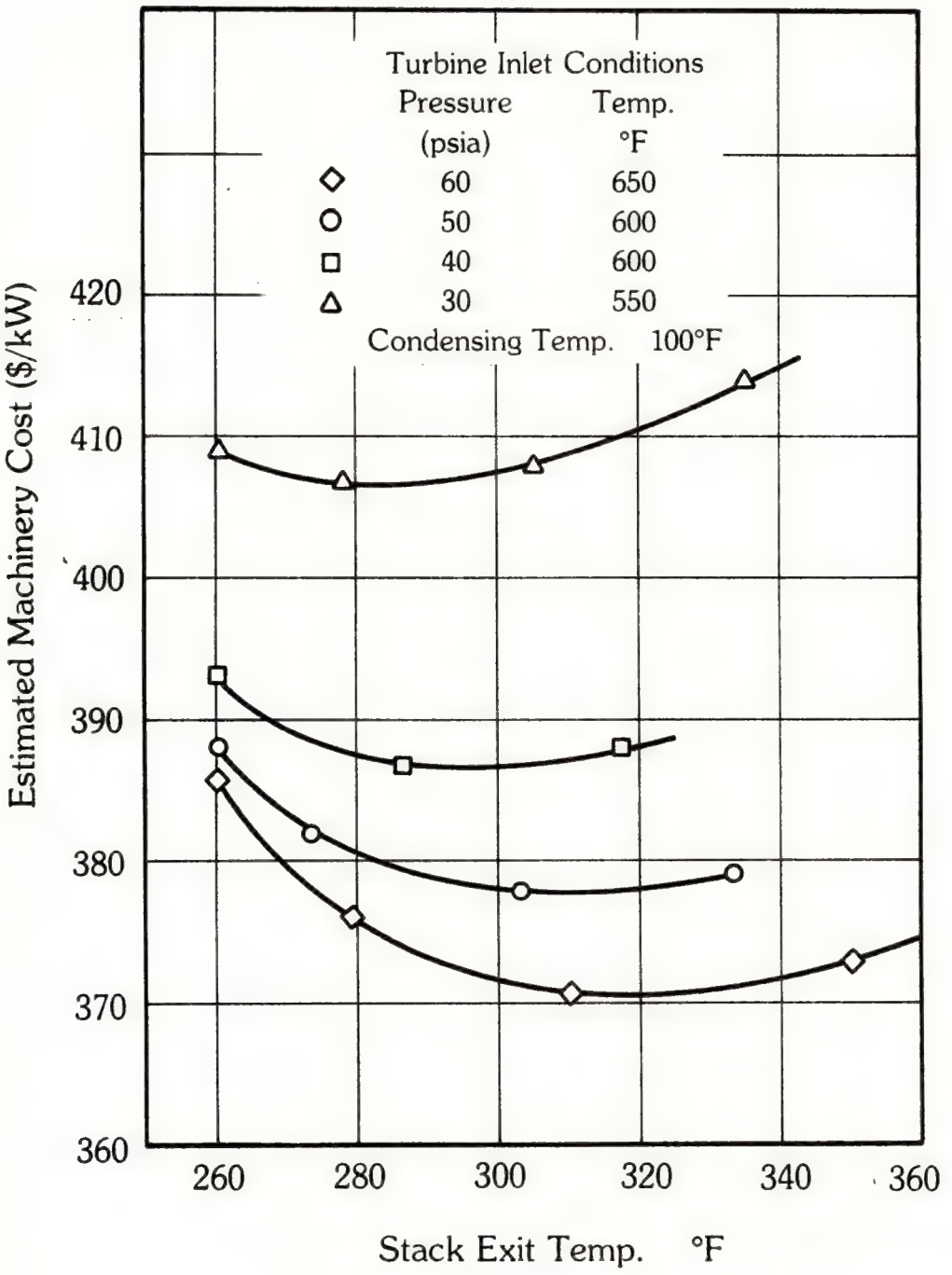

Figure 28 Cost Comparison of Various Cycle Conditions With Simple Steam With 700°F Hot Gas Source

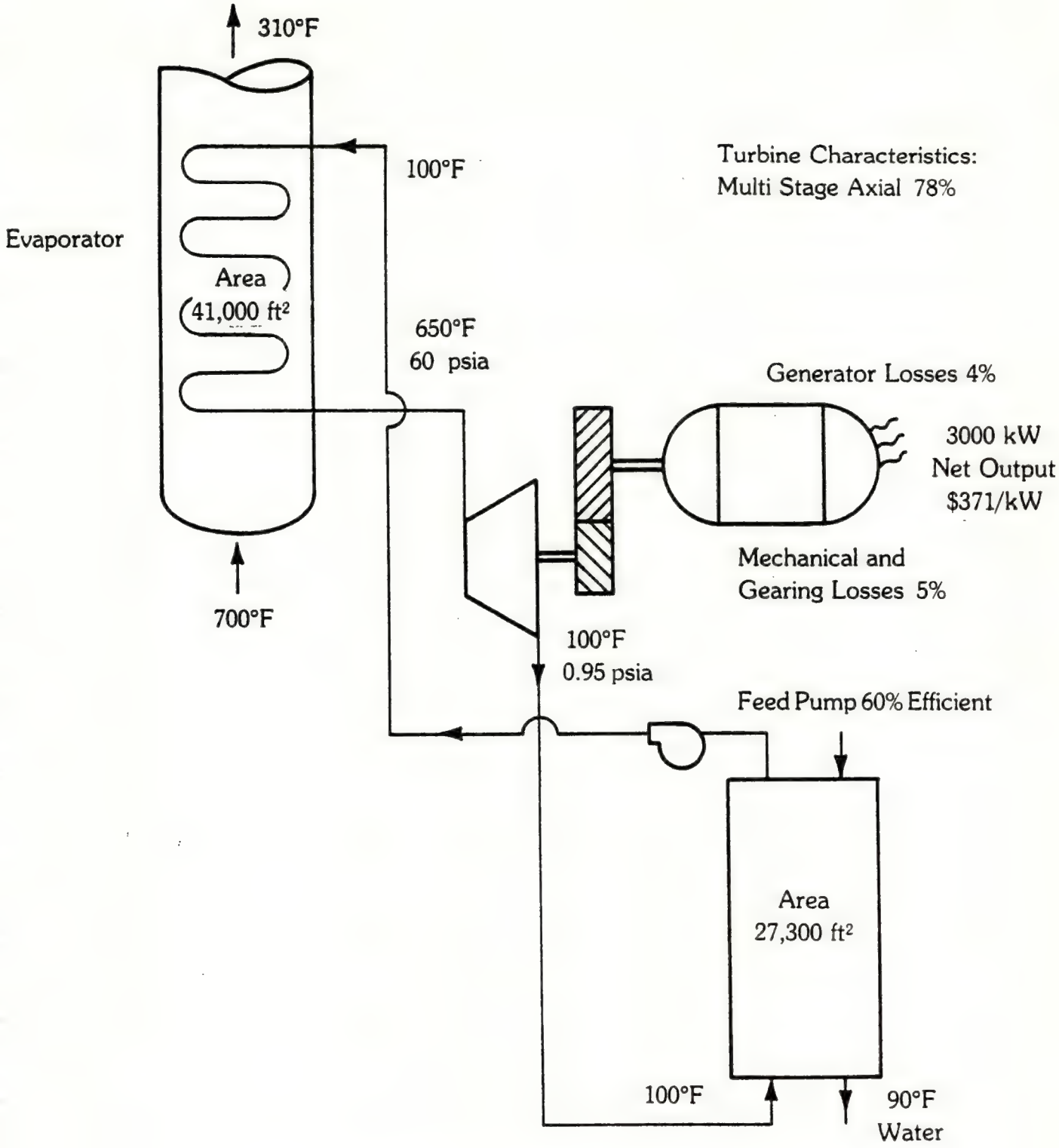

Figure 29 Illustration of Rankine Cycle With Simple Steam For Most Cost Effective Case Considered

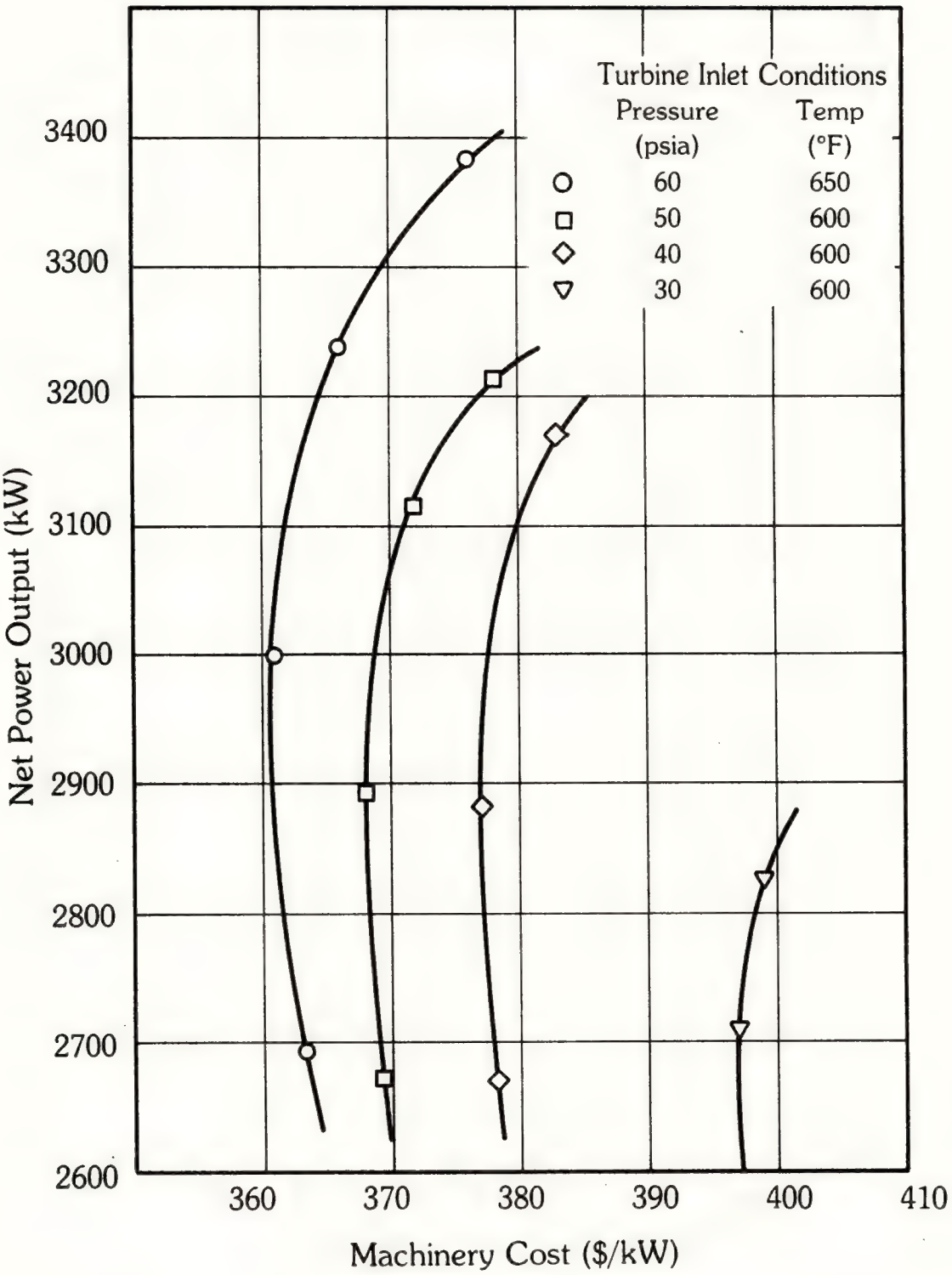

Figure 30 Power Output and Machinery Cost for Various Steam Cycles With a 700°F Hot Gas Source

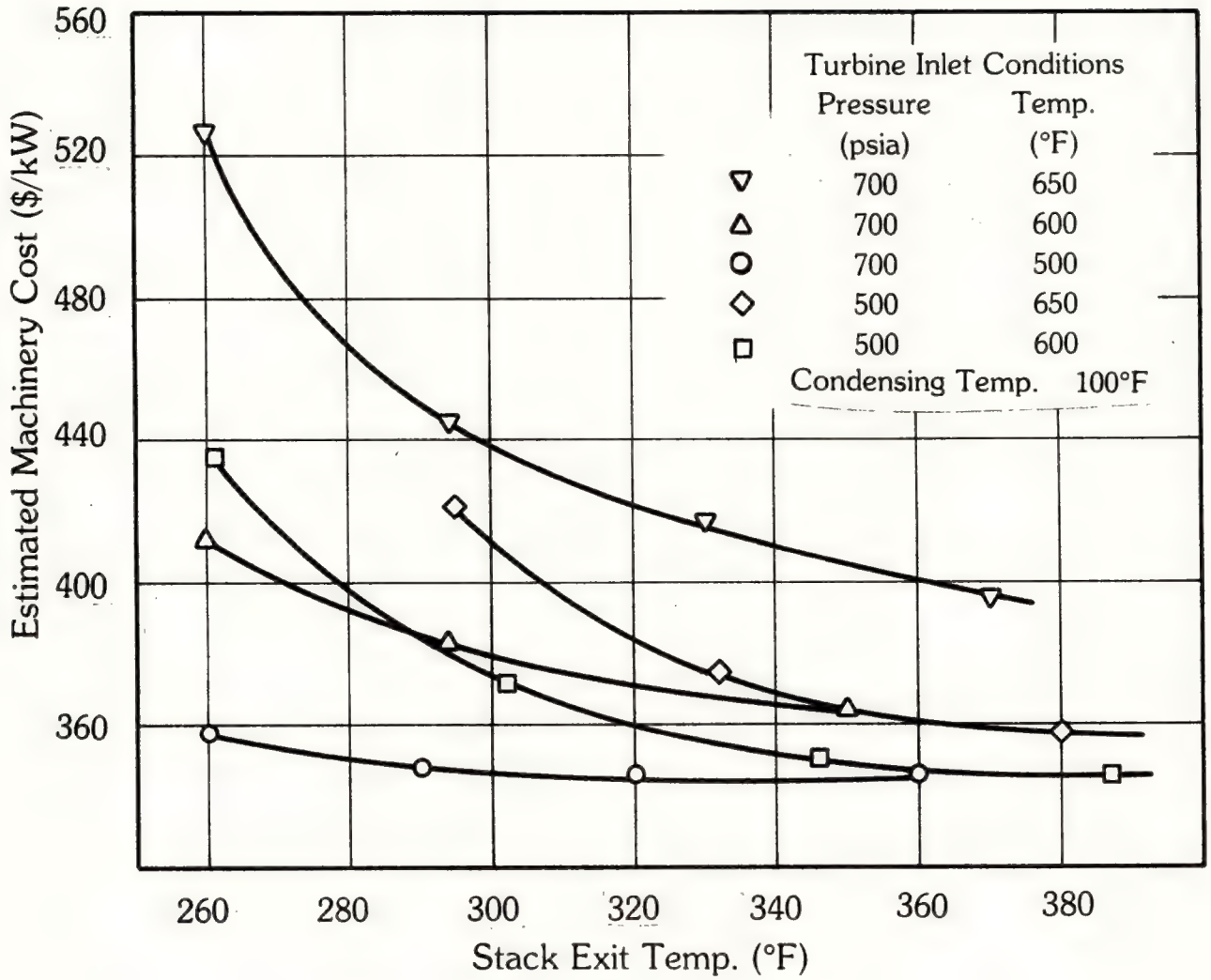

Figure 31 Cost Comparison of Various Cycle Conditions With Fluorinol-85 With 700°F Hot Gas Source

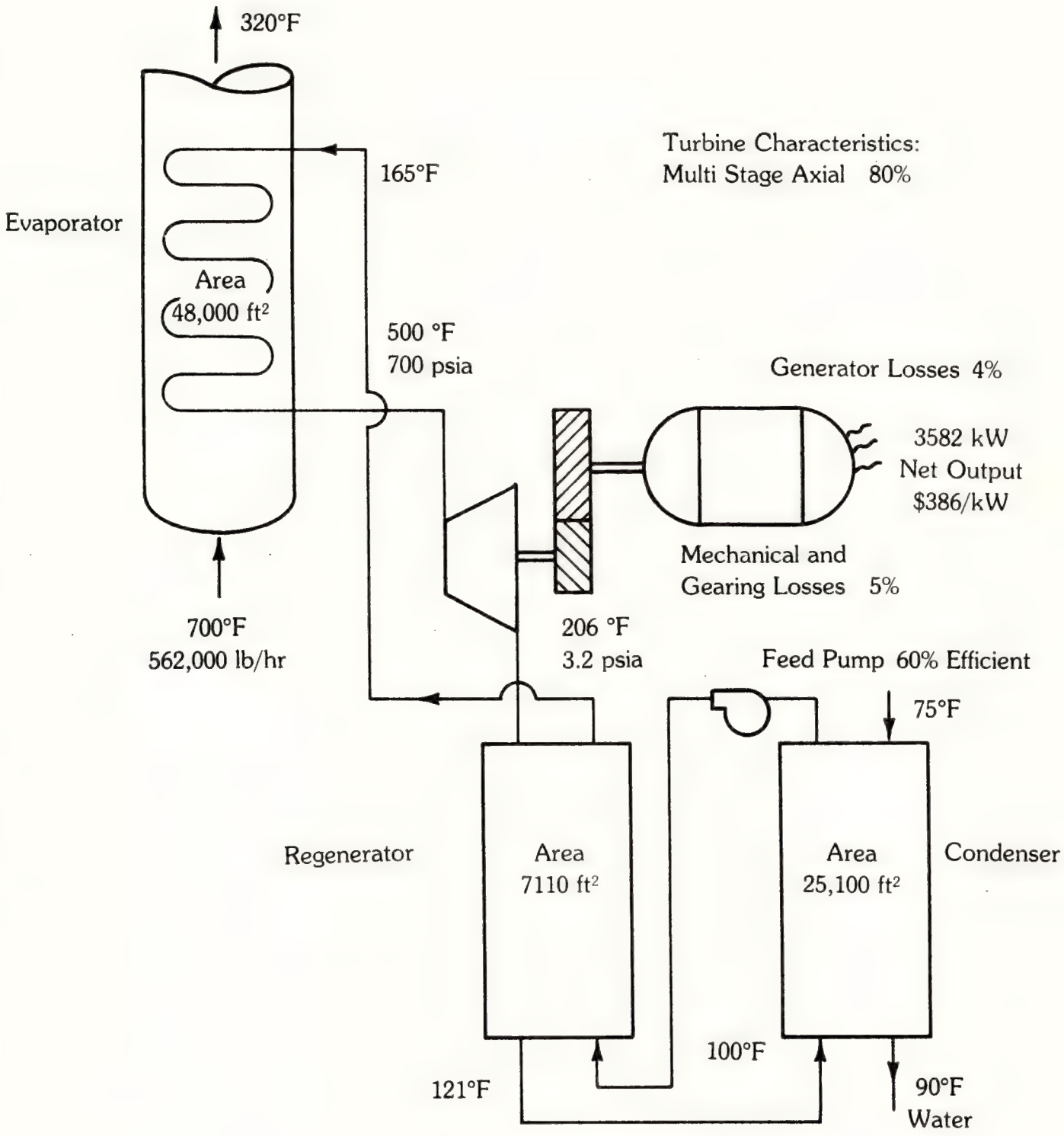

Figure 32 Illustration of Rankine Cycle With Flourinol-85
For Most Cost Effective Case Considered

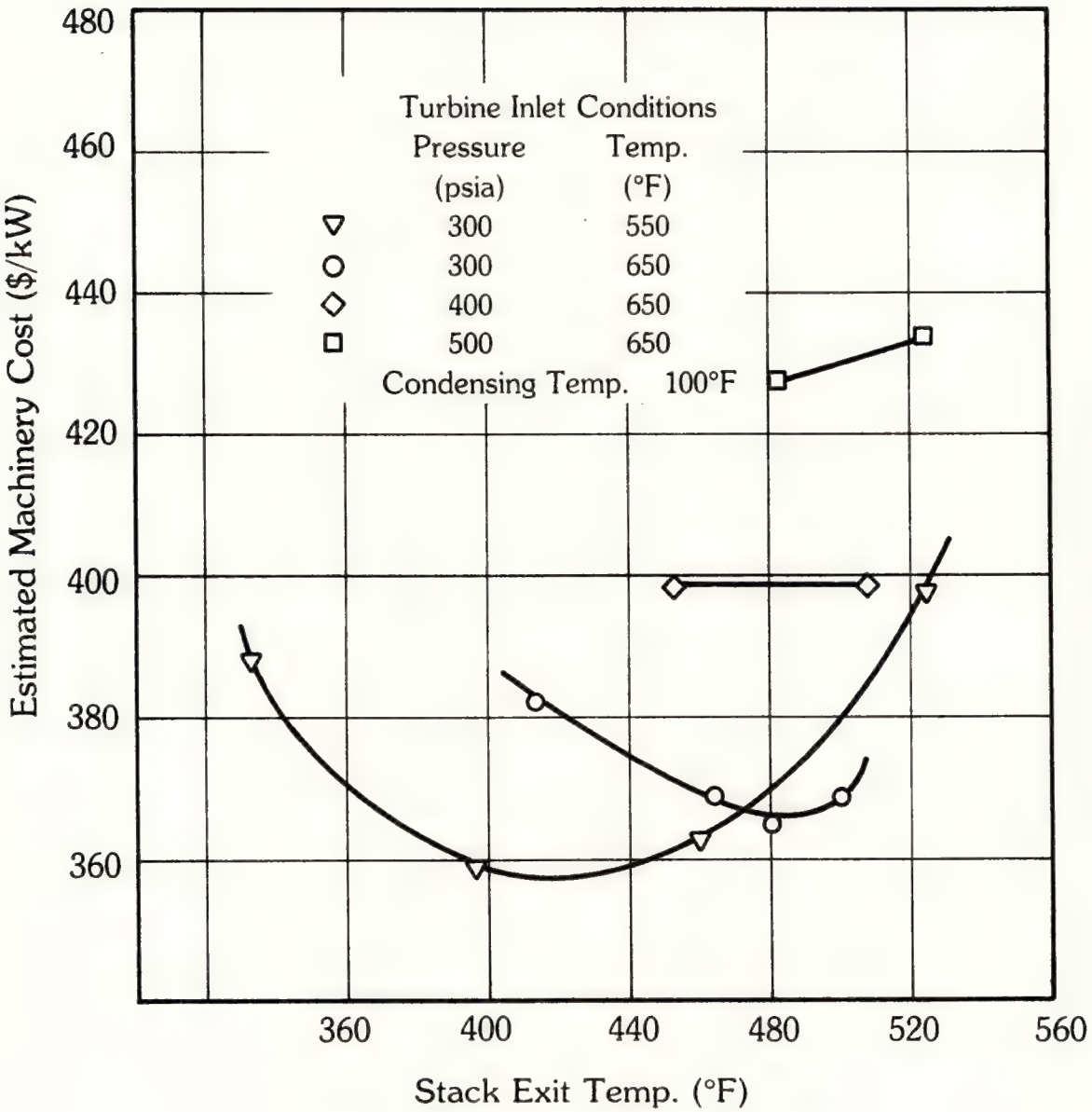

Figure 33 Cost Comparison of Various Cycle Conditions With Toluene With 700°F Hot Gas Source

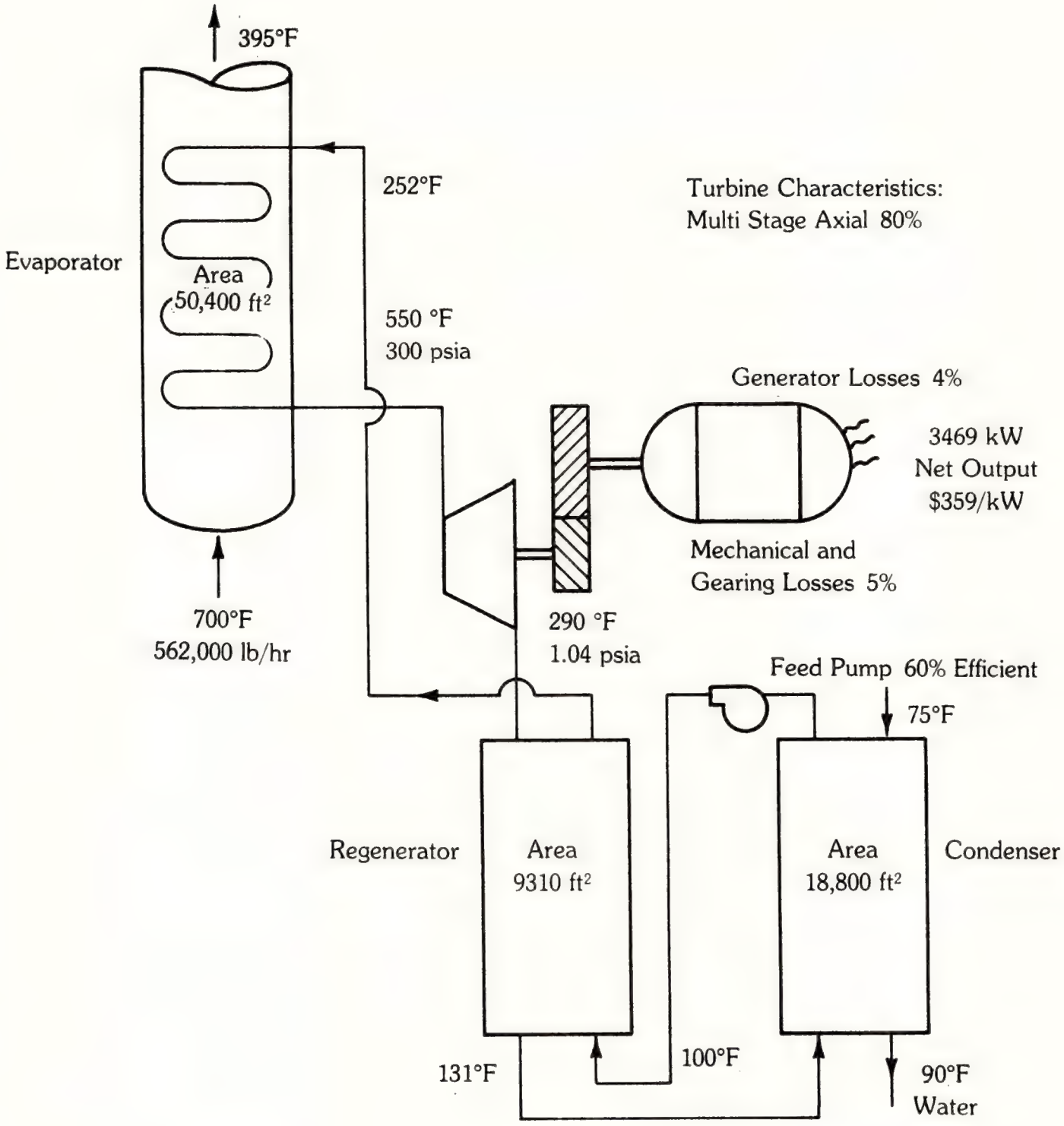

Figure 34 Illustration of Rankine Cycle With Toluene For Most Cost Effective Case Considered

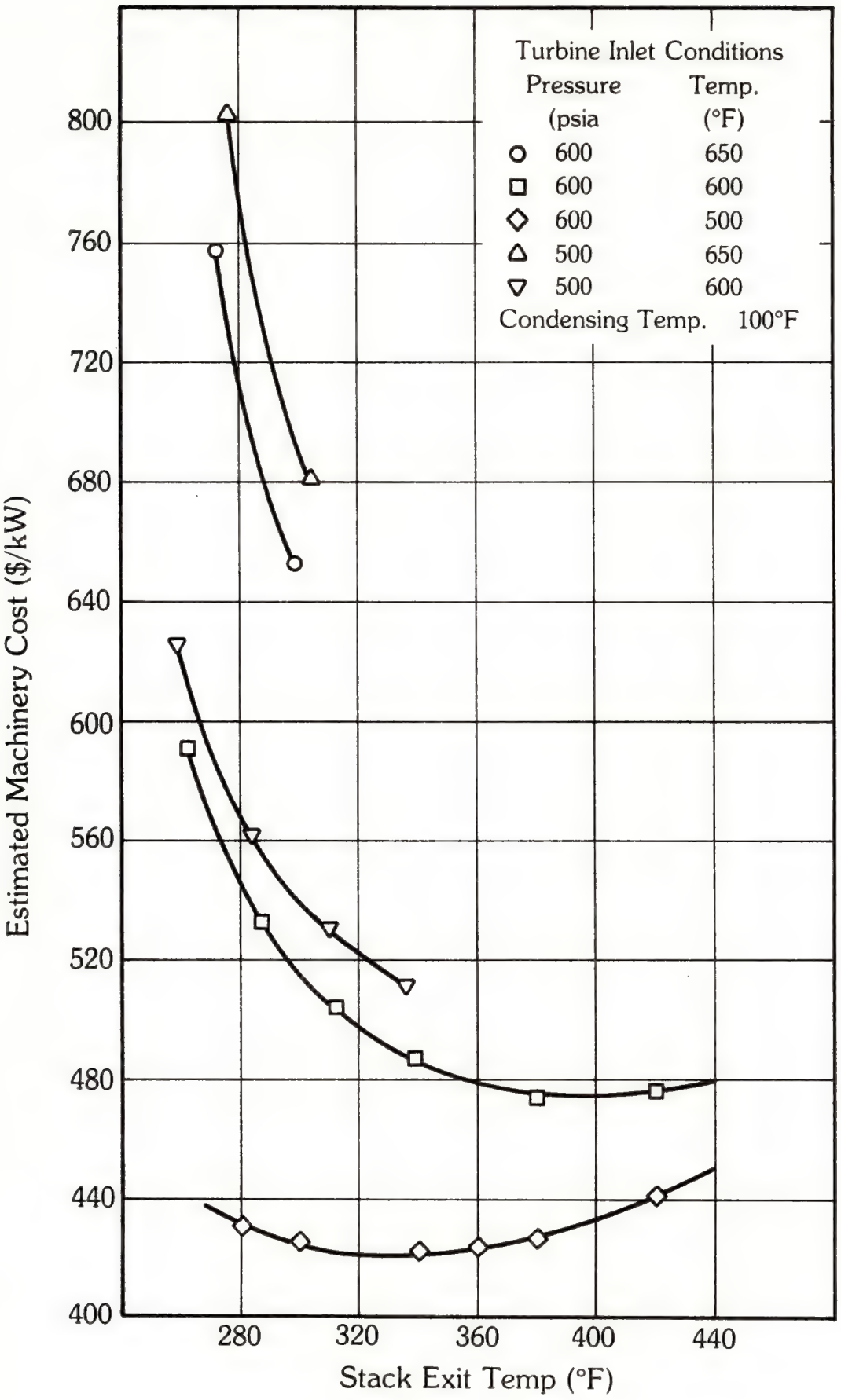

Figure 35 Cost Comparison of Various Cycle Conditions With Butane With 700°F Hot Gas Source

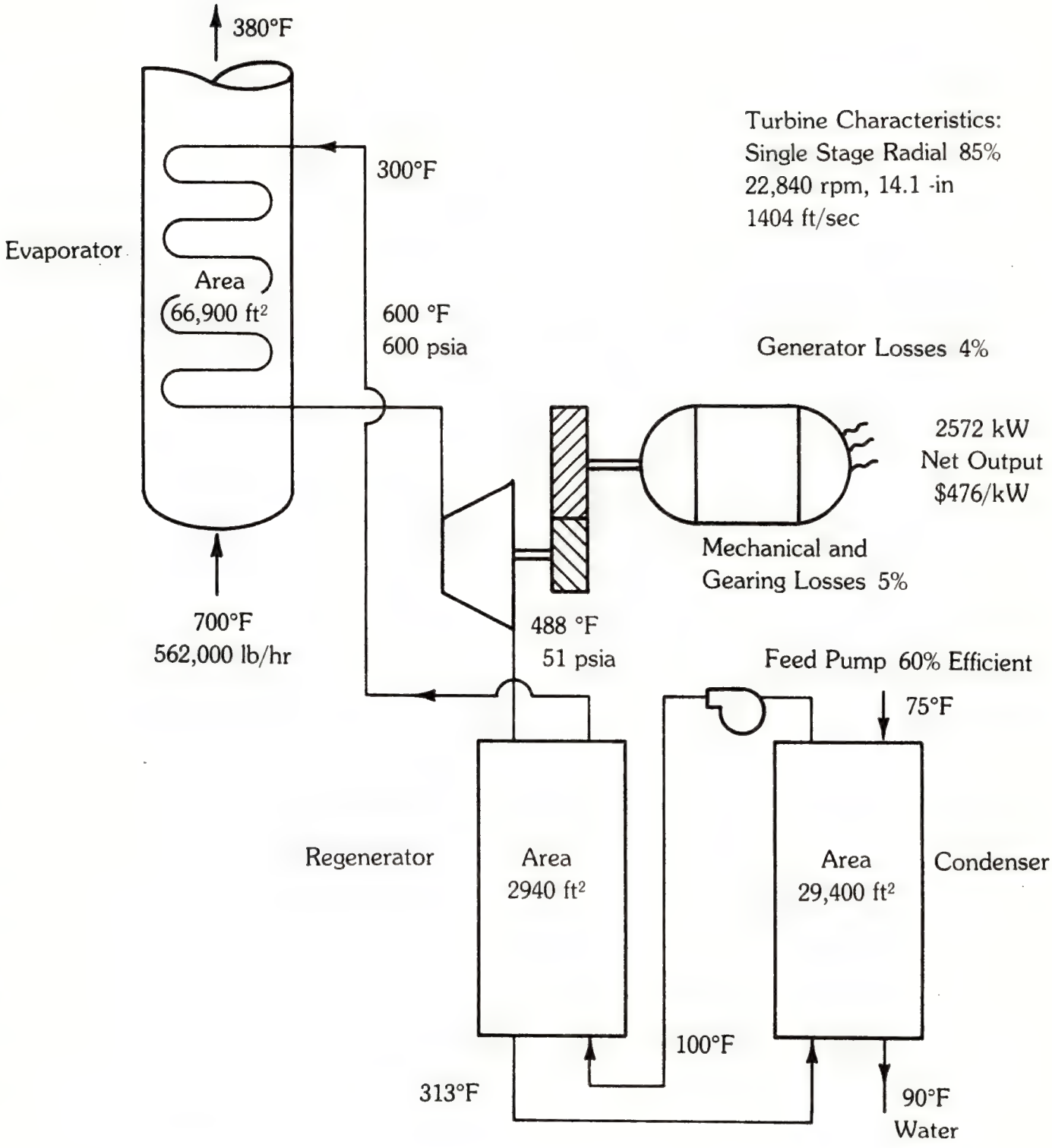

Figure 36 Illustration of Rankine Cycle With Butane For Most Cost Effective Case Considered for a 600°F Turbine Inlet

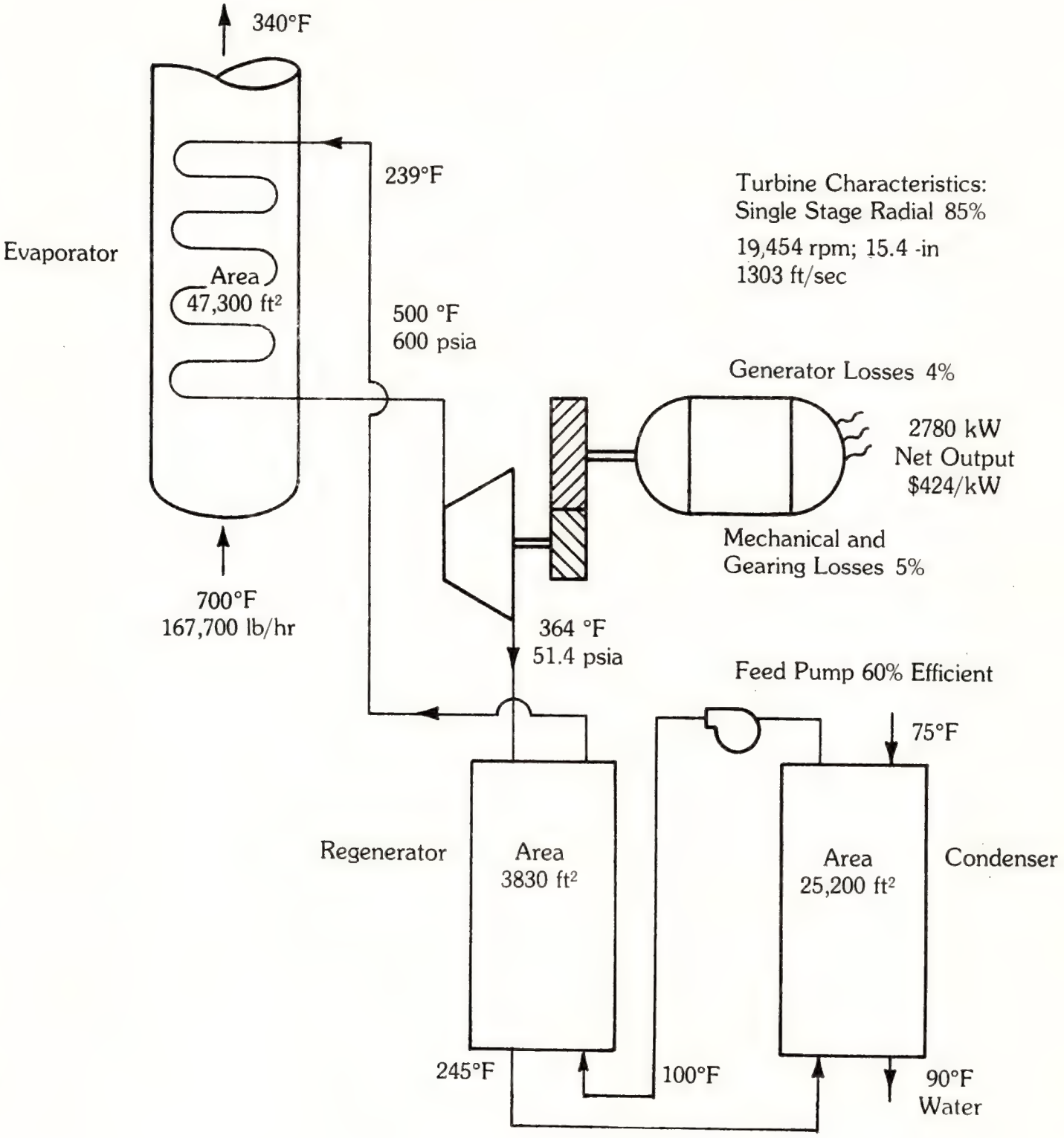

Figure 37 Illustration of Rankine Cycle with Butane For Most Cost Effective Case Considered for a 500°F Turbine Inlet Case.

TABLE 12

COMPARISON OF THE EFFECT OF TURBINE INLET TEMPERATURES WITH A SUPERCRITICAL BUTANE CYCLE

Turbine Inlet Temperature	600°F	500°F
Turbine Inlet Pressure	600 psia	600 psia
Evaporator Surface Area	66,900 ft^2	47,300 ft^2
Evaporator Surface Area/Unit Output	26.0 ft^2/kw	17.0 ft^2/kw
Regenerator Surface Area	2,940 ft^2	3830 ft^2
Condenser Surface Area	29,400 ft^2	25,200 ft^2
Stack Exit Temperature	380°F	340°F
Heat Flow Used	45.9 x 10^6 Btu/hr	51.7 x 10^6 Btu/hr
Delivered Power	2,572 kw	2,780 kw
Overall Efficiency	19.1 percent	18.4 percent
Estimated System Cost	$476/kw	$424/kw

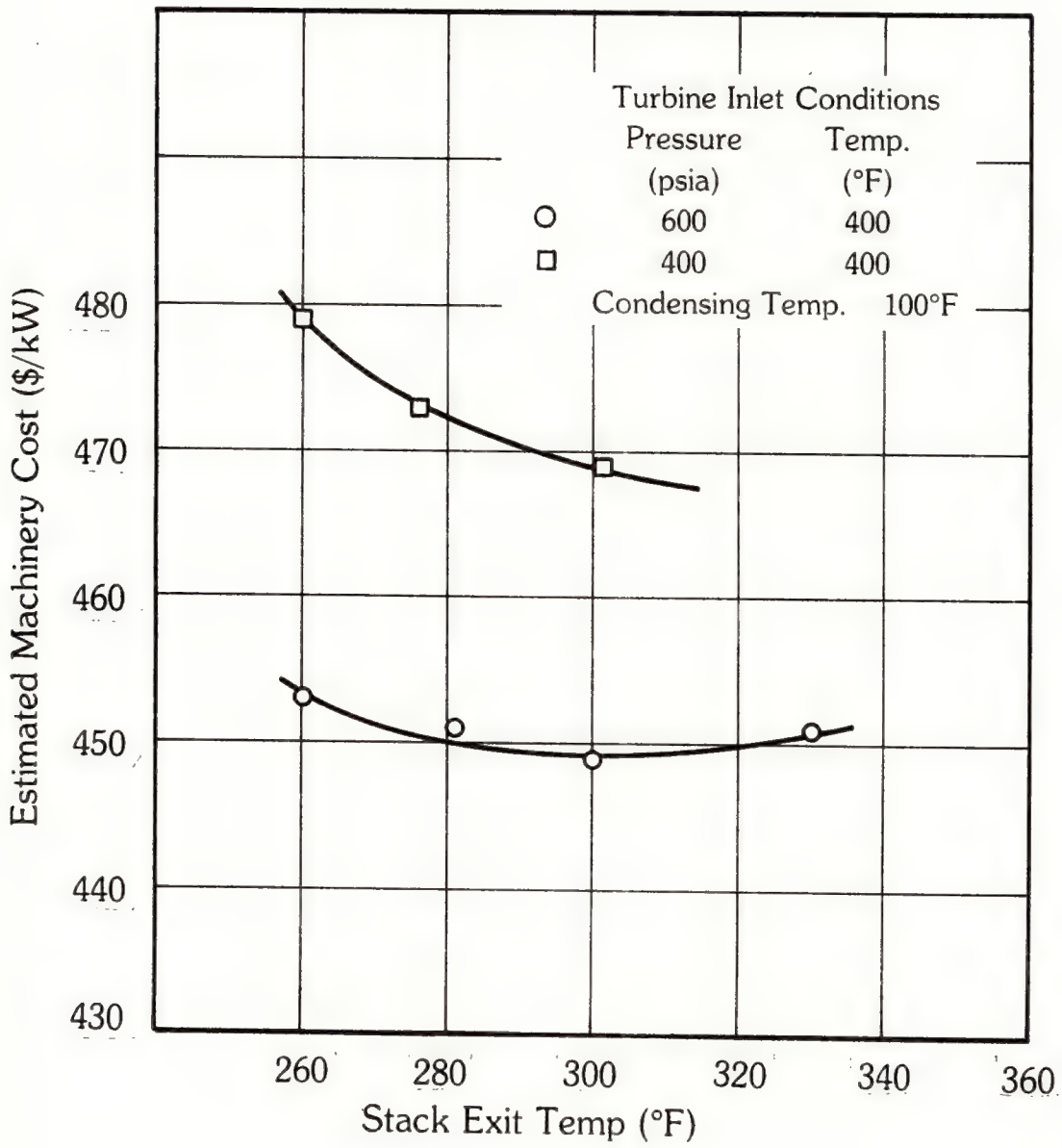

Figure 38 Cost Comparison of Various Cycle Conditions With R-114 With 700°F Hot Gas Source

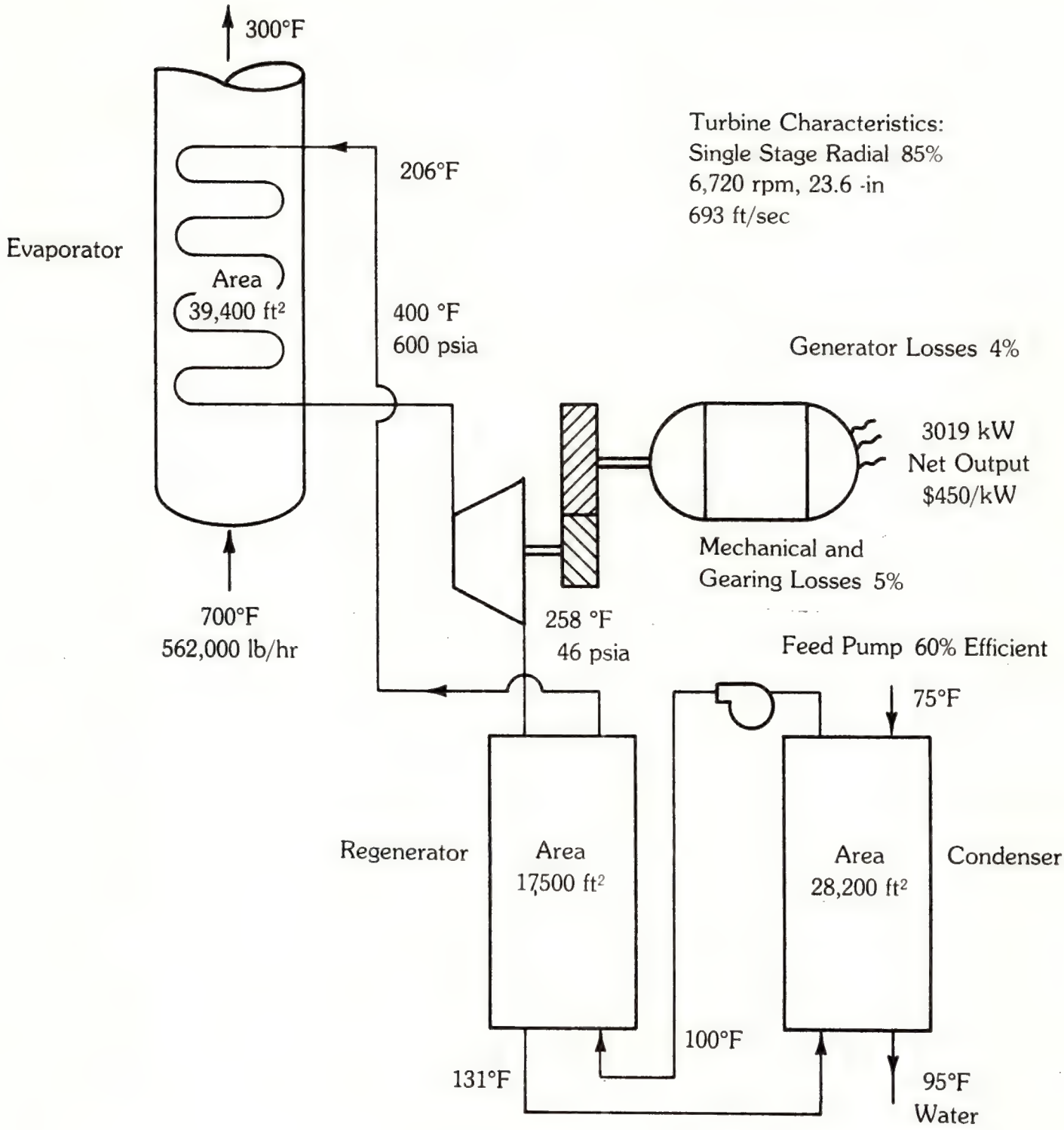

Figure 39 Illustration of Rankine Cycle With R-114
For Most Cost Effective Case Considered

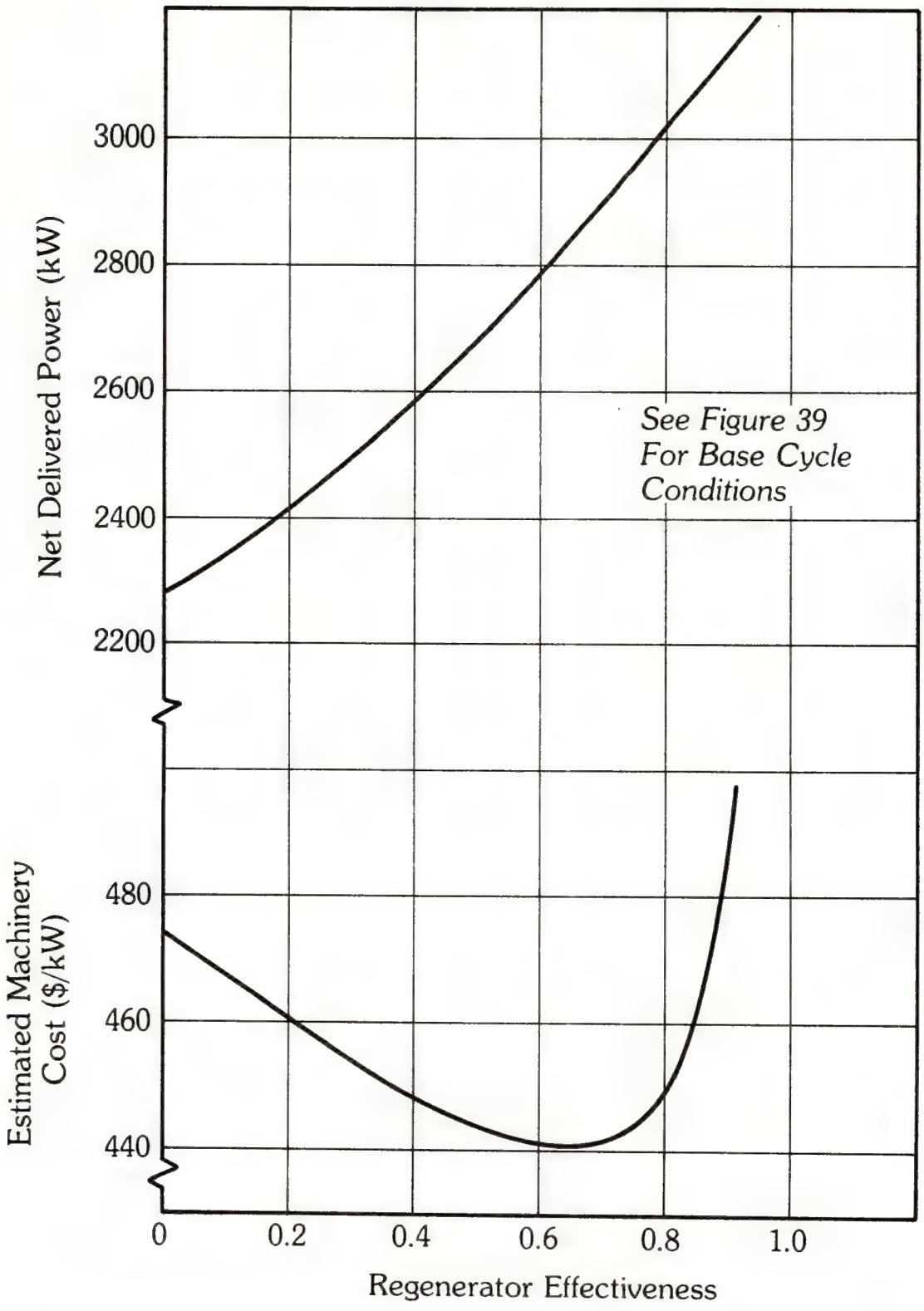

Figure 40 The Effect of Regeneration on System Cost and Power Output For an R-114 Cycle With 600 psia and 400°F Turbine Inlet Conditions

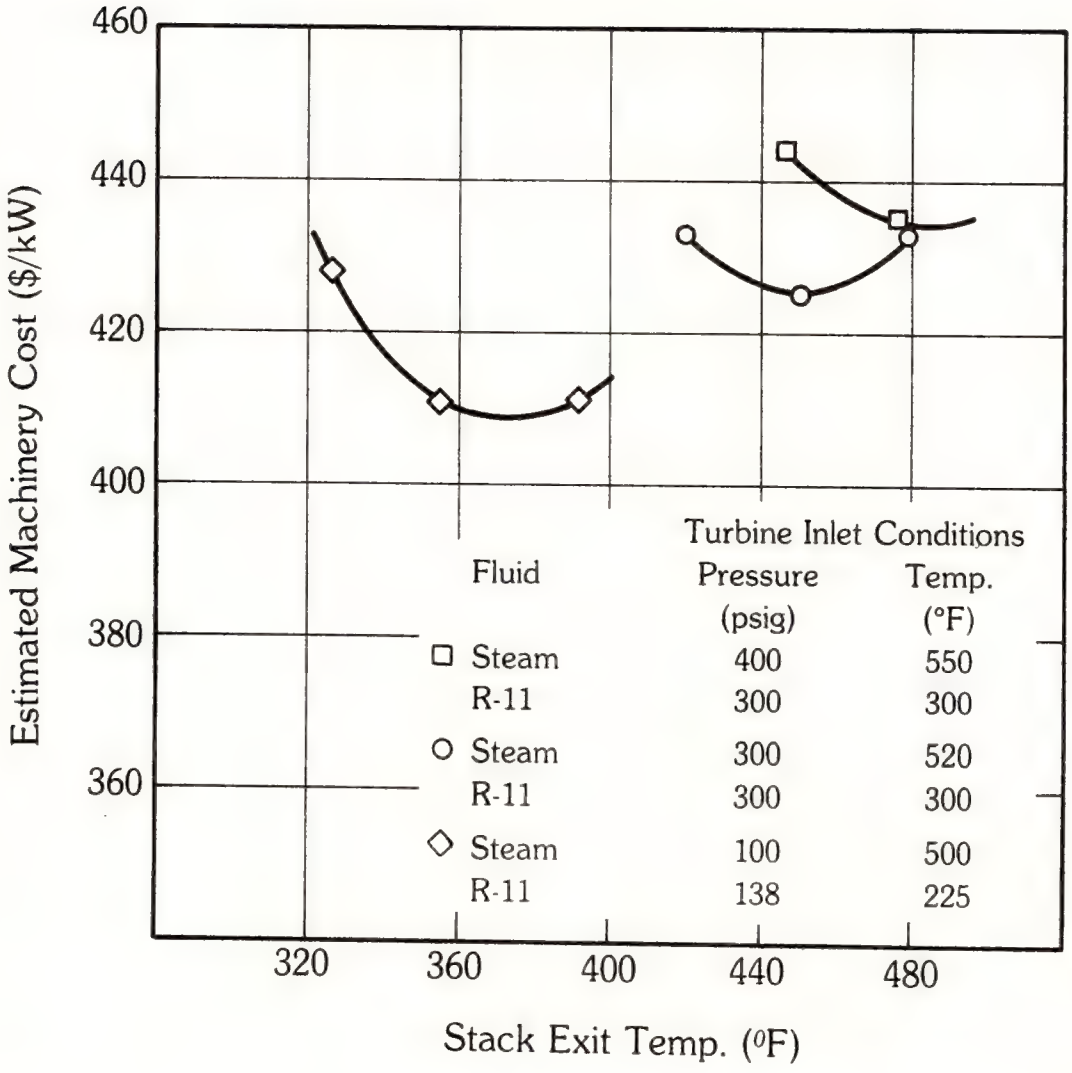

Figure 41 Cost Comparison For a Binary Steam/R-11 System With 700°F Hot Gas Source

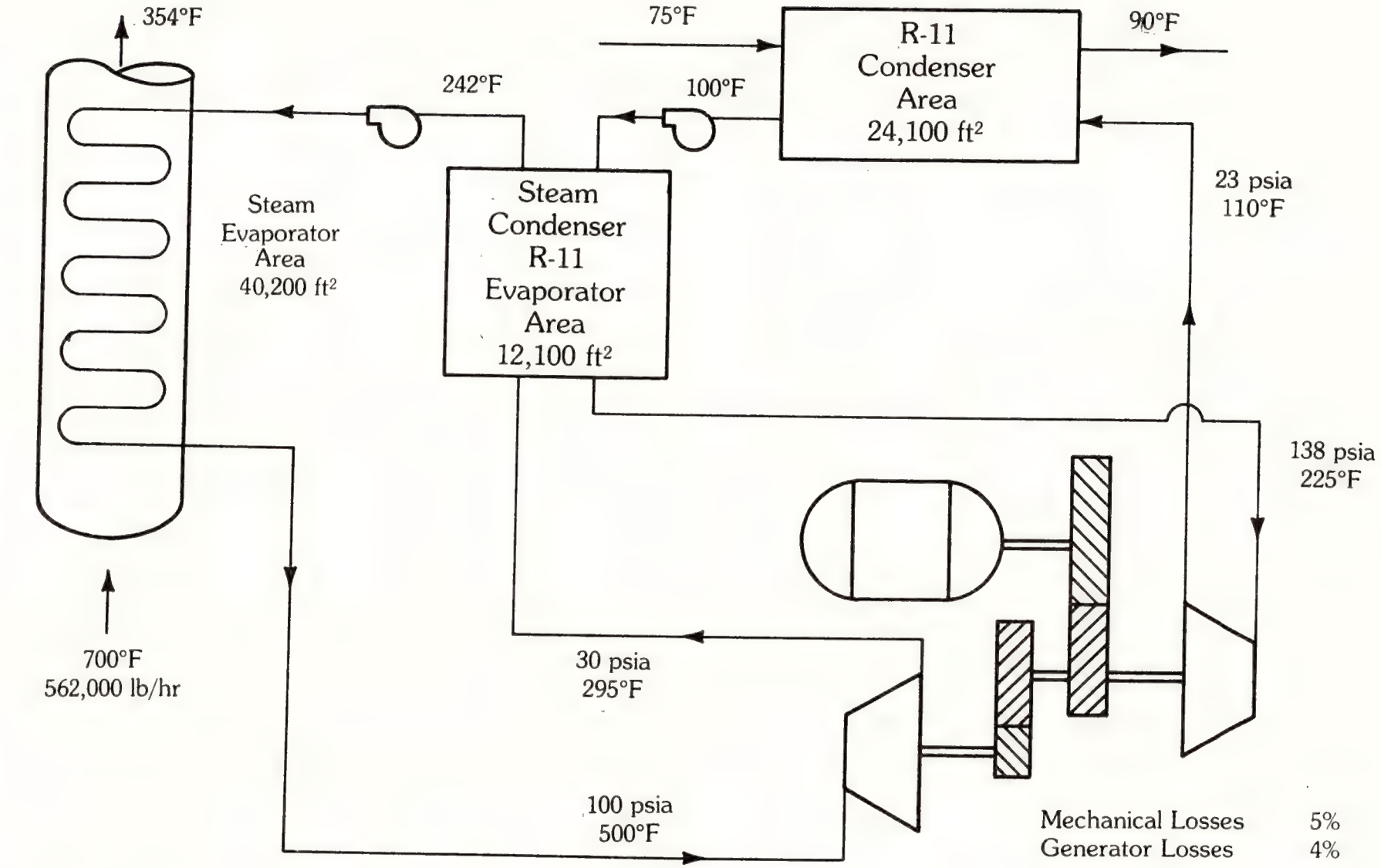

Figure 42 Schematic of Binary Steam/R-11 Cycle

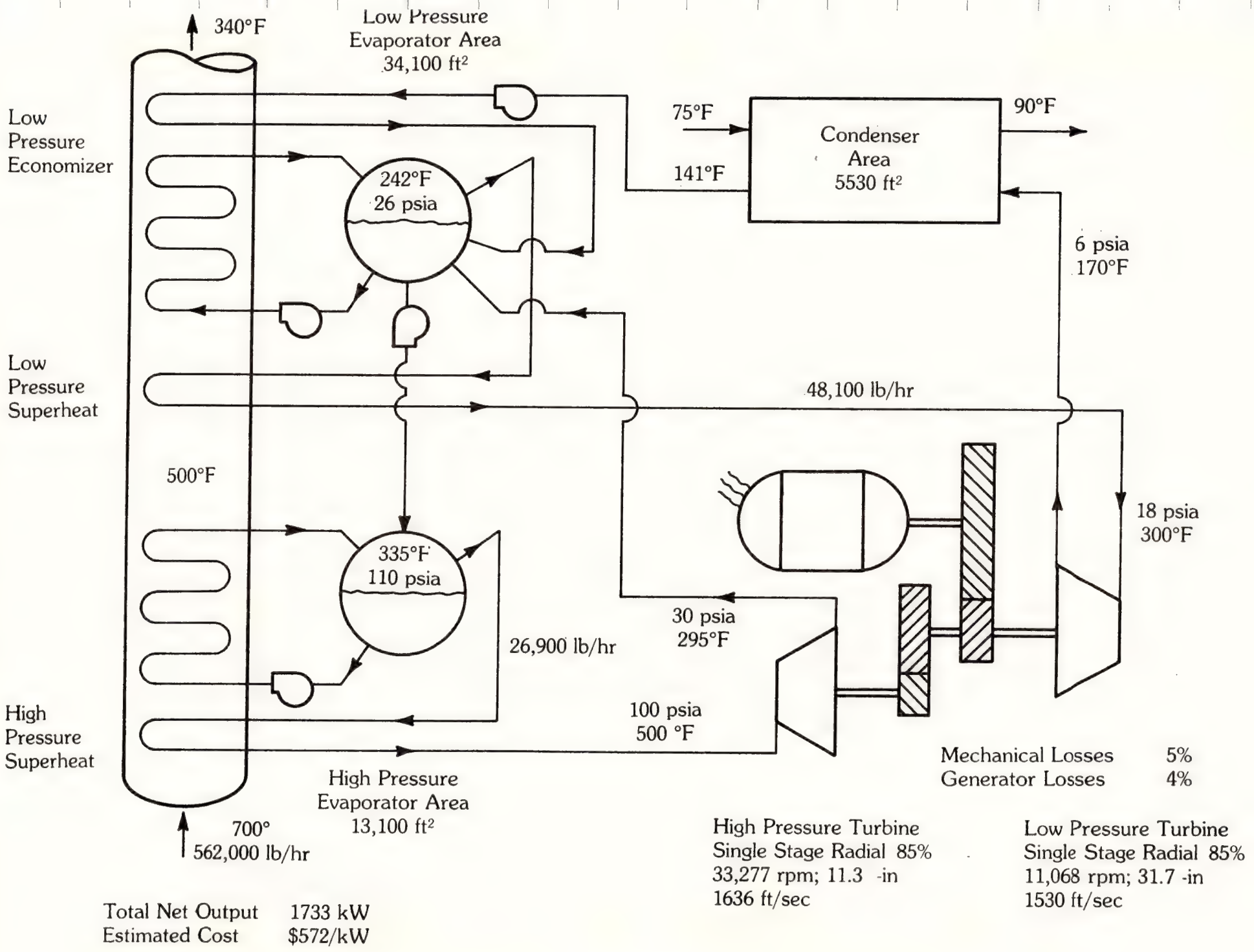

Figure 43 Schematic of Simple Two Level Steam Cycle

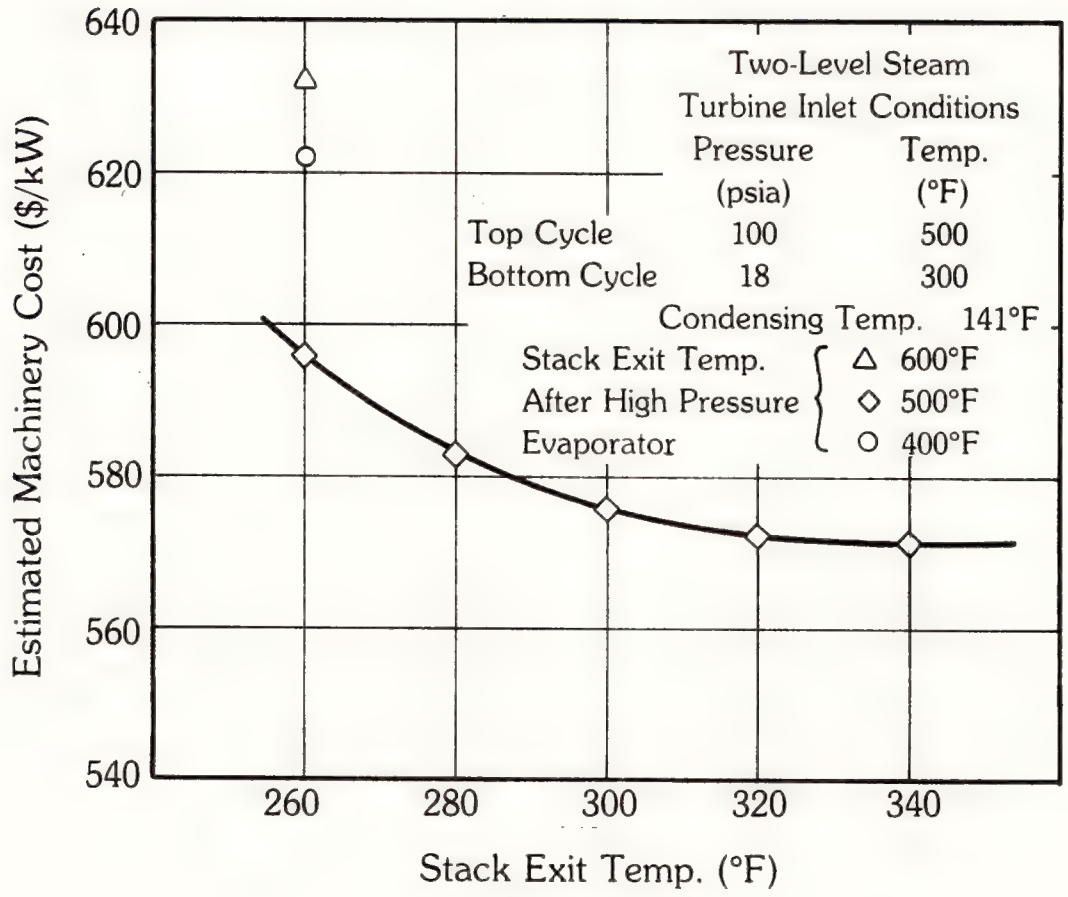

Figure 44 Cost Comparison of Various Cycle Conditions With Two Level Steam With 700°F Hot Gas Source

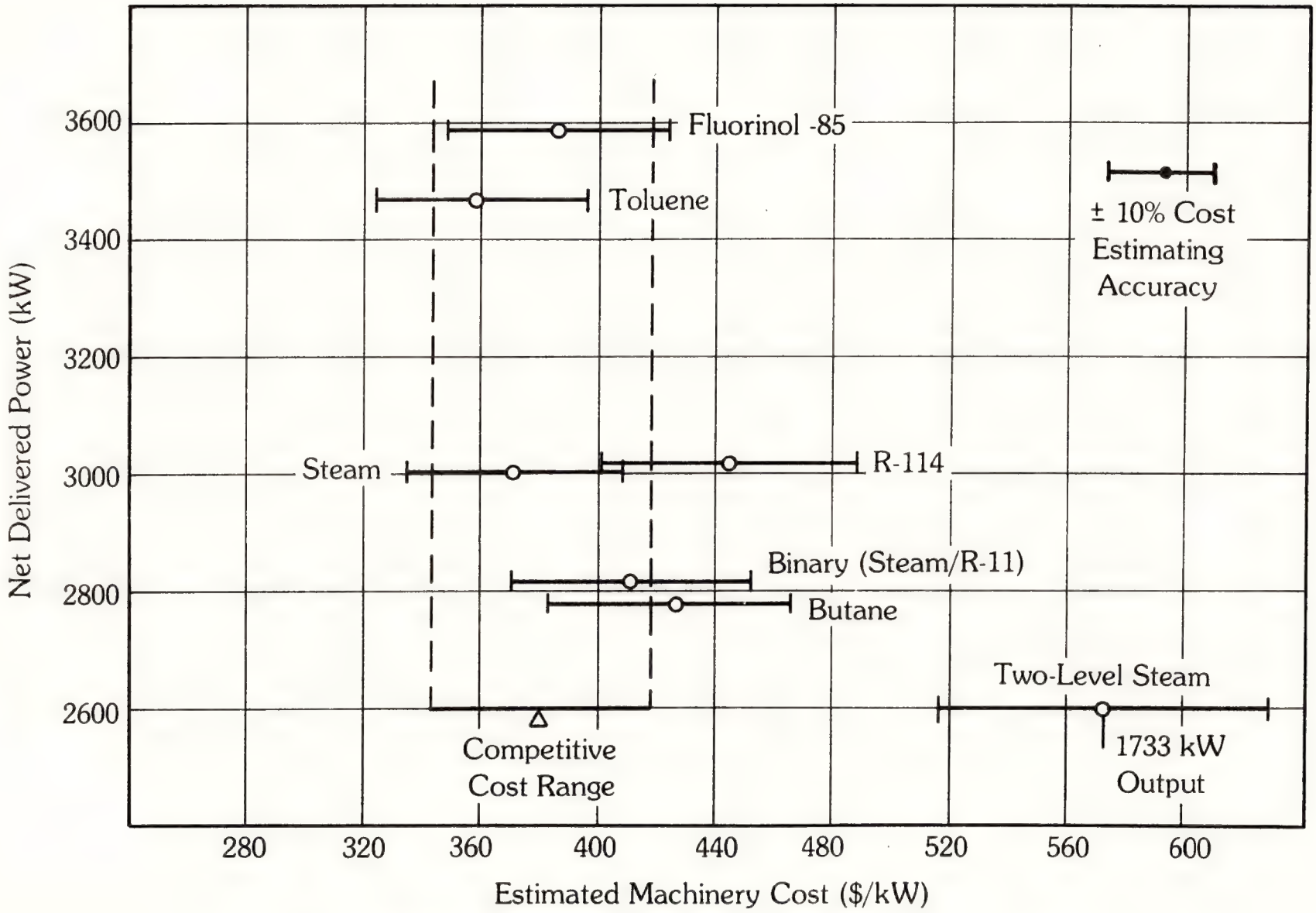

Figure 45 Alternate Working Fluids For Cost Optimized Heat Recovery With A 700°F Waste Gas Source and 100°F Condensing Temperature

- ☐ Separate Machinery Components
- ☐ Costly Field Interconnections
- ☐ High and Low Speed Couplings in the Field
- ☐ Maximum Space Required
- ☐ Numerous Seals with Attendant Leakage
- ☐ Extended Field Supervision Machinery
- ☐ Start-up and Check-out Done in the Field

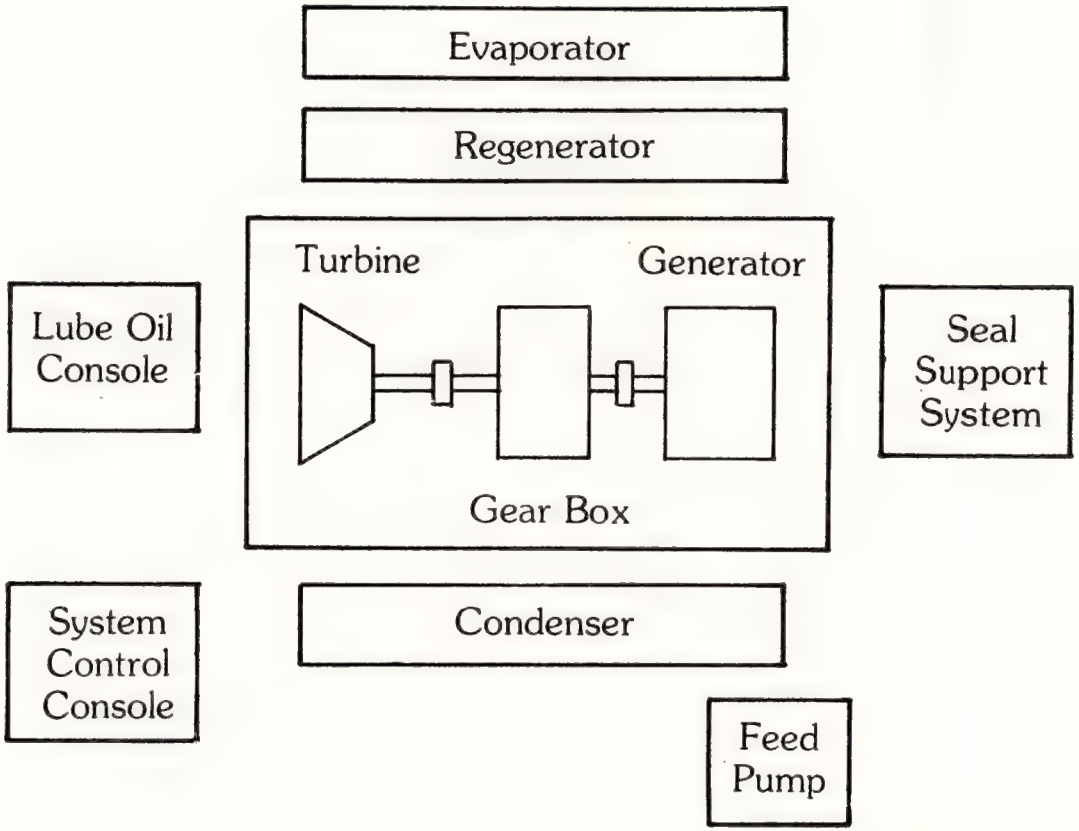

Figure 46 Conventional System Design Approach

- ☐ Unitized Machinery and Control Construction
- ☐ No Field Interconnections for Machinery System
- ☐ No High Speed Coupling
- ☐ Reduced Space Requirements
- ☐ Reduced Seal Requirements and Leakage
- ☐ Reduced Field Supervision
- ☐ Machinery Started-up and Checked-out at Factory

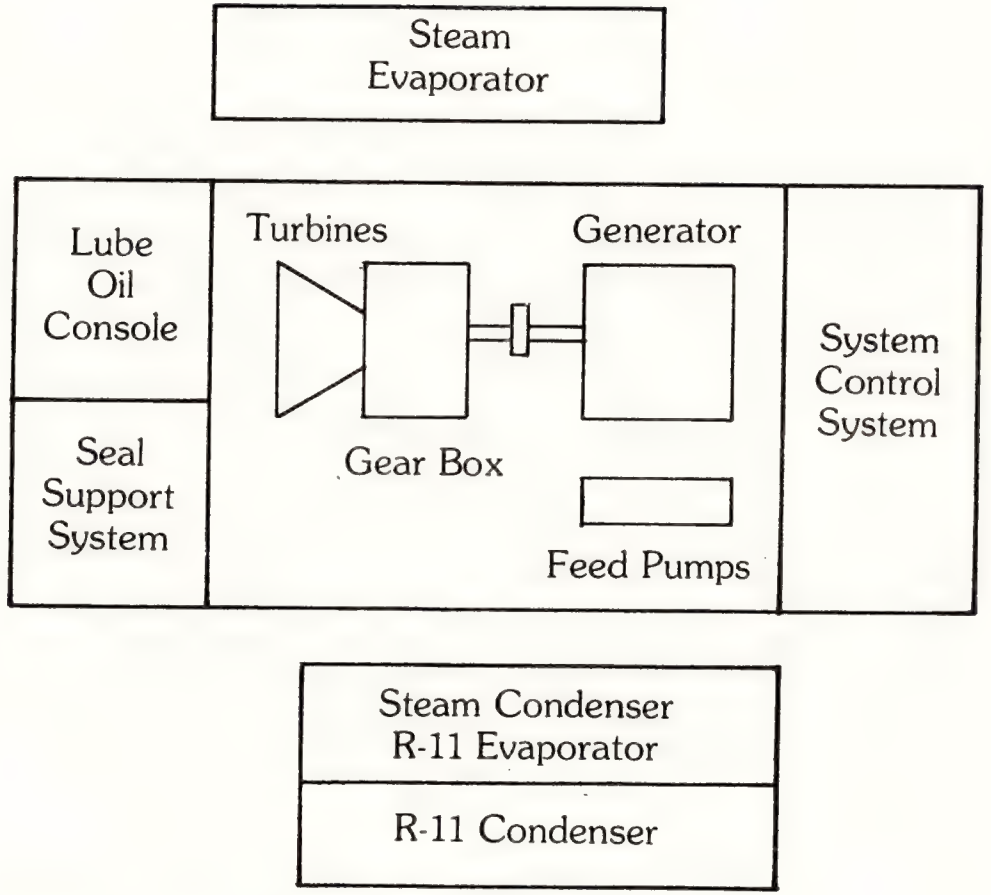

Figure 47 MTI/Turbonetic System Design Approach

TABLE 13

WORKING FLUID COMPARISON FOR HEAT RECOVERY
FROM A 700°F WASTE GAS SOURCE

SYSTEM CONSIDERATION	WORKING FLUID					
	BINARY	FLUORINOL	TOLUENE	STEAM	BUTANE	R-114
Machinery Unit Cost	Competitive	Competitive	Competitive	Competitive	High	Highest
Design Approach	Packaged	Packaged	Built-up[1]	Built-up[3]	Packaged	Packaged
Turbomachinery	Two radial stages; Two gear reductions	Multiaxial; Single spool; Single gear reductions	Multiaxial;[2] Two spool; Two gear reductions	Multiaxial[3] Two spool; Two gear reductions	Single radial; Single gear reduction	Single radial; Single gear reduction
Fluid Stability	No Problems	Questionable	No Problems	No Problems	Possible Problems	Possible Problems
Fluid Safety	No Problems	Toxicity (?)	Toxicity (?) Flammable	No Problems	Flammable	No Problems
Fluid Availability	General	Limited	General	General	General	General
System Pressure Range	1.6 to 9.4 atm	0.22 to 47.6 atm	0.07 to 20.4 atm	0.06 to 4.1 atm	3.5 to 40.8 atm	3.1 to 40.8 atm
Heat Exchangers	Binary Condenser/ Evaporator	Regenerator	Regenerator	Feed Preheater	Regenerator	Regenerator
Expected Total Installed Cost	Competitive	Competitive-High	Competitive-High	High	Competitive-High	High
Output Ranking	5	1	2	4	6	3

1 Conventional turbomachinery approach would involve field erection. Reference 11 uses packaged design. See note 2.

2 Conventional turbomachinery approach; Reference 11 using single stage axial in packaged system.

3 Reference 7 indicates a packaged system with a single spool multistage turbine direct driving a 3,600 rpm alternator.

4.0 SYSTEM COMPARISON FOR MEDIUM TEMPERATURES

Power recovery from gaseous waste heat sources in the 400°F to 600°F range is that range in which organics begin to have clear performance, operational, and cost advantages over binary systems. To compare the performance of these fluids, an application was selected to recover the heat from the exhaust of a Diesel engine. The assumptions and cycle limitations enumerated in the prior section are followed here.

The application selected is the recovery of waste heat from a single Nordberg Model TSGL-2110-SC dual fuel Diesel engine rated at 7675 BHP. While the actual exhaust temperature is in the 510°F to 520°F range, a 500°F exhaust temperature was assumed for this comparative analysis. The exhaust flow rate is 167,700 lb/hr which would provide a recoverable heat potential of 10,224,000 Btu/hr (2996 kw-hr) when cooled to an exit temperature of 260°F. This application is similar to an actual binary demonstration system that is being installed in a municipal power plant in Rockville Centre, New York, by MTI under a contract with the U.S. Department of Energy. The difference between the demonstration and this screening analysis is that the demonstration uses the output of two Diesel engines in order to assure high ultilization of the binary system. The demonstration program is discussed further in Section 5.0.

The fluids considered in the comparative analysis in this section are steam, Fluorinal-85, toluene, butane, R-114, and a binary steam/R-11 system with state points identical to the demonstration systems for Rockville Centre.

The condensing medium for all comparisons is water which is being supplied from a cooling tower at 61°F. A 6°F temperature rise is allowed. The cooling tower design performance is based on the weather conditions at Rockville Centre, New York. The resulting condensing temperature for the working fluids in the power cycle is 81°F.

4.1 Cycle Comparisons

4.1.1 Simple Steam Cycle

A simple steam cycle was considered with a turbine inlet temperature of 450°F and a condensing temperature of 81°F. Requiring a dry expansion with an 80 percent efficient multistage axial turbine fixed the turbine inlet pressure at 10 psia. The 450°F turbine inlet condition was selected for the 500°F source since the optimum cycle for the 700°F source was 650°F turbine inlet. Extensive cycle optimizations were not carried out for this analysis. The resulting cycle conditions are shown in Figure 48. The cycle optimization for selection of the stack exit temperature is shown in Figure 49. As with the other simple steam cycle, a feed preheater will be required to avoid stack gas condensation.

The pressure levels in the cycle are extremely low and are subatmospheric throughout the entire operational range. Variations in cycle conditions including a relaxation on the requirement for a dry exhaust will not significantly increase the peak cycle pressure. The problems of running low pressure steam turbines will be compounded in a small scale system as will result here. From an operational standpoint, steam will be undesirable in such an application. Further, when a detail design and costing of such a system is conducted, it would probably result in higher costs than the screening cost estimates.

4.1.2 Fluorinol Cycle

A number of Fluorinol-85 cycle points were evaluated for the heat recovery conditions in this section. A multistage axial turbine with an 80 percent total efficiency was assumed. As before, an 80 percent effective regenerator was assumed. The results are shown in Figure 50. The schematic of the cost optimized cycle is shown in Figure 51.

4.1.3 Toluene Cycle

A number of toluene cycles were considered. The optimum system, as shown in Figure 52, has a turbine inlet condition of 400°F and 55 psia. The schematic of the cycle is shown in Figure 53.

As with the previous analysis, a multistage axial turbine with an overall efficiency of 80 percent and an 80 percent effective regenerator was assumed.

4.1.4 Butane Cycle

A number of butane cycles were considered for the heat source considered in this section. These cycles included two supercritical and two regular cycles, with one of each having an inlet temperature of 400°F and 350°F. The cost optimizations are shown in Figure 54. In this analysis, as with the previous, a single stage radial turbine with an efficiency of 85 percent was assumed even though the pressure ratio is of the order of 16 rather than 6. Also, a 45 percent effective regenerator was assumed. The schematic of the cost optimized cycle is shown in Figure 55.

As can be seen in Figure 54, the supercritical cycles are more effective in terms of cost than the regular cycle. The differences between the 400°F inlet cases are most striking. Table 14 presents some comparative data for these two cycles. Two factors contribute to the supercritical cycle's being more cost effective. First, in the case of butane, the supercritical cycle is 5 percent more efficient (20.6 percent versus 19.5 percent). This is due to the properties of the fluid. Second, there is significantly less (10 percent) boiler surface required for the supercritical cycle. This is due to the fact that in the supercritical case, only 80 Btu/lb is added in the superheat region, while in the regular cycle, 88 Btu/lb is added in the superheat region and 68 Btu/lb is added in the vaporization region. The overall heat transfer coefficient in both the superheat and vaporizing regions is about 60 percent of that in the economizing region. The net result is that more heat transfer surface and cost is required for a given unit output. The reduced boiler surface area and the high cycle output make the supercritical cycle cost about 5 percent less than the regular cycle.

4.1.5 R-114 Cycle

Three R-114 cycles were considered for the waste heat source in this section, one of which is a supercritical cycle. As with the previous R-114 cases, an 85 percent

efficient single stage radial turbine was assumed even though the pressure ratio is of the order of 16 rather than 6. The regenerator was taken as 80 percent effective. The results of the cost optimization are shown in Figure 56. The schematic of the cost optimized system is shown in Figure 57.

As in the case of butane, the supercritical R-114 cycle is more cost effective than the regular cycle. Table 15 presents some comparative data for the two cycles. The most significant difference is in the amount of boiler surface needed per unit output. The regular cycle requires about 15 percent more surface. Again, this is due to the relative amounts of heat input in the superheat and vaporization region for each cycle. The cycle efficiency is almost equal for each cycle. This means that heat transfer costs account for the 5 percent difference in machinery costs for the two cycle.

4.1.6 Binary Steam/R-11 Cycle

The binary steam/R-11 cycle selected for the heat source considered in this section is the cycle optimized for virtually an identical condition for an ongoing demonstration program. The differences between the cycle shown in Figure 58 and the one discussed in Section 5.0 are due to the slightly lower supply temperature (500°F versus 520°F) and a slightly lower design heat flow (167,000 lb/hr versus 205,000 lb/hr). The demonstration system will be discussed in detail in Section 5.0. The cost optimization for the stack gas exit temperature is shown in Figure 59.

4.2 System Comparisons

As in the previous section, the six cycles considered here are presented in Figure 60 as a plot of estimated machinery cost and net delivered power. The varability in cost among the systems is about the same in this case as in the 700°F case. The varability in power output is about twice as great in the 500°F case (a 60 percent variation from the lowest to the highest) as in the 700°F case (a 30 percent variation from the lowest to the highest). The selection of the "best" system from Figure 60 would appear to be somewhat less difficult than from Figure 45 (the 700°F case). The R-114 cycle has the lowest estimated machinery cost and almost the highest delivered power. However, let's evaluate some other selection criteria.

Selection criteria are present in Table 16. This table is abbreviated from Table 13, but the considerations in Table 13 are equally applicable here.

The only fluid that could have a stability problem in this range of application is R-114. While the operating temperature is within the upper stability limits, the supply gas temperature does exceed the temperature limits of R-114. This means that R-114 can be exposed to temperatures above its stability point if there are hot spots in the boiler or a plugged boiler tube. Depending upon the unit startup procedure, the working fluid might be required to be exposed to the full temperature of the heat source.

Toluene and butane present flammability problems and a perceived safety risk. Fluroinol is not generally available. Fluorinol, toluene, and steam have very low condensing pressures.

While the binary system does not offer as high a potential for recovered power as some other cycles, it does offer a system that does not pose any fluid stability or safety problems (perceived or actual), and offers a reasonable operating pressure range at a unit installed cost that is competitive with the other systems. These factors make it acceptable to potential users and, thus, make it a desirable concept from a potential manufacturer's point of view.

MEDIUM TEMPERATURE GAS SOURCE

NORDBERG MODEL TSGL-2110-SC
DUAL FUEL DIESEL ENGINE
7675 bhp
167,700 lb/hr
500°F

78P79

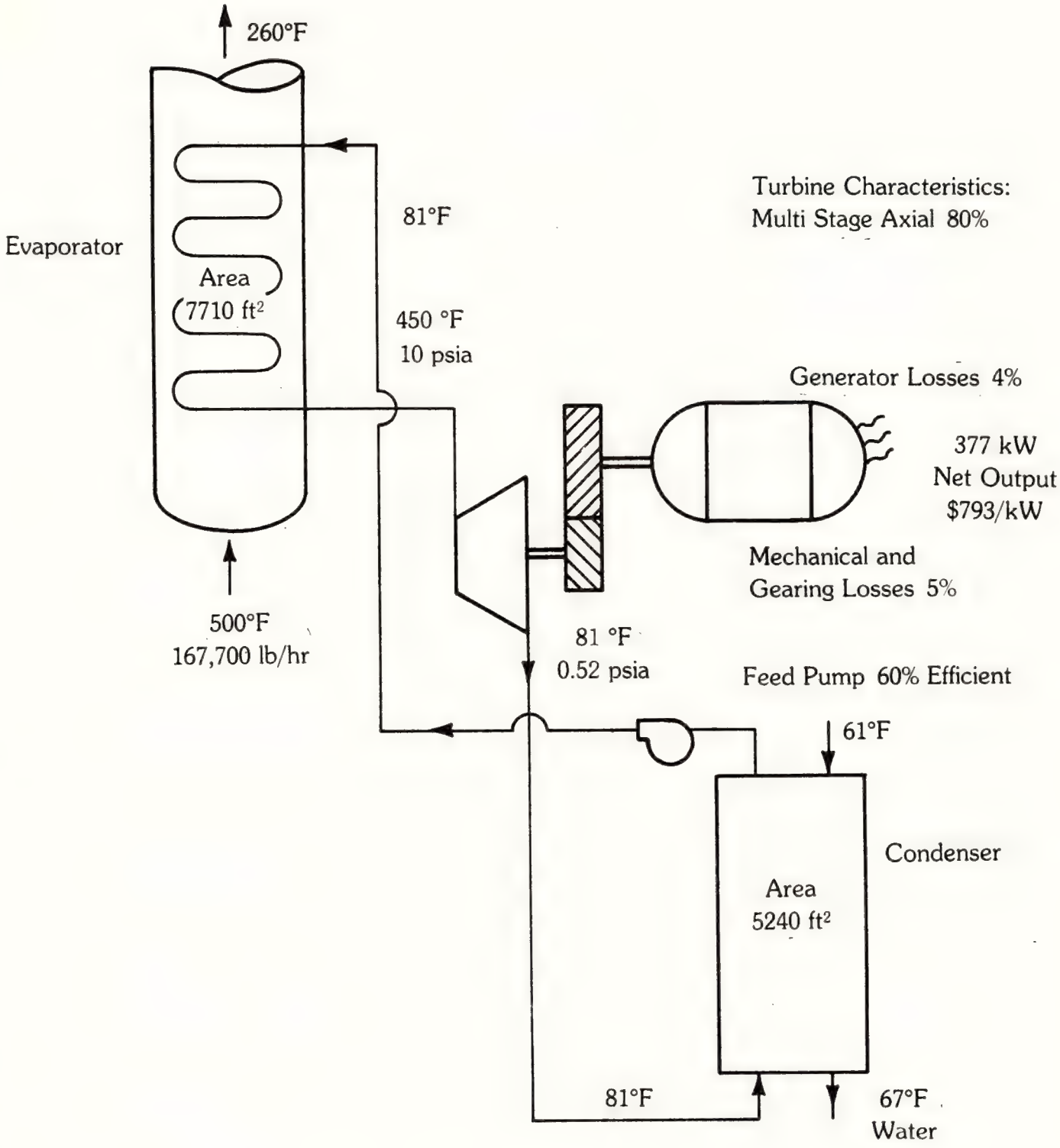

Figure 48 Illustration of Rankine Cycle With Simple Steam Cycle For Most Cost Effective Case Considered With 500°F Gaseous Source

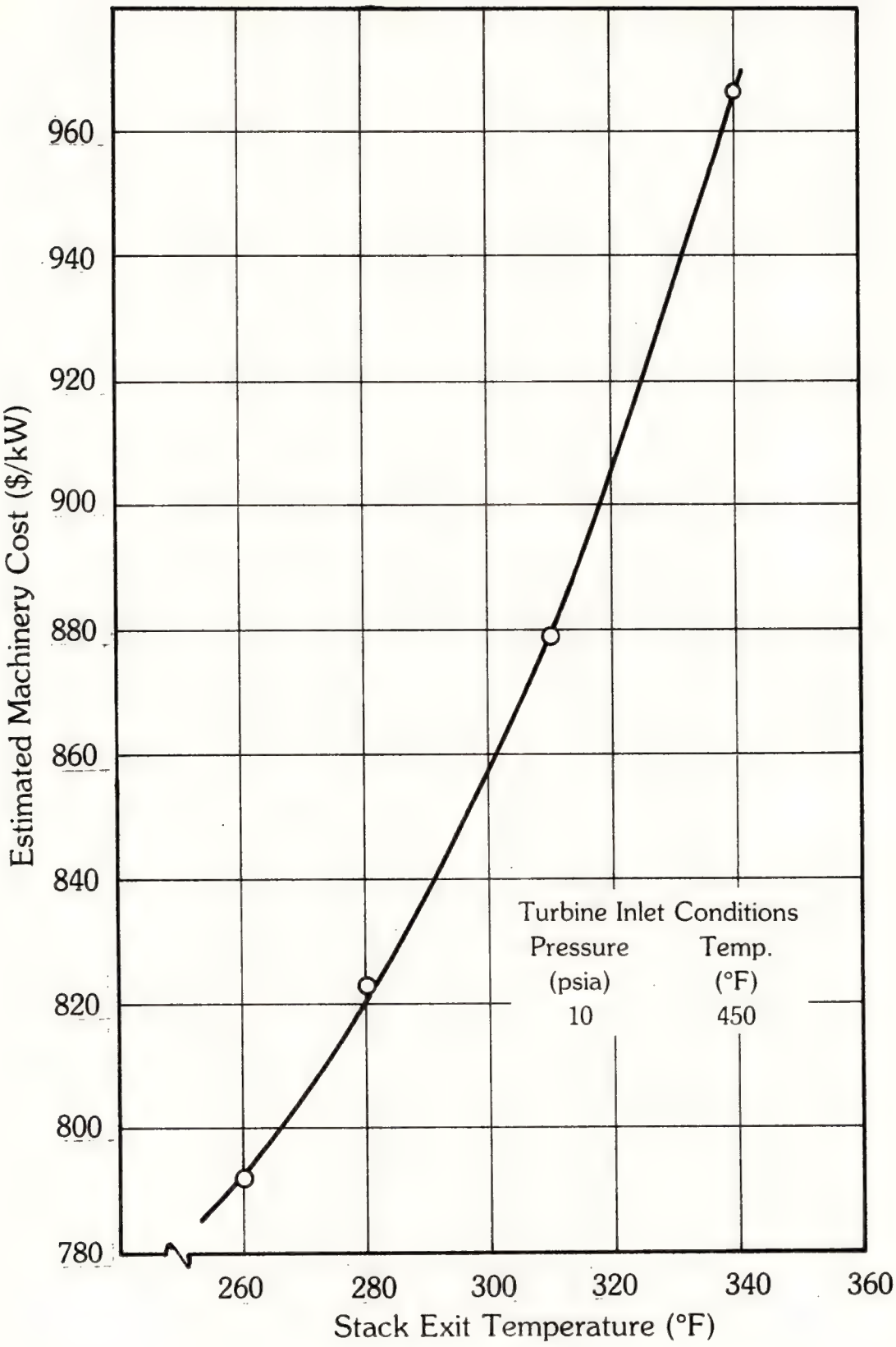

Figure 49 Cost Comparison of Simple Steam Cycle With 500°F Hot Gas Source

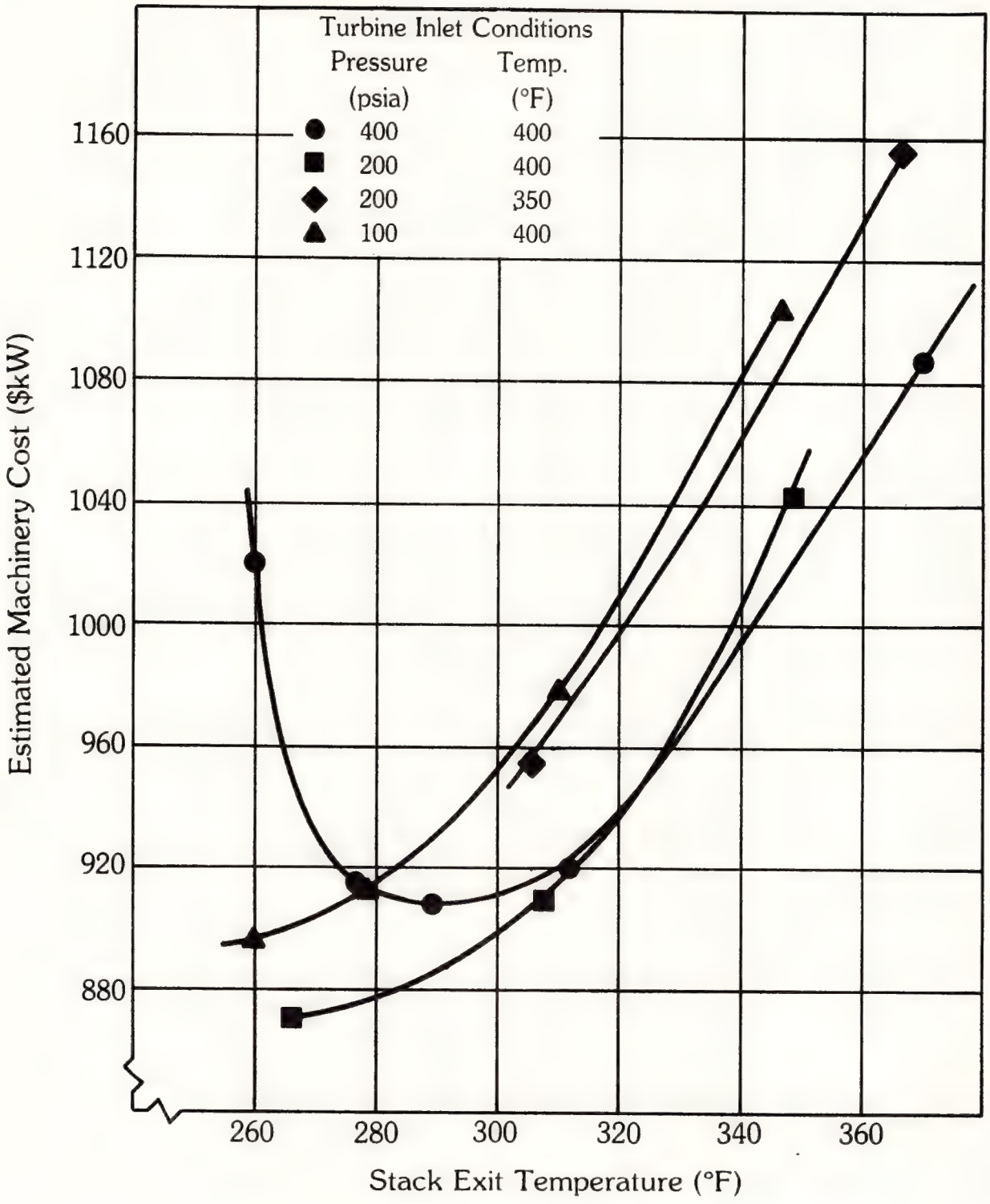

Figure 50 Cost Comparison of Fluorinol-85 Cycles With 500°F Hot Gas Source

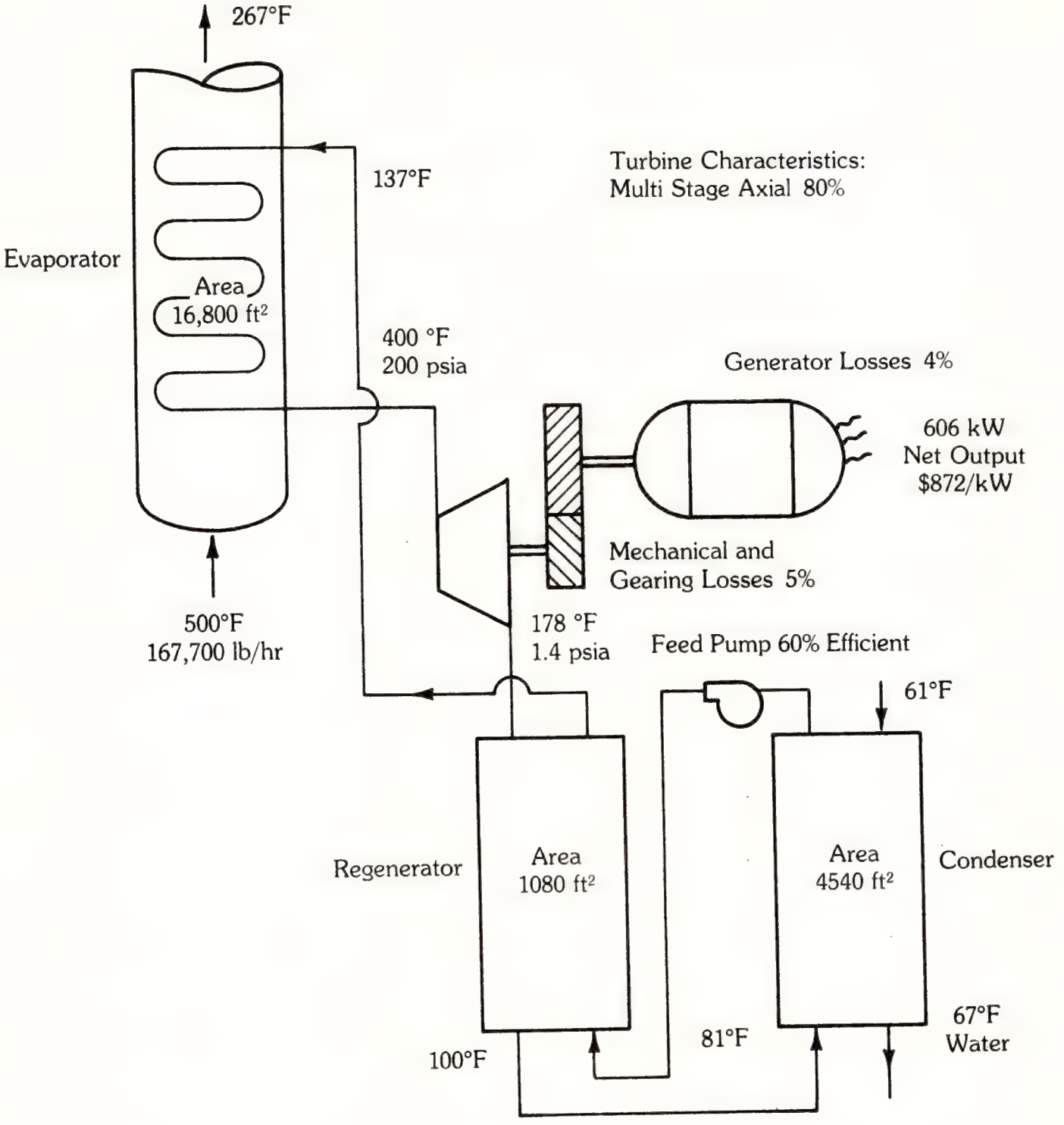

Figure 51 Illustration of Rankine Cycle With Fluorinol-85 For Most Cost Effective Case Considered With 500°F Gaseous Source

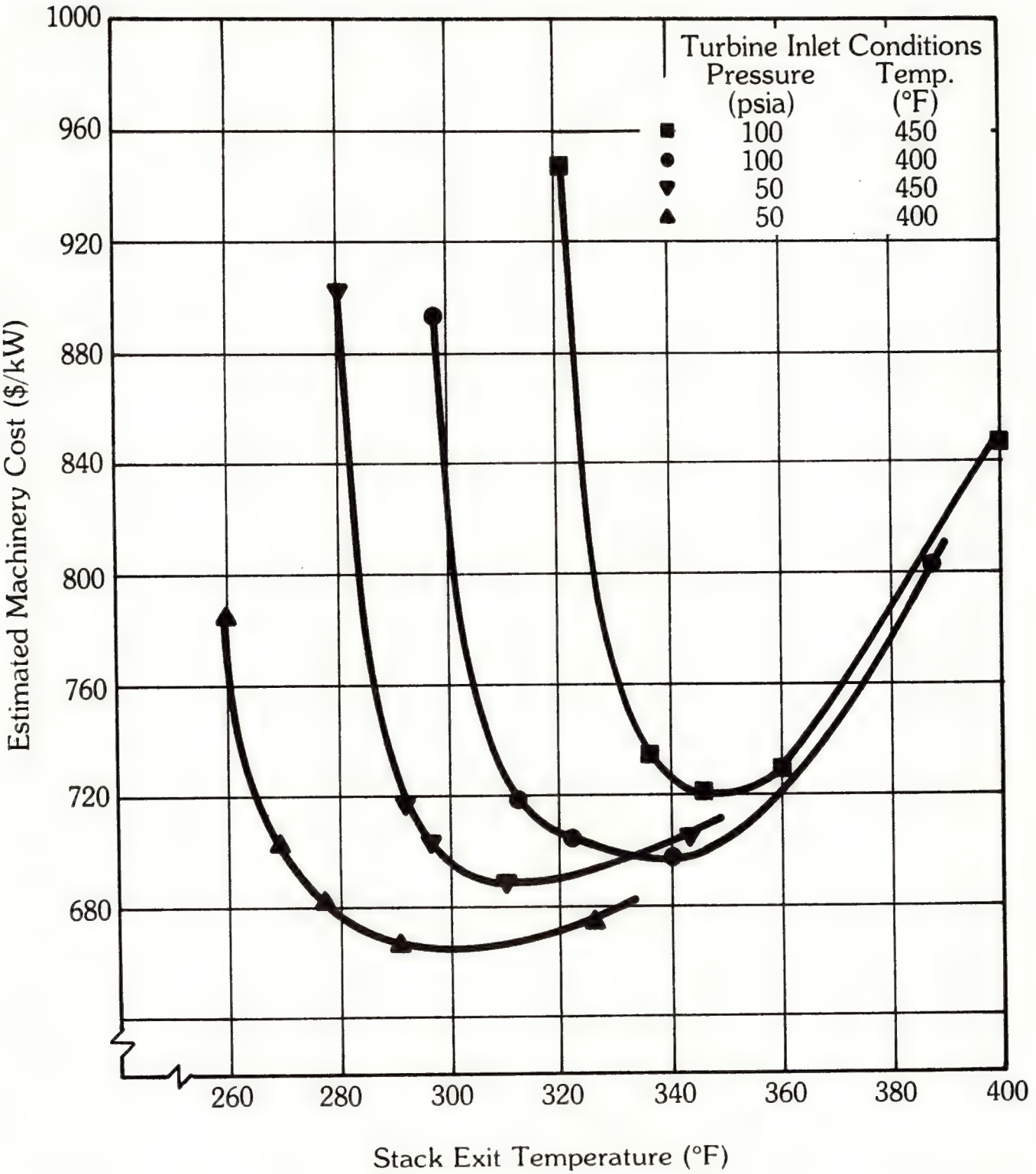

Figure 52 Cost Comparison of Toluene Cycle With 500° Gas Source

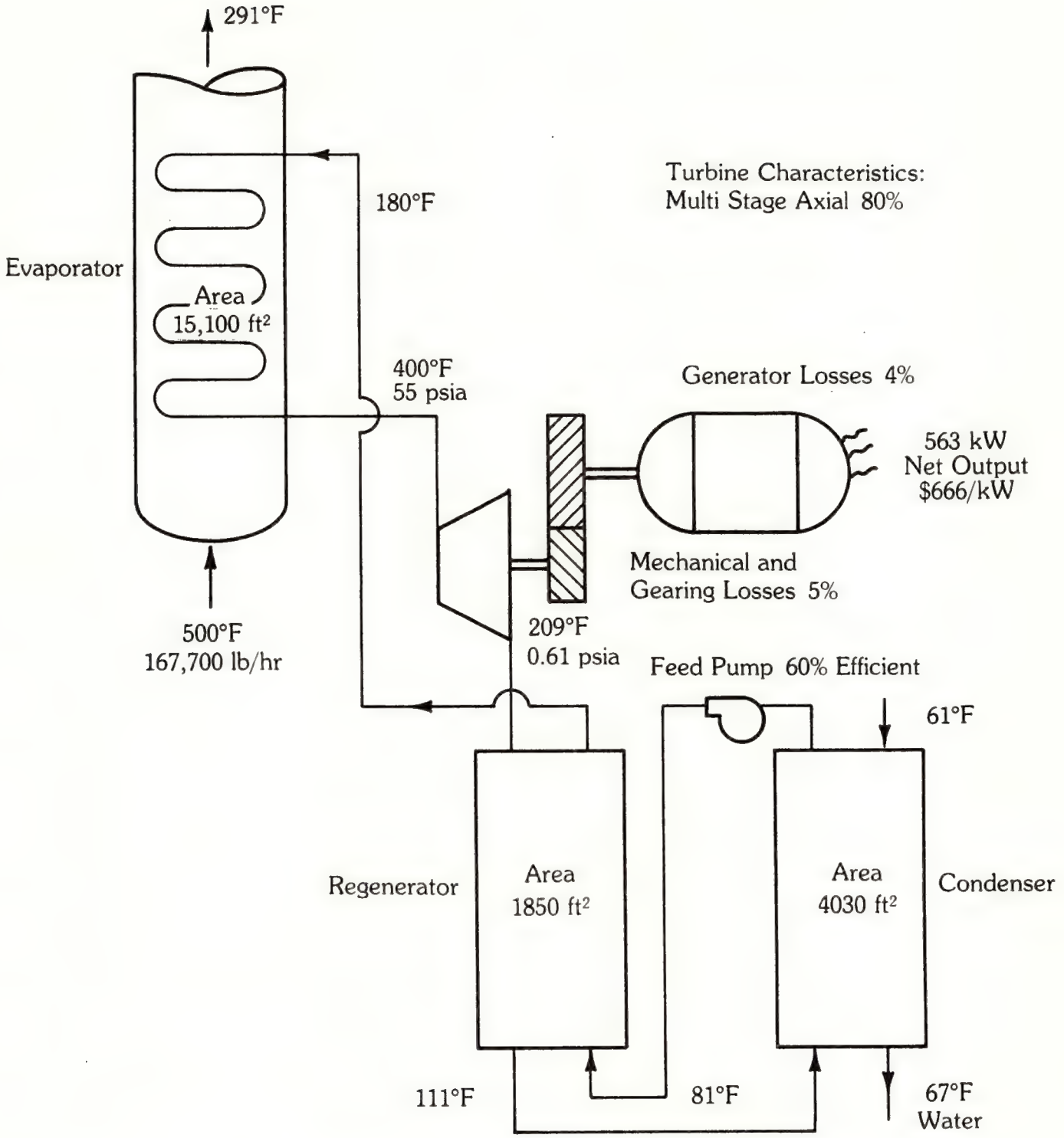

Figure 53 Illustration of Rankine Cycle With Toluene For Most Cost Effective Case Considered With 500°F Gaseous Source

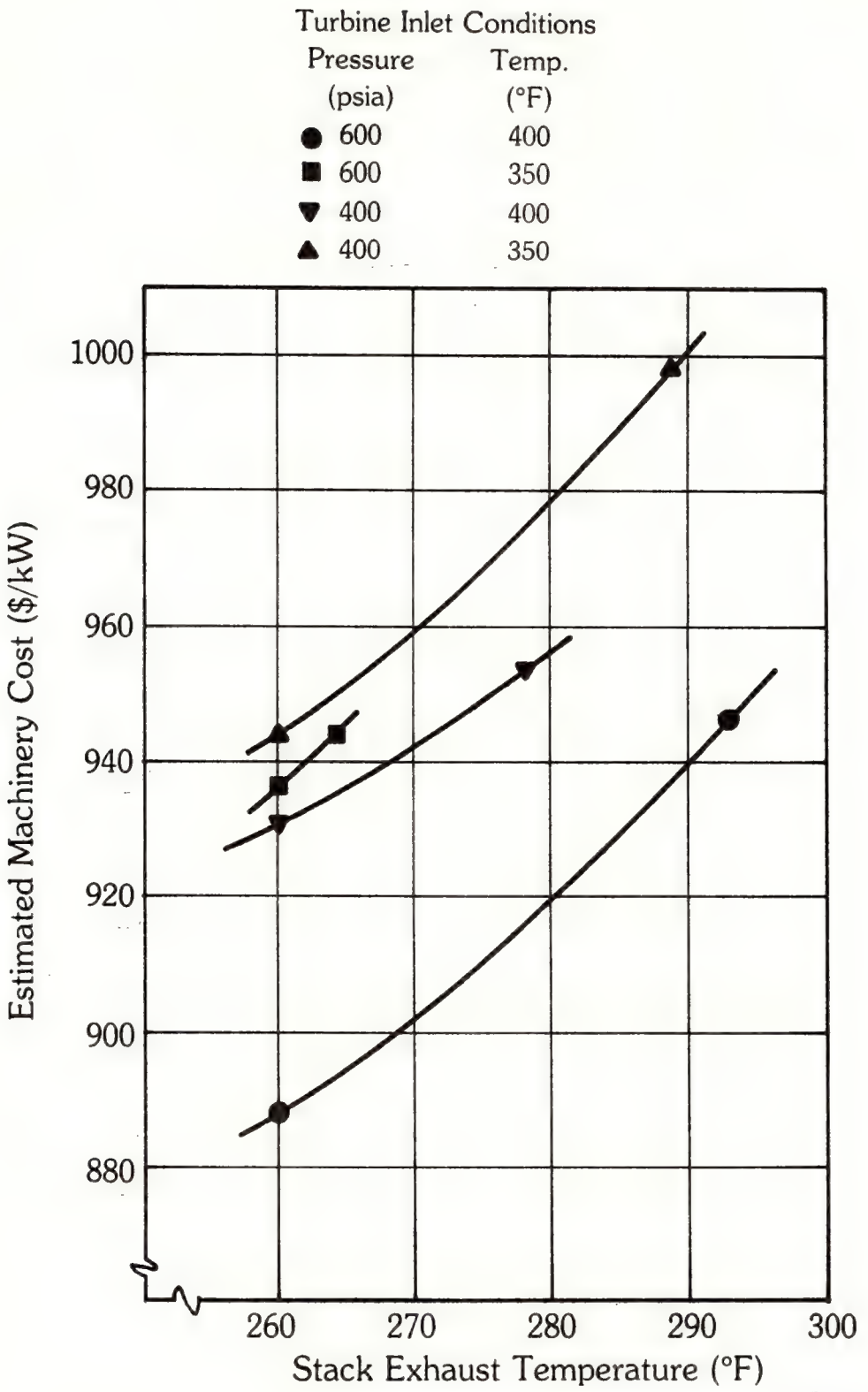

Figure 54 Cost Comparison of Butane Cycles With 500°F Hot Gas Source

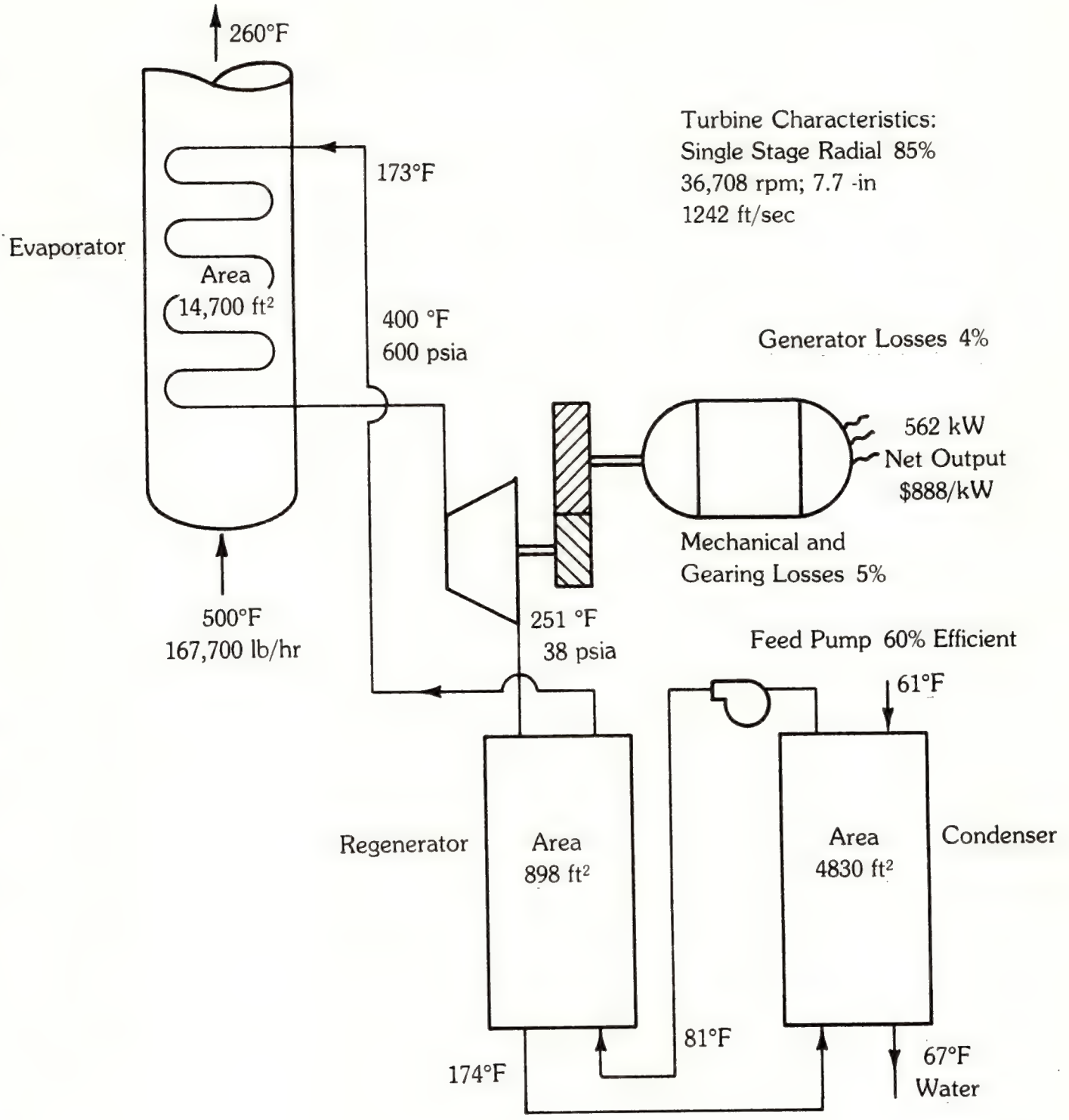

Figure 55 Illustration of Rankine Cycle with Butane For Most Cost Effective Case Considered With 500°F Gaseous Source

TABLE 14

COMPARISON OF BUTANE SUPERCRITICAL AND REGULAR RANKINE CYCLES

Comparison Parameter	Supercritical	Regular
Turbine Inlet Temp (°F)	600	400
Turbine Inlet Pressure (psia)	400	400
Turbine Exit Temp (°F)	251	278
Turbine Exit Pressure (psia)	38	38
Boiler Area Total (ft^2)	14,700	15,000
Boiler Area Per Unit Output (ft^2/kw)	26.2	28.2
Regenerator Area (ft^2)	898	832
Condenser Area (ft^2)	4830	4900
Heat Input (kw)	2988	2988
Power Output (kw)	562	532
Thermal Efficiency	20.6	19.5
Machine Cost ($/kw)	887.60	931.82

78P79

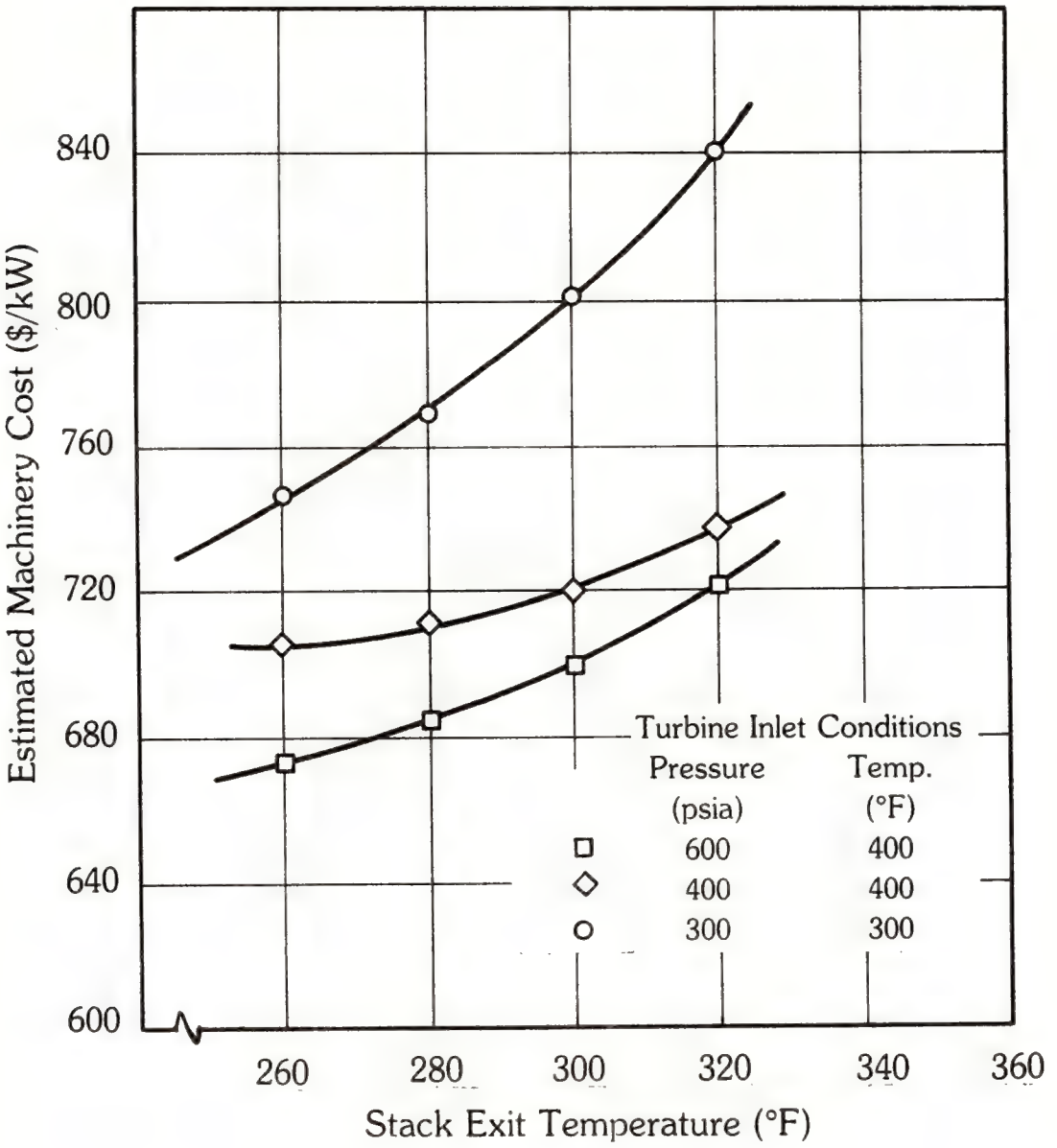

Figure 56 Cost Comparison of R-114 Cycles With 500°F Hot Gas Source

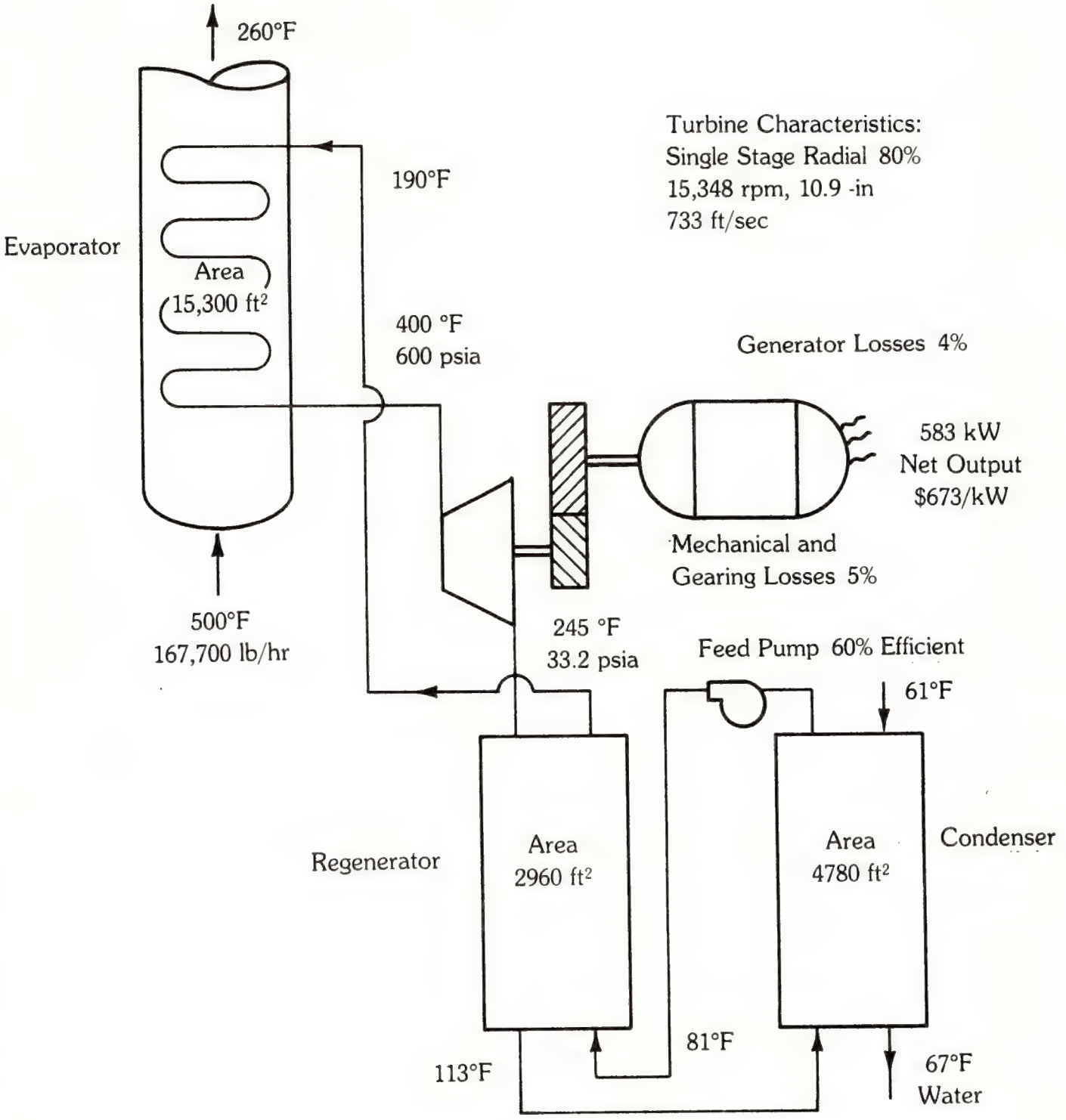

Figure 57 Illustration of Rankine Cycle With R-114 For Most Cost Effective Case Considered With 500°F Gaseous Source

TABLE 15

COMPARISON OF R-114 SUPERCRITICAL AND REGULAR RANKINE CYCLES

Comparison Parameter	Supercritical	Regular
Turbine Inlet Temp (°F)	400	400
Turbine Inlet Pressure (psia)	600	400
Turbine Exit Temp (°F)	245	276
Turbine Exit Pressure (psia)	33.2	33.2
Boiler Area Total (ft^2)	15,300	17,300
Boiler Area Per Unit Output (ft^2/kw)	26.2	30.0
Regenerator Area (ft^2)	2960	2620
Condenser Area (ft^2)	4780	4790
Heat Input (kw)	2988	2988
Power Output (kw)	583	577
Thermal Efficiency	21.3%	21.1%
Machine Cost ($/kw)	673.60	706.11

78P79

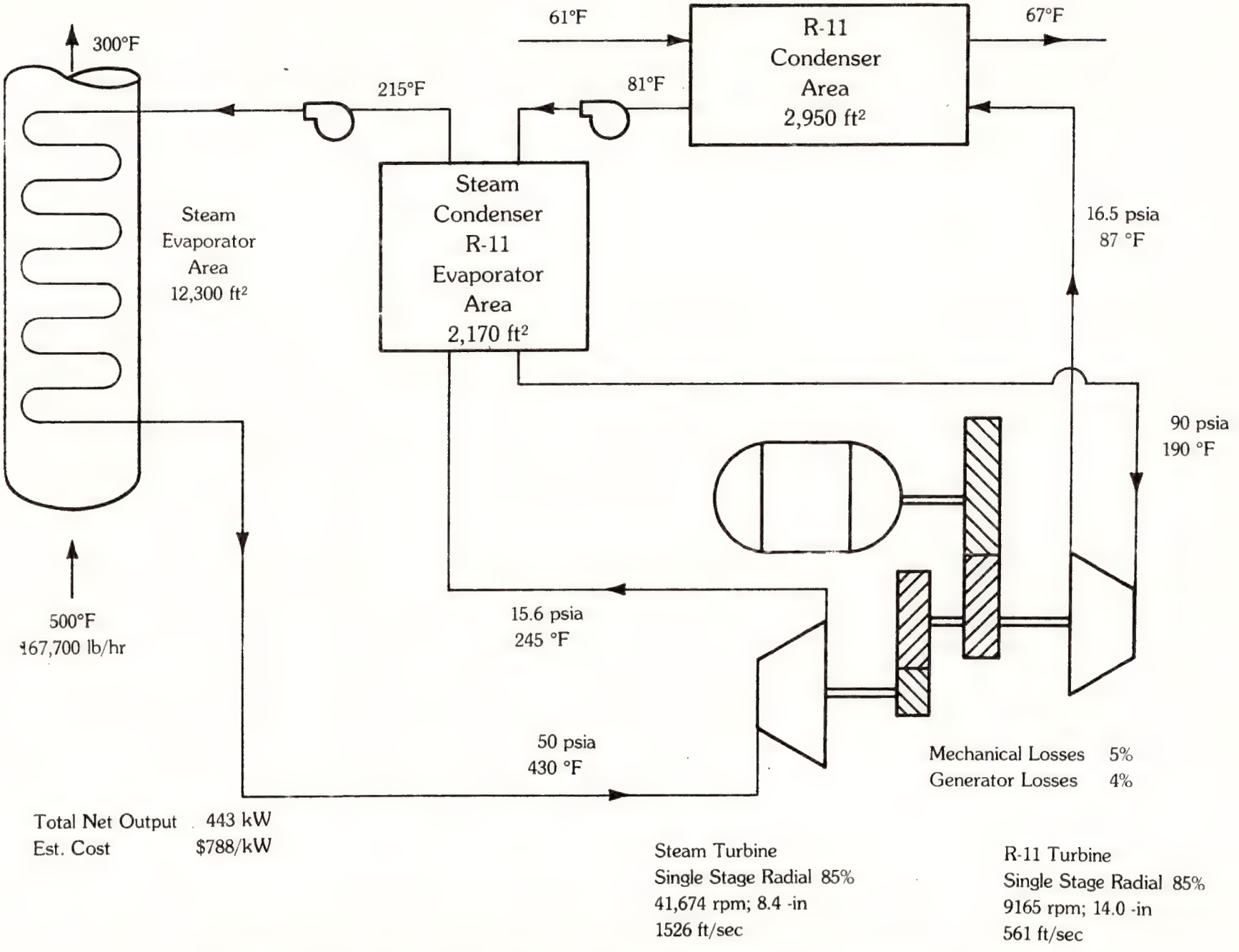

Figure 58 Schematic of Binary Steam/R-11 Cycle With a 500°F Hot Gas Source

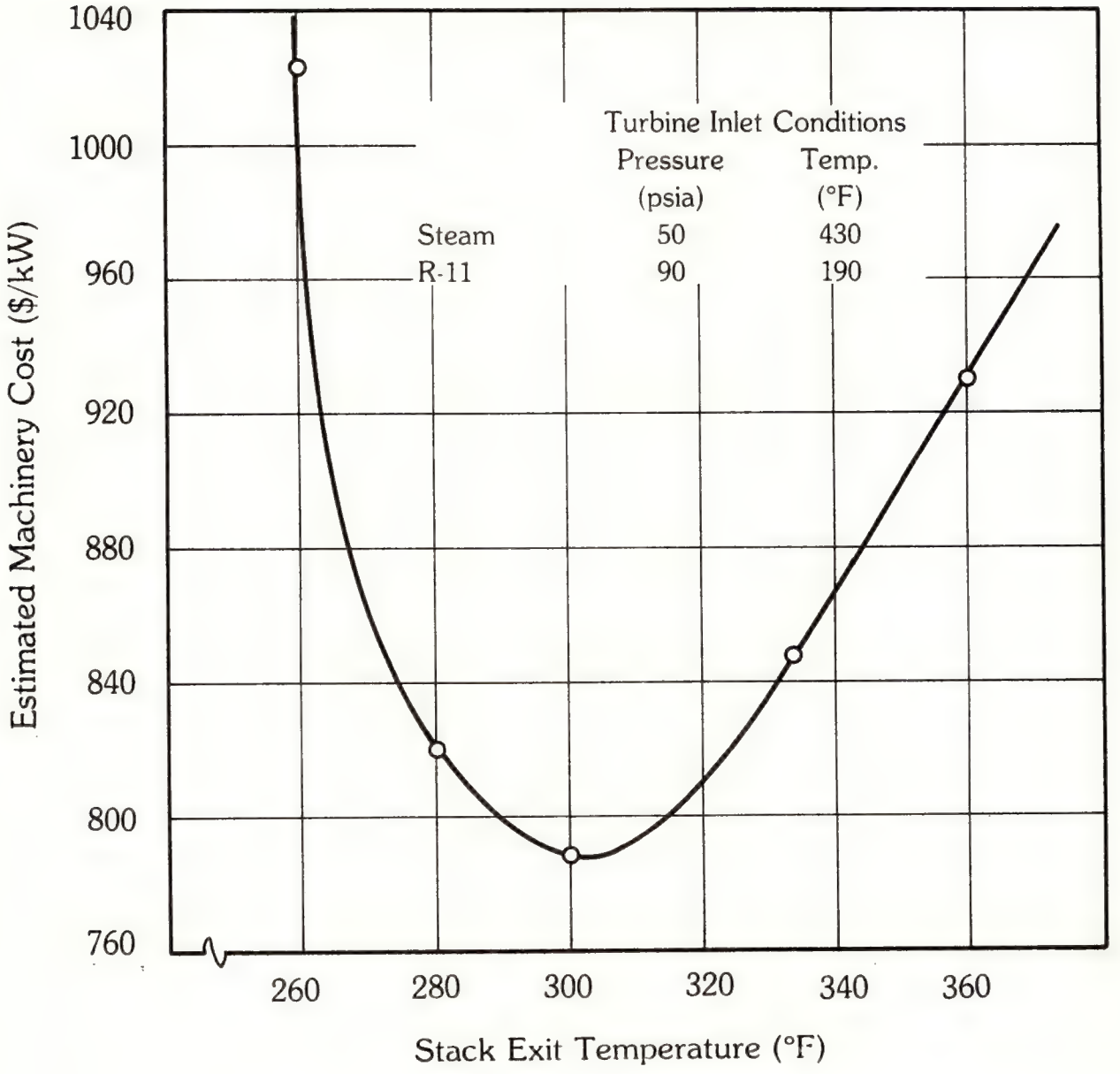

Figure 59 Cost Comparison of Binary Steam/R-11 Cycle With 500°F Hot Gas Source

TABLE 16

WORKING FLUID COMPARISON FOR HEAT RECOVERY FROM A 500°F WASTE GAS SOURCE

SYSTEM CONSIDERATION	WORKING FLUID					
	BINARY	FLUORINOL	TOLUENE	STEAM	BUTANE	R-114
Machinery Unit Cost	Competitive	Competitive-High	Low-Competitive	Competitive	High-Competitive	Low
Fluid Stability	No Problems	No Problems	No Problems	No Problems	No Problems	Questionable
Fluid Safety	No Problems	Toxicity (?)	Flammable	No Problems	Flammable	No Problems
Fluid Availability	General	Limited	General	General	General	General
System Pressure Range atm	6.12 to 1.06	13.6 to 0.09	6.8 to 0.04	0.68 to 0.03	40.8 to 2.6	40.8 to 2.3
Expected Total Installed Cost	Competitive	Competitive -High	Competitive	Competitive -High	High-Competitive	Lowest
Output Ranking	5 (See Notes)	1	4	6	3	2

1 Conventional turbomachinery approach would involve field erection. Reference 11 uses packaged design. See note 2.

2 Conventional turbomachinery approach; Reference 11 using single stage axial in packaged system.

3 Reference 7 indicates a packaged system with a single spool multistage turbine direct driving a 3,600 rpm alternator.

78P79

5.0 BINARY STEAM/R-11 DEMONSTRATION

The U.S. Department of Energy is sponsoring a number of programs to demonstrate the use of Rankine bottoming cycles for the recovery of waste heat. The first such program was initiated with MTI [4,5] in 1976 to design, build, and demonstrate a binary Rankine system on a base loaded Diesel generator set in Rockville Centre, N.Y. This program is now nearing completion. The system has been designed, built, and tested at MTI and is now (mid-April 1978) being installed at the Municipal Power Station in Rockville Centre. The Department of Energy and MTI have recently concluded a cooperatively funded agreement to produce three more demonstration units over the next four years and an engineering development test unit. The Department of Energy is sponsoring two other programs to produce a Fluorinol unit [14] and five toluene units [11]. The Fluorinol unit and three toluene units are scheduled for installation on base load Diesel generator sets. A Hawthorn Leslie steam unit is scheduled for installation in a Diesel power plant in England. Apparently, there is interest in France [34] in Rankine bottoming cycles on Diesel power plants.

As indicated in Section 4, MTI believes that the binary cycle is the best cycle for heat recovery from 400°F to 800°F gaseous sources because the binary system uses fluids that are acceptable to the end user. Water, R-11, and the other fluorocarbon refrigerants are inexpensive, readily available in unlimited quantities, nonflammable, nontoxic, nonexplosive, compatible with most materials, entail no development risk, and carry no "psychological" barriers to ready acceptance throughout industry. In addition, the water - R-11 binary cycle has thermodynamic flexibility which allows the technology demonstration to be applied in a wide spectrum of waste heat recovery applications. The remainder of this section is devoted to a detailed description of the system and the demonstration.

5.1 General System Description

As discussed in earlier sections, the binary steam/R-11 system extracts heat from a hot gas stream with a steam waste heat boiler. The steam is expanded through a single stage radial turbine and is condensed against R-11. The evaporated R-11 is expanded through a single stage radial turbine and is condensed against cooling water. The output of both turbines is coupled through

a single gear box integrated into and with the turbine housings to a conventional 1,800 rpm synchronous generator. The specific arrangement and cycle conditions are shown in Figure 61.

The power conversion machinery package incorporates design features similar to those embodied in MTI centrifugal compressor systems, which are in operation world-wide in sizes up to 3,500 hp.

The cycle design provides a close approximation to Carnot efficiency, and while operating at low pressures (90 psia maximum), has no subatmospheric pressures and thus requires only minimal air removal equipment. Segmentation of the cycle into high temperature and low temperature portions also insures that relatively warm heat exchange surfaces are in contact with the Diesel exhaust. As previously noted, condensation of the exhaust gases is to be avoided. The water returning to the waste heat boiler is at 215°F. This eliminates the potential for condensation with fuel with sulfur contents up to 1 percent (see Figure 27).

Figure 62 shows a perspective of the general arrangement of equipment at the Rockville Centre site. As shown in the figure, four specific modules are required, as follows: (1) the primary steam generator, located on the roof of the Diesel building; (2) the heat recovery machinery building; (3) the shell and tube heat exchanger skid, located adjacent to the heat recovery machinery building; and (4) the cooling tower system.

During the design of the system, a detailed examination of engine exhaust flow rates, conditions, and operating schedules was made. The engine's exhaust flows are presented in Table 17. Table 18 presents the normal maintenance schedule for the engines. As will be shown in the next section, the economics of a Rankine bottoming cycle are extremely sensitive to annual operating time. A 14.7 percent downtime was deemed to be an unnecessary economic penalty. Therefore, it was determined to use about 60 percent of the exhaust from two engines to supply the waste heat gas flow. This provides the advantage that the Rankine system is capable of being "up" 100 percent of the time, assuming that at least one of the two engines is operating, If one engine is down, as will occur 28 percent of the time, the Rankine system will

operate at 80 percent capacity. The resulting design exhaust flow conditions are presented in Table 19. A schematic of the exhaust gas ducting arrangement is shown in Figure 63a.

To provide for maintenance personnel safety, two manually installed blocking plates (isolation dampers) and a ventilating door between the plates are located in the ducts between each engine and the steam generator.

This positive isolation is provided between each engine and the heat recovery system to permit normal operation of both engines (if the recovery system is off line) or to permit operation of either engine with the recovery system when the opposite engine is down for maintenance. With this arrangement, maintenance personnel can enter the exhaust ducts of the idle engine with assured safety while the second engine and recovery system are operating. The existing silencers will be left in place with this piping arrangement.

Figure 63b shows a mockup of the exhaust gas management system. The turbo-generator, controls, valving, pumps, and receiver tanks are packaged in an integrated building located about 100 feet from the Diesel stack area. Figure 64 shows the machinery building mockup. The building is constructed in two pieces for disassembly and shipping after factory test of the assembly. The heat exchanger skid is located adjacent to the machinery building and is configured such that, after test, the skid can be disassembled in two major sections for shipment. The top exchanger on the skid receives slightly superheated steam turbine exhaust at the shell side flange. The tube side of this exchanger comprises a forced circulation evaporator in conjunction with a vapor separator to provide saturated R-11 at the separator discharge. As shown in the Figure 62 schematic, two sets of U tubes are utilized within the same shell. The lower set preheats subcooled condensate to approximately saturated conditions, and the upper set vaporizes saturated Freon, withdrawn from the separator, in the forced circulation loop. Figure 65 shows the general arrangement in mockup form. The lower heat exchanger condenses near saturated Freon against water. With the exception of the structural members added to support the skid assembly, the condenser utilizes conventional refrigeration design practice. The cooling tower is of standard wet tower construction and will be packaged with an integral cooling water pump. Special controls have been added to prohibit freezing during winter operation of the system.

5.2 Component Descriptions

5.2.1 Steam Evaporator

The steam evaporator (waste heat boiler) is designed around an array of finned steel tubes. The exhaust gas flows over the outside of the tubes while the working fluid (water) flows through the tubes. Figure 66 shows the tube dimensions and spacing patterns used in the Rockville Centre demonstration unit. The heat exchanger specifications (including the tube array pattern) was developed by MTI. An experimental verification of the gas side pressure drop was made due to the sensitivity of the Diesel engine to exhaust back pressure. Table 20 presents some design information for the steam evaporator. Figure 67 presents the overall external configuration of the evaporator.

The spacing of the fins and the general layout of the heat exchanger take into account that it will be used with the exhaust from oil-fired engines. The fin size and spacing was selected to minimize soot fouling and promote cleaning with standard soot blowers. The system steam could be used in soot blowing.

The heat exchanger is divided into an economizer, a vaporizer, and a superheater section, as implied in Figure 61. Figure 68 shows the internal construction detail of the steam evaporator. Tubes are connected in series flow circuits by U bends butt welded at each end of the tubes. The tubes are supported at each end of the OD of the fins by thick "tube sheets" which have holes slightly larger than the fin OD cut through at each tube location. Tubes are free to slide within these holes to accommodate thermal expansion. Exhaust gas leakage through the clearance between tube-sheet holes and tube fins is contained in a "header box" which covers the U bends at each end of the tube bank. Horizontal baffles in these header boxes prevent excessive bypass leakage through the header boxes. The steam side heat transfer design data is presented in Table 21. This design is based on the use of a forced circulation vaporizer section, with a recirculation flow rate five times the through-put rate. The vaporizer thereby delivers steam of 20 percent quality to the steam drum. Vortex separating units in the steam drum would be employed to separate vapor from liquid and deliver steam of 99.5 percent quality to the superheater section. A "canned motor" is used for the boiler circulating pump. The canned motor pump requires no shaft seal on the pump, since the pumped fluid is

allowed to flow through the motor housing. This reduces downtime and maintenance load for changing shaft seals, but does impose penalties of decreased pump efficiency and higher first cost.

5.2.2. Other Heat Exchanges

The steam condenser/R-11 evaporator heat exchanger and the R-11 evaporator are conventional shell and tube units, and draw heavily from industrial packaged chiller practice.

5.2.3. Power Conversion Machinery

Figure 69 presents a gearbox section and isometric of the assembled package. The steam turbine operates at superheated inlet conditions and at a speed of 42,200 rpm. At the design pressure ratio of 3.3, the turbine isentropic enthalpy drop is about 100 Btu/lb. These operating conditions provide optimum specific speed characteristics; the turbine performance exceeds 85 percent isentropic efficiency. The steam turbine output is speed reduced to 9,540 rpm and combined at the R-11 turbine output shaft. The low speed pinion thus passes all of the recovered power through the bull gear mesh to the 1,800 rpm generator shaft. The gearing allows both turbines to be independently optimized at maximum aerodynamic efficiency. Multiple shaft outputs are also available to drive other high speed loads, such as centrifugal pumps and compressors.

Figure 70 shows the steam turbine nozzle ring wheel and volutes and Figure 71 compares the R-11 and steam wheels. The steam turbine operates at high tip speed, and at these conditions, some radial growth of the pilot diameter occurs. Accordingly, a polygon spline is used for self centering under load torque conditions. The lower tip speed R-11 turbine utilizes the wheel bore for piloting. Both turbines utilize axial tie bolts to attach the wheels and shafts.

The high speed steam turbine shaft is supported on 5-shoe tilting-pad journal bearings with the wheel end diameter selected to resist shaft bending; the opposite end bearing diameter is selected to minimize friction losses. The pads are preloaded for rotor stability. Minimal overhang length and weight of turbine wheel have been utilized to preserve a high first critical speed and rotor bearing stability.

The R-11 turbine shaft utilizes four axial groove cylindrical bearings at a unit pressure loading of 260 psi; gravity and gear tooth forces combine to produce high bearing loads vertically downward at full turbine load. A hydrodynamic pressure pocket in the top sector of the bearing produces a hydrodynamic force at low eccentricity which internally loads and stabilizes the rotor bearing system.

The gearbox output shaft uses two groove cylindrical bearings at 270 psi unit loading. Figure 72 summarizes the critical speed maps for the three shaft system. The steam turbine rotor operates between the first and second critical speeds. The Freon turbine and generator shafts operate below their first critical speeds at full load conditions.

5.2.3.1 Turbine Design. A number of aerodynamic turbine design programs are available at MTI. The process in which they are applied and some of the results are presented in the following paragraphs.

The starting point for the turbine design is the simlitude plots of Balje [25] and Wood [26]. A specific speed, velocity ratio, and efficiency are selected and used in the Rankine Design Program. This program permits the Rankine cycle to be optimized, and produces specifications of turbine power, rotative speed, inlet pressure, inlet temperature, and mass flow rate. Calculations are made on significant design variables to examine turbine performance. The variables include stator exit angle, rotor-exit-to-inlet radius ratio, rotor exit hub-to-tip radius ratio, and the rotor exit distribution of tangential velocity. The program calculations include turbine loss estimates based on separate loss models to determine boundary layer loss at stator and rotor walls, and tip clearance, disc friction, and rotor exit velocity losses. The program output provides overall stage performance, component losses, absolute and relative velocities, and flow angles through the stage. Dimensionally, diameters are calculated at stator inlet and exit, rotor inlet, and rotor exit at both hub and tip. Nozzle vane width and the number of vanes and rotor blades are also provided. The program can be used in a parametric analysis to optimize a radial inflow turbine based on the specific input requirements, thus providing a comparative analysis of key turbine variables.

The preliminary design computer program is normally applied to optimize turbine geometry. Turbine design parameters are typically varied to determine their effects on the component losses and overall turbine performance. An example of the parametric treatment is shown in Figure 73. Rotor hub-tip radius ratio, rotor exit-to-inlet radius ratio, and stator exit angle are varied to determine the effect on stage efficiency. Cross-plotted over these characteristics, the 65° exducer tip angle represents a nominal rotor design and illustrates the attainable stage efficiency within the range of the variables examined. Other parameters are varied in a similar manner so that the optimum turbine configuration is defined for the particular requirements.

The steam turbine was sized accordingly. Specific speed for the turbine stage has a nominal value of 72.7, with a stage static-to-total efficiency of 87.5 percent. The flowpath cross-section for the steam turbine is shown in Figure 74 including the scroll area required at the stage inlet.

The R-11 gas has a higher molecular weight than steam, and the turbine data generated typically shows higher Mach number characteristics at lower rotational speeds. The overall performance, however, is comparable to the steam turbine; the specific speed value is 73.6 at an overall stage efficiency of 90 percent. The dimensions of the flowpath cross-section for the R-11 turbine are shown in Figure 75.

Next, a performance estimate for a radial inflow turbine at off-design conditions is made. The basis of the analysis is a one dimensional solution of flow conditions along the mean streamline of the turbine flowpath. Program inputs consist of stator and rotor geometry, flow conditions, and rotor speed. The program calculates turbine performance for a range of pressure ratios at a given speed, based on incremental values of stator-exit critical-velocity ratio. An internal loss model assesses stator and rotor incidence and rotor viscous losses. The stator loss calculation is based on the kinetic energy loss across the nozzle vanes, weighted by a stator loss coefficient. Incidence loss is based on deviation from the calculated optimum incidence angle; the loss coefficient differentiates positive and negative incidence from the optimum angle. Rotor viscous losses are calculated based on the average kinetic energy

through the rotor flowpath. Similar to the stator loss calculation, a rotor loss coefficient is used to weigh the magnitude of the viscous losses. Provisions for stator trailing edge blockage are included in the computer program to determine stator choking points. Rotor choking is also calculated based on the maximum flow per unit area at the rotor exit station.

A calculation of cross-sectional areas to develop a scroll for a turbine inlet is made. The analytical method calculates areas to produce a constant pressure around the circumference on areas adjoining the rotor. The program can be used to calculate area according to a single free vortex distribution, or to increase flow areas to account for frictional losses in the scroll.

The R-11 turbine is manufactured from an alloy steel such as AISI 4130 and is hard coated by electrolyzing to protect it from corrosion and erosion. Titanium alloy 6Al-4V was the choice for the steam turbine wheel. This wheel material selection included a detailed analysis of the stress distribution in this rotor. Although the steam temperature is only moderate, the high tip speed of the steam turbine wheel requires close attention to bore stress and material strength at operating temperature. A finite element stress design analysis indicated that some configuration modifications were needed at the rear of the turbine wheel. This design change reduced peak stresses in the wheel to 90 percent of yield strength of the material when the wheel is at full turbine inlet temperature and operating at 125 percent design speed. This analysis was confirmed in a test pit run-up of the turbine wheel. As an additional safety feature, the turbine shrouds are designed to fully contain the wheel should there be a catastrophic failure.

An addition construction feature is the use of Polygon splines with tie bolts for wheel-to-shaft attachment for both turbines. The Polygon geometry accurately pilots the wheel on the shaft to maintain dynamic balance and provides ample torque capacity with no stress risers and low shaft stresses.

5.2.3.2. Gearing. The use of gearing is necessary to optimize the turbine design speed for maximum turbine efficiency. The binary system uses an integral double reduction, high speed gearing. While such gearing can present severe reliability problems if incorrectly designed, similiar high speed gearing is being used in critical duty machinery in the process industry.

Gear reliability begins with design. MTI has achieved an enviable record of gear performance and reliability of the high speed rotoating machinery designed and built by its subsidiary, Turbonetics Inc. The same design concepts which achieve reliability and high performance in Turbonetics gearing is used for the gearing in the binary system.

MTI recognizes that the most reliable techniques and data available for the evaluation of the load carrying capabilities of gearing are the "Load Rating Standards" developed by the American Gear Manufacturers Association. These standards are quite involved and must be used with considerable care and judgment.

- Abrasive Wear - Abrasive wear is usually caused by foreign particles in the oil. It is MTI's practice to filter the oil to 10 microns, thus keeping the particle size below the operating film thickness.
- Pitting - Pitting is a surface fatigue failure of the gear materials. It can best be avoided by designing the gears with a Hertzian compressive stress below the levels at which the specific gear material will pit.

  The reliability of the gear drives produced by MTI is achieved in part by the special consideration given to the concept of service life. A turbine operating at 14,000 rpm for 10 years, for example, will accumulate 7.4×10^{10} fatigue cycles on each pinion tooth. The AGMA standard for the type of gearing considered in this proposal assigns a life factor $C_L = 1$. (See solid line, Figure 76). Experience has shown that the fatigue curve shown in Figure 76 should really be an extension of the slope for cycles less than 10^7. Thus, the MTI value for life factor would be 0.601 instead of 1. This results in a more conservative gear design. This concept is also shown in certain of the AGMA aerospace standards where reliability is essential.

  Experience has shown that gears designed with this concept show little or no initial pitting and no destructive pitting.

- Scoring - Scoring is a lubricating film failure. Conditions of heat, load, surface finish, and lubricant characteristics may be such that

the film cannot prevent localized welding of the contacting surfaces. As these welds tear loose, the resultant surface damage destroys the correct form of the active profiles of the teeth. The likelihood that a gear set may score can be evaluated from the results of the scoring index. This index is evaluated for all MTI gear designs and must be a conservative value before the design is accepted.

- Plastic Flow of the Tooth Surfaces - In the case of hard (case carburized) gearing, plastic flow is not observed as a cause of tooth failure.

These standards were developed to provide load rating data for most types of gearing used by industry. A wide range of factors are included in each rating technique in the anticipation that each segment of the gear industry will develop the specific modifying factors that apply to the gears used within that segment of the industry.

Highest reliability and performance demand the following:

- Gearing of very high accuracy in order to minimize noise, vibration, and dynamic loads, while operating at high pitch line velocities frequently required for high performance turbomachinery drives.
- Highest quality metallurgy in order to achieve assurance against failures caused by material imperfections or from zones within the gears wherein the materials were not properly hardened. Optimum metallurgy also permits the design of smaller gearing for given loads, thereby minimizing starting loads, pitch line velocities, dynamic meshing loads, and the amount of material required in both gears and housings.
- Profile modification - In high speed power gearing sets in which smoothness of operation is essential, it is desirable to modify the profiles of the gear teeth and the pinion teeth so as to compensate for the deflections and the resultant displacement that gear teeth experience under load. The profile modifications on the tips of the pinion teeth are specified so as to assure smooth engagement and a uniform deflection of the tooth to its full load position as it enters mesh.

- Helical overlap - The pitch, face width, and helix angles have been chosen such as to assure the maximum practicable number of helical tooth overlaps. This will contribute greatly to the smoothness of operation. This feature assures that at all times there are between three and four teeth in contact in all phases of involute profile mesh.
- Absence of common factors - The numbers of teeth in pinion and gear are selected so that no divisor other than 1 exists common to both members. This is the criteria for a "hunting tooth". Hunting tooth design has been shown in extensive testing to increase the fatigue capability of a gear set some 20 to 30 percent over nonhunting designs.
- Fatigue life - The resistance to bending fatigue is determined in accordance with the procedures published by the American Gear Manufacturers Association. Their standard, AGMA 211.02, "AGMA Standard for Surface Durability (Pitting) of Helical and Herringbone Gear Teeth", is used to determine the resistance to both surface fatigue stresses (pitting), and resistance to bending fatigue stresses.

In order to design gearing that will perform a long and useful service reliably, it is necessary to recognize the types of failures to which the gears may be subject.

Gear failures may occur in any one or more of a combination of the following modes. The principal modes of gear tooth failure as recognized by AGMA may be classed as follows:

1. Wear of the tooth surfaces
   a) Normal wear
   b) Abrasive wear
2. Pitting of the tooth surfaces
   a) Initial pitting
   b) Destructive pitting
3. Scoring of the tooth surfaces
4. Plastic flow of the tooth surfaces
5. Tooth breakage

The following considerations are made by MTI at the design stage to eliminate all of the above types of failures:

- Normal wear - Normal wear is minimized by proper lubrication and by the use of hard gear materials. Proper lubrication includes the use of an oil which is both clean and of sufficient viscosity to provide a correct film thickness. In the gearing considered in this proposal, the gears must be made hard to resist pitting (discussed below) and to resist wear; thus, these gears have two reasons for being hard. It is anticipated that very little wear will be found during the life of the equipment as a result of this approach.
- Tooth breakage - Tooth breakage occurs when the load on the tooth exceeds its beam strength at the time the load is applied. When assessing the strength of a gear tooth, it is necessary to evaluate the dynamic load imposed on the tooth and the number of fatigue cycles that will occur. A desired fatigue life is assured by choosing a tooth material which will have a strength at the end of that life (or number of fatigue cycles) which is greater than the bending stress created by the applied loads.

The design data for the gear set to be employed in the dual turbine unit of Figures 69 and 77 are summarized in Table 22. These data were extracted from computer output data for MTI's design program, "Surface durability and strength of spur and helical gears".

5.2.3.3. Seals. Each turbine shaft must be sealed where it passes through the wall of the gear housing to prevent leakage of steam or R-11 into the gear housing. Leakage of this nature would represent a loss of working fluid and would contaminate the lubricating oil. In addition, the working fluids should be protected against contamination by oil.

Each turbine wheel carries a multi-tooth labyrinth seal which confines the high pressure to an outer annulus on the back of the wheel. The inner annulus in back of the wheel would be vented to the turbine exhaust pressure. The shaft seal, therefore, must seal between exhaust pressure back of the turbine wheel and atmospheric pressure in the gear housing. Floating-ring seals with a close radial clearance would be employed on each turbine shaft. In addition,

a buffer fluid such as dry air or lube oil would be used at the R-11 turbine shaft seal, to prevent leakage of R-11 into the gear housing. Using oil as a buffer, the "sour oil", or mixture of oil and R-11, can be separated externally merely by heating the mixture to about 200°F, driving off the R-11 as vapor to be pumped into the turbine exhaust. This seal approach avoids the rapid wear and frequent replacement problems associated with face-type seals.

5.2.4. Controls and Accessories

The system can be operated from a single supervisory location on either a semi-automatic or a full automatic or a full automatic basis. Start up of the system is carried out off-line as the heat transfer systems are brought up to full operating heat flows, and as proper fluid distributions are established by liquid level controllers. During this phase of operation, both turbines are fully bypassed and the machinery is not rotating. Spin up of the turbomachinery is accomplished by regulating a speed/time ramp on the governor set-point. The control system is capable of maintaining speed at partial or full load operation on or off line. Synchronization with the line is accomplished at the Rockville Center site by closing the generator breaker using the existing station hardware and in a manner identical to the synchronizing procedure on the existing Diesel generating sets.

Figure 78 shows the linearized speed loop block diagram which applies for off-line operation. A novel feature in the control mode design comprises the use of turbine inlet pressure as an internal feedback around the turbine control valves. Torque is proportional to turbine inlet pressure; therefore, the non-linear throttle valve characteristics are compensated by the feedback loop.

The lubrication system is completely self-contained and uses the turbine generator base as an oil sump. The main oil pump is gear driven from the gear-box output shaft and an auxiliary motor-driven oil pump is used for start-up and back-up. An oil-to-water cooler and sump oil heater with a thermostatic mixing valve regulate bearing oil temperatures.

Local monitoring instruments and remote warnings are provided for oil temperature, oil pressure, oil sump level, and high speed shaft vibration.

5.3 System Operation

Figure 79 is a detailed schematic of the binary system identifying the various control valves and pumps. This figure will be used to describe the start-up and normal operation of the system.

The start-up sequence can be separated into three phases:

- Fluid circulation
- Turbine-generator start
- Output power

Initially, the turbine stop valves are closed and the water and Freon fluids are located in receiver tanks. Selection of the stack heat source is made by proper positioning of the damper valves. Cooling water is circulated through the Freon condenser and cooling tower by starting the coolant pump.

Isolation valves on the receiver tanks are now opened and the automatic start sequence initiated. Water is pumped from the receiver tank through the preheater section of the steam generator and into the vapor drums. As soon as the proper water level has been detected in the steam vapor drum, the water circulation pump is turned on. The water is now forced through the vaporizer section and back to the drum. Eventually, saturated steam is generated in the steam drum. This steam flows out of the drum, through the superheater section, and into the steam supply line leading to the turbine. As soon as the steam pressure reaches the design level, a bypass pressure control valve directs the steam flow to the steam condenser, thereby maintaining the design steam pressure.

At the same time water is pumped to the steam generator, R-11 is pumped through the preheater section of the steam condenser/R-11 vaporizer and into the R-11 vapor drum. When the level of the R-11 reaches the design point, the R-11 circulator pump is turned on and pumps R-11 through the vaporizer section of the combined steam condenser/R-11 vaporizer heat exchanger. Saturated R-11 vapor is eventually produced and flows into the R-11 turbine supply line. As soon as the R-11 pressure builds up to the design level, a second bypass control valve directs the R-11 flow to the R-11 condenser, thus maintaining the R-11 drum pressure at its design value.

The steam condensate formed in the steam condenser is returned to the water receiver tank by means of a condensate pump. Here the water cycle is continued as it flows back to the steam generator via the feed pump. In a similar manner, the R-11 condensate is returned to the R-11 receiver tank and then back to the vaporizer by means of the feed pump.

The binary heat recovery system can continue to operate in this bypass mode indefinitely or until it is decided to start the turbine-generator. The system can always be returned to this mode of operation by simply closing the stop valves which automatically initiates the bypass action.

Start-up of the turbine-generator is accomplished by opening the steam stop valve (R-11 stop valve remains closed). The steam turbine will now accelerate the generator, together with the R-11 turbine. At approximately 90 percent rated speed, the speed governor takes control and modulates the steam control valve in order to arrive at 100 percent rated speed.

Synchronizing and paralleling the generator to the main system bus is carried out from the generator control panel. The operator energizes the exciter, adjusts the generated voltage to match line voltage, adjusts frequency by means of a motor-driven rheostat connected to the governor speed set point, and finally closes the generator breaker when the phase of the generator and line are matched. These steps are initiated by the operator with protective relay back-up on phase sequence, under voltage, and synchronism.

Once the generator is connected to the line, it is loaded by simply opening the R-11 turbine stop valve and steam turbine control valve. This action is accomplished by means of a load selector switch on the generator control panel. In the "load" position, the system will develop up to the maximum power as limited by the bypass control around the turbines, or the available heat in the stack gas. In the "no load" position, the system will return to an idle condition with the R-11 turbine bypassed and the steam turbine operating at its no-load condition.

5.4 Current Status

As of mid-April 1978, the binary steam/R-11 system has complete system shakedown and acceptance testing. Having achieved full rated power and a continuous

200 hour acceptance test at the MTI Energy Systems Test Facility, the unit is being dismantled for shipment and installation in the Rockville Centre power plant. The installation is expected to be completed by the end of September with the unit coming on-line in October 1978.

BINARY STEAM/R-11

DEMONSTRATION

78P79

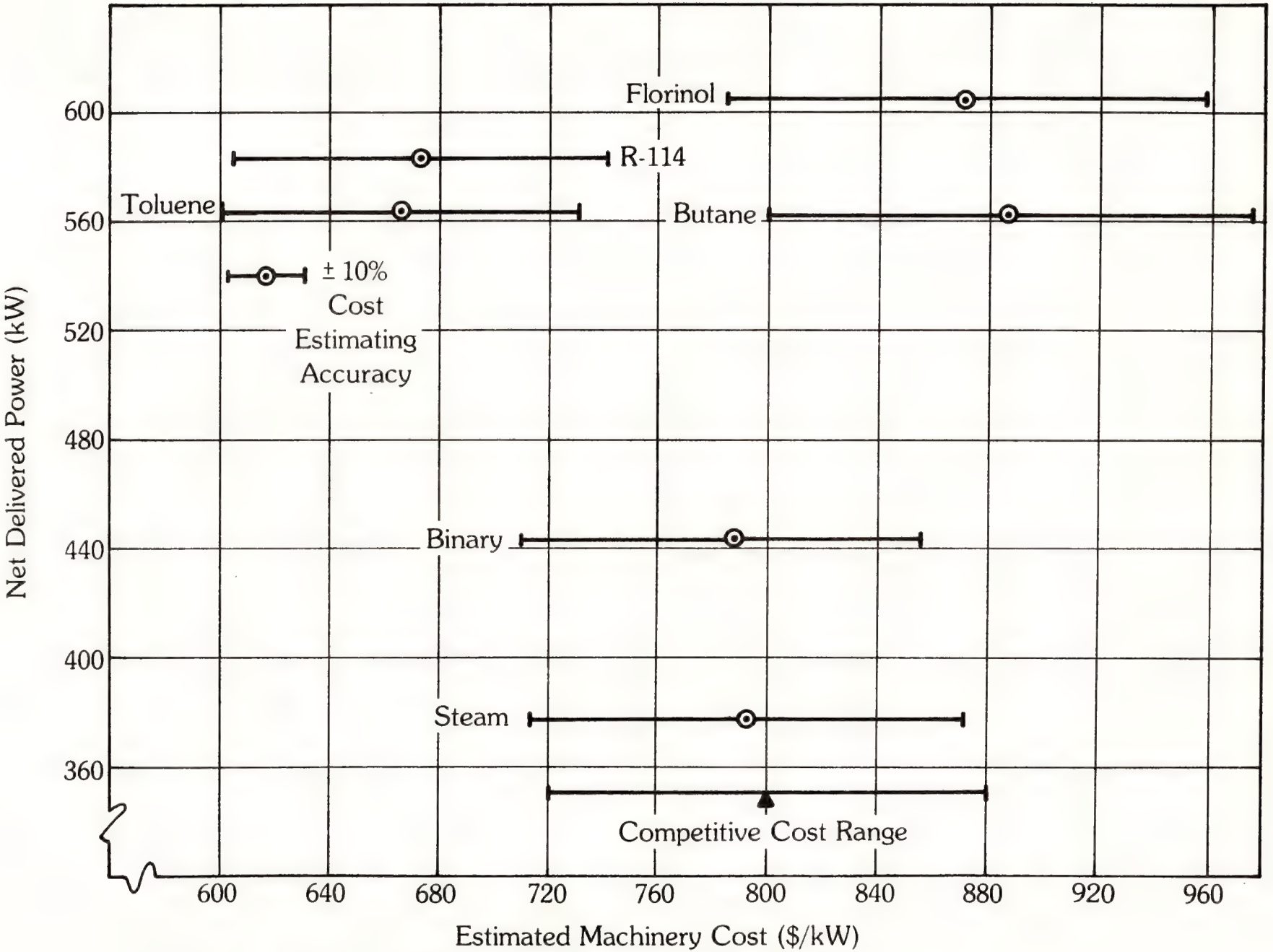

Figure 60 Alternate Working Fluids For Cost Optimized Heat Recovery With A 500°F Waste Gas Source and 81°F Condensing Temperature

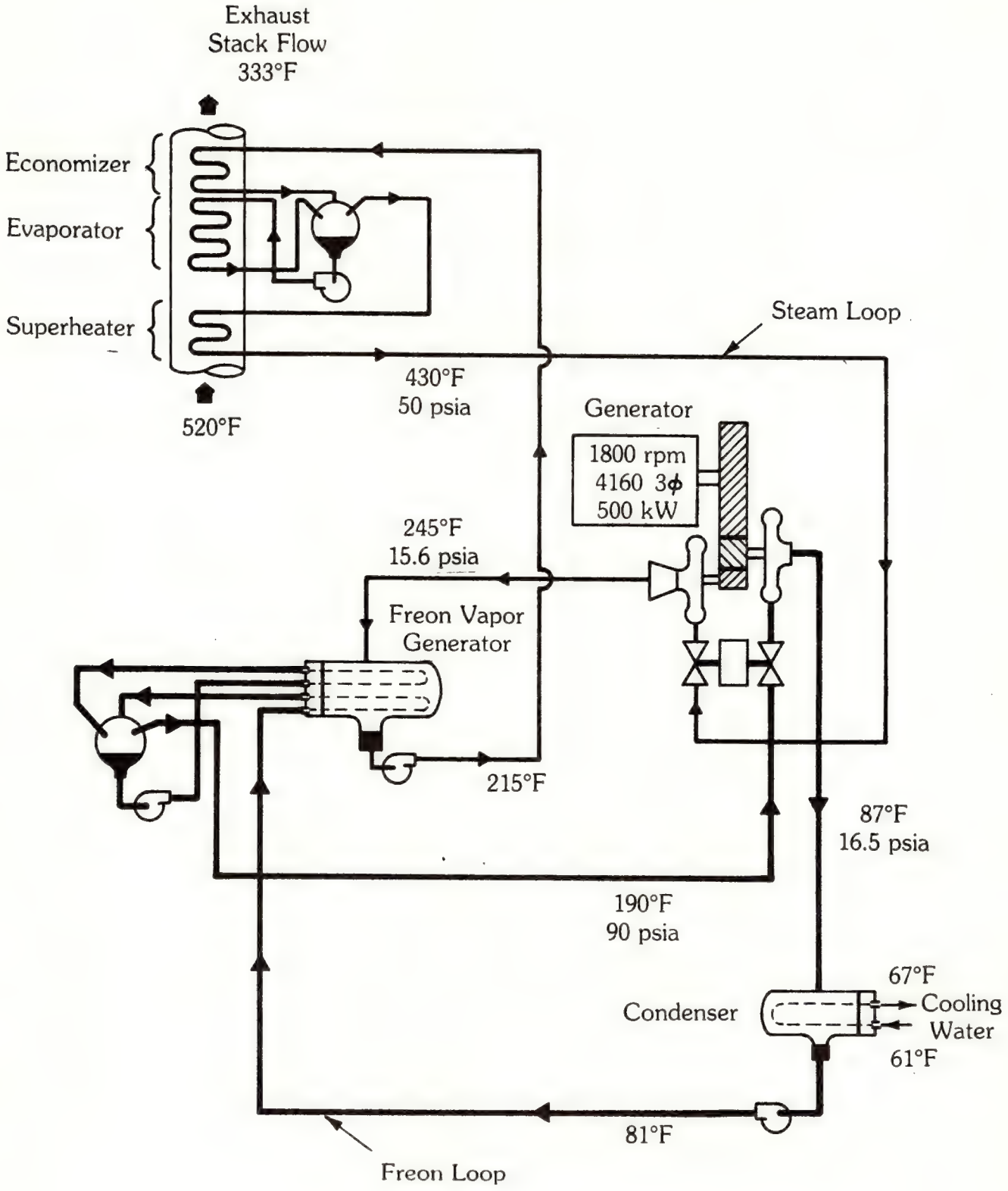

Figure 61 Cycle Schematic For Binary Demonstration System

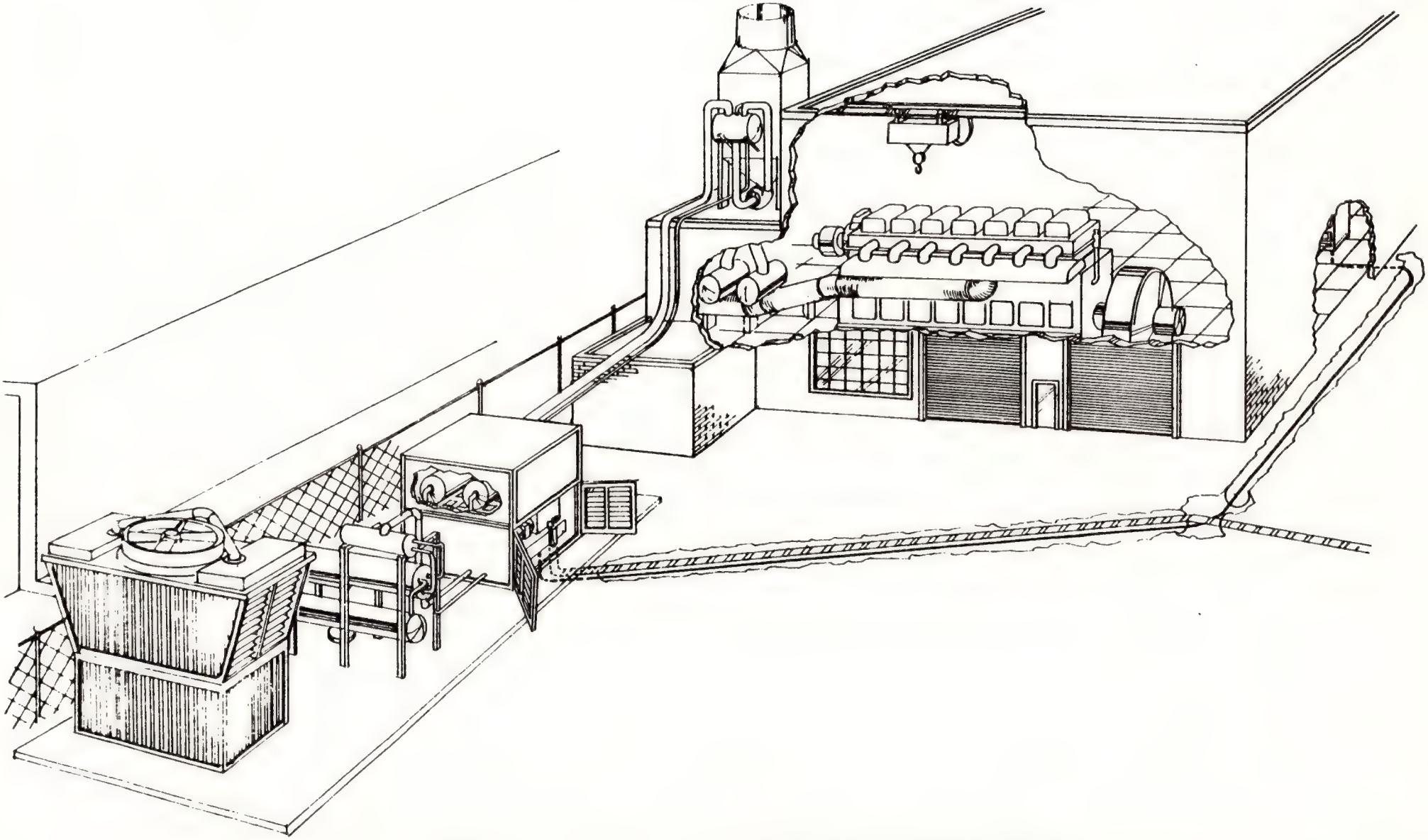

Figure 62 General Arrangement of MTI Binary Rankine Cycle System
For Waste Heat Recovery/Electric Power Generation

TABLE 17

HEAT ENERGY AVAILABLE FOR RECOVERY

Measured Values of Mass Flow and Temperature for Diesel-Engine Exhaust Gas (Nordberg Model TSGL-2110-SC)

	UNIT 12	UNIT 13
Air Flow to the Engine, lb/hr	168,800.	175,300.
Calculated Fuel Flow, lb/hr*	2,700.	2,700.
Total Exhaust Mass Flow, lb/hr	171,500.	178,000.
Measured Exhaust Temperature, °F	505.	490.
Measured Back Pressure at Silencer Inlet, Inches H_2O	6.0	5.0
Total Heat Content for a 325°F Stack Discharge Temperature, Btu/hr	7.73×10^6	7.36×10^6

*Based on SFC = .5184 lb/kw-hr

A Conservative Value for Minimum Boiler Stack-Gas Outlet Temperature From the Standpoint of Fuel Sulfur Content and Avoidance of Sulfuric Acid Corrosion

Selected Minimum Temperature = 325°F

TABLE 18

DIESEL ENGINE MAINTENANCE REQUIREMENTS

MAINTENANCE REQUIREMENT	DOWNTIME
Annual Shutdown for Overhaul	1008 Hrs
Preventive Maintenance (1 day per month for 10 months)	240 Hrs
TOTAL	1248 Hrs
PERCENT DOWNTIME	14.2%

TABLE 19

DESIGN POINT EXHAUST FLOW CONDITIONS

	Unit 12	Unit 13
Nominal Exhaust Flow (lb/hr)	165,000	165,000
Nominal Exhaust Flow Temperature (°F)	520	520
Available Heat Flow, 333°F Exit Temp (Btu/hr)	7,726,000	7,726,000
Rankine System Output (kw)	402	402
Design Exhaust Flow Rate (lb/hr)	205,000	
Design Heat Flow, 333°F Exit Temp (Btu/hr)	9,600,000	
Design Rankine System Output (kw)	500	

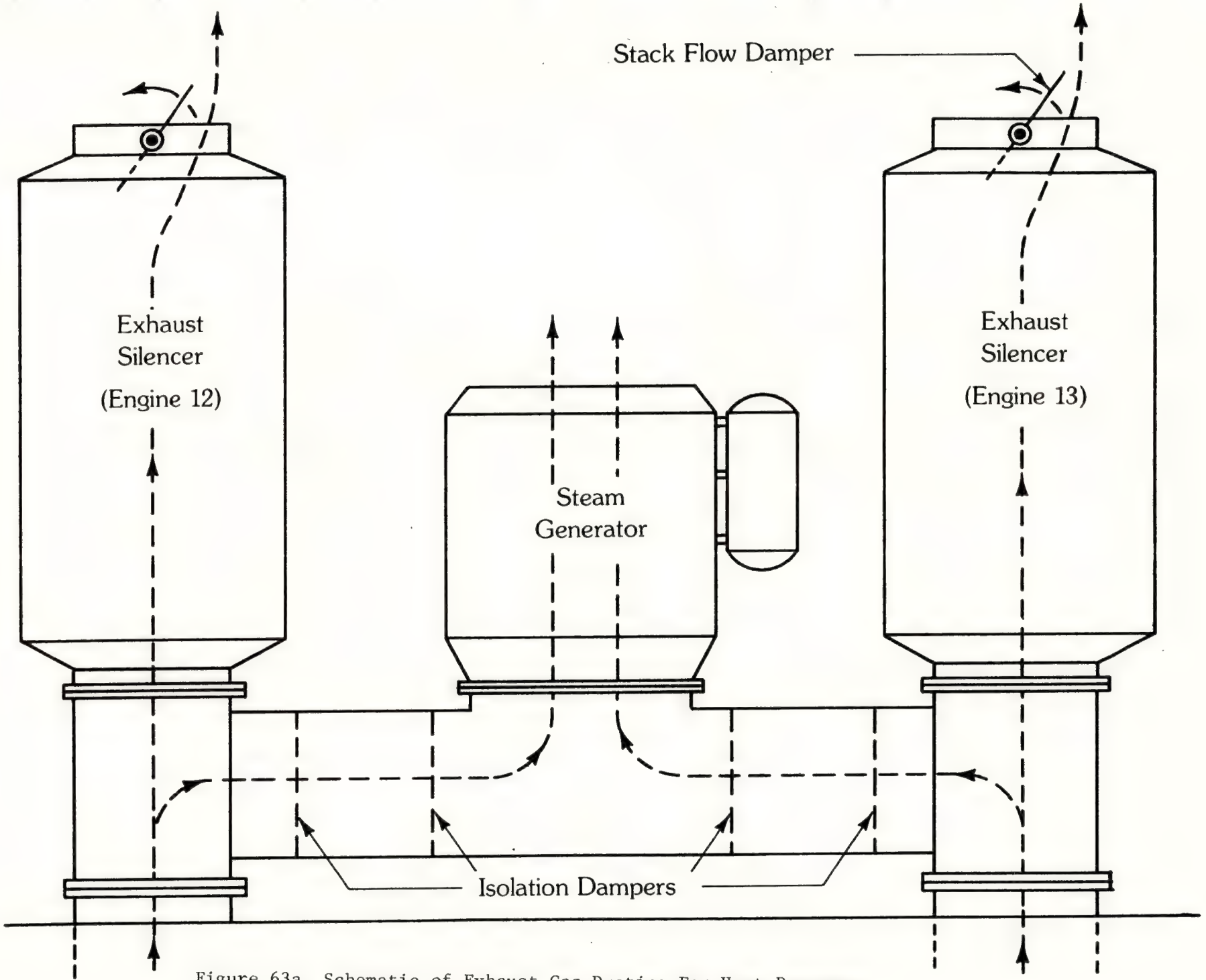

Figure 63a Schematic of Exhaust Gas Ducting For Heat Recovery

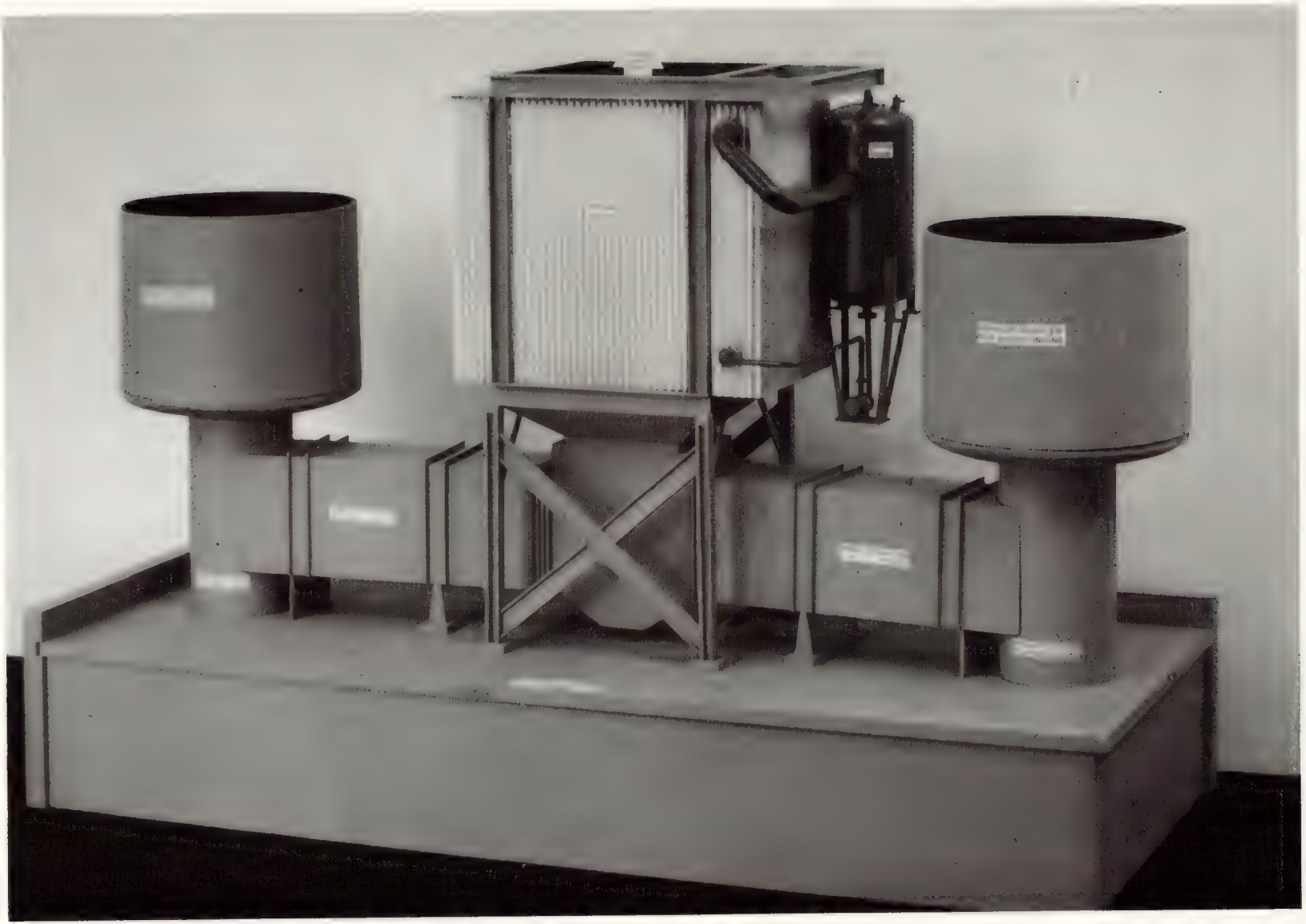

Figure 63b Mockup of Exhaust Gas Management System and Steam Generator

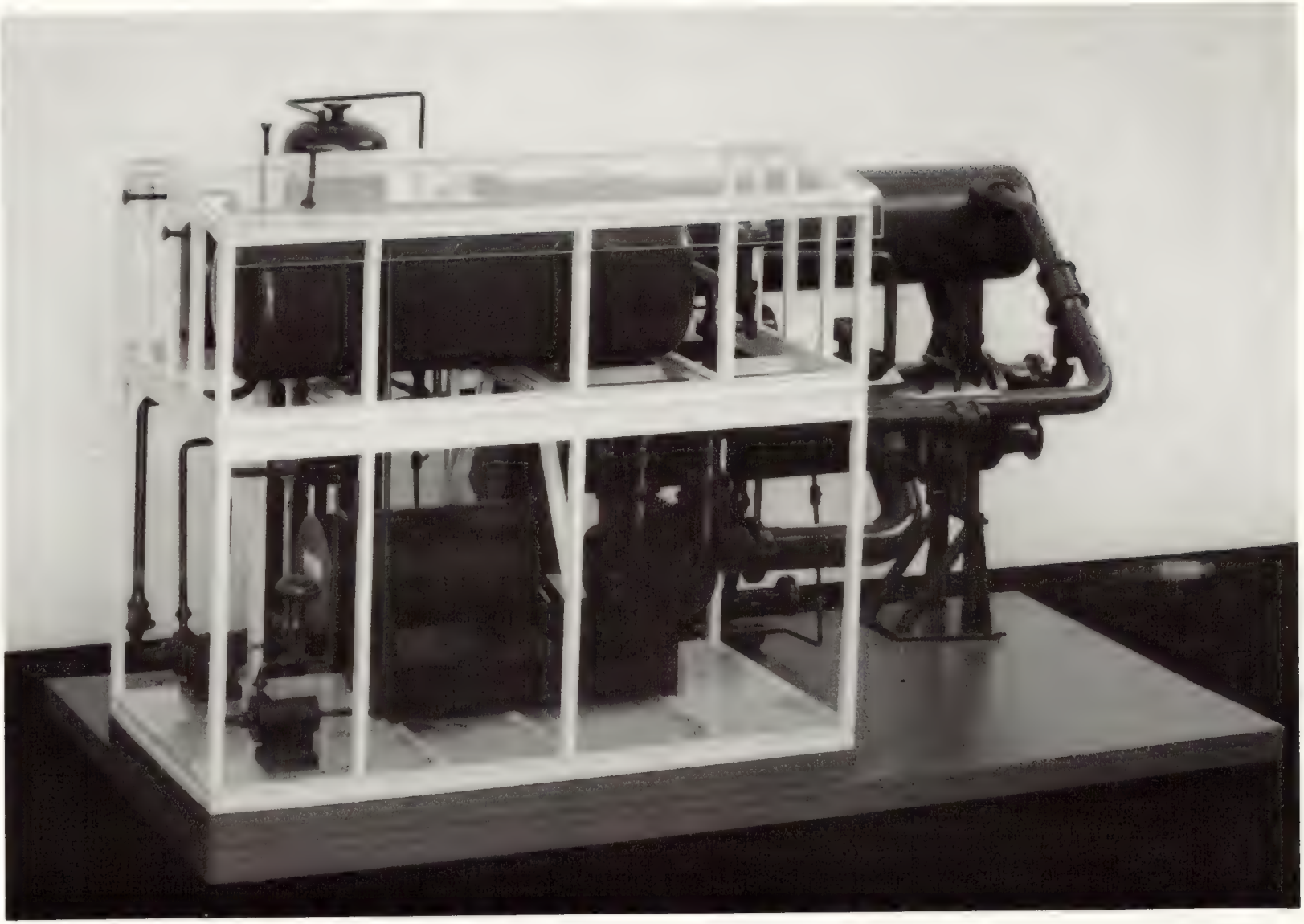

Figure 64 Machinery Building Mockup

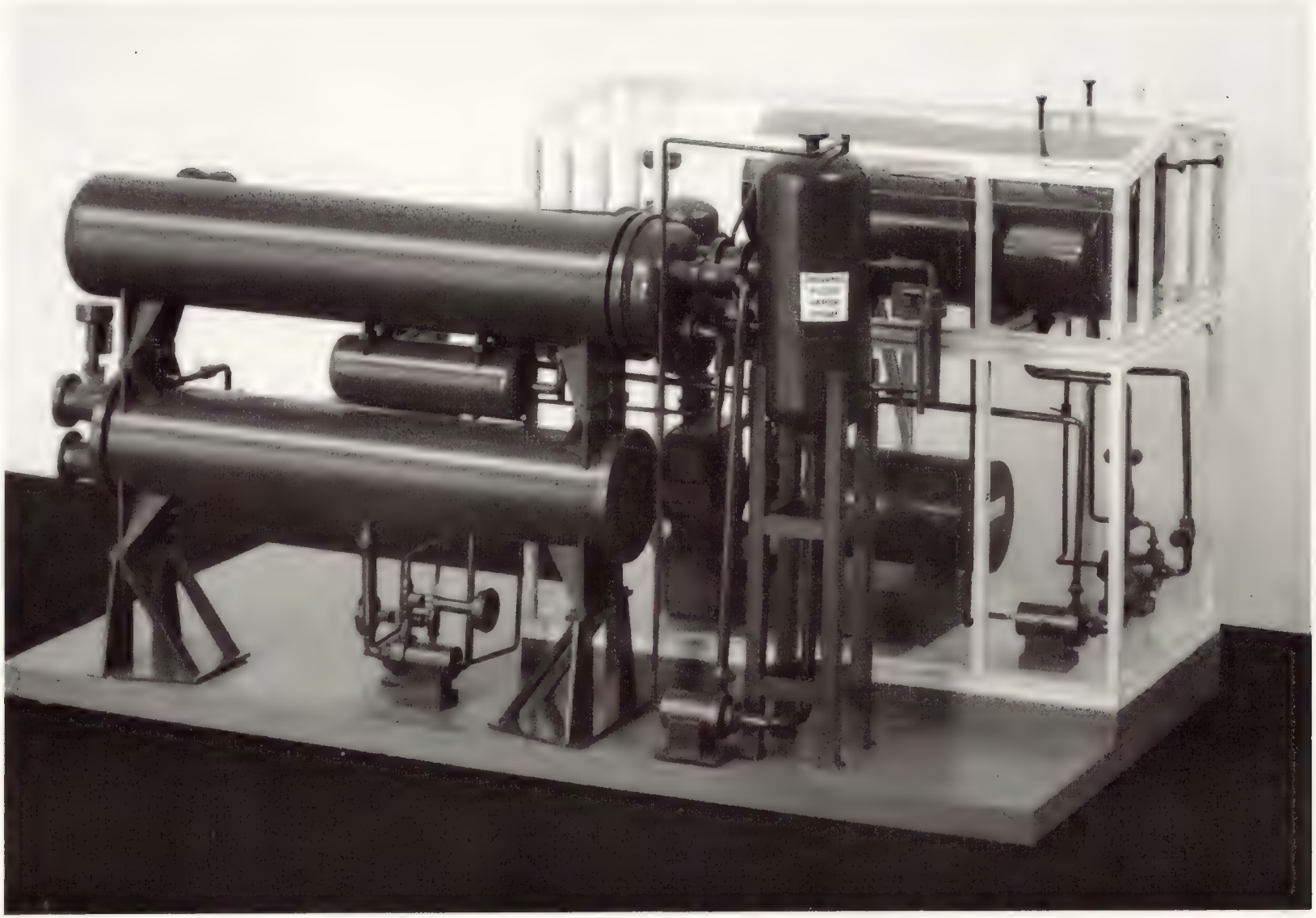

Figure 65 Mockup of Heat Exchanger Skid

MTI-17965

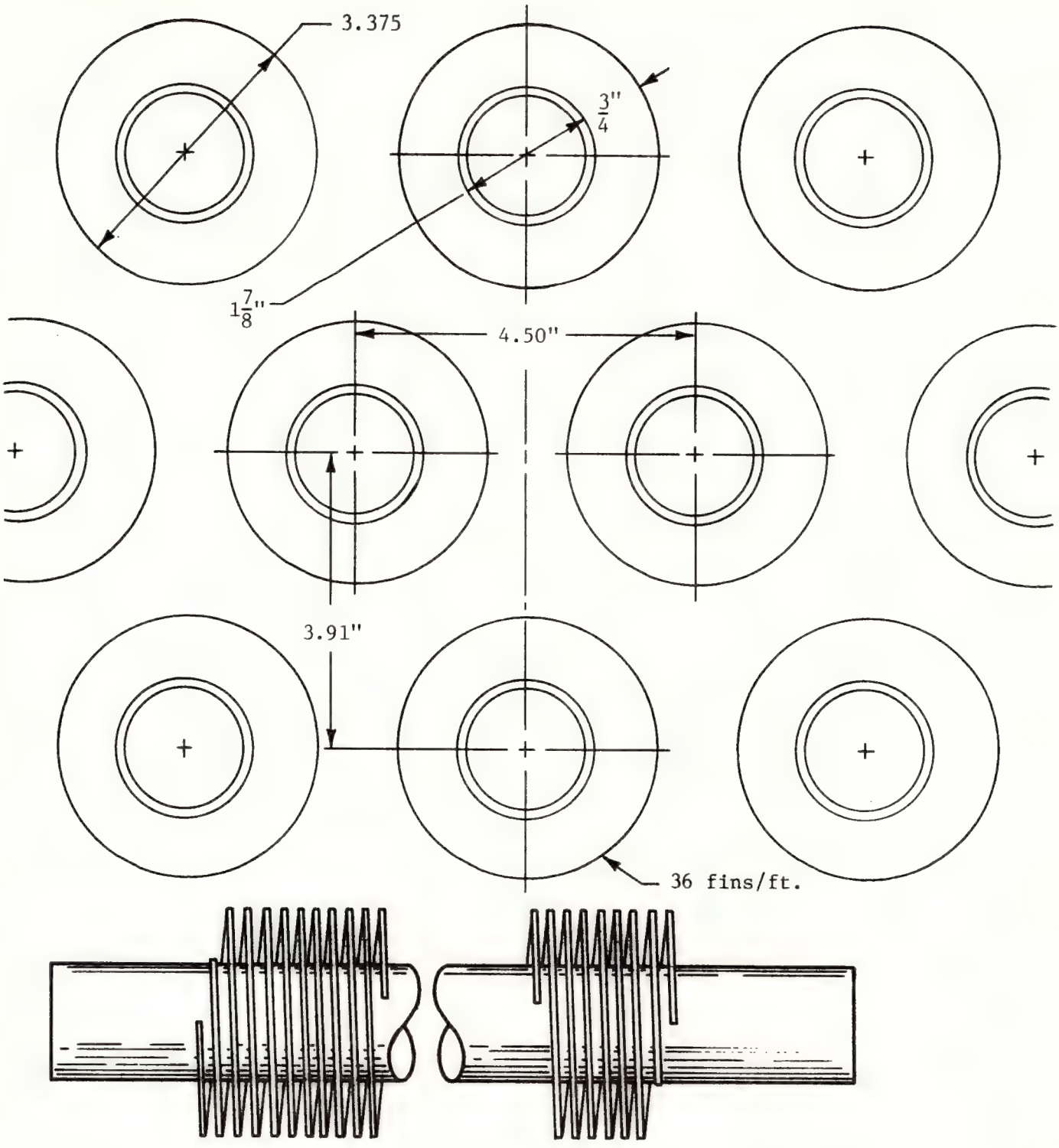

Tube O.D.	1.875″
Tube Wall Thickness	0.090″
O.D. of Fins	3.375″
Fin Height	0.75 ″
Fin Thickness	0.060″
Fin Spacing	3 per inch
Tube Pitch in Horizontal Layer	4.5 per inch
Vertical Spacing of Layers	3.91 per inch

Figure 66 Dimensions and Spacing Pattern For Steam Evaporator

TABLE 20

GAS SIDE DATA FOR STEAM EVAPORATOR

Frontal area at entrance to boiler, sq ft	47.5
Net free area through tube row, sq ft	26.89
Mass flow rate G. lb/hr-ft^2	2.117
Gas side film coefficient, h	14.45 Btu/hr$ft^{2o}F$
Coefficient h, including .01 fouling factor	12.63 Btu/hr$ft^{2o}F$
Fin efficiency of fouled surface	.807
Stack gas pressure drop across finned tubes	4.2 inches of water

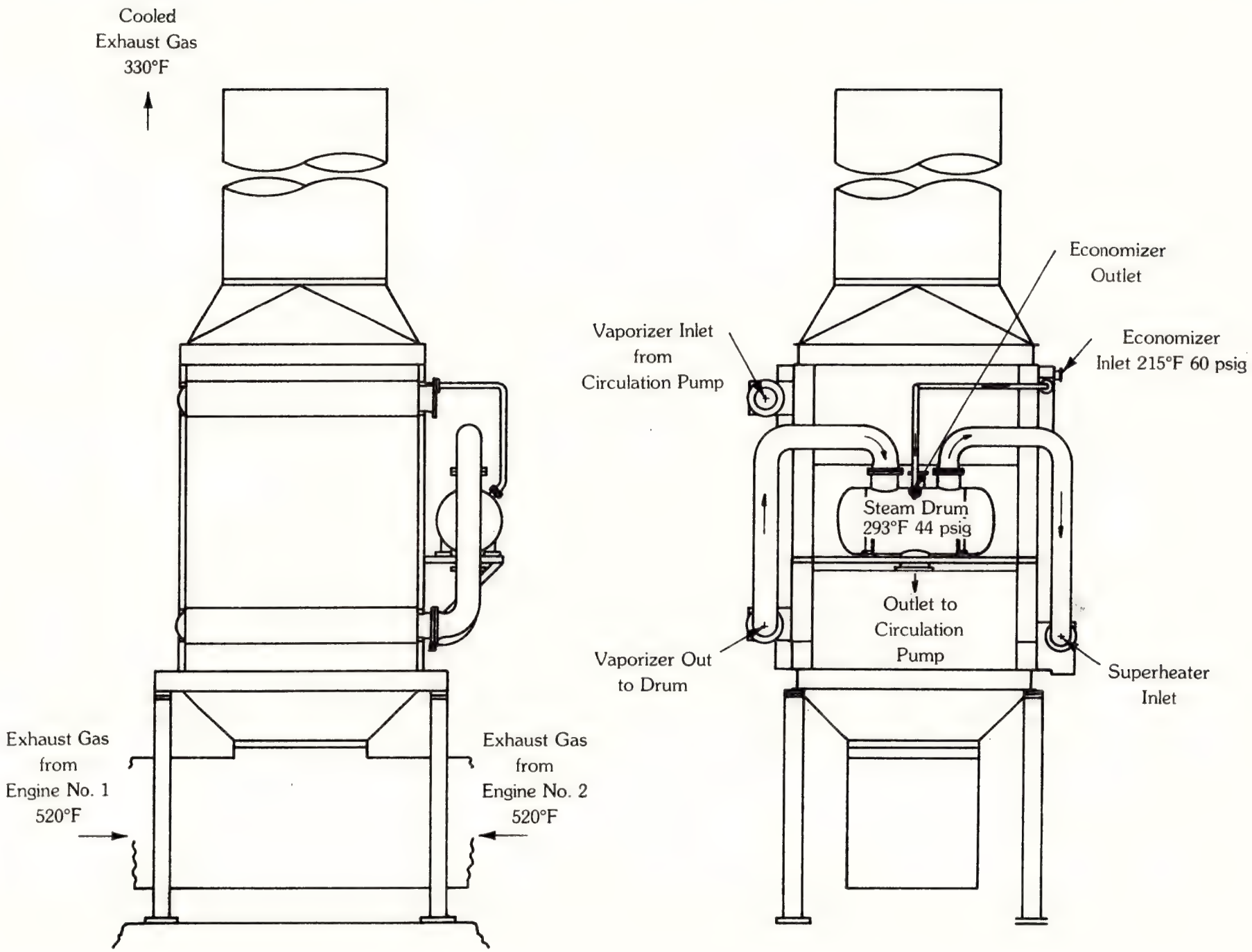

Figure 67 Layout of Waste Heat Recovery Vaporizer System

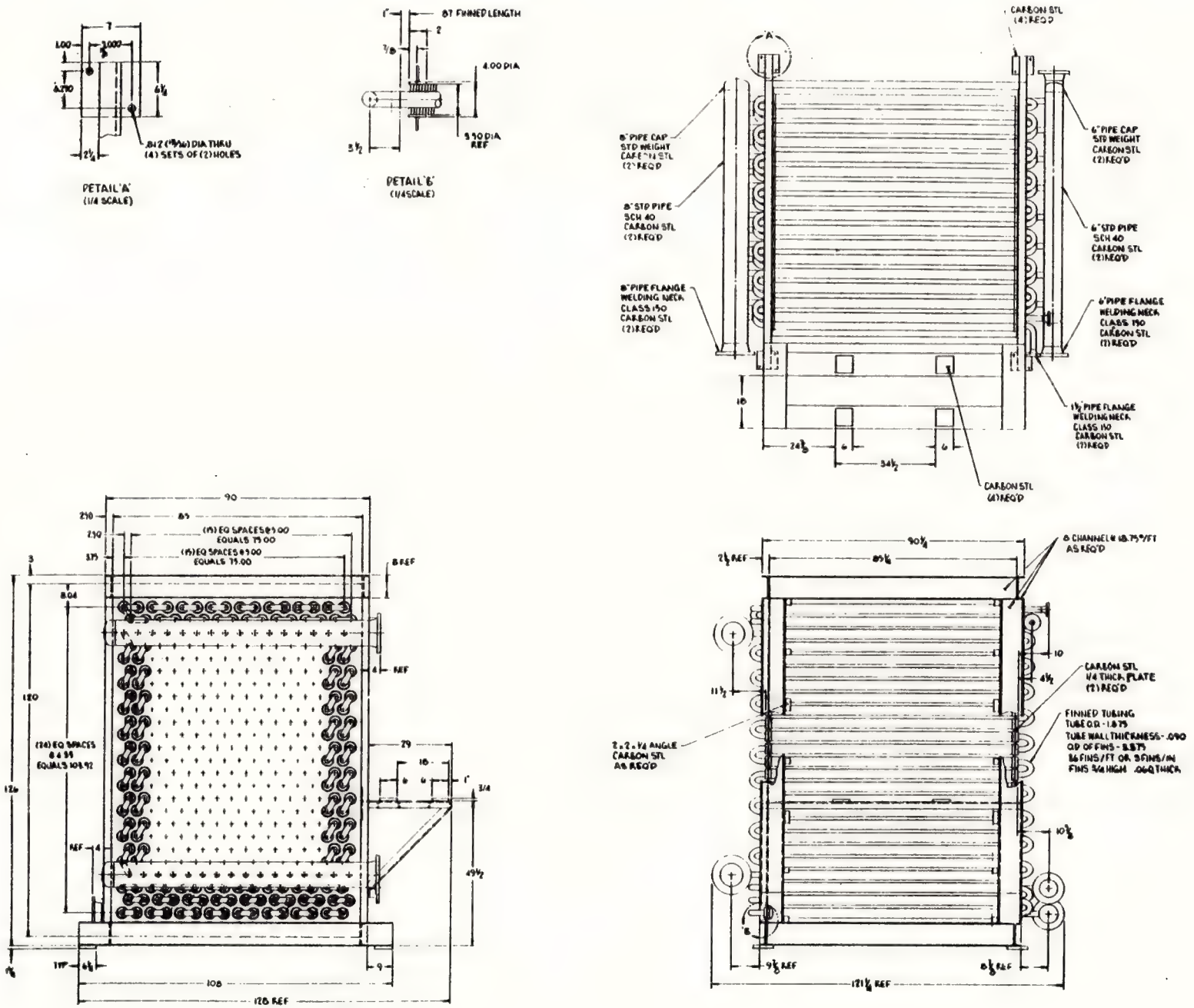

Figure 68 Construction Details of Steam Evaporator

TABLE 21

STEAM SIDE DATA FOR STEAM EVAPORATOR

	Preheater	Vaporizer	Superheater
Fin side surface area, sq ft	816	8160	1124
Number of tube rows	2	20	3
Heat transfer rate, Btu/hr	713,700	8,237,800	648,900
Average conductance, U, Btu/hrft^2^{o}F	9.27	8.54	4.41
Steam side film coefficient	1090	493	65.6
Steam side flow circuit	All tubes in series	16 tubes in parallel	8 tubes in parallel
Steam side pressure drop, psi	2.29	6.17	2.06
Log mean temperature difference, ^{o}F	81	114.7	142.8
Stack gas temperature, entering, ^{o}F	345.6	506.1	520
leaving, ^{o}F	333	345.6	506.1
Steam (water) temperature entering, °F	215	293	293
leaving, °F	293	293	430
Steam side flow rate, lb/hr	9,000	45,000	9,000

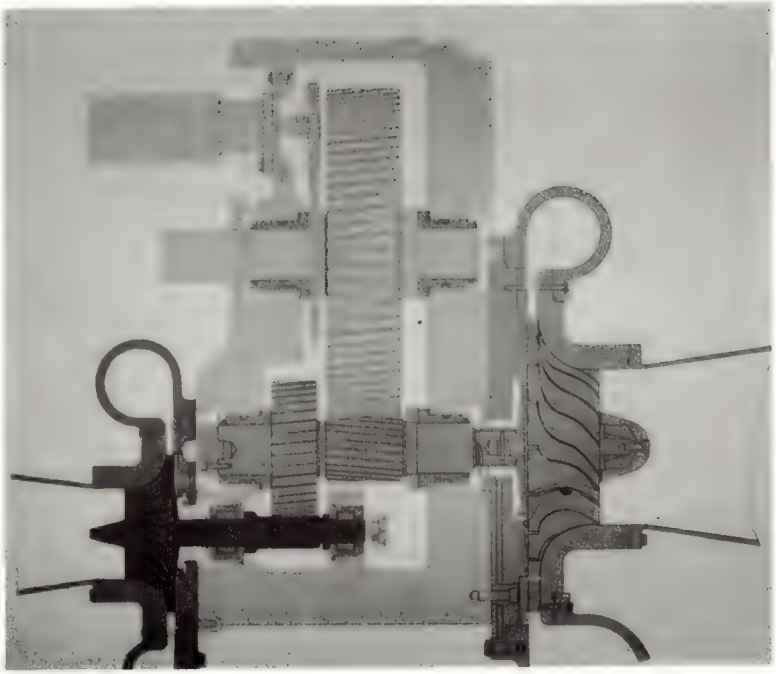

Gearbox Section

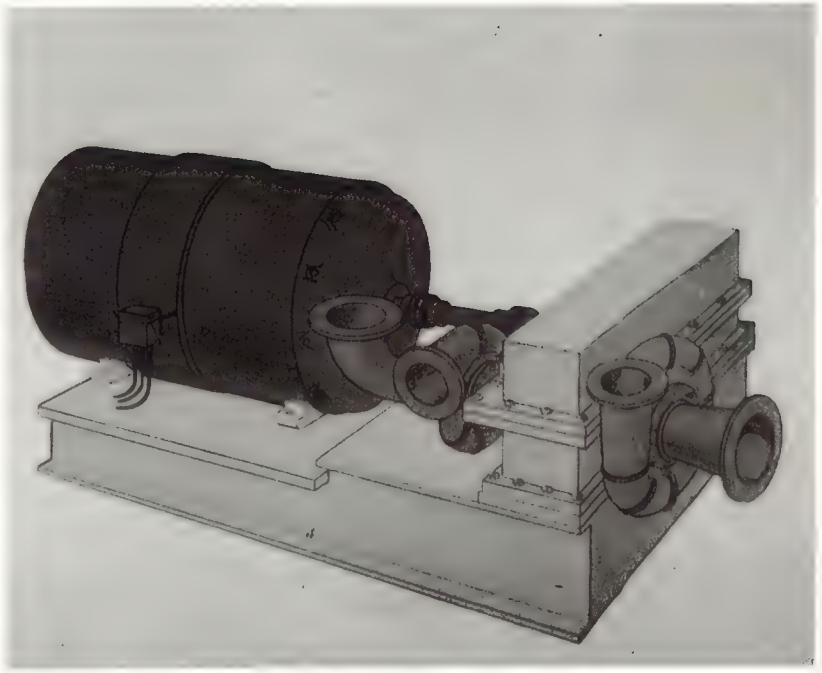

Assembled Machinery Package

Figure 69 Gearbox and Assembled Machinery Package for the Binary Steam/R-11 System

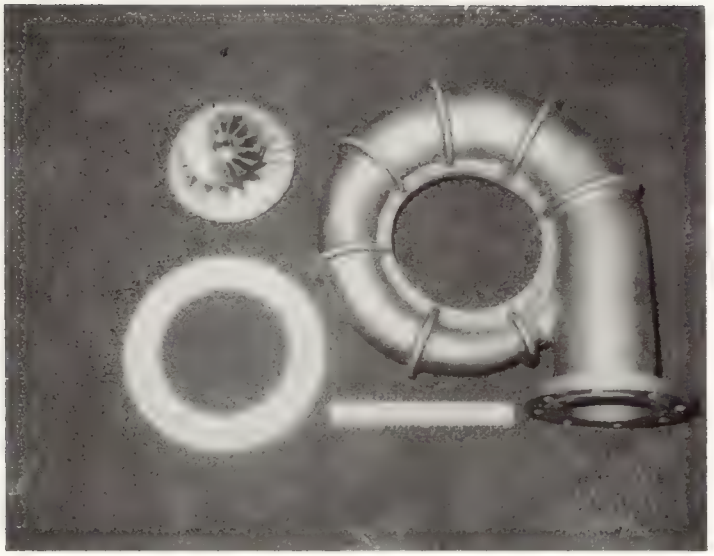

Figure 70 Steam Turbine Components

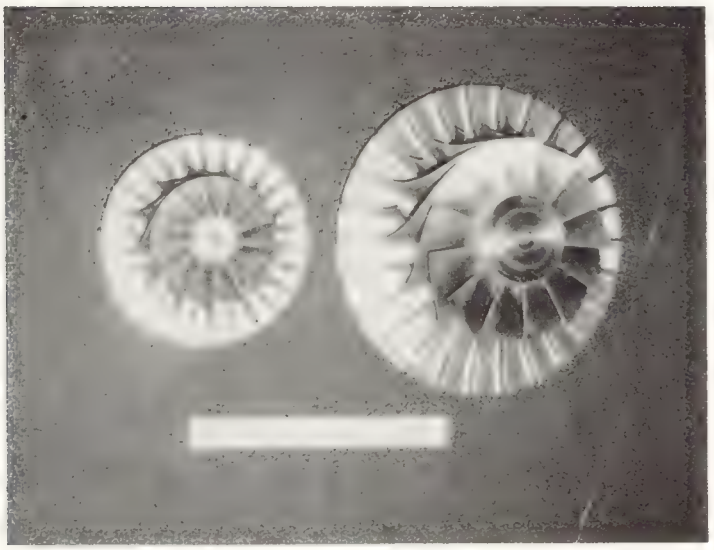

Figure 71 Steam and Freon Turbine Wheels

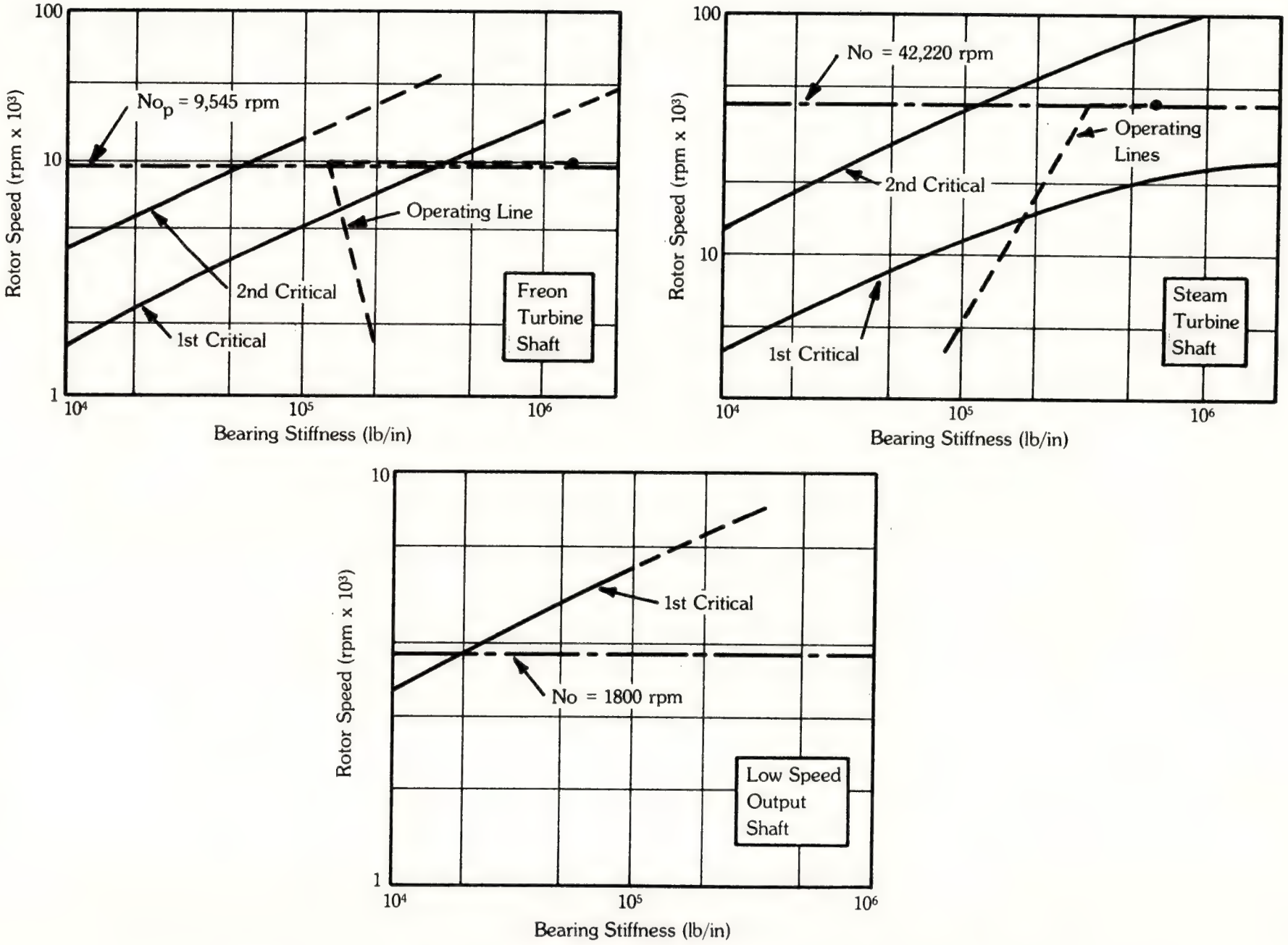

Figure 72 Critical Speed Map For the Three Shafts of the Binary Steam/R-11 System

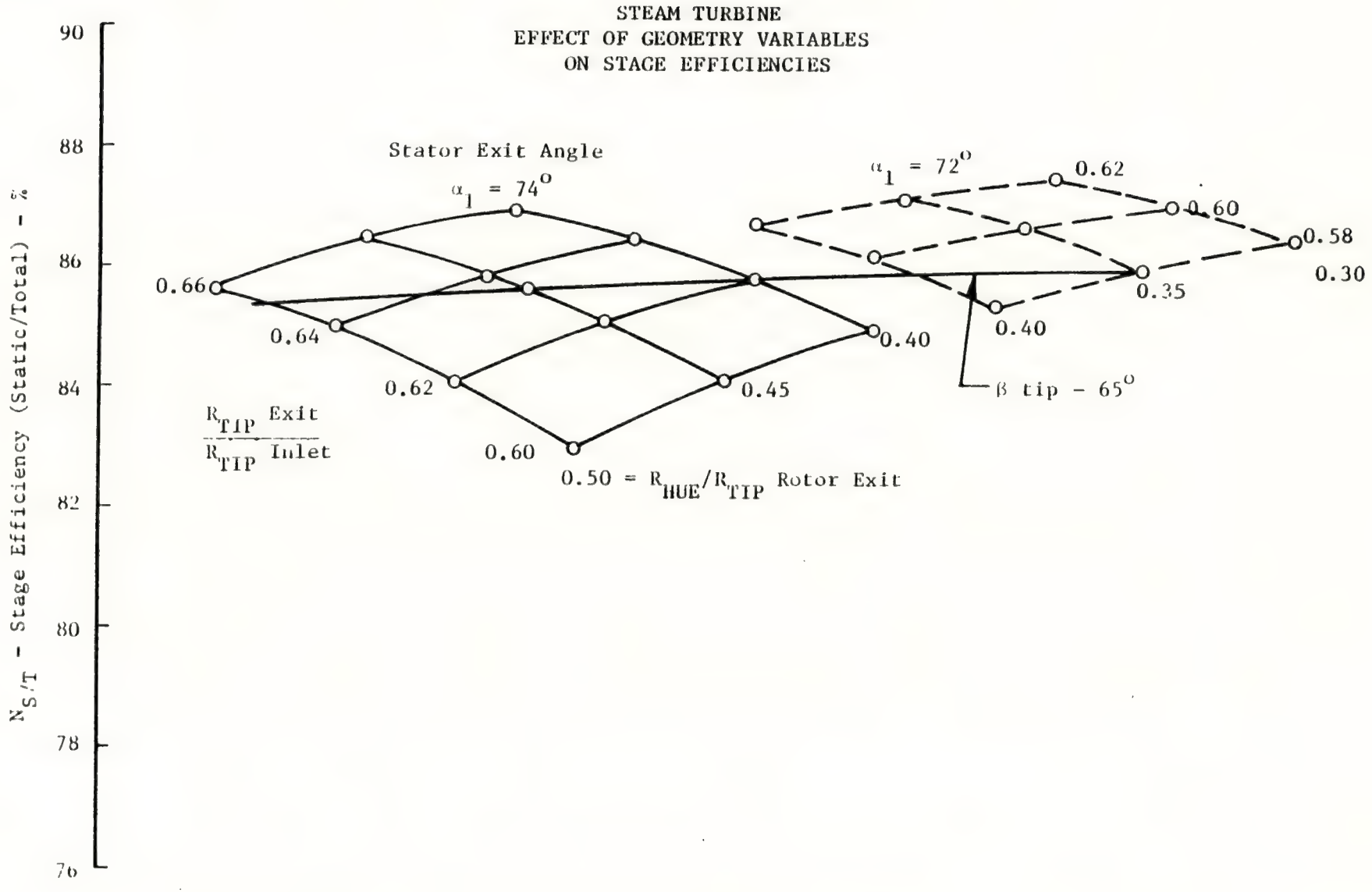

Figure 73 Parametric Plot of Radial-Inflow Turbine Geometry Variables

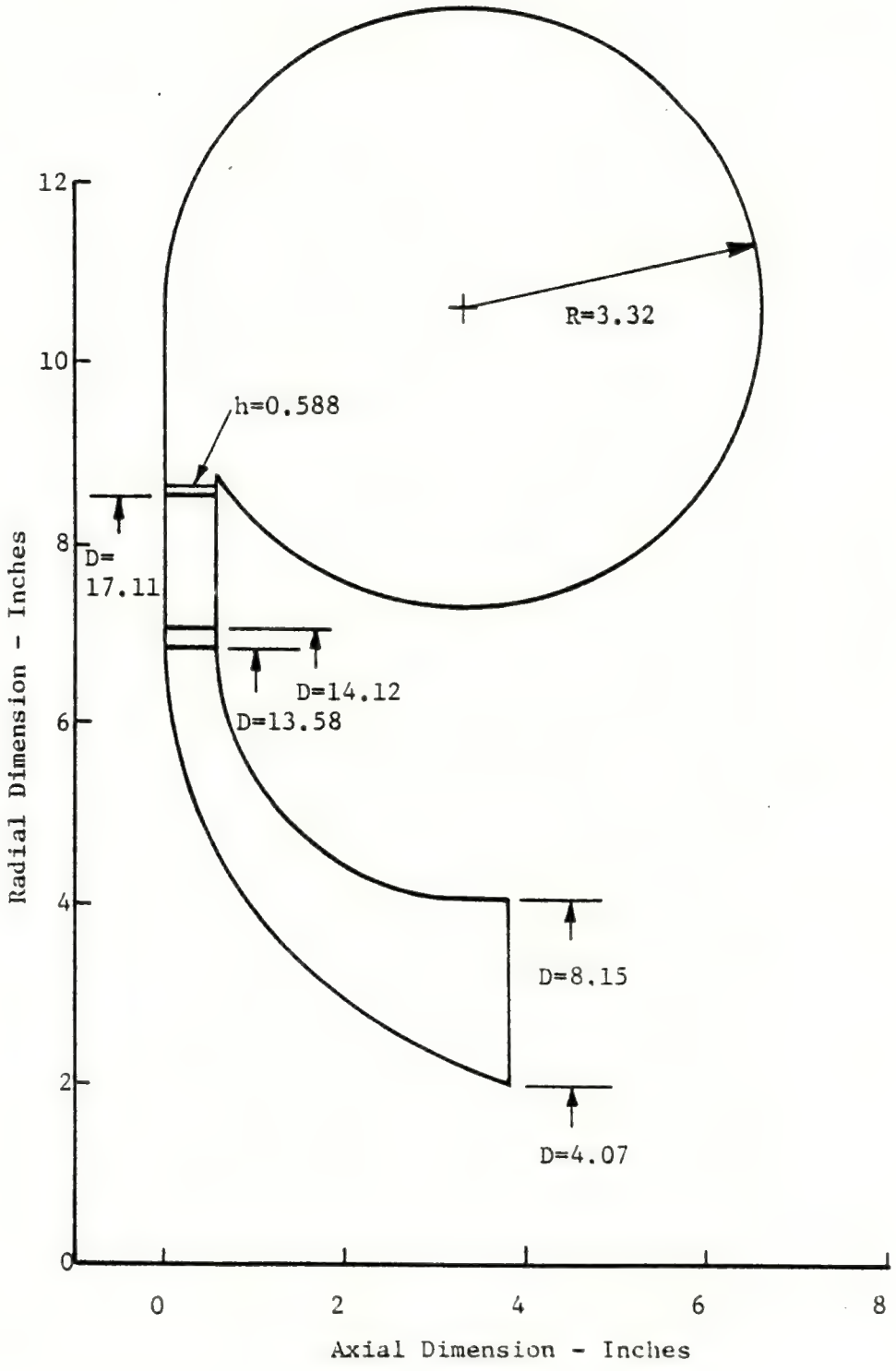

Figure 74 Flowpath Cross-Section for Radial-Inflow Steam Turbine

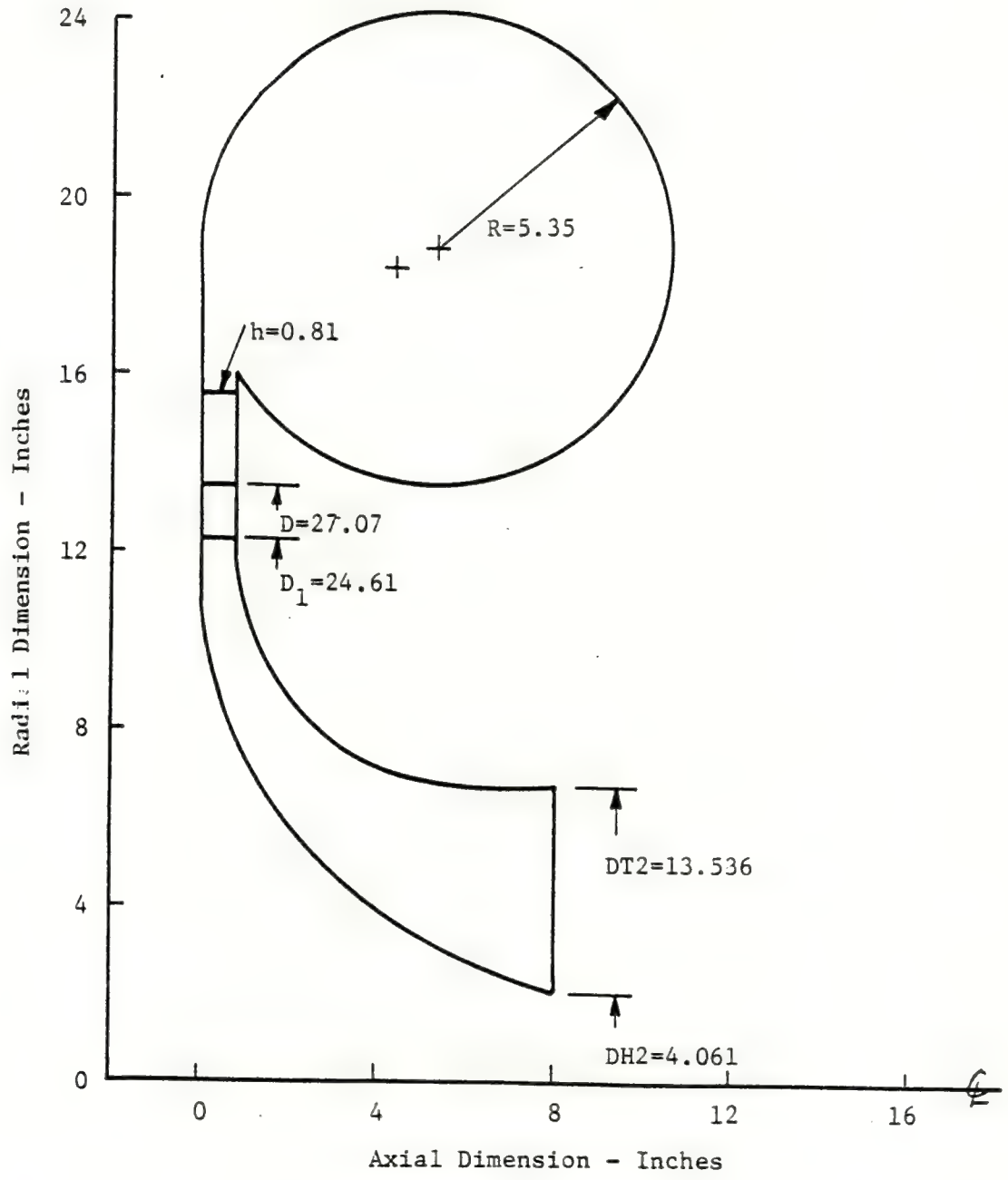

Figure 75 Flowpath Cross-Section for Radial-Inflow R-11 Turbine

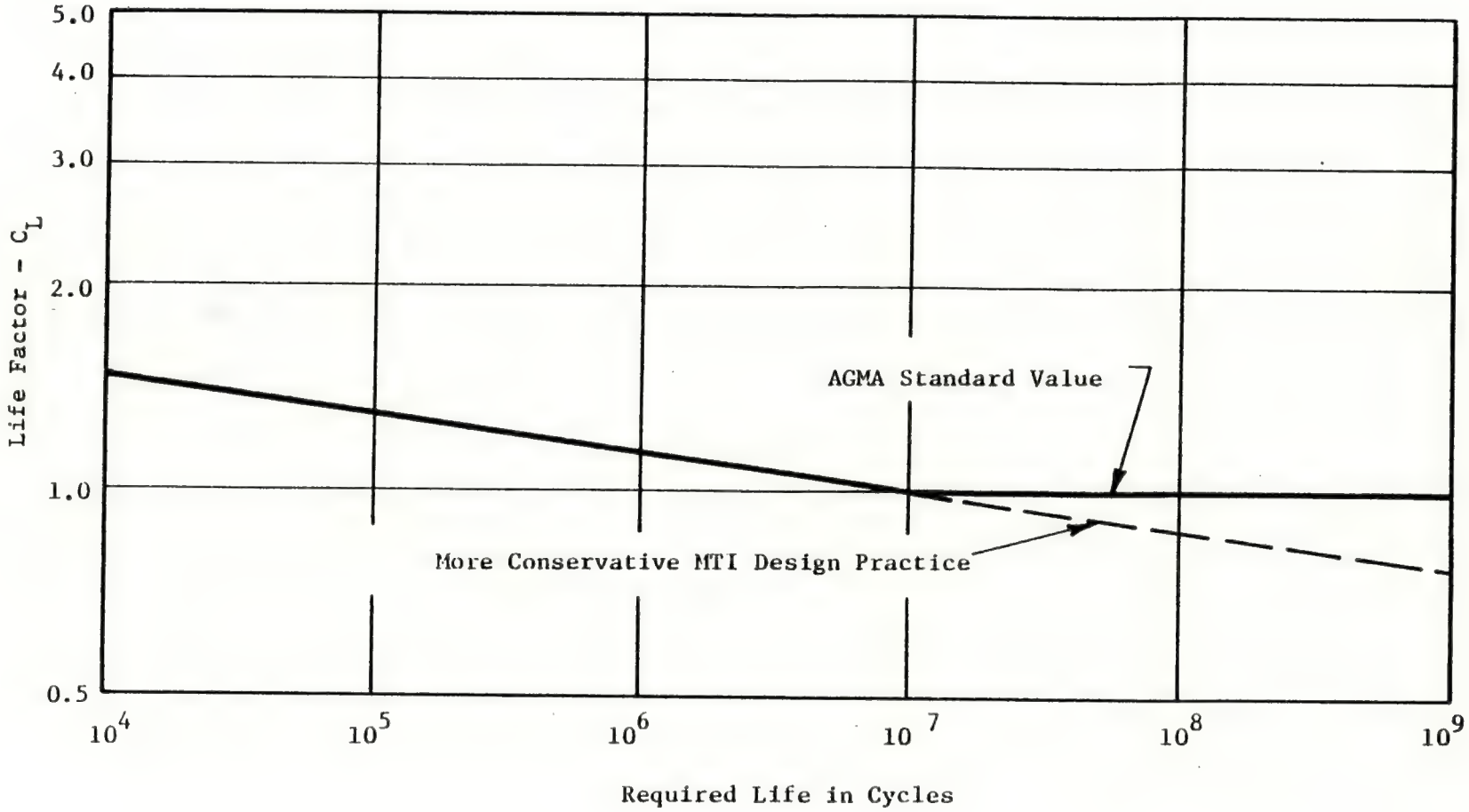

Figure 76 Gear Life Factor Versus Number of Fatigue Cycles, Illustrating Conservative MTI Practice Compared to AGMA Standard

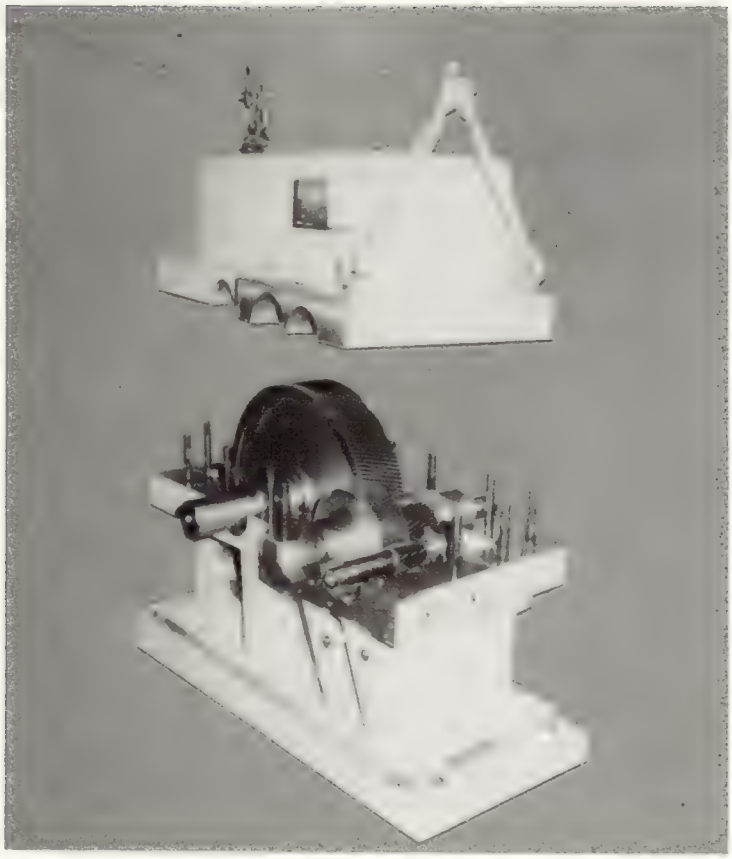

Figure 77 Partial Assembly of Gearbox

TABLE 22

GEAR DATA FOR BINARY SYSTEM INTEGRAL DOUBLE GEAR SET

Low Speed Gear Set	Generator Shaft (Gear)		R-11 Turbine (Pinion)
Shaft speed, rpm	1800		9545.5
Number of Teeth	175		33
Pitch diameter, inches	18.007		3.396
Face width, inches		4	
Speed ratio		5.303	
Helix angle, degrees (single helical gear)		13.628	
AGMA quality number		12	
Pitch-line velocity, ft/min		8486	
Design power, horsepower		750	
Design life, continuous operation*		10 Years	
Material	E-9310 Steel, case carburized to R_c56.		

High Speed Gear Set	R-11 Turbine (Gear)		Steam Turbine (Pinion)
Shaft speed, rpm	9545.5		42,220
Number of teeth	115		26
Pitch diameter, inches	7.441		1.682
Face width, inches		2.5	
Speed ratio		4.423	
Helix angle, degrees (single helical)		15.0	
AGMA quality number		12	
Pitch-line velocity, ft/min		17,750	
Design power, horsepower		300	
Design life, continuous operation*		10 Years	
Material	E-9310 Steel, case carburized to R_c56.		

*Fewer than 1 failure out of 100 gear sets for 10 years of continuous operation

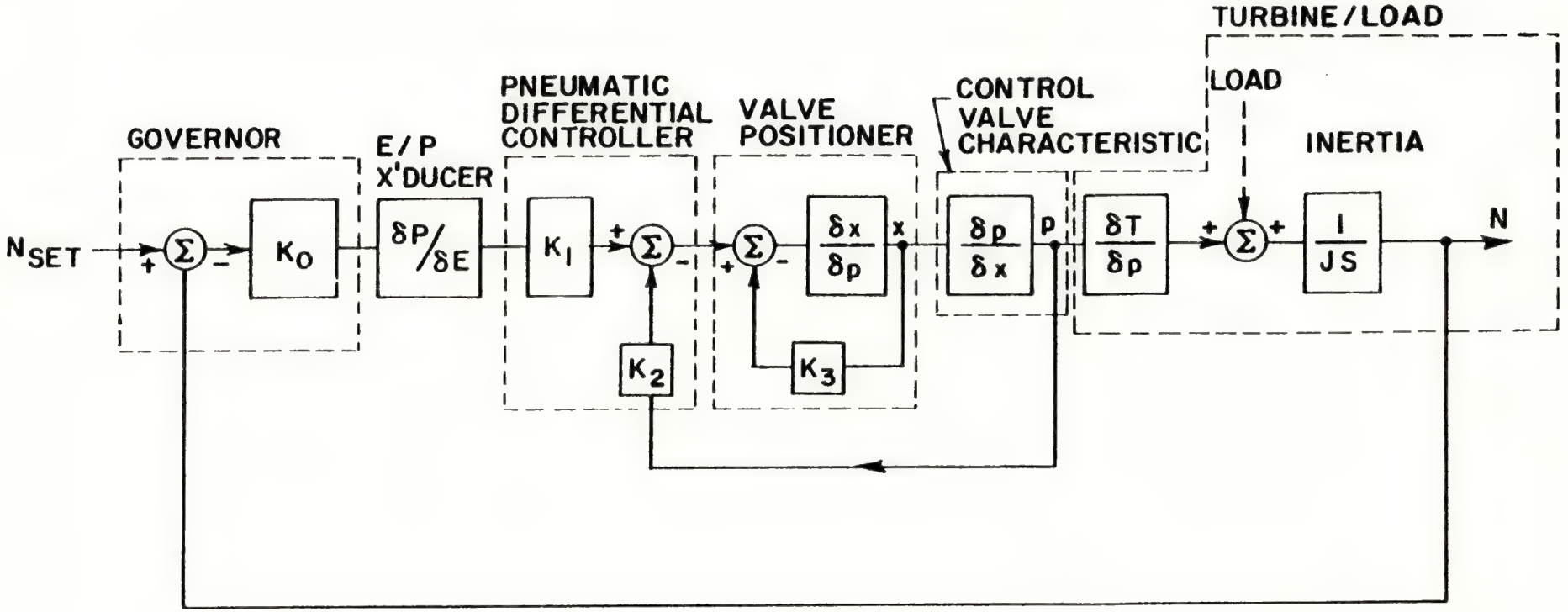

Figure 78 Linearized Controller Block Diagram

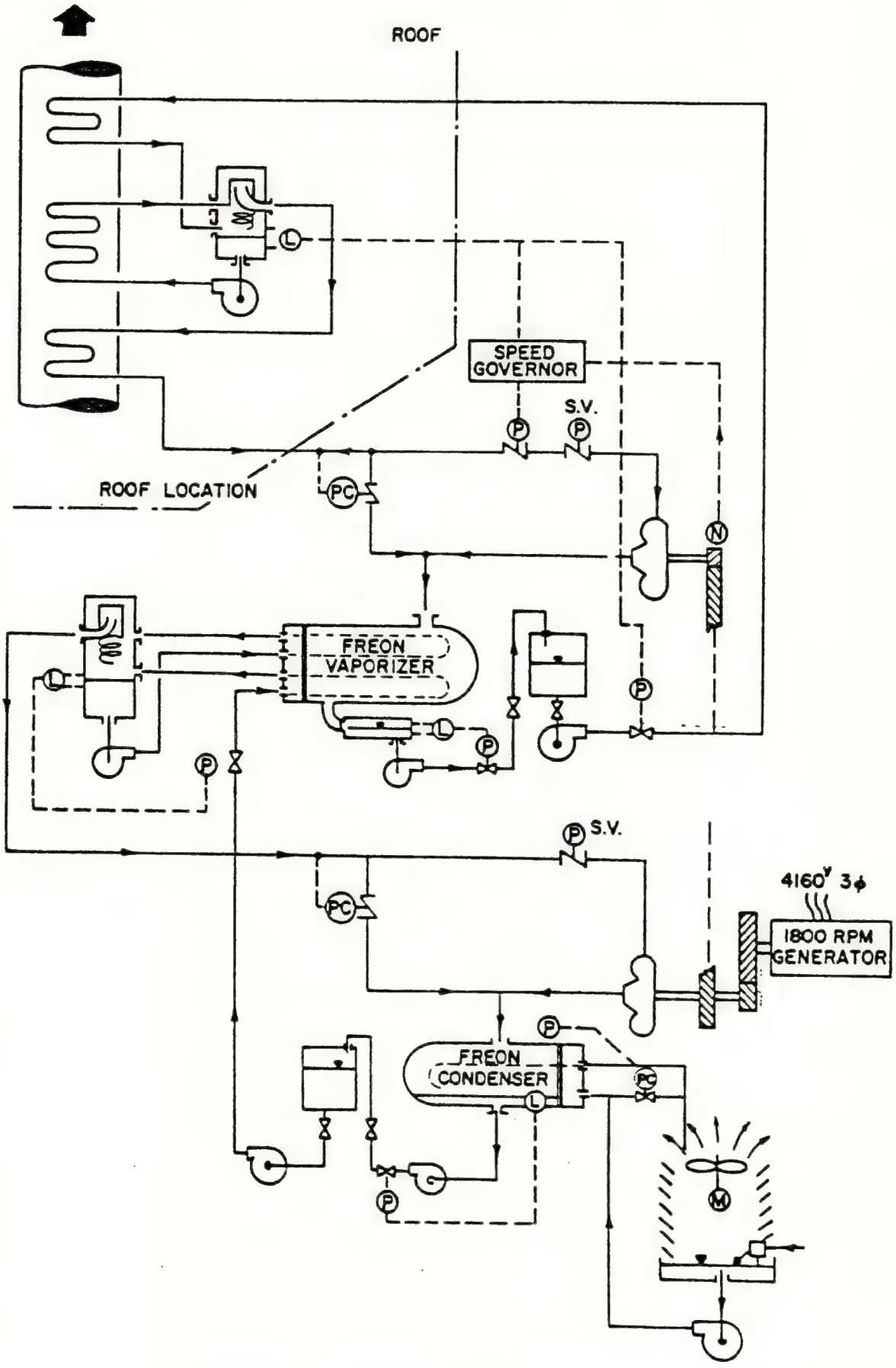

Figure 79 System Schematic

6.0 NON-UTILITY POWER GENERATION ECONOMICS

6.1 The Investment Decision

While various conservation technologies have been suggested for the industrial sector, most emphasis has been placed upon cogeneration and in-plant power generation with Rankine power recovery systems [35-41]. The economics of power generation in the non-utility environment was investigated in Reference 41 and has recently been brought to the attention of business management. Both References 41 and 42 speak of the differences between utility and non-utility investment decisions for power generation, and the impact of government policy on those decisions. The effects of positive or negative regulation are obvious. The effect of tax policy and rates is not so obvious. This is one aspect that will be discussed in this section.

Another effect is the influence of inflation. We are all aware of the results of inflation in general terms. The effects of expected future rates of inflation and the differential between different commodities can have a significant effect on the investment decision process. This too will be discussed in this section.

The basic criteria for investment decisions is the rate of return that investment provides the stockholder or bondholder (e.g., a return that is adequate to pay the interest and principal over the life of the bond). If an analysis is made of the actual return on equity experienced by industrial and utility companies, one could determine an investment threshold. This type of exercise was conducted in Reference 41 and presented here in Figure 80. There is an obvious difference between utilities and industrials. Utilities, whether publicly or privately owned, are monopolies with a guaranteed minimum return and a prohibited maximum return. Industry has more opportunity to make money as well as lose money. With an inherent higher risk, the industrials have higher returns. The rates of return indicated in Figure 80 do not, in fact, represent investment thresholds. They represent the average return on investment. The profit motivation (as well as bonuses and stock options) forces companies to seek investments that will improve their average return. The return premium demanded depends upon the perceived risk of the investment and the type of investment. The perceived risk is a subjective or objective evaluation of the

probability that the investment will achieve its performance goals. Technical and safety risks influence this valuation. The types of investment include defensive investments necessary for the company to maintain its business or market share, product expansion investments, and discretionary cost reduction investments. In-plant power generation falls into this last category. As pointed out in Reference 42, management has often imposed an investment return threshold that is twice that indicated in Figure 80 for discretionary investments.

Investment in in-plant generation will soon become a defensive investment. Energy costs are becoming increasingly important. In some industries, fuel costs approach 20 to 30 percent of operating costs. As this point, energy cost savings will significantly affect product cost. Thus, the companies that save the most energy can reduce their selling price and obtain both a larger market share and more profit. However, even in this case, the investment must show at least the returns indicated in Figure 80.

In order to evaluate an investment decision, a basic financial investment analysis must be made. This analysis is called by various names, such as Discounted Cash Flow (DCF) or Internal Rate of Return. Basically, the analysis determines a single figure of merit for the investment which is an effective interest rate, or DCF. This DCF interest rate indicates to the investor the return that investment would provide if it were a simple bond. The DCF interest rate can be compared directly to the values in Figure 80, or to alternative investments. The DCF interest rate is a function of tax rates, energy costs, inflation, depreciation rates, and investment tax credit. The next section will develop the DCF analysis, and is followed by an evaluation of the effects of the various input factors on the DCF rate, particularly the effects of governmental tax policies.

6.2 Discounted Cash Flow

Modern capital investment decision analyses and all based on the time value of money. This concept is simply illustrated by the following example. If you were offered a dollar today or a dollar next year, the dollar today would be worth more. This is due to the fact that you can take the dollar today, invest it in a zero risk bond at, for example, 6 percent. Thus, one year from now, the dollar you receive today is worth $1.06 (this ignores inflation and

taxes). The use of a discounted cash flow (also called "internal rate of return") provides an investor with a single rate of return or interest rate for a capital investment which will make the present value of the future flows of investment and returns identical. Mathematically, this can be written as:

$$\sum_{n=1}^{N} R_n (1 + r)^{-n} = \sum_{n=1}^{N} I_n (1 + r)^{-n}$$

where

N is the economic life of the investment

R_n is the return to the investor in year n

I_n is the investment in year n

r is the rate of return or interest rate

The returns and investments for each period are specified, and the relation is solved for the value of r which satisfy the equality.

The value for the investment in the case of power recovery systems is the total installed cost of the machinery. In the U.S., an investment tax credit is permitted for qualifying productive investments. The investment tax credit has the effect of reducing the cost of any investment by the amount of the investment tax credit. Assuming the investment tax credit is realized in the same year as the investment, the investment is given by:

$$I_n = C_n (1 - T_i)$$

where

C_n is the equipment and installation cost incurred in year n

T_i is the investment tax credit rate

Currently, the investment tax credit is 10 percent. There is legislation proposed to increase the investment tax credit to 20 percent or 30 percent for qualifying cogeneration and waste heat recovery investments.

The returns on the investment are composed of avoided electric and fuel costs, less the operating costs as might be adjusted by income tax considerations.

In this case, the returns are given by:

$$R_n = H_o c_e K (1+i_e)^n - H_L c_L (1+i_L)^n + c_m (1+i_m)^n -$$

$$T_m [H_o c_e K (1+i_e)^n - H_L c_L (1+i_L)^n + c_m (1+i_m)^n - D_n]$$

where

H_o is the number of operating hours per year

c_e is the avoided cost of electricity ($/kw-hr)

K is system capacity

i_e is the inflation rate for electricity

H_L is the number of labor hours for operation and maintenance

c_L is the average hourly labor cost

i_L is the inflation rate for labor

c_m is the miscellaneous maintenance cost (e.g., fluid make-up, maintenance parts, etc.)

i_m is the inflation rate for materials

T_m is the marginal income tax rate

D_n is the depreciation charges per year

Waste heat recovery has no fuel charge. A cogeneration system would include the fuel cost associated with the electric generation.

For the purpose of screening, the operating costs are assumed to be zero (i.e., neglibible on a per kw-hr basis). Also, it is assumed that a lump sum investment is made at the beginning of the first year. Thus, the relation for computing the DCF rate is:

$$C (1-T_i) = \sum_{n=1}^{N} [(1-T_m) H_o c_e K (1+i_e)^n + T_m D_n] (1+r)^{-n}$$

or

$$\bar{C} (1-T_i) = \sum_{n=1}^{N} [(1-T_m) H_o c_e (1+i_e)^n + T_m \bar{D}_n] (1+r)^{-n} \qquad (17)$$

where

$\bar{C}_n$ is the installed cost per unit delivered power

$\bar{D}_n$ is the depreciation charge per unit of delivered power

This latter relationship permits the examination of the investment desirability on a $/kw basis. Also, it makes it easier to look at the investment sensitivity to various parameters.

In order to quantify the effects of these various parameters, a series of investment analyses were made. In these investment analyses, an economic project life of 10 years was assumed. The depreciation method used is the sum-of-the-years-digits. The annual depreciation charge with this method is given by:

$$\bar{D}_n = \bar{C} \frac{(M+1-n)}{\sum_{1}^{M} n} \qquad \text{for } n \leq M$$

$$\bar{D}_n = 0 \qquad \text{for } n > M$$

where

M is the tax life of the investment

For example, if the investment has a 10 year life, the first year charge is .1818 (=10/55) of the investment base. However, in order to more clearly show the effect of the depreciation life, we can use a simple straight line depreciation rate and rewrite Equation 17 as:

$$\bar{C}\,(1-T_i) = \sum_{n=1}^{N} [(1-T_m)\, H_o c_e\, (1+i_e)^n + \frac{Tm\ \bar{C}}{M}\, (1+r)^{-n}$$

The quantitative sensitivity analyses are presented in Section 6.3 using the sum-of-the-years depreciation.

Examination of Equation 17 shows that the returns are affected by the installed unit cost, the investment tax credit, the marginal income tax rate, the hours of operation, the avoided unit electric cost, the inflation rate of electric costs, and the depreciation charges. The government can easily control the investment tax credit, the marginal tax rate, and the depreciation charges.

Increasing the investment tax credit decreases the effective cost of a system and thus increases the DCF for a given system. The marginal tax rate operates in two ways. A decrease in the marginal tax rate increases the operating savings that stay with the company. This will increase the DCF. However, a decrease in the tax rate decreases the effect of the depreciation charges which will tend to decrease the DCF. The relative sizes of the savings and depreciation charges are such that a decrease in the marginal tax rate will increase the DCF. The depreciation charge depends upon the allowed tax life and the depreciation method. Obviously, depreciation charges early in the economic life of the investment have more value than in later years. This is why various accelerated depreciation schedules are permitted and used. The tax life of an investment need not have a direct relationship to the economic life. For most investments in the U.S., there are guidelines for determining the tax life of an investment which approximate its economic life. However, exceptions have been allowed for certain classes of investments such as pollution control equipment. A government policy to permit similar short write-offs for energy conservation equipment is very possible.

6.3 Investment Sensitivity Analysis

An investment analysis designed for examining investments in waste heat recovery systems was used to analyze the sensitivity of the DCF to total installed cost ($\overline{C}$), the avoided electric unit cost (c_e), the energy inflation rate (i_e), the annual hours of operation (H_o), the marginal tax rate (T_m), the investment tax credit rate (T_i), and finally, the depreciation life (M). A sample output from the investment analysis program is shown in Figure 81. In this parametric sensitivity analysis, the unit price of installed machinery specified for the program is taken to include all costs including site preparation, construction, tie-in, startup and end user engineering costs. Operating costs were assumed to be negligible. The economic project life was assumed to be 10 years. Local taxes and insurance was taken as 3 percent of the initial investment.

The effect of DCF to avoided electricity is shown in Figure 82 with no inflation effects. This shows why there has not been interest in power generation from waste heat. Current average industrial electric cost in the U.S. is about 2.5¢/kw-hr. Without any inflation, the cost will remain at that

level. The DCF at an installed cost of $800/kw is only 12 percent with 2.5¢/kw-hr. Referring back to Figure 80, it is clear that very few companies would invest at this level of DCF. A more reasonable and expected investment threshold would be a 20 percent DCF. The expected installed cost of a bottoming system is indicated on Figure 82 as in the range of $800 to $1,000/kw for a 1,000 kw system. This implies that if a company now has electric costs of the order of 4¢/kw-hr or greater, waste heat power recovery would be an attractive investment.

In Figures 83 through 87, an area is indicated as being the region of expected near term economic acceptability for waste heat recovery systems. This region is the same for all the figures and helps to indicate the effect of the sensitivity parameter being illustrated. This area indicates the expected economic parameters that will characterize the initial commercial purchases of waste heat power recovery systems in the 1979 to 1982 time frame.

Figure 83 presents the effect of electric cost inflation rate on the DCF. A variation of $\pm$12 percent from an 8 percent inflation rate does not have much effect (about $\pm$1 percent in DCF). Therefore, an exact estimate of the inflation rate is not too important as long as it is a reasonable estimate. For the U.S., an electric inflation rate of 8 percent seems to be an accepted estimate.

Another parameter that has significant effect on economic acceptability is the annual hours of operation. Since waste heat recovery systems are tied to a primary operating cycle typical of a given industry, Figure 84 implies that only those industries having high annual utilization of their plant will be attracted to use waste heat power recovery. For example, a single shift operation will have at best 2,080 hours of operation in a year (40 hours/week). In order to get 7,000 hours of operation, a plant has to be on a three shift operation, six days per week. This would tend to suggest a process type operation. As noted in Section 5, a base loaded Diesel generator has only 7,500 hours per year of operation.

The parameters covered thus far are parameters that are not easily controlled or even significantly affected by the central government. The next three parameters are readily controlled by the government and can be used by the government

to promote the economics of energy saving investments. Figure 85 shows the effect of the marginal income tax rate. Currently, the marginal federal income tax rate for U.S. industry is 48 percent. State taxes will be added but will be somewhat reduced by deductions in the federal tax base. Income tax rates are not an appropriate means of influencing specific investments. However, there have been some suggestions for changes in the tax rate for overall economic stimulation. Figure 85 shows that a charge of 10 percent in the tax rate produces about a 2 percent change in the DCF. This is not a very effective stimulant for investing specifically in energy saving equipment.

Legislation has already been introduced to increase the investment tax credit for energy conservation equipment. Figure 86 shows that an increase of 10 percent in the investment tax credit raises the DCF by 3 percent. This could move a marginal investment into the acceptable region. An increase of 20 percent in the investment tax credit will raise the DCF by about 6 percent. This could move a marginal investment into the attractive region.

Figure 87 shows the effect of permitting a rapid write-off of energy conservation equipment. Reducing the depreciation period from 10 years to 5 years increases the DCF by 4 percent. A combination of rapid write-offs plus an increased investment tax credit will significantly improve the economics of waste heat utiliztion technologies in the industrial sector.

NON-UTILITY POWER

GENERATION ECONOMICS

78P79

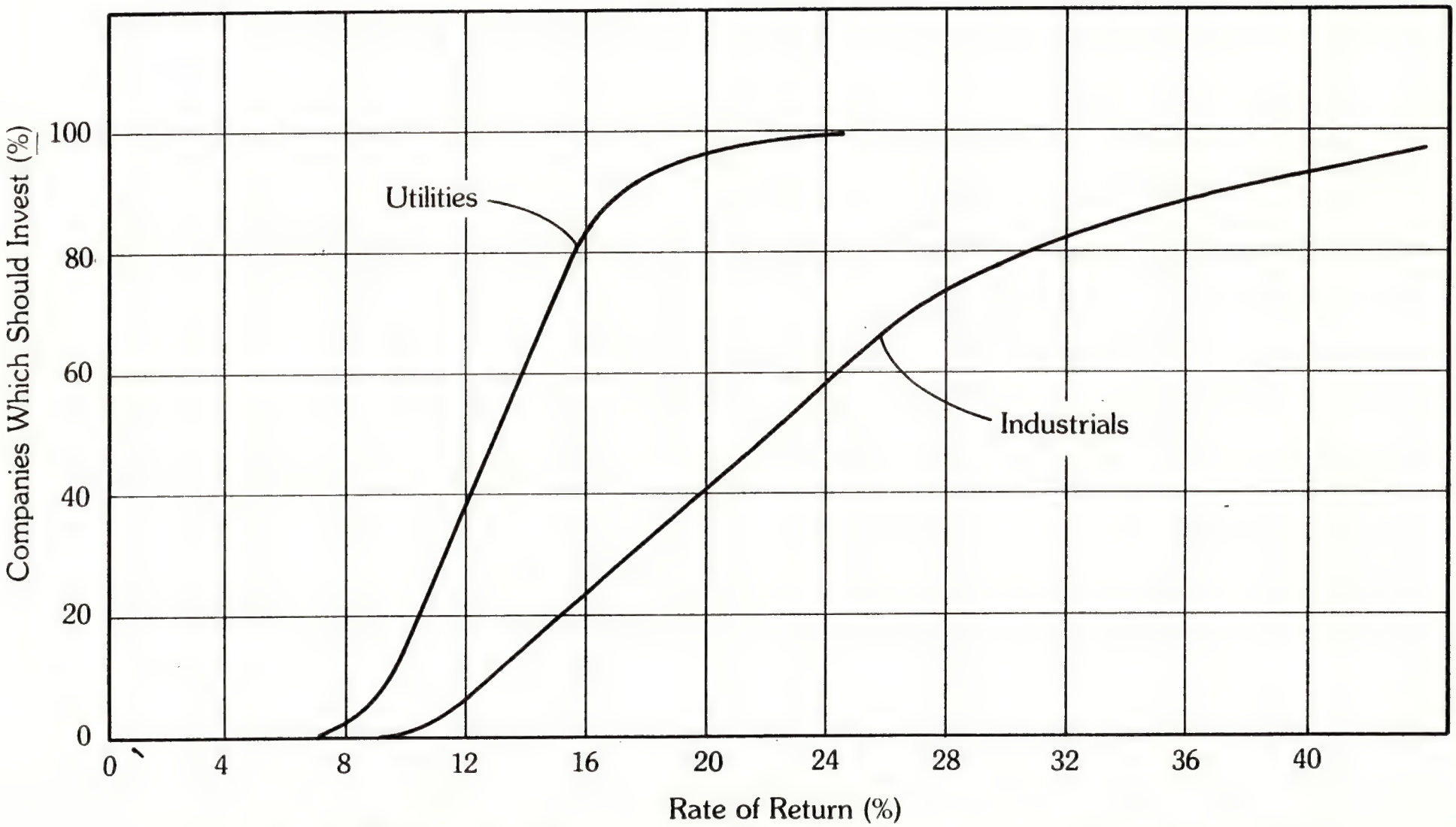

Figure 80 Accumulative Distribution of Industries and Utilities That Should Be Willing To Invest at a Given Rate of Return (Source: Reference 41)

DISCOUNTED CASH FLOW

$$\sum_{n=1}^{N} R_n (1+r)^{-n} = \sum_{n=1}^{N} I_n (1+r)^{-n}$$

78P79

VON KARMAN PAPER

INVESTMENT INPUTS

UNIT PRICE OF INSTALLED MACHINERY, DOLLARS/KW.....	1000.00
CUSTOMER SITE PREP, CONSTRUCTION AND TIE-IN COST (PERCENT).....	0.00
INSTALLED TOTAL UNIT COST, DOLLARS/KW.....	1000.00
RATED POWER, KW.....	1000.00
TOTAL INVESTMENT.....	$1000000.00

OPERATING INPUTS

ENERGY RATE, CENTS/KW HR.....	3.50
PERCENTAGE RISE IN ENERGY RATE PER YEAR.....	8.00
OPERATING HOURS PER YEAR.....	8760.00
OPERATING LABOR HOURS PER YEAR.....	0.00
MISC. OPERATING COST, DOLLARS PER YEAR.....	0.00
PERCENTAGE RISE IN MISC. OP. COST PER YEAR.....	0.00
OPERATING LABOR RATE, DOLLARS/HOUR.....	0.00
PERCENTAGE RISE IN OP. LABOR RATE PER YEAR.....	0.00

FINANCIAL INPUTS

YEARS ANALYZED.....	10
DEPRECIATION PERIOD YEARS.....	10
DEPRECIATION METHOD 0 FOR STRAIGHT LINE 1 FOR SUM OF THE YEARS DIGITS.....	1
LOCAL PROPERTY TAXES AND INSURANCE, PERCENT.....	3.00
COMBINED FEDERAL AND STATE INCOME TAX RATE, PERCENT....	50.00
INVESTMENT TAX CREDIT, PERCENT.....	10.00
INTEREST RATE ON REINVESTED CASH FLOWS, PERCENT...	0.00

OUTPUT TABLE (IN THOUSANDS OF DOLLARS)

END OF YEAR	UNDEPRECIATED BALANCE	GROSS INCOME	COST OF OP. INCL. DEPR.	AFTER TAX INCOME	CASH FLOW	CUM. NET CASH FLOW
0	1000.00	0.00	0.00	0.00	0.00	-1000.00
1	818.18	306.60	209.09	148.75	330.57	-669.43
2	654.55	331.13	185.73	72.70	236.34	-433.09
3	509.09	357.62	162.91	97.35	242.81	-190.28
4	381.82	386.23	140.64	122.80	250.07	59.79
5	272.73	417.13	118.91	149.11	258.20	317.99
6	181.82	450.50	97.73	176.38	267.29	585.28
7	109.09	486.54	77.09	204.72	277.45	862.73
8	54.55	525.46	57.00	234.23	288.77	1151.50
9	18.18	567.50	37.45	265.02	301.38	1452.89
10	-.00	612.89	18.45	297.22	315.40	1768.29

DISCOUNTED CASH FLOW, PERCENT.....	24.272
BREAK EVEN POINT, YEARS.....	3.76

Figure 81 Sample Printout from the Waste Heat Recovery Investment Analysis Program

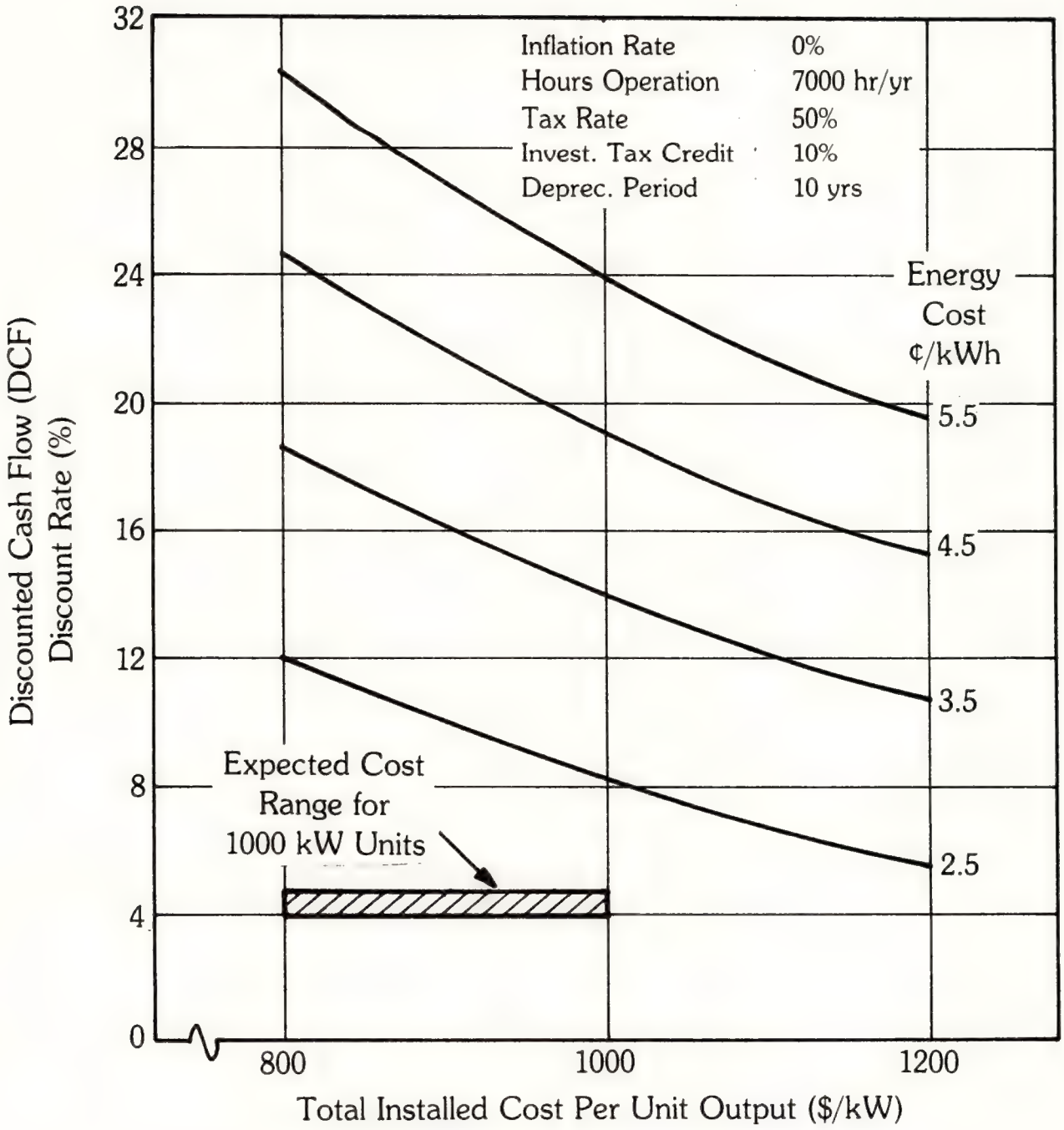

Figure 82 Effect of Energy Cost on the Discounted Cash Flow

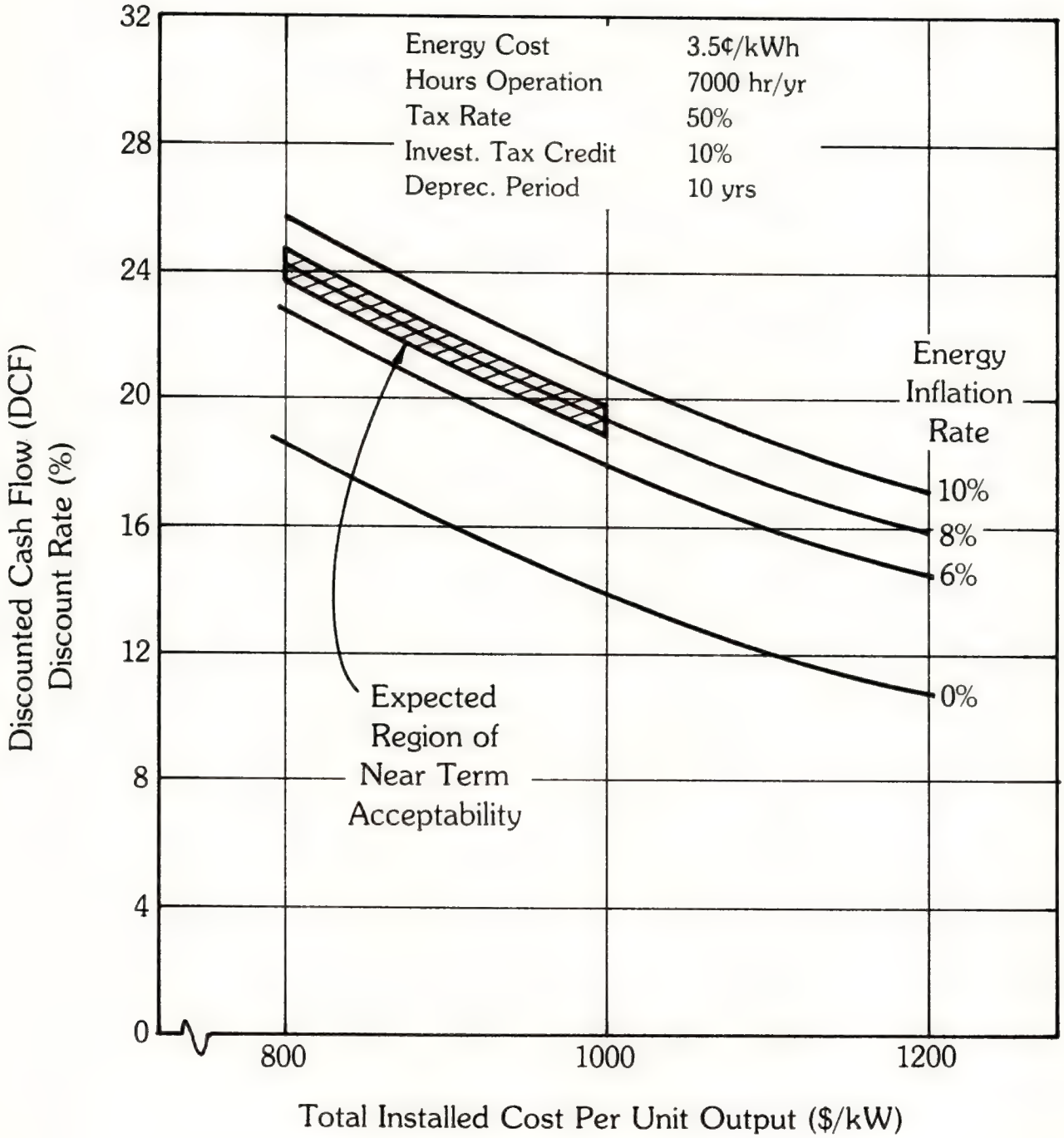

Figure 83 Effect of Energy Inflation Rate on the Discounted Cash Flow

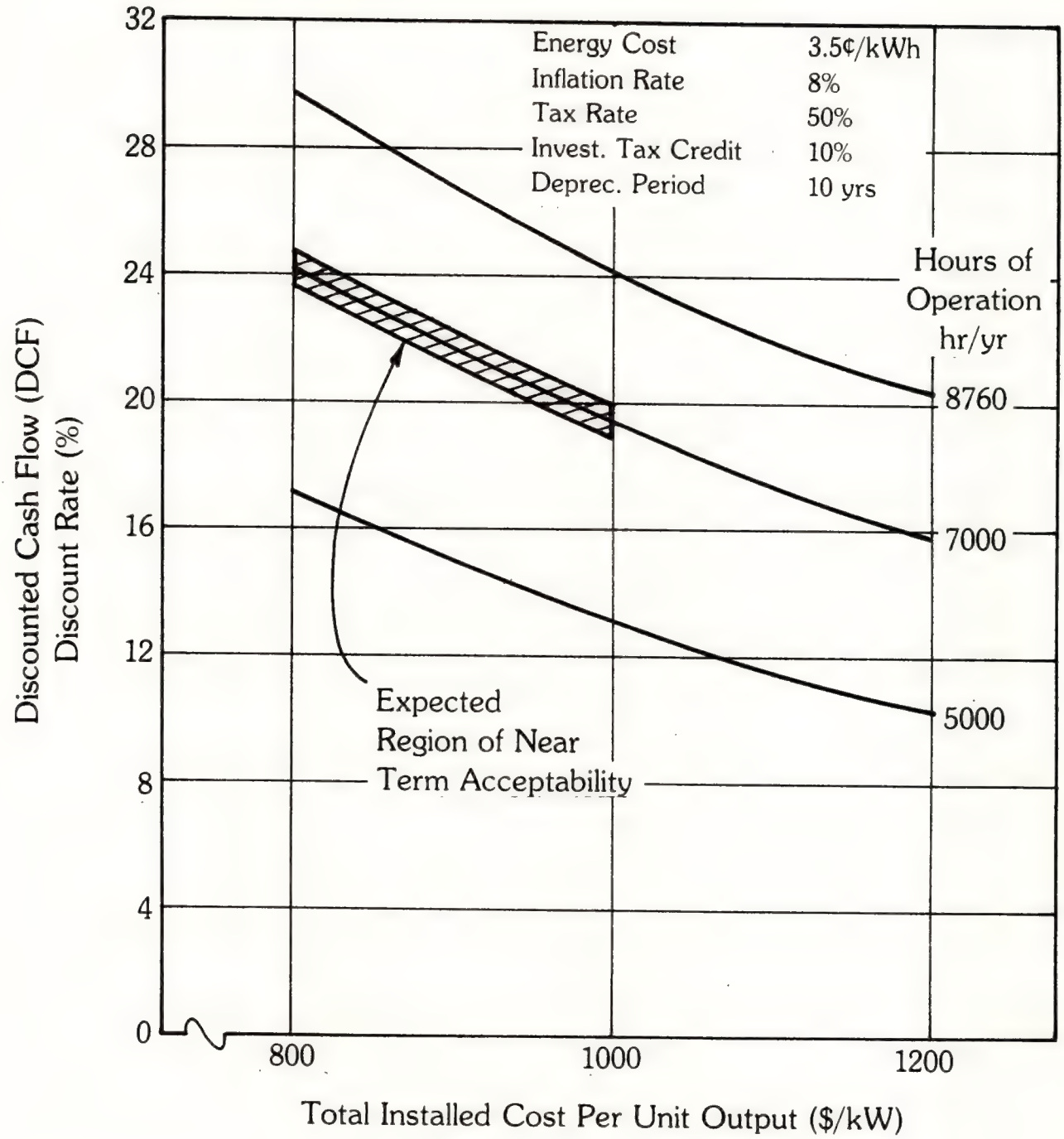

Figure 84 Effect of Annual Operating Hours on Discounted Cash Flow

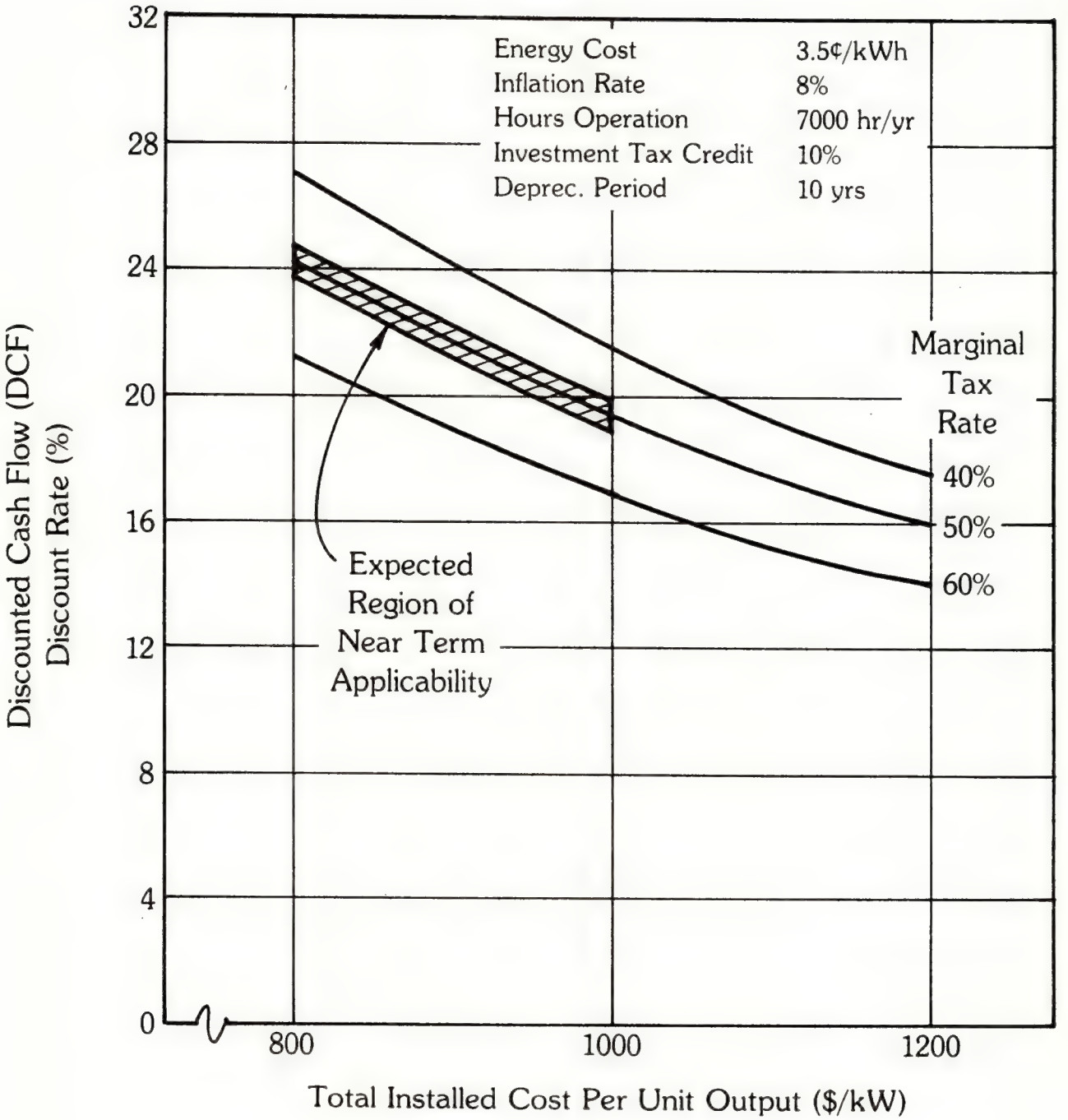

Figure 85 Effect of Marginal Tax Rate on the Discounted Cash Flow

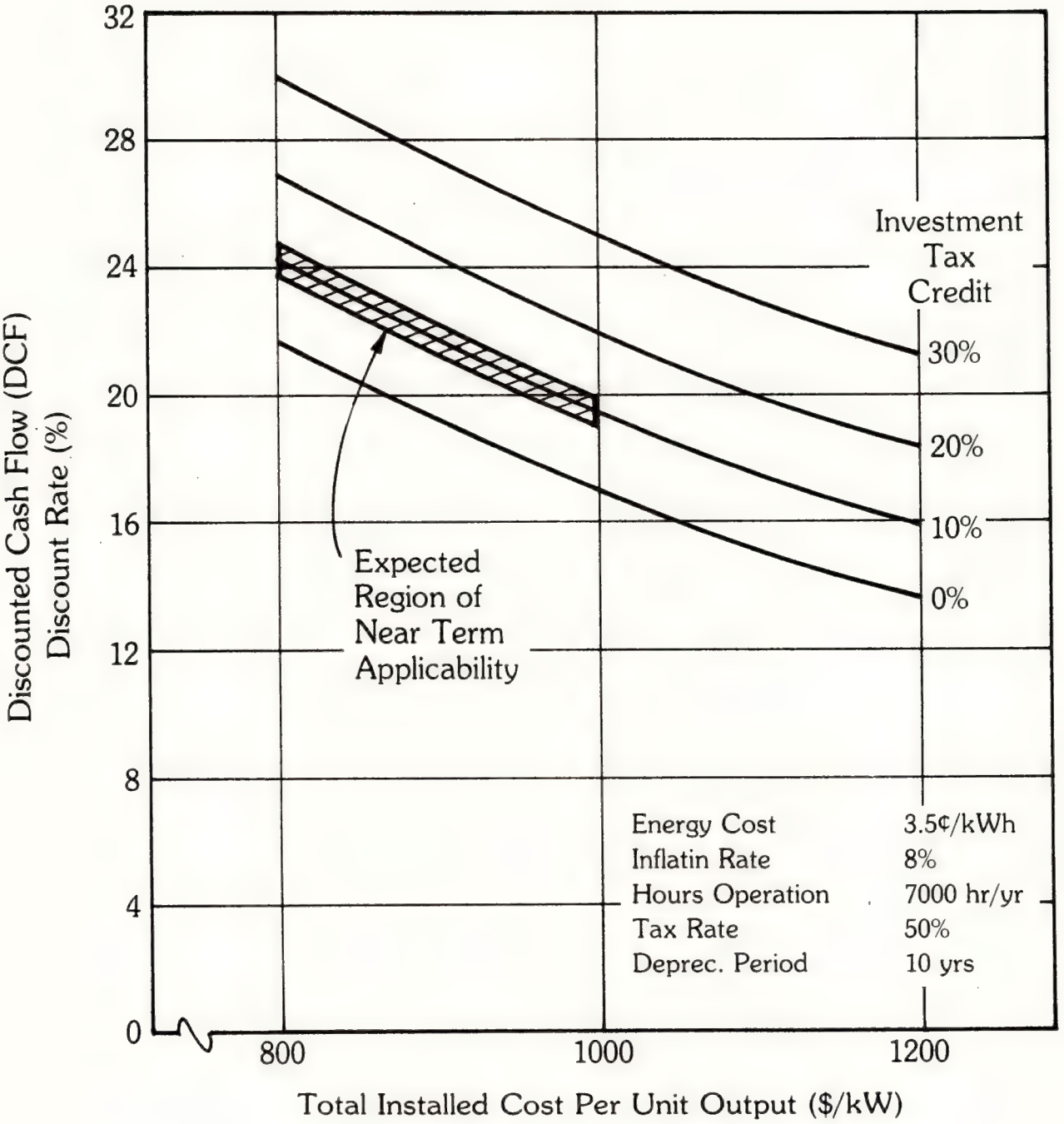

Figure 86 Effect of Investment Tax Credit Rate on the Discounted Cash Flow

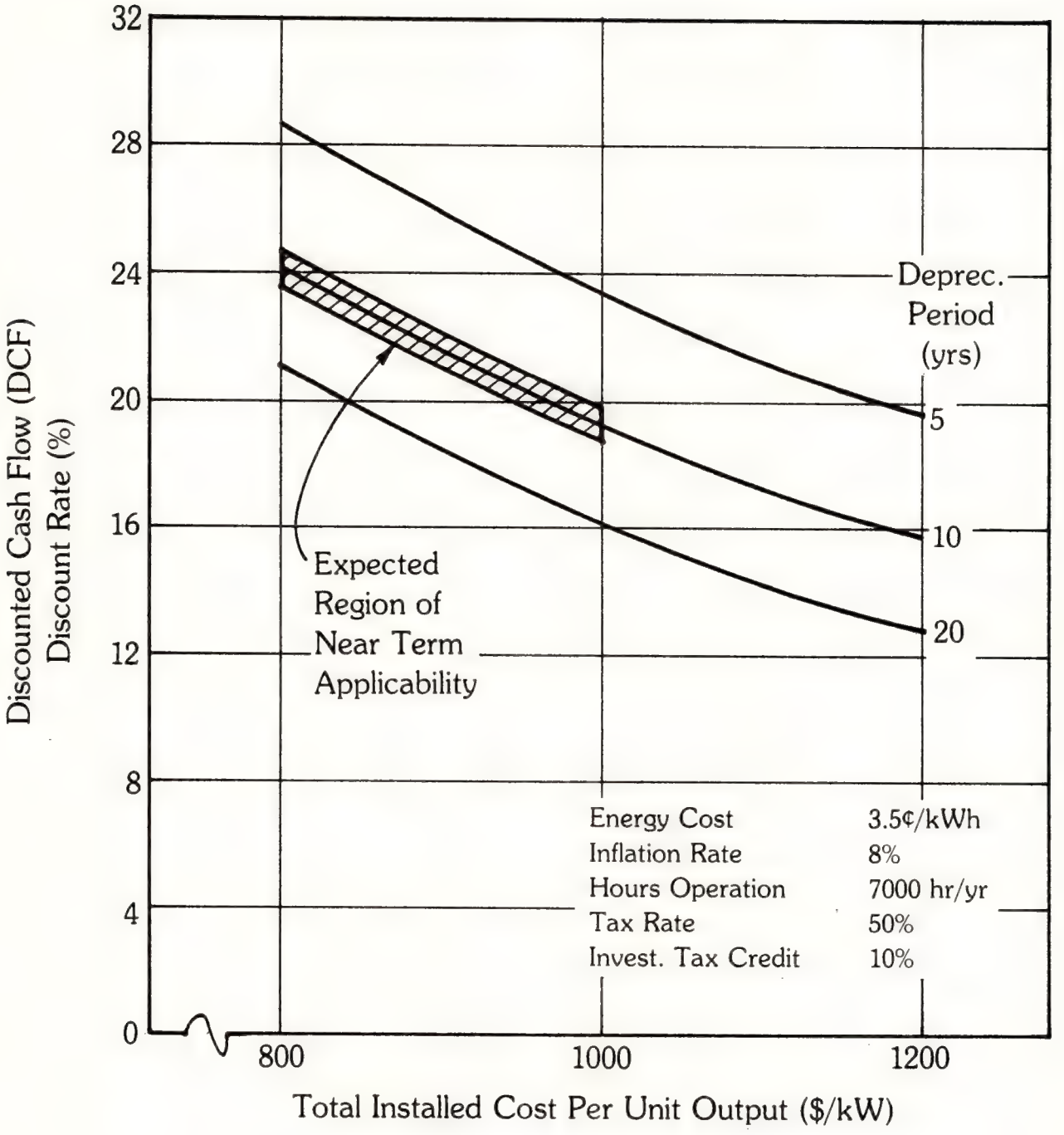

Figure 87 Effect of Depreciation Period on the Discounted Cash Flow

7.0 ECONOMIC ACCEPTANCE OF BOTTOMING CYCLES

Up to this point, we have examined the applicability of a given fluid or cycle as a bottoming cycle in an application range, and have seen that binary cycles are cost competitive with other fluids in the temperature range of 400°F to 800°F, and that under 400°F, the fluorocarbon refrigerants should have clear cost and performance advantages. We have seen in the previous section that a rather straightforward relationship exists between the installed cost of a bottoming cycle and its economic return based on a number of parameters. We have not yet discussed if the best bottoming cycle in a range will meet the economic investment criteria of industry so that it will be purchased. This subject will be addressed in this section.

7.1 Economic Screening Criteria

A series of investment analyses were conducted using the technique described in the previous section. The chief difference between the investment analysis conducted for developing an economic acceptance screening and that conducted in the previous section is that the machinery cost is estimated and the installation charge is specified as a percentage of machinery cost. This results in a DCF discount rate being expressed as a function of the machinery cost. The estimated machinery cost resulting from the Rankine design program can then be used to identify a DCF for the particular cycle and application. Table 23 presents the economic factors used for the economic acceptance screening as compared to the base case factors used in Section 6.

7.2 Rankine Cycles for Screening

Four organic cycles using common fluorocarbon refrigerants (R-11 and R-114) and three binary cycles with steam and R-11 were analyzed with a number of source temperatures and heat flows for condensing (latent) and hot gas (sensible) heat sources. The state points and fluids for these seven cycles are shown in Table 24. The source temperature and exit temperature were set based on a boiler effectiveness that has appeared to give the optimium cycle economics during numerous cycle optimization studies. Having determined the source and exit temperatures, four levels of heat flow into the Rankine cycle were specified. Physically, this means simply increasing the flow rate of exhaust gas or condensing fluid to achieve a level of heat flow for a given temperature drop. This analysis format permits the effect of different source temperatures

and heat flows (e.g., net delivered power) on various cycles to be studied. Conversely, given a specific source temperature and physical flow, a heat/flow can be computed and a near optimum cycle identified.

7.3 Economic Acceptance Screening

7.3.1 Condensing Heat Sources

Condensing sources of heat are not unusual in petroleum refining or chemical processes. One specific type of condensing waste heat stream is a clean cut off a distillation column. Another example is a stream of steam used to drive off contaminants from and reactivate an activated carbon adsorption system. Currently, the heat from these condensing waste streams is simply dumped to cooling water. The recovery of this waste heat through a bottoming cycle can be both energy conserving and economic.

Figure 88 presents the economics of power recovery from a condensing waste stream. This figure illustrates that heat recovery economics depends not only on the temperature of the waste stream, but also on the size of the waste stream. If a waste condensing stream of 30 million Btu/hr is available, a source temperature of 205°F would show a DCF of about 25 percent. This is an attractive enough DCF to warrant a more detailed look. If the heat flow were 10 million Btu/hr, a source temperature of about 300°F would be necessary to achieve a DCF of 25 percent.

This type of plot permits very rapid screening of possible heat recovery applications. Local economic conditions can be quickly taken into account with sufficient accuracy for screening purposes by using the following relation:

$$DCF_{Actual} \approx DCF_{Figure} \left[\frac{\text{Actual Electric Rate}}{3.5}\right] \left[\frac{\text{Actual Hours}}{7{,}000}\right]$$

Referring to the example of a 30 million Btu/hr flow at 205°F, the DCF from Figure 88 is 25 percent. If the actual electric rate is 2.5¢/kw-hr and the actual hours is 8,000, the screening DCF for that particular application would be about 20 percent, which is economically marginal considering the simplifying assumptions made for the screening purpose.

7.3.2 Hot Gas Sources

A hot gas source can be screened in the same way as described for the condensing waste heat source. Figure 89 presents the variation of DCF for some organic and binary cycles with a hot gas waste heat source at various temperatures and heat flows. The screening approaches described for the condensing heat sources are applicable here. As can be seen, a shift from organic cycles (Cases A to C) to binary cycles (Cases E and G) was made in the plot. The question of whether this shift is economically or operationally justfied needs to be addressed.

Figure 90 presents the variation of the cycle DCF with source temperature for a given heat flow of 10-million Btu/hr. The solid curves in Figure 90 indicate the locus of the most cost effective cycles for a given source temperature, and the economic cost of selecting the non-optimum cycle. For example, selection of a system represented by case A would have a DCF of about 2.7 percent less than a system represented by Case B with a 350°F source. As would be expected from the results in Section 4 (Figure 60), the organic cycle represented by Case D has a higher DCF than the binary cycle represented in Case E. However, due to fluid stability, use of the common fluorocarbons with source temperatures above 400°F is questionable, and above 500°F, not acceptable. Thus, a switch from fluorocarbons to a binary should be made between 400°F and 500°F for reasons of stability. System economics would dictate a change at about 575°F where the DCF for Cycle D would cross the DCF for the optimum binary cycle.

Figure 90 would suggest that a binary steam/R-11 cycle would have better economics than a simple organic at lower temperatures. This would not be a logical expectation since the binary has more machinery, a loss of thermodynamic potential across the steam/R-11 heat exchanges, and an extra heat exchanger at the lower temperatures where regeneration is not economic. This implication of the curves is simply the result of the cycles selected. The economics of the binary cycle will degrade very rapidly with source temperatures below 450°F, and thus, such cycles were not analyzed. An indication of the rapid performance degradation of the binary cycle's performance relative to the organic can be seen in Figure 91. This figure shows the variation of delivered power with source temperature for the cycles considered. As can be seen,

the binary cases have a steeper slope than the organic cases, and at source temperatures below 525°F, has less delivered power. A simple extrapolation of the binary case would suggest that it would have no net delivered power at a source temperature of 350°F.

A comparison of Figures 90 and 91 gives an indication of the effect of the added costs in a binary system over an organic system. Figure 90 indicates an economic break even at a source temperature of 575°F. Figure 91 indicates a power break even at 525°F. The additional 50°F of source temperature is needed to offset the capital cost difference between the two approaches.

7.4 Economic Acceptance Conclusions

Current average industrial power rates in the U.S. are of the order of 2.5¢/kw-hr. Recent discussions with a number of industrail clients indicates that a project DCF of 20 percent is needed to justify an energy conservation investment. If we use Figures 88 and 89 for screening, an extra 5 percent in DCF should be required to account for the simplifying assumptions made. If we also constrain our discussion to the process type industries that have operations of over 8,000 hours per year, we can define a screening DCF as:

$$\text{DCF}_{\text{Screen}} = \text{DCF}_{\text{Required}} \left[\frac{3.5}{\text{Actual Rates}}\right] \left[\frac{7,000}{\text{Actual Hours}}\right]$$

or

$$\text{DCF}_{\text{Screen}} = 25 \left[\frac{3.5}{2.5}\right] \left[\frac{7,000}{8,000}\right] = 30.6\%$$

Since this a screening analysis, we will use 30 percent as the threshold DCF in Figures 88 and 89. Figure 92 presents the results showing the current source temperatures and heat flows in process industries that might be judged economically acceptable for the use of Rankine bottoming cycles. In general, applications with heat flows into the Rankine cycle of less than 15 million Btu/hr seem to be uneconomic under the criteria used in this screening.

From discussions with companies in the process industries, there seems to be a large number of applications that fall at or above the economic threshold lines in Figure 92. Thus, there is now an economic need for bottoming cycles that will increase as the energy cost increase relative to equipment cost.

What is needed to make this need into a viable business for manufacturers of packaged bottoming cycle systems is actual demonstration of such systems in process applications.

ECONOMIC ACCEPTANCE OF BOTTOMING CYCLES

78P79

TABLE 23

ECONOMIC FACTORS USED IN ECONOMIC ACCEPTANCE ANALYSIS

	Economic Acceptance Analysis	Base Case Section 6.0
Machinery Unit Cost ($/kw)	Specified	-----
Installation Cost (as a percent of Machinery Cost)	25%	-----
Total Installed Unit Cost ($/kw)	Computed	Specified
Energy Rate (¢/kwh)	3.5	
Energy Inflation Rate (%)	8.0%	
Operating Hours in Year	7000	
Other Operating Costs	0	
Project Life	10 yrs	
Depreciation Period	10 yrs	
Depreciation Method	Sum-of-the-years-digits	
Local Property Tax and Insurance	30%	
Marginal Income Tax Rate	50.0%	
Investment Tax Credit	10.0%	

TABLE 24

CYCLES FOR INVESTMENT SCREENING

Case	Fluid	Turbine Inlet Conditions Pressure (psia)	Turbine Inlet Conditions Temperature (°F)	Condensing Temperature (°F)
A	R-11	79	180	79
B	R-11	163	240	79
C	R-11	300	300	79
D	R-114	600	400	81
E	Steam	44	433	204
	R-11	79	180	79
F	Steam	121	492	264
	R-11	163	240	79
G	Steam	288	555	324
	R-11	300	300	79

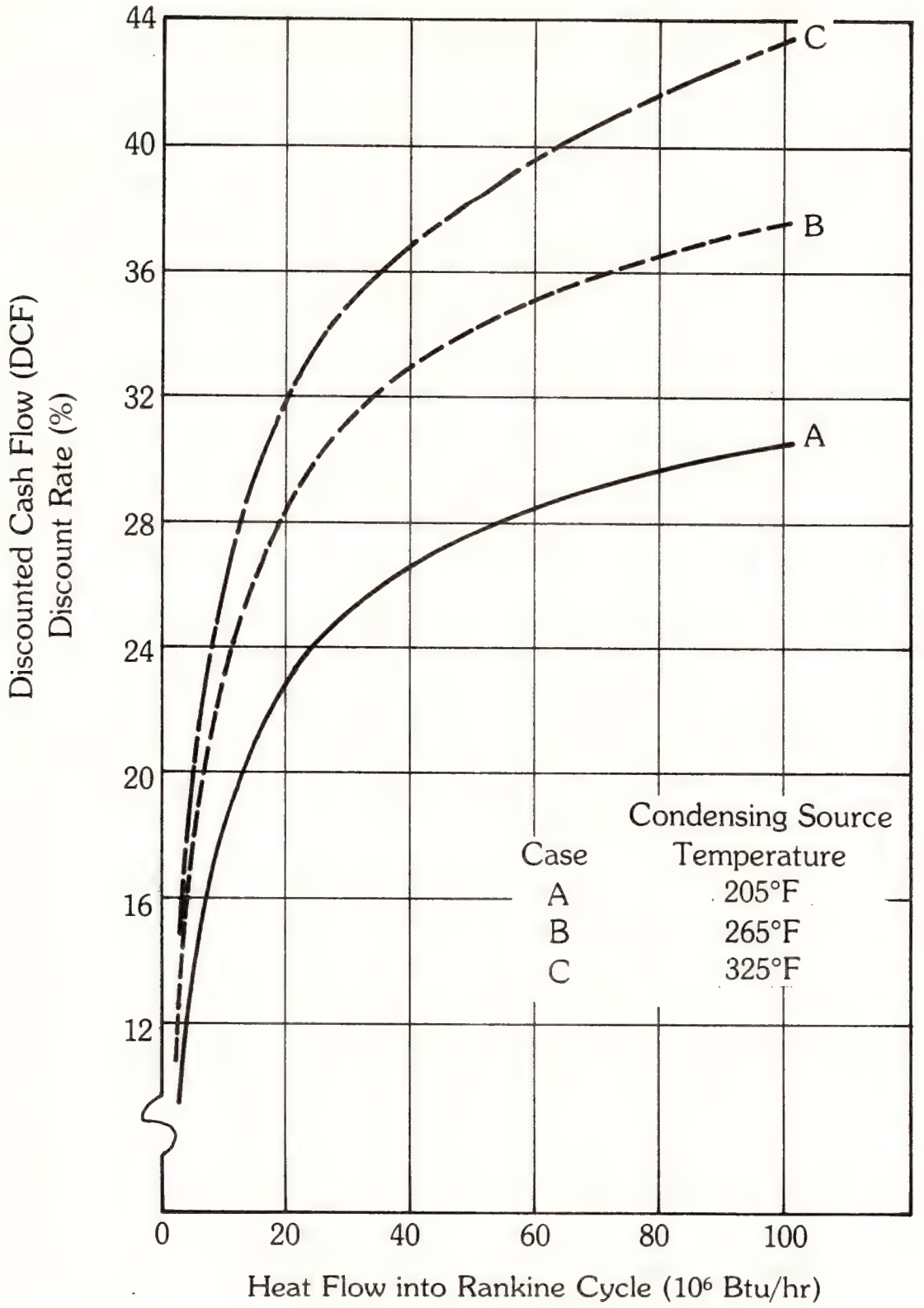

Figure 88 Variation of DCF With Available Heat Flow For Organic Cycles With a Condensing Heat Source

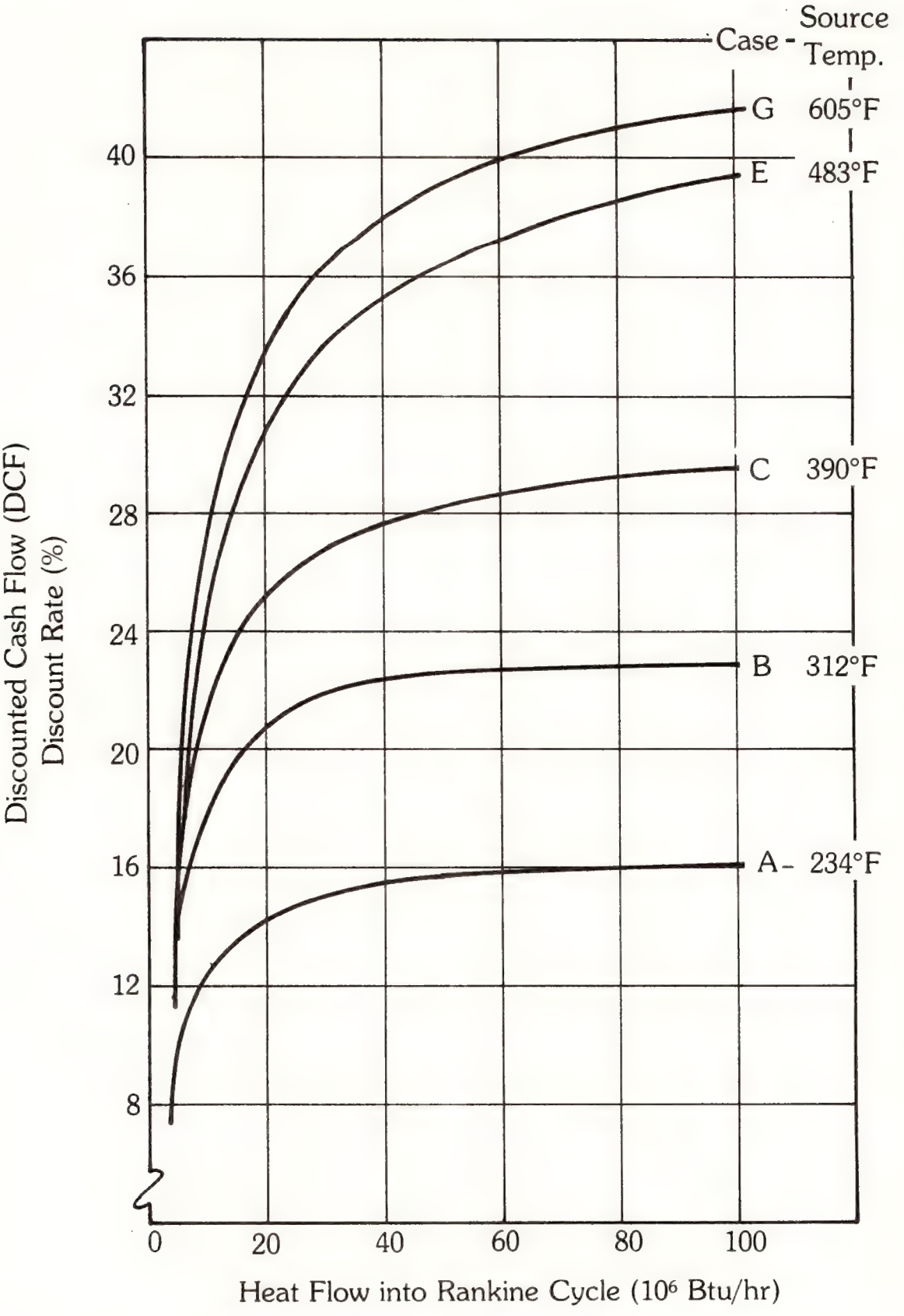

Figure 89 Variation of DCF With Available Heat Flow For Organic and Binary Cycles With a Sensible Hot Gas Source

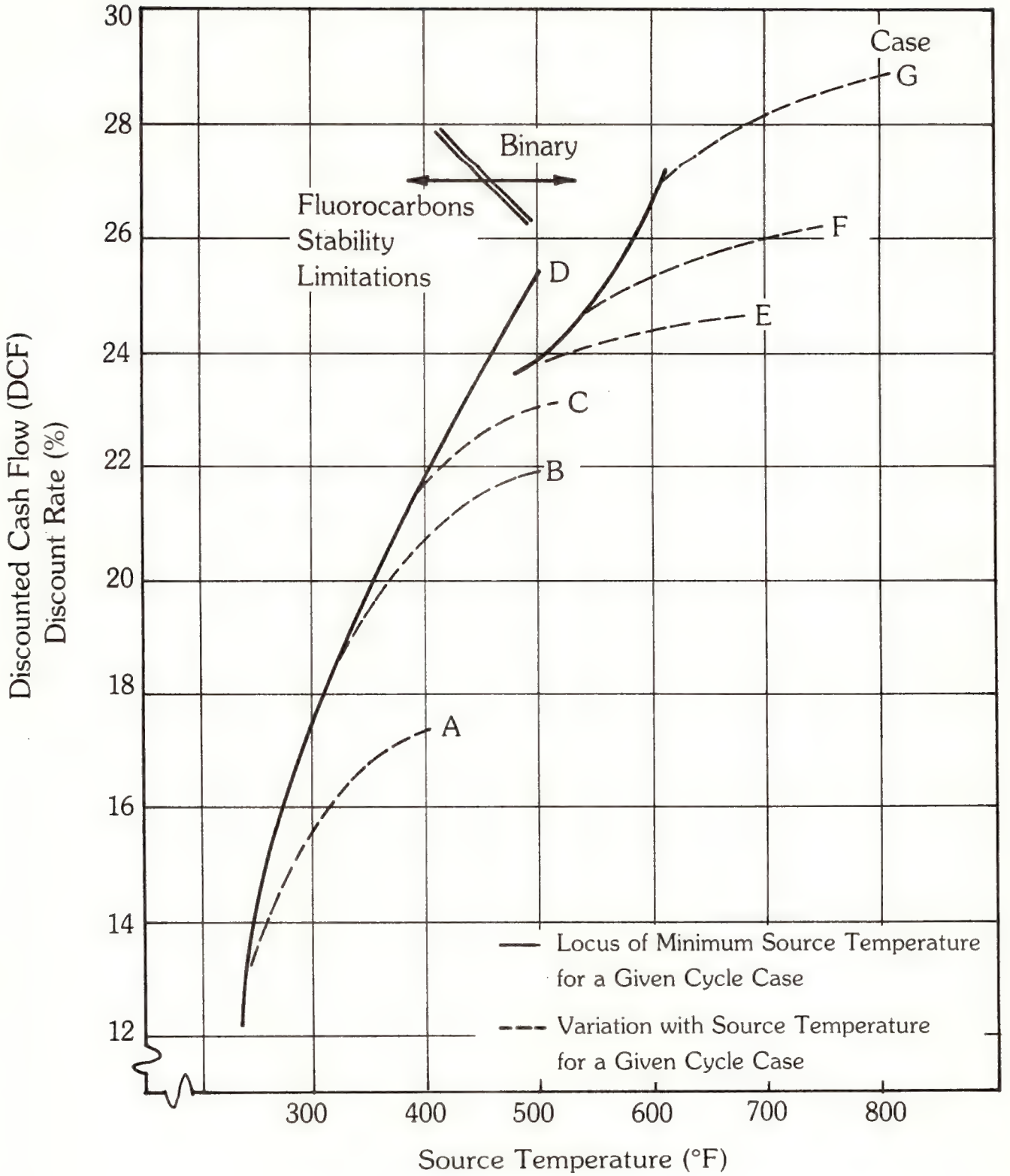

Figure 90 Variation in DCF With Hot Gas Source Temperature For Organic and Binary Cycles With a 10-million Btu/Hr Heat Flow

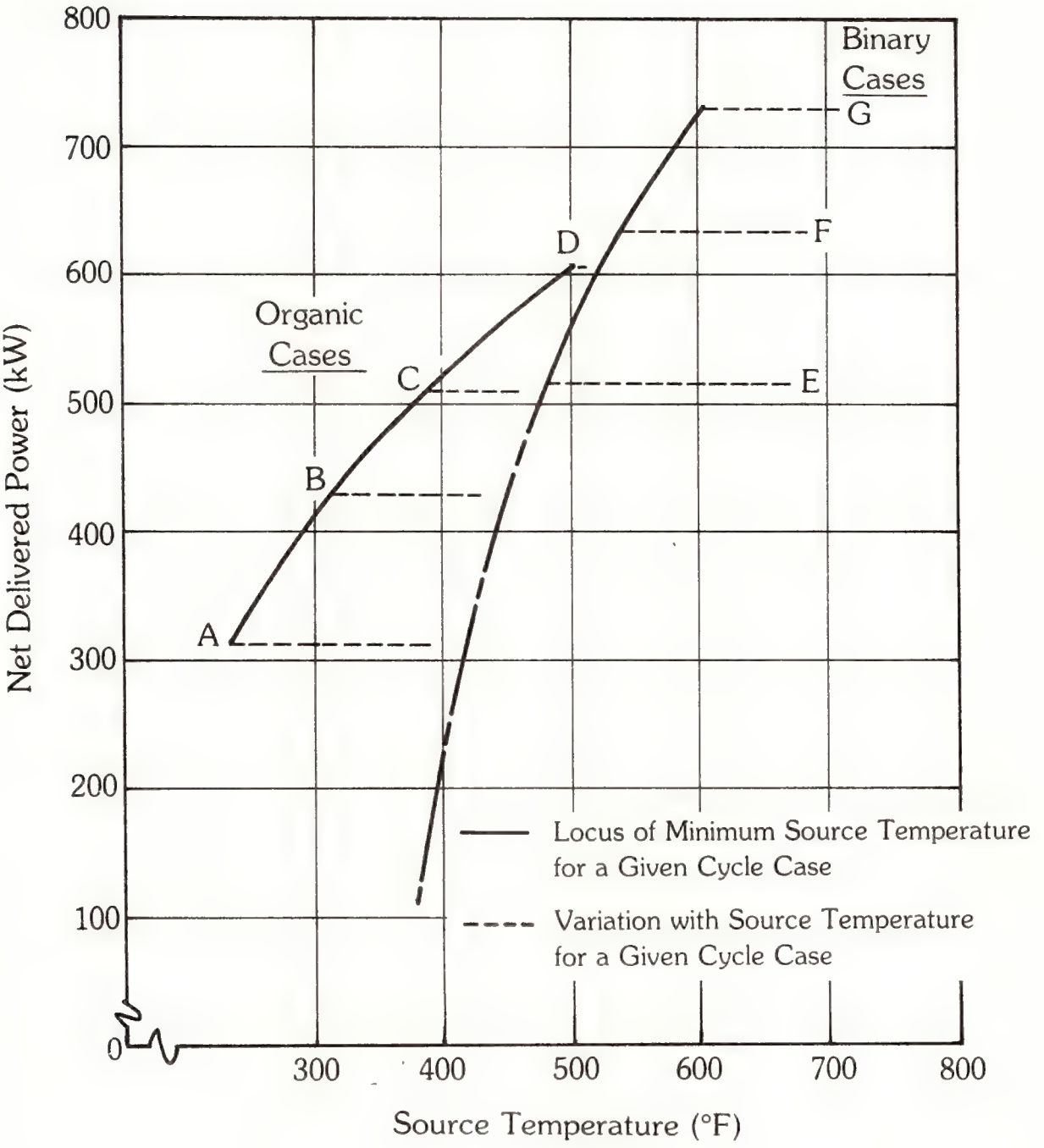

Figure 91 Variation in Delivered Net Power With Hot Gas Source Temperature For Organic and Binary Cycles With a 10-million Btu/Hr Heat Flow

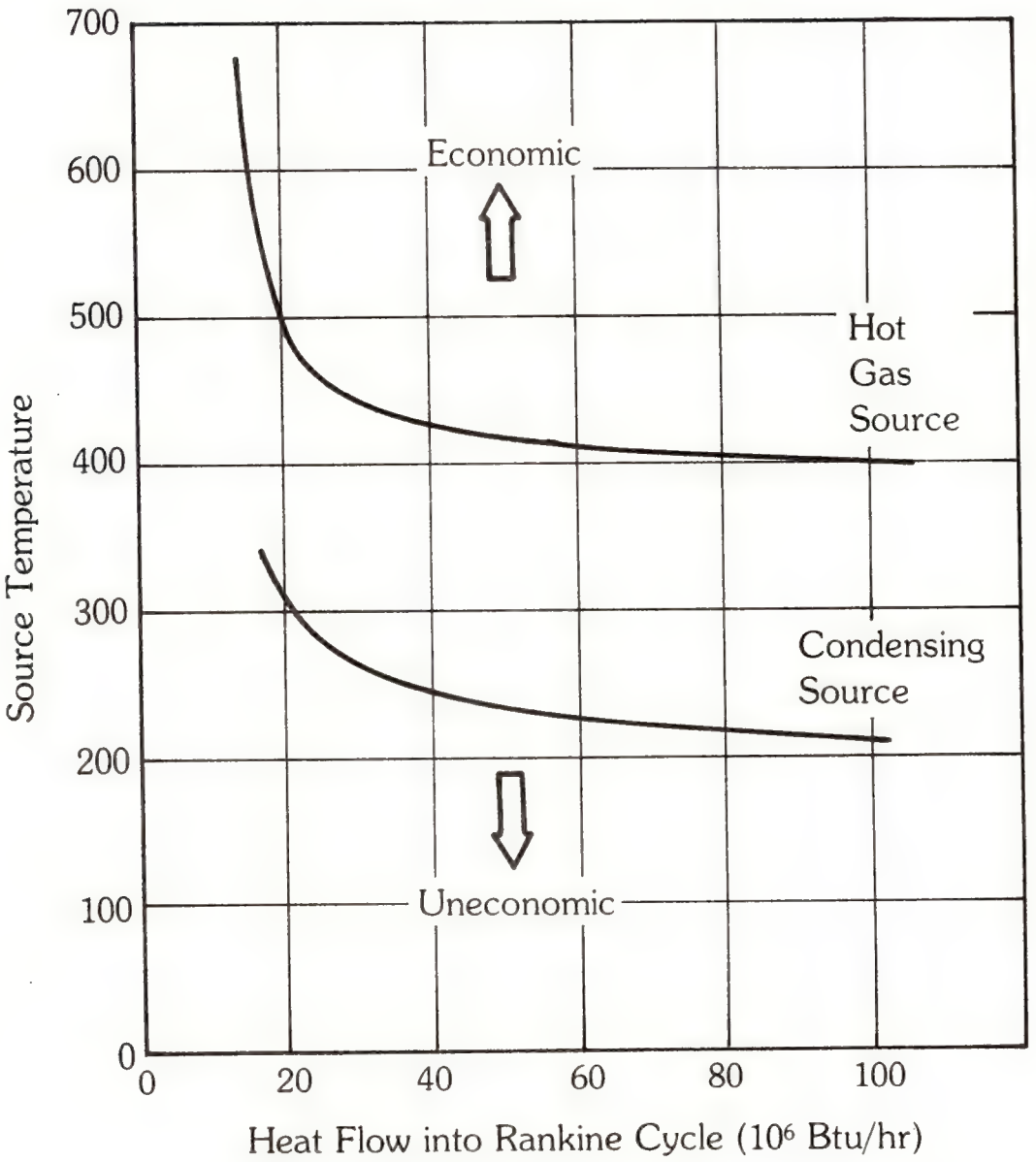

Figure 92 Economic Applications For Bottoming Cycles

8.0 SUMMARY AND CONCLUSIONS

Non-utility companies now have economic justification to generate power by combining a power generation cycle with a process cycle. The individual power generation units will be typically small, in the 1,000 kw range and almost always less than 4,000 kw. The power generation cycle should pose neither operating problems nor any perceived or actual risks to the end user, and should have a total installed capital cost as good as any other system which might offer higher performance but with operating or risk problems. A product family based on fluorocarbon refrigerants and steam appears to MTI to satisfy the product requirements. Additionally, the product needs to be reliable to enable the operating returns to be realized, compactly packaged for the lowest installed cost, and simple to operate. Again, a product line based on fluorocarbons and steam can satisfy these requirements.

It is obvious in Sections 3 and 4 that Fluorinol and toluene can deliver more power from a given waste stream than a competitive binary system. A reasonable question results: With such performance, cannot a Fluorinol or toluene system overcome the risk problems and acually produce a lower priced system? The answer would have to be yes if the total Rankine bottoming cycle market consisted of applications in the range where these fluids excel. However, it is very clear that the bulk of the waste heat applications is going to be at temperatures much less than those at which these fluids have performance advantages [References 39 and 40]. Figure 93 illustrates this qualitatively.

Looking at Figure 93, a product manager will ask this question:

> How can I achieve the most market penetration with a product family that minimizes production and distribution costs?

It is obvious that fluorocarbon and steam systems will be used, plus something else in the range of 400°F to 800°F. The applications over 800°F will use multistage axial flow steam turbines, possibly with two spools operating at different speeds (Reference 6). The fluorocarbon applications will use single stage radial inflow turbines. If a manufacturer is already in the fluorocarbon turbine market, the use of a binary steam/fluorocarbon permits the 400°F to 800°F market to be served with two single stages of radial turbines. This

offers possible manufacturing cost advantages. For example, the entire market from 200°F to 800°F might be served with six turbine designs (three organic and three steam).

As time progresses, the radial steam turbine on the binary system might be replaced by high speed, multistage axial steam turbines from the higher temperature market. This would improve the performance of the binary cycle and possibly extend its range into higher temperatures (see Reference 3).

Thus, there is a strong belief at MTI that steam and fluorocarbon refrigerants either singly or in binary system can best satisfy the needs of small scale power generation in non-utility applications. A program cooperatively funded by the U.S. Department of Energy and MTI has been initiated to demonstrate the acceptability of this concept.

SUMMARY AND CONCLUSIONS

78P79

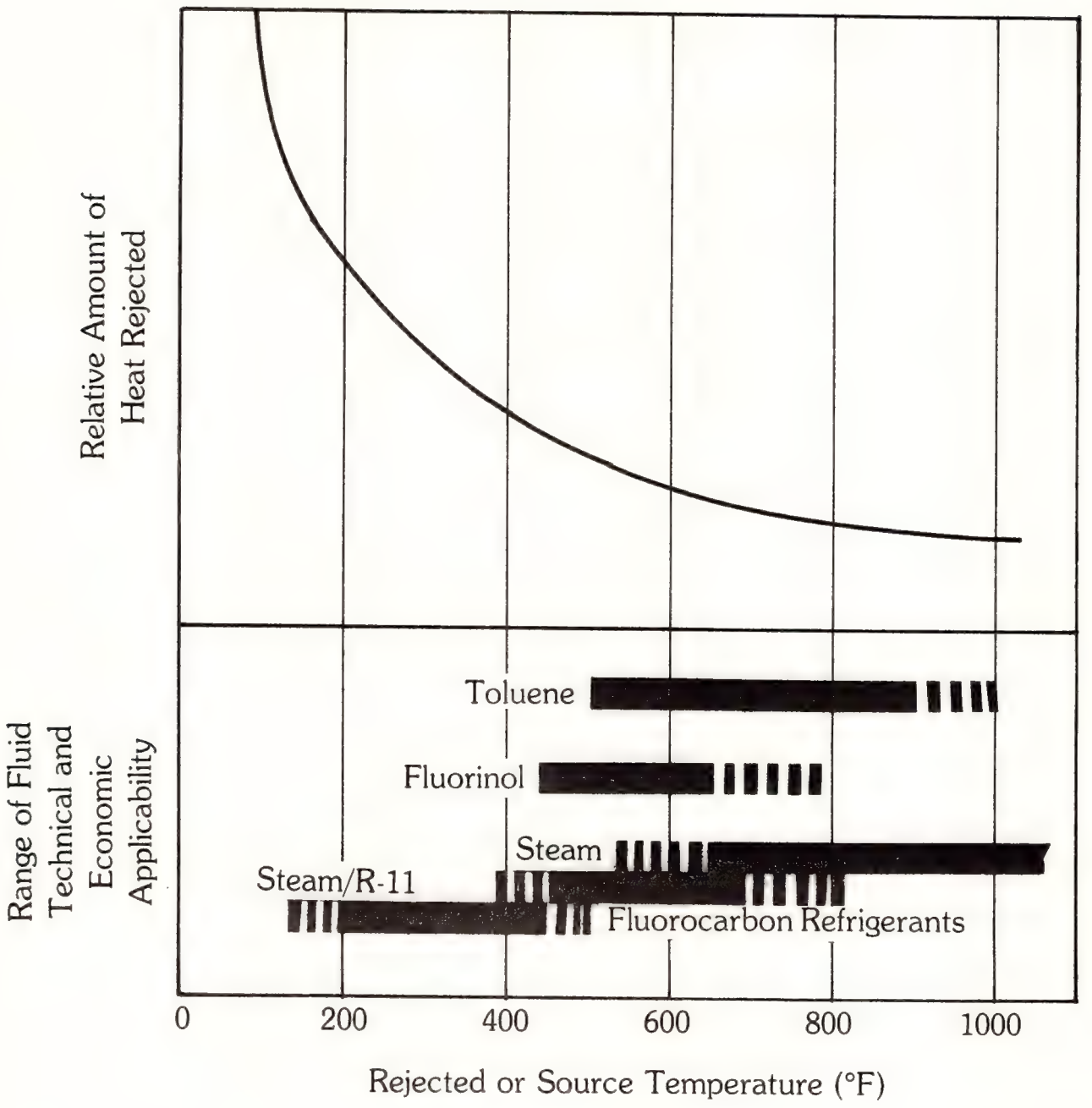

Figure 93 Comparison of Rejected Heat and Suitable Power Fluids

REFERENCES

1. Hackett, H. N., "Mercury-Steam Power Plants", Mechanical Engineering, July 1951, pp. 559-564.

2. Sternlicht, B., "Waste Heat Utilization: A Conservation Measure Whose Day Has Come", Presented at the Symposium on Implications of Energy Conservation and Supply Alternatives, American Chemical Society, January 30, 1978.

3. Horn, G., and Norris, I. D., "The Selection of Working Fluids Other Than Steam for Future Power Generation Cycles", The Chemical Engineer, November 1966, pp. 298-305.

4. Rhinehart, H. L., Ketler, C. P., and Rose, R. K., "Development Status: Binary Rankine Cycle Waste Heat Recovery System", Paper 779175 presented at the 12th IECEC, 1977.

5. Woodson, C. W., "Shipboard Heat Recovery Program for US Merchant Ships", MTI Report No. 77TR16, December 1976, prepared for the US Department of Commerce, Maritime Administration, Contract No. 6-38048.

6. Wardall, R. M., and Doorly, E. E., "Current Prospects for Efficient Combined Cycles for Small Gas Turbines", presented at the ASME Gas Turbine Conference, March 1976.

7. "Sea Joule: Outline Specifications", Hawthorn Leslie Engineers Ltd.

8. Herman, S. W., and Cannon, J. S., Energy Futures: Industry and the New Technologies, INFORM, Inc., 25 Broad Street, NY, NY 10004.

9. Meacher, J. S., "Feasibility Study of Power Recovery From Gas Turbine Exhaust Heat for Alaskan Oil Pipeline and Texas Gas Pipeline", MTI Report No. 76TR30, March 1976, US ERDA Report COO-2835-1.

10. Therma Technology Inc., "Power Recovery Package for Pipeline Pump Turbines", Press Release dated December 5, 1977.

11. Cheek, R. M., and Lacey, P. D., "600 kw Organic Rankine Cycle Waste Heat Power Conversion System", Paper 779176 presented at the 12th IECEC, 1977.

12. Morgan, D. T., and Davis, J. P., "High Efficiency Decentralized Electrical Power Generation Utilizing Diesel Engines Coupled with Organic Working Fluid Rankine-Cycle Engines Operating on Diesel Reject Heat", Thermo-Electron Report No. TE4186-27-75, prepared for The National Science Foundation, November 1974.

13. Doyle, E., Helekan, S., and Raymond, R., "Diesel- rganic Rankine Compound Engine Development", Paper 779170 presented at the 12th IECEC, 1977.

14. Soini, H. E., Patel, P. S., Morgun, D. T., and Batra, S. K., "Combined Diesel-Organic Rankine Cycle Powerplant", Paper 7/9177 presented at the 12th IECEC, 1977.

15. Lewis, P. G., Smith, R. D., Harkness, W. P., Yamada, M., and Ickiki, N., Sulfuric Acid Plant Rankine Cycle Waste Heat Recovery", Paper 769209 presented at the 11th IECEC, 1976.

16. "IHI FRON TURBINE SYSTEM", Ishikawajima-Harima Heavy Industries Co., Ltd.

17. McAnneny, A. W., "Binary Cycle Gas Fired Turbines for Gas Compression Service", ASME Paper 62-GTP-17.

18. Mangan, J. L. and Pettit, J. L., "A Highly Efficient Steam Turbine-Gas Turbine Cycle", ASME Paper 63-GT-51.

19. Bjerklie, J. W., "Working Fluid as a Design Variable for a Family of Small Rankine Power Systems", ASME Paper 67-GT-6.

20. Garay, P. N., "Application of Chemical Fluids in a Rankine Cycle Plant", Paper 759029 presented at the 10th IECEC, 1975.

21. Shepard, D. G., "A Comparison of Three Working Fluids for the Design of Geothermal Power Plants", Paper 779128 presented at the 12th IECEC, 1977.

22. Klooster, H. J., "Practical Rankine Cycles for Process Plants", paper 759210 presented at 10th IECEC, 1975.

23. Eskesen, J. H., "Study of Practical Cycles for Geothermal Power Plants", Department of Energy Report COO-2619-1, UC-66, April 1976.

24. Angelino, G., and Moroni, V., "Perspectives for Waste Heat Recovery by Means of Organic Fluid Cycles", Transactions of the ASME Journal of Engineering For Power, April 1973, pp. 75-83.

25. Balje, O. E., "A Study on Design Criteria and Matching of Turbomachines: Part A - Similarity Relations and Design Criteria of Turbines", Transactions of the ASME Journal of Engineering for Power, January 1962, pp. 83-102.

26. Wood, H. J., "Current Technology of Radial-Inflow Turbines for Compressible Fluids", Transactions of the ASME Journal of Engineering for Power, January 1963, pp. 72-83.

27. Rohsenow, W. M., and Choi, H. Y., Heat, Mass and Momentum Transfer, Prentice-Hall, Inc., 1961.

28. Lord, R. C., Minton, P. E., and Slusser, R. P., "Design of Heat Exchangers", Chemical Engineering, January 26, 1970.

29. Chen, N. H., "Graphs Speed Evaluation of Condensing and Boiling Coefficients of Heat Transfer", Chemical Engineering, March 9, 1957.

30. Rohsenow, W. M., and Sukhatme, S. P., "Condensation", Chapter 10 in Developments in Heat Transfer, W. M. Rohsenow, Ed., The MIT Press, 1964.

31. Fanaritis, J. P., and Bevevino, J. W., "How to Select the Optimum Shell-and-Tube Heat Exchanger", Chemical Engineering, July 5, 1976, pp. 62-71.

32. Werner, D. K., "Comparison of Water Trifluoroethanol/Water Mixtures, and Fluorozene-M as Rankine Cycle Working Fluids", Barber-Nichols Engineering, report dated April 3, 1974.

33. Abbin, J. P., "Rankine Cycle Energy Conversion System Design Considerations for Low and Intermediate Temperature Sensible Heat Sources", Sandia Laboratories, Report No. SAND-76-0363, October 1976.

34. Daugas, C. F., "Diesel and Dual Fuel Engines With Heat Recovery", ASME Paper 77-DGP-20.

35. Gyftopoulos, E. P., Lazaridis, L. J., and Widmer, T. F., Potential Fuel Effectiveness in Industry; A Report to the Energy Policy Project of the Ford Foundation, Ballinger Publishing Co., Cambridge, Mass., 1974.

36. Barber, R. E., "Rankine-Cycle Systems for Waste Heat Recovery" in Chemical Engineering, November 25, 1974, pp. 101-106.

37. Svoboda, K. J. and Klooster, H. J.,"Proper Waste Heat Utilization Reduces Air Pollution and Saves Energy" presented at the 69th Annual Meeting of the Air Pollution Control Association, June, 1976.

Sternlicht B, "The Equipment Side of Low Level Heat Recovery", Power Magazine, June, 1975.

38. Klooster, H. J. "Practical Rankine Cycles for Process Plants" Paper 759210, presented at the IECEC, 1975.

39. "Industrial Applications Study" US Energy Research and Development Administration Report CONS/2862-1, -2, -3, -4, -5, (Five Volumes), January, 1977.

40. "Industrial Applications Study" US Department of Energy Report HCP/T2862-01, -02, -03, -04, -05, (Five Volumes), March, 1978.

41. Nydick, S.E., Davis, J. P., Denlay, J., Rain S., and Sukhuja, R., "A Study of In-Plant Power Generation in the Chemical, Petroleum Refining and Paper and Pulp Industries", US Federal Energy Administration Report FEA/D-76/321, June, 1976 (Available through NTIS PB 255-659).

42. Hatsopoulos, G. N., Gyftopoulos, E. P., Sant, R. W., and Widmer, T. F., "Capital Investment to Save Energy" Harvard Business Review, March-April 1978, pp. 111-122.

References For Fluid Properties

Keenan, J. H., and Keyes, F. G., Thermodynamic Properties of Steam, John Wiley & Sons, Inc.

Properties of Commonly Used Refrigerants, Air-Conditioning and Refrigeration Institute, Arlington, VA, 1967, Edition.

Canjan, L. N., and Manning, F. S., Thermodynamic Properties and Reduced Correlations for Gases, Gult Publishing Co., 1967.

"Tables of Thermodynamic Properties of Fluorinol", Halocarbon Products Corporation, 82 Burlews Court, Hackensack, NJ, 07601, March, 1978.

Handbook of Chemistry and Physics, Dr. R. Weast, Ed., Chemical Rubber Publishing Company.

BIBLIOGRAPHY

Barret, R. W., Garcia, R, and Waters, W. M., "Organic Rankine Power Unit Testing", Aerojet Nuclear Systems Company, Azusa, California.

Biancardi, Frank R. and Meader, Maurice D., "A Unique Rankine-Cycle Heat Pump System", United Technologies Research Center, East Hartford, Conneticut 06108.

Boretz, J.E., "Low Peak Temperatures and Hydrodynamic Bearings-Key to Long Life Organic Rankine Cycle Systems", Systems Group of TRW, Inc., Redondo Beach, California 90278.

Clay, W. and Teagan, Dr. W. P., 3KW Closed Rankine-Cycle Powerplant with a Turbine Expander, Thermo Electron Corporation, 85 First Avenue, Waltham, Massachusetts 02154.

Eckard, Spurgeon E., "Test Results for a Rankine Engine Powered Vapor Compression Air-Conditioner for 366°K Heat Source", General Electric Company, Space Division, Evendale, Ohio.

Elliott, David G., "Comparison of Geothermal Power Conversion Cycles", Jet Propulsion Laboratory, Pasadena, California.

Eskesen, John H., "Cost and Performance Comparison of Flash Binary and Steam Turbine Cycles for the Imperial Valley, California", Medium Steam Turbine Department, General Electric Company, Lynn, Massachusetts.

Hankin, J. W., Hogue, R. A., Cassel, T. A. V., and Fick, T. R., "Effect of Reservoir Temperature Decline on Geothermal Power Plant Design and Economics", Bechtel Corporation, P.O. Box 3965, San Francisco, California 94119.

Henry, Charles D. and Fazzolare, Rocco, "Optimal Cycle Analysis for Low Temperature Applications", University of Arizona, Tucson, Arizona U.S.A.

Hoagland, Lawrence C., "Summary of Recent Developments in Small Rankine Cycle Power Systems", CTi-Cryogenics, Waltham, Massachusetts.

Miller, D. R., Thompson, Q. E., Null, H. R., Monsanto Research Corporation, St. Louis, Missouri 63166, and Barber, K. F., Environmental Protection Agency, Ann Arbor, Michigan 48105, "Working Fluids for Automotive Rankine Engines".

Monahan, John and McKenna, Ron, "Development of a 1-KW, Organic Rankine Cycle Power Plant for Remote Applications", Sundstrand Energy Systems, Rockford, Illinois.

Niggemann, R. E., "3000 Hour Endurance Test of a 6 KWE Organic Rankine Cycle Power System", Sundstrand Aviation, Division of Sundstrand Corporation, Rockford, Illinois.

Niggemann, R. E., Bland, T. J., and Wigmore, D. B., "A 6 KWe Organic Rankine Power Conversion System for Space Applications", Sundstrand Aviation, Division of Sundstrand Corporation, Rockford, Illinois.

Pope, W. L., Pines, H. S., Silvester, L. F., Green, M. A., and Williams, J. D., "Multiparameter Optimization Studies on Geothermal Energy Cycles", Lawrence Berkeley Laboratory, University of California, Berkeley, California 94720.

Reistad, G. M., Department of Mechanical Engineering, Oregon State University, Corvallis, Oregon, Yao, B., Power Train and Chassis Division, Ford Motor Co., Dearborn, Michigan, and Gunderson, M., Environmental and Energy Systems, AlResearch Manufacturing Co. of California, Torrance, California, "A Thermodynamic Study of Heating with Geothermal Energy".

Schapiro, A. R., and Hajela, A. R., "Geothermal Power Cycle Analysis", Atomics International Division, Rockwell International, 8900 DeSoto Avenue, Canoga Park, California 91304.

Sheinbaum, I., "Power Production from High Temperature Geothermal Waters", I. Sheinbaum Co., Pasadena, California.

Somekh, George S., "Water-Pyridine Azeotrope is an Excellent Rankine Cycle Fluid", Union Carbide Corporation, Chemicals and Plastics, Research and Development Department, P.O. Box 65, Tarrytown, New York 10591.

Spechtenhauser, Alfred M., "Fundamentals on the Suitability of the Reaction-Type Steam Turbine for Compressor and Pump Drive", Brown Boveri Corp., Baden, Switzerland.

Starling, K. E., Fish, L. W., Iqbal, K. Z., West, H. H., "The Use of Mixture Working Fluids in Geothermal Binary Power Cycles", The University of Oklahoma.

Starling, K.E., Fish, L. W., West, H., Johnson, D. W., Iqbal, K. Z., Lee, C. O., Vasudevan, M. K., Resource Utilization Efficiency Improvement of Geothermal Binary Cycles: Phase I, School of Chemical Engineering and Materials Science, University of Oklahoma, Normal, Oklahoma.

Walter, Ronald A. and Wilson, Stephen W., "Economic Optimization of Binary Fluid Cycle Power Plants for Geothermal Systems", Battelle, Pacific Northwest Laboratories, Richland, Washington, U.S.A.

Wigmore, D. B. and Niggemann, R. E., Sundstrand Aviation, Division of Sundstrand Corporation, Rockford, Illinois and O'Sullivan, J. B., U.S. Army Mobility Equipment Research and Development Center, Fort Belvoir, Virginia, "The Specification of an Optimum Working Fluid for a Small Rankine Cycle Turboelectric Power System".